Journal of Research

of the

National Bureau of Standards

[redacted]

[redacted]

PERIODICALS OF THE NATIONAL BUREAU OF STANDARDS

Journal of Research

The National Bureau of Standards is the principal agency of the Federal Government for fundamental research in physics, chemistry, and engineering. It has the custody of the national standards of physical measurement in terms of which all existing standards for measurement in science and industry are calibrated, and carries on research necessary to keep these standards abreast of progress in such disciplines and methods of measurement. It also has a broad program of general research in physics, chemistry, and engineering, and the development of fundamental methods for testing materials and equipment. It determines physical constants and properties of materials, tests and calibrates standard measuring equipment and reference standards, and develops technical processes. The results of the Bureau's research and investigations are published in the JOURNAL OF RESEARCH.

Research Papers

Reprints of individual articles appearing in the JOURNAL OF RESEARCH. They are made available to serve the needs of research workers, technical groups, and others for full reprints papers relating to the special subjects in which they are interested.

Technical News Bulletin

Contains short but complete summaries of research, development, and testing in progress at the Bureau, comments of the Bureau's technical and administrative officers, scientific and technical announcements of new plans and programs, and a list of publications by members of the staff. It is a prompt and reliable source of official information of value to those who desire to keep in touch with the general activities of the Bureau.

Basic Radio Propagation Predictions

This is a monthly publication for those concerned with radio communication in determining the best sky-wave frequencies over any path at any time of day for average conditions for the month of prediction, which are made three months in advance. Charts of ionospheric-wave critical frequency for the F2 layer and of operationally usable frequency for a transmission distance of 4,000 km, of highest frequency of sporadic E (in excess of 15 Mc) are included. In addition, there are various maps, charts, diagrams, and nomograms needed to make practical application of the world-center charts, together with examples of their use.

JOURNAL OF RESEARCH of the National Bureau of Standards. 12 monthly issues (2 volumes), paper covers	[illegible]	$4.00
Bound volume (½ year, 1 volume), [illegible]	[illegible]	5.00
RESEARCH PAPERS	[illegible]	[illegible]
TECHNICAL NEWS BULLETIN, 12 [illegible]	[illegible]	1.50
BASIC RADIO PROPAGATION PREDICTIONS, 12 monthly issues	1.50	2.00

The prices of the separate Research Papers appearing in the JOURNAL [illegible] are listed in the Contents [illegible] of current issues of each separate publication. A discount of 25 percent is allowed on orders for 100 or more copies of any publication mailed to one address. Remittances should be made payable to the Superintendent of Documents, U. S. Government Printing Office, Washington 25, D. C. [illegible] Orders for publications should designate the publication desired by its full name and not by reference to the number of copies to be supplied. [illegible] and usually no more copies can be furnished than are sold. Only publications [illegible] can be sold.

Published with approval of Director of the Budget

U. S. DEPARTMENT OF COMMERCE
W. Averell Harriman, Secretary
NATIONAL BUREAU OF STANDARDS
E. U. Condon, Director

JANUARY 1947
VOLUME • 38
NUMBER 1

JOURNAL OF RESEARCH

of the

NATIONAL BUREAU OF STANDARDS

Contents

RP		Page
1758.	Vibrational frequencies of semirigid molecules: A general method and values for ethylbenzene. William J. Taylor and Kenneth S. Pitzer. (Price 15 cents)	1
1759.	Analysis of a standard sample of natural gas by laboratories cooperating with the American Society for Testing Materials. Martin Shepherd. (Price 20 cents)	19
1760.	Purification, purity, and freezing points of 8 nonanes, 11 alkylcyclopentanes, 6 alkylcyclohexanes, and 4 butylbenzenes of the API-Standard and API-NBS series. Anton J. Streiff, Evelyn T. Murphy, Janice C. Cahill, Helen F. Flanagan, Vincent A. Sedlak, Charles B. Willingham, and Frederick D. Rossini. (Price 20 cents)	53
1761.	Infrared absorption of some experimental glasses containing rare earth and other oxides. Ralph Stair and Conrad A. Faick. (Price 10 cents)	95
1762.	Properties of water-repellent fabrics. John W. Rowen and Domenick Gagliardi. (Price 10 cents)	103
1763.	Adsorption of water vapor by untanned hide and various leathers at 100° F. Joseph R. Kanagy. (Price 10 cents)	119
1764.	Concentration of the isotopes of mercury by free evaporation in a 10-cell counter-current reflux still. A. Keith Brewer and Samuel L. Madorsky. (Price 10 cents)	129

or sale by the Superintendent of Documents, U. S. Government Printing Office, Washington 25, D. C. - Price 30 cents,
$3.50 per year on subscription

UNITED STATES GOVERNMENT PRINTING OFFICE, WASHINGTON : 1947

U. S. Department of Commerce
National Bureau of Standards

Research Paper RP1758
Volume 38, January 1947

Part of the Journal of Research of the National Bureau of Standards

Vibrational Frequencies of Semirigid Molecules: A General Method and Values for Ethylbenzene [1]

By William J. Taylor [2] and Kenneth S. Pitzer [3]

It is shown that in normal coordinate calculations of the vibrations of molecules it is sometimes advantageous to calculate the kinetic-energy matrix, rather than the reciprocal kinetic-energy matrix. Explicit formulas are given for the elements of the kinetic-energy matrix. Illustrative calculations are given for propane, toluene, and ethylbenzene. A semiempirical assignment of the vibration frequencies of ethylbenezene is made on the basis of these calculations and the spectroscopic data.

I. Introduction

For the purpose of calculating the thermodynamic functions (particularly the entropy) of molecules by statistical methods, it is important that the low frequencies of vibration be assigned as accurately as possible. When these frequencies have not been observed in the spectra, the assignment must be made either by analogy with other molecules, or on the basis of a normal coordinate calculation, using force constants determined from other molecules. Even when the frequencies have been observed, a preliminary assignment by analogy or calculation is often necessary for the identification of the observed frequencies. However, a complete normal coordinate analysis for molecules with many atoms is so time-consuming as to be impracticable in most investigations. Therefore, an approximate method of calculating the low skeletal frequencies of large molecules should be of considerable value in connection with thermodynamic calculations.

In this paper there is described an approximate method that is based on the replacement of the actual molecule by a semirigid model (of the same dimensions and masses) in which certain groups of atoms move as rigid units. In this way the number of internal coordinates of the molecule may be reduced sufficiently to make the calculation of the low skeletal frequencies practicable. The semirigid model should be satisfactory, provided that all the frequencies of internal motion of the groups assumed to be rigid are either considerably higher than the frequencies to be calculated, or else do not interact seriously with them because of molecular symmetry or other factors. In order to reduce the error due to interactions, it is desirable that the necessary force constants be determined by analogous (semirigid model) calculations on other molecules in which the frequencies are known.

The analysis given in this paper shows that the kinetic-energy matrix of a semirigid molecule is usually more easily calculated than the reciprocal kinetic-energy matrix. The reverse is true for a complete normal coordinate calculation for the molecule. Formulas are given that reduce the calculation of the kinetic-energy matrix to a consideration of the masses, moments of mass, and moments of inertia of the rigid groups.

[1] This investigation was performed at the National Bureau of Standards as part of the work of the American Petroleum Institute Research Project 44 on the "Collection, Analysis, Calculation, and Compilation of Data on the Properties of Hydrocarbons".

[2] Research Associate on the American Petroleum Institute Research Project 44 at the National Bureau of Standards.

[3] Associate Supervisor, American Petroleum Institute Research Project 44; Professor of Chemistry, University of California, Berkeley, Calif.

An illustrative calculation is given for ethylbenzene by using force constants determined from propane and toluene. A semiempirical assignment of the vibrational frequencies of ethylbenzene is made on the basis of this calculation and the spectroscopic data. These calculations for ethylbenzene were completed in September 1945, were and used in the tables of the thermodynamic properties of ethylbenzene issued November 30, 1945, by the American Petroleum Institute Research Project 44.

II. Mathematical Analysis

1. Kinetic Energy of Semirigid Molecules

The first step in the normal coordinate analysis of a vibrating system is the computation of the kinetic-energy matrix, or of its reciprocal. Certain general features of the calculation will first be considered. Let the system of n particles be characterized by $3n$ generalized coordinates, q, six of which refer to over-all translation and rotation of the system (external coordinates), and the remainder of which specify the configuration of the system (internal coordinates). The present discussion is concerned only with small distortions of the system from its equilibrium configuration, so that the internal coordinates may pe assumed to measure this distortion and to have the value zero at the equilibrium configuration.

The kinetic energy is a quadratic form in the coordinate velocities, the $\dot{q}$'s,

$$2T=\tilde{\dot{q}}S\dot{q}. \tag{1}$$

In this equation $\dot{q}$ is a column matrix, $\tilde{\dot{q}}$ is a row matrix (the transpose of $\dot{q}$), and S is the square symmetric kinetic-energy matrix. In general, the elements of S are functions of the q's (not of the $\dot{q}$'s), but because of the restriction to configurations near the equilibrium configuration, S is to be regarded as a constant matrix here.

For reasons that will appear presently, it will be convenient to assume that the coordinates are of three types, and to partition the column matrix q accordingly.

$$q=\begin{bmatrix} q_1 \\ q_2 \\ q_3 \end{bmatrix} \tag{2}$$

The kinetic-energy matrix, S may be partitioned into the corresponding submatrices, and it will also be convenient to designate by G the reciprocal of S and to partition G,

$$S=\begin{bmatrix} S_{11} & S_{12} & S_{13} \\ \tilde{S}_{12} & S_{22} & S_{23} \\ \tilde{S}_{13} & \tilde{S}_{23} & S_{33} \end{bmatrix}, \quad G=S^{-1}=\begin{bmatrix} G_{11} & G_{12} & G_{13} \\ \tilde{G}_{12} & G_{22} & G_{23} \\ \tilde{G}_{13} & \tilde{G}_{23} & G_{33} \end{bmatrix} \tag{3}$$

The concept of a semirigid molecule, with which this paper is principally concerned, will now be introduced. A semirigid molecule, as defined here, is one in which some of the internal coordinates, say the group q_3, remain zero throughout the molecular motion, so that $q_3=0$, and $\dot{q}_3=0$. Thus, if parts of the molecule move as rigid units in their equilibrium configurations, the internal coordinates of these parts will remain zero.

The kinetic-energy matrix for a semirigid molecule reduces to

$$\begin{bmatrix} S_{11} & S_{12} \\ \tilde{S}_{12} & S_{22} \end{bmatrix}, \tag{4}$$

as $\dot{q}_3=0$. The equivalent expression for the kinetic energy is

$$2T=\tilde{\dot{q}}_1S_{11}\dot{q}_1+2\tilde{\dot{q}}_1S_{12}\dot{q}_2+\tilde{\dot{q}}_2S_{22}\dot{q}_2. \tag{5}$$

The form of the potential-energy expression will now be considered. As $q_3=0$, these coordinates do not influence the variable part of the potential energy (the assumption that $q_3=0$ is equivalent to setting the force constants for these coordinates equal to infinity). In addition, there will be a group of coordinates, say q_1 that do not occur in the expression for the potential energy, although $\dot{q}_1$ occurs in the kinetic energy. This group of coordinates of zero frequency includes the external coordinates and possibly (as an approximation) some very low frequency internal coordinates, in particular torsional motions. Finally, it will be assumed that the potential energy is a quadratic form in the remaining coordinates (harmonic vibrations) so that,

$$2V=\tilde{q}_2F_{22}q_2, \tag{6}$$

where F_{22} is the symmetric potential-energy matrix.

If the Lagrangian equations of a system for which the kinetic and potential energies are given by eq 5 and 6, respectively, are to be integrable, it is necessary to remove by a suitable

transformation the cross term between q_1 and q_2 in the kinetic energy. The existence of this cross term is a consequence of the fact that the initial coordinates, q_1 have been defined in such a way that their conjugate momenta, $p_1=(\partial T/\partial \dot{q}_1)$, are not independent of $\dot{q}_2$. As a result, the momenta p_1 are not conserved, as they should be, because the coordinates q_1 do not enter into the potential-energy expression, and are therefore not acted upon by any forces.

As it is desired to find the proper kinetic-energy matrix for the (arbitrary) internal coordinates q_2, it follows that the transformation should leave these coordinates unchanged. The most general linear transformation of this type is

$$\begin{bmatrix} q_1' \\ q_2 \end{bmatrix} = \begin{bmatrix} T_{11} & T_{12} \\ 0 & E_{22} \end{bmatrix} \begin{bmatrix} q_1 \\ q_2 \end{bmatrix}, \tag{7}$$

where E_{22} is the unit matrix with the appropriate number of rows and columns. The matrices T_{11} and T_{12} are subject only to the condition that the transformed kinetic-energy matrix have the form

$$\begin{bmatrix} S_{11}' & 0 \\ 0 & S_{22}' \end{bmatrix} \tag{8}$$

The equivalent expression for the kinetic energy is

$$2T=\tilde{\dot{q}}_1' S_{11}' \dot{q}_1' + \tilde{\dot{q}}_2 S_{22}' \dot{q}_2. \tag{9}$$

The transformed kinetic-energy matrix is obtained by multiplying the original kinetic-energy matrix from the right by the reciprocal of the transformation matrix, and from the left by the transpose of the reciprocal (congruent transformation). Therefore,

$$\begin{bmatrix} S_{11}' & 0 \\ 0 & S_{22}' \end{bmatrix} = \begin{bmatrix} \tilde{T}_{11}^{-1} & 0 \\ -\tilde{T}_{12}\tilde{T}_{11}^{-1} & E_{22} \end{bmatrix} \begin{bmatrix} S_{11} & S_{12} \\ \tilde{S}_{12} & S_{22} \end{bmatrix} \begin{bmatrix} T_{11}^{-1} & -T_{11}^{-1}T_{12} \\ 0 & E_{22} \end{bmatrix} \tag{10}$$

Equation 10 is equivalent to the relations

$$S_{11}' = \tilde{T}_{11}^{-1} S_{11} T_{11}^{-1} \tag{11}$$

$$0 = \tilde{T}_{11}^{-1}(S_{12} - S_{11}T_{11}^{-1}T_{12}) \tag{12}$$

$$0 = (\tilde{S}_{12} - \tilde{T}_{12}\tilde{T}_{11}^{-1}S_{11})T_{11}^{-1} \tag{13}$$

$$S_{22}' = S_{22} - \tilde{T}_{12}\tilde{T}_{11}^{-1}S_{12} - \tilde{S}_{12}T_{11}^{-1}T_{12} + \tilde{T}_{12}\tilde{T}_{11}^{-1}S_{11}T_{11}^{-1}T_{12} \tag{14}$$

Equations 12 and 13 are equivalent, and yield

$$T_{11}^{-1}T_{12} = S_{11}^{-1}S_{12} \tag{15}$$

as the condition that there be no cross term between $\dot{q}_1'$ and $\dot{q}_2$ in the kinetic energy.

Equation 15 does not determine T_{11} or T_{12} separately, but only the product $T_{11}^{-1}T_{12}$, and therefore S_{11}' is not uniquely determined. However, S_{22}' is unique, as the combination of eq 14 and 15 yields

$$S_{22}' = S_{22} - \tilde{S}_{12}S_{11}^{-1}S_{12} \tag{16}$$

The matrix S_{22}' will be called the reduced kinetic-energy matrix for the internal coordinates (excluding those that do not occur in the expression for the potential energy). A result equivalent to eq 16 has been obtained by Majantz [1] [4] by an argument less fundamental than that presented here.

When applied to the external coordinates, the transformation of eq 7 is equivalent to the application of the conditions that the linear and angular momenta of the entire molecule are independent of the $\dot{q}_2$'s. When applied to an internal torsional motion, the transformation is equivalent to the condition, previously stated by Sayvetz [2, 3], that the momentum conjugate to the torsion should be independent of the (remaining) $\dot{q}_2$'s.

An important property of transformations of the type of eq 7 may now be stated. The proof is given in appendix 1. The coordinates q_1 may be divided into two or more groups in various ways, and the transformation applied consecutively to each group. The over-all transformations from q_1 to q_1' will not, in general, be identical. However, the theorem states that all possible transformations of this type lead to the same reduced matrix S_{22}'. The importance of this theorem is that in practice it is convenient to apply the transformation consecutively to translation, rotation, and finally, in some cases, to certain internal coordinates.

The Lagrangian equations for the system may now be written as

$$\dot{p}_1' = S_{11}'\ddot{q}_1' = 0 \tag{17}$$

$$S_{22}'\ddot{q}_2 + F_{22}q_2 = 0 \tag{18}$$

[4] Figures in brackets indicate the literature references at the end of this paper.

The first equation shows that the momenta p_1' are conserved. The second equation may also be written

$$\ddot{q}_2 + G_{22}' F_{22} q_2 = 0, \tag{19}$$

where

$$G_{22}' = (S_{22}')^{-1} \tag{20}$$

is the reduced reciprocal kinetic-energy matrix for the internal coordinates q_2. In eq 16, S_{22}' is defined in terms of the submatrices of S. It is proved in appendix 2 that G_{22}' may be expressed in terms of the submatrices of G, eq 3, by the equation

$$G_{22}' = (S_{22}')^{-1} = G_{22} - G_{23} G_{33}^{-1} \tilde{G}_{23}. \tag{21}$$

This result has been obtained previously by Wilson [4], although not explicity for the case in which coordinates of the types q_1 and q_3 are present simultaneously.

As is well known, eq 18 and 19 lead to the following secular equations for the determination of the normal frequencies of vibration of the coordinates q_2:

$$|F_{22} - \lambda S_{22}'| = 0, \tag{22}$$

or,

$$|G_{22}' F_{22} - \lambda E_{22}| = 0, \tag{23}$$

where $\lambda = 4\pi^2\nu^2$ (ν = normal frequency). In the present method, in which S_{22}' rather than G_{22}' is computed, it is convenient to convert eq 22 to the secular equation of a single matrix, in the form

$$|S_{22}' F_{22}^{-1} - \lambda^{-1} E_{22}| = 0. \tag{24}$$

In practice, F_{22} is diagonal, or nearly so, and therefore easily reciprocated. The roots of eq 24 are, of course, the reciprocals of the λ's.

It is possible now to state clearly the relative advantages of calculating S_{22}' and G_{22}' (see eq 3, 16, and 21). In calculating S_{22}', the coordinates q_3 are ignored, but all the elements for q_1 and q_2 must be computed. Conversely, in calculating G_{22}', the coordinates q_1 are ignored, but all the elements for q_2 and q_3 must be computed. It should also be noted that even with the simplifications described later in this paper, the elements of S are more difficult to compute than those of G[5] (this statement does not apply to the elements for the external coordinates, but these are just the elements of G that may be ignored). From these considerations it is obvious that the calculation of G_{22}' is to be preferred when all or most of the internal coordinates are included in the calculation (so that the number of coordinates of type q_3 is zero or small). On the other hand, S_{22}' is often to be preferred in calculations by the semirigid molecule approximation as the number of coordinates of the type q_3 is then relatively large, and the number of coordinates remaining in the calculation (type q_2) is relatively small.

If the molecule has the symmetry of one of the point groups, the internal coordinates fall into sets equivalent under the group. The coordinates in an equivalent set may be transformed into each other by the operations (rotations and reflections) of the group. In this case, just as is the case when working with the reciprocal kinetic-energy mtarix [4, 5], it is desirable to construct new coordinates, symmetry coordinates, which are linear combinations of equivalent internal coordinates, and which reduce the group. That is, the symmetry coordinates are chosen in such a way that each transforms according to one of the irreducible representations of the group. The advantage of the use of symmetry coordinates is, that there are no interaction elements in the kinetic- or potential-energy matrices between coordinates which transform according to different irreducible representations. The matrices therefore factor into submatrices (the number of identical submatrices for each representation is equal to the dimension, or degeneracy, of the representation), and the secular equation factors into the corresponding equations of lower degree [6, 7].

It will now be shown that the symmetry coordinates may be constructed either before or after applying the transformation of eq 7, provided that none of the symmetry coordinates involve linear combinations of coordinates of types q_1 and q_2. With this restriction the symmetry coordinates may be represented by

$$\begin{bmatrix} U_{11} & 0 \\ 0 & U_{22} \end{bmatrix} \begin{bmatrix} q_1 \\ q_2 \end{bmatrix}, \tag{25}$$

The matrices U_{11} and U_{22} are usually, although not necessarily, orthogonal. The transformed kinetic energy matrix is

[5] Wilson [4] has described a now well-known method for the calculation of G. A detailed exposition of the method has been given by Meister and Cleveland [5]. A method similar to Wilson's has been developed independently by the Russian workers M. Eliashevich, B. Stepanov, and M. Wolkenstein. References to the papers of these workers are not given here, as we are not directly concerned with the calculation of G.

$$\begin{bmatrix} \tilde{U}_{11}^{-1} & 0 \\ 0 & \tilde{U}_{22}^{-1} \end{bmatrix}\begin{bmatrix} S_{11} & S_{12} \\ \tilde{S}_{12} & S_{22} \end{bmatrix}\begin{bmatrix} U_{11}^{-1} & 0 \\ 0 & U_{22}^{-1} \end{bmatrix}$$

$$=\begin{bmatrix} \tilde{U}_{11}^{-1}S_{11}U_{11}^{-1} & \tilde{U}_{11}^{-1}S_{12}U_{22}^{-1} \\ \tilde{U}_{22}^{-1}\tilde{S}_{12}U_{11}^{-1} & \tilde{U}_{22}^{-1}S_{22}U_{22}^{-1} \end{bmatrix} \quad (26)$$

The reduced kinetic-energy matrix is then,

$$\begin{aligned}&\tilde{U}_{22}^{-1}S_{22}U_{22}^{-1}- \\ &\quad \tilde{U}_{22}^{-1}\tilde{S}_{12}U_{11}^{-1}(\tilde{U}_{11}^{-1}S_{11}U_{11}^{-1})^{-1}\tilde{U}_{11}^{-1}S_{12}U_{22}^{-1} \\ &\quad =\tilde{U}_{22}^{-1}S_{22}U_{22}^{-1}-\tilde{U}_{22}^{-1}\tilde{S}_{12}S_{11}^{-1}S_{12}U_{22}^{-1} \\ &\quad =\tilde{U}_{22}^{-1}(S_{22}-\tilde{S}_{12}S_{11}^{-1}S_{12})U_{22}^{-1}, \end{aligned} \quad (27)$$

which is identical with the result obtained by transforming the original matrix S'_{22} of eq 16 by U_{22}. It will also be observed that the matrix S'_{22} is unaffected by symmetry combinations formed with the coordinates q_1 (such, for example, as a rotation of axes).

When U_{22} is orthogonal the transformed kinetic-energy matrix is $U_{22}S'_{22}\tilde{U}_{22}$, but for nonorthogonal U_{22} the general form $\tilde{U}_{22}^{-1}S_{22}U_{22}^{-1}$ must be used. An illustration of the use of a nonorthogonal transformation will occur in the calculations at the end of this paper.

2. Calculation of the Kinetic-Energy Matrix

(a) Equations for Generalized Coordinates

Explicit formulas for the calculation of the elements of the kinetic-energy matrix for generalized internal coordinates are presented in this section. Denote by m_i the mass of the ith atom, and by $\mathbf{R}_i$ the position vector of the ith atom with respect to a point stationary in an inertial system. Then the kinetic energy of the system of particles is

$$2T=\sum_i m_i\dot{\mathbf{R}}_i\cdot\dot{\mathbf{R}}_i, \quad (28)$$

where $\dot{\mathbf{R}}_i$ is the vector velocity of the ith atom.

It will be assumed here, as in the preceding section, that the positions of the n particles are specified by $3n$ generalized coordinates q, some of which, as before, remain zero for a semirigid molecule.[6] We may then define a set of vectors,

$$\mathbf{s}_{mi}=(\partial\mathbf{R}_i/\partial q_m). \quad (29)$$

[6] In this section specific coordinates will be indicated by letter subscripts, as q_m and q_n.

Thus $\mathbf{s}_{mi}$ is a vector pointing in the direction in which the ith atom moves when q_m increases from zero (for the equilibrium configuration) to a small positive value, all other q's remaining zero, and the magnitude of $\mathbf{s}_{mi}$ is equal to the displacement of the ith atom per unit change in q_m. Then,

$$\dot{\mathbf{R}}_i=\sum_m \mathbf{s}_{mi}\dot{q}_m, \quad (30)$$

and

$$\begin{aligned}2T&=\sum_i m_i\Big(\sum_m \mathbf{s}_{mi}\dot{q}_m\Big)\cdot\Big(\sum_n \mathbf{s}_{ni}\dot{q}_n\Big) \\ &=\sum_{m,n}\dot{q}_m\dot{q}_n\Big(\sum_i m_i\mathbf{s}_{mi}\cdot\mathbf{s}_{ni}\Big) \end{aligned} \quad (31)$$

But from eq 1,

$$2T=\sum_{m,n}S_{mn}\dot{q}_m\dot{q}_n, \quad (32)$$

where S_{mn} is the element in the mth row and nth column of the symmetric kinetic-energy matrix S. It follows from eq 31 and 32 that

$$S_{mm}=\sum_i m_i\mathbf{s}_{mi}\cdot\mathbf{s}_{mi}, \quad (33)$$

$$S_{mn}=S_{nm}=\sum_i m_i\mathbf{s}_{mi}\cdot\mathbf{s}_{ni} \quad (34)$$

In order to proceed further, define an orthogonal system of x, y, z,-axes in the molecule, and denote the unit vectors, directed positively along the axes, by **x**, **y**, and **z**. Let the system be right-handed, so that $\mathbf{x}\times\mathbf{y}=\mathbf{z}$. The position of the origin of the system, and the directions of the unit vectors, must be uniquely determined with respect to the molecule for any arbitrary (small) displacements of the internal coordinates, but the choice of axes is otherwise arbitrary. In particular, it is not necessary that the origin be at the center of mass of the molecule.

The coordinates of the ith atom are x_i, y_i, and z_i. For a given choice of axes these coordinates are completely determined when the values of the internal coordinates are given. The position vector of the ith atom with respect to the origin is

$$\mathbf{r}_i=\mathbf{x}x_i+\mathbf{y}y_i+\mathbf{z}z_i. \quad (35)$$

Three of the generalized coordinates will be taken to be the translations of the origin of the axes in the (instantaneous) directions of the **x**-, **y**-, and **z**-vectors. The **r**-vectors of eq 29 are identical for each atom, for each translation, and are simply the unit vectors

$$\mathbf{s}_x=\mathbf{x},\ \mathbf{s}_y=\mathbf{y},\ \mathbf{s}_z=\mathbf{z}. \quad (36)$$

Three more coordinates will be taken to be the three rotations, by angles ϕ_x ϕ_y and ϕ_z about the x-, y-, and z-axes. The **S**-vectors for these are easily shown to be the vector products,

$$\mathbf{s}_{\phi x i}=\mathbf{x}\times\mathbf{r}_i,\ \mathbf{s}_{\phi y i}=\mathbf{y}\times\mathbf{r}_i,\ \mathbf{s}_{\phi z i}=\mathbf{z}\times\mathbf{r}_i. \quad (37)$$

For the remaining coordinates, the $(3n-6)$ internal coordinates,

$$\mathbf{s}_{mi}=(\partial\mathbf{r}_i/\partial q_m) \quad (38)$$

where,

$$(\partial\mathbf{r}_i/\partial q_m)=\mathbf{x}(\partial x_i/\partial q_m)+\mathbf{y}(\partial y_i/\partial q_m)+\mathbf{z}(\partial z_i/\partial q_m). \quad (39)$$

Explicit formulas for the elements of the kinetic-energy matrix may now be obtained from eq 33 and 34, combined with eq 36 to 39. The reductions of the scalar products of the **s**-vectors are made by the standard methods of vector analysis. The reduction process of eq 16 may then be applied explicitly to the translations. In this reduction, S_{11} in eq 4 and 16 represents the submatrix for translation, and is a 3×3 diagonal matrix, with each diagonal element equal to the total mass of the molecule, M. S_{22} represents the submatrix for rotations and internal coordinates, and S_{12} the submatrix for the interaction of these coordinates with translation. The elements of S_{12} are simply the x-, y-, and z-components of linear momentum of the rotations (about the x, y, z-axes) and internal coordinates.

The reduced matrix for the rotations and internal coordinates, corresponding to S'_{22} in eq 16, which is obtained in this way may be written,

	ϕ_x	ϕ_y	ϕ_z	q_m	q_n
ϕ_x	I_x	$-I_{xy}$	$-I_{xz}$ . . .	H_{xm} . . .	H_{xn} . . .
ϕ_y	$-I_{xy}$	I_y	$-I_{yz}$ . . .	H_{ym} . . .	H_{yn} . . .
ϕ_z	$-I_{xz}$	$-I_{yz}$	I_z . . .	H_{zm} . . .	H_{zn} . . .
.	.	.	.	.	.
.	.	.	.	.	.
.	.	.	.	.	.
q_m	H_{xm}	H_{ym}	H_{zm} . . .	K_{mm} . . .	K_{mn} . . .
.	.	.	.	.	.
.	.	.	.	.	.
.	.	.	.	.	.
q_n	H_{xn}	H_{yn}	H_{zn} . . .	K_{nm} . . .	K_{nn} . . .
.	.	.	.	.	.
.	.	.	.	.	.
.	.	.	.	.	.

(40)

The elements for rotation are the moments and products of inertia of the molecule about axes parallel to the x,y,z-axes, but passing through the center of mass of the molecule,

$$\left.\begin{aligned}
I_x&=\sum_i m_i(y_i^2+z_i^2)-M(y_M^2+z_M^2)\\
I_y&=\sum_i m_i(z_i^2+x_i^2)-M(z_M^2+x_M^2)\\
I_z&=\sum_i m_i(x_i^2+y_i^2)-M(x_M^2+y_M^2)\\
I_{xy}&=\sum_i m_i x_i y_i-Mx_My_M\\
I_{yz}&=\sum_i m_i y_i z_i-My_Mz_M\\
I_{zx}&=\sum_i m_i z_i x_i-Mz_Mx_M
\end{aligned}\right\} \quad (41)$$

The total mass of the molecule has been denoted by M, and the coordinates of the center of mass of the molecule, for the equilibrium configuration, by x_M, y_M, and z_M. The first term in each equation of 41 is the moment or product of inertia about the arbitrary origin; the second term arises from the reduction process of eq 16, and vanishes if the origin coincides with the (equilibrium) position of the center of mass.

The elements for the interaction of rotation and internal coordinates may be written

$$H_{xm}=\mathbf{x}\cdot\mathbf{H}_m,\ H_{ym}=\mathbf{y}\cdot\mathbf{H}_m,\ H_{zm}=\mathbf{z}\cdot\mathbf{H}_m, \quad (42)$$

where $\mathbf{H}_m$ is the vector

$$\mathbf{H}_m=\sum_i m_i\mathbf{r}_i\times(\partial\mathbf{r}_i/\partial q_m)-\mathbf{r}_M\times\sum_i m_i(\partial\mathbf{r}_i/\partial q_m) \quad (43)$$

The vector from the origin of the axes to the center of mass of the molecule has been represented by $\mathbf{r}_M$,

$$\mathbf{r}_M=M^{-1}\sum_i m_i\mathbf{r}_i=\mathbf{x}x_M+\mathbf{y}y_M+\mathbf{z}z_M. \quad (44)$$

If the origin of the x,y,z-axes coincides with the (equilibrium) position of the center of mass of the molecule, the vector $\mathbf{r}_M$, and the second term in eq 43, vanish. The second term arises from the reduction process of eq 16. The first term in eq 43 represents the vector angular momentum of the motion q_m about the origin, while $\mathbf{H}_m$ represents the vector angular momentum of q_m about the (equilibrium) center of mass. The quantities H_{xm}, H_{ym}, *and* H_{zm} are therefore the components of angular momentum of q_m about axes through the center of mass parallel to the x, y, z-axes.

For internal coordinates,

$$K_{mm}=\sum_i m_i(\partial\mathbf{r}_i/\partial q_m)^2-M^{-1}\Big[\sum_i m_i(\partial\mathbf{r}_i/\partial q_m)\Big]^2 \quad (45)$$

and for the interaction of two internal coordinates,

$$K_{mn}=K_{nm}\sum_i m_i(\partial\mathbf{r}_i/\partial q_m)\cdot(\partial\mathbf{r}_i/\partial q_n) - M^{-1}\Big[\sum_i m_i(\partial\mathbf{r}_i/\partial q_m)\Big]\cdot\Big[\sum_i m_i(\partial\mathbf{r}_i/\partial q_n)\Big] \quad (46)$$

The second term in eq 45 may also be written $M(\partial\mathbf{r}_M/\partial q_m)^2$, and therefore vanishes if the position of the center of mass of the molecule is independent of q_m. Similarly, the second term in eq 46 is $M(\partial\mathbf{r}_M/\partial q_m)\cdot(\partial\mathbf{r}_M/\partial q_n)$, and vanishes if the center of mass is independent of either q_m or q_n (or both). However, the vanishing of the (equilibrium) vector $\mathbf{r}_M$ is not, of itself, sufficient to cause these terms to vanish. The second terms in eq 45 and 46 represent the kinetic energy of translation of the center of mass of the molecule, and arise in the reduction process of eq 16. The first terms in these equations represent the kinetic energy of the internal coordinates computed with respect to the arbitrary origin. Subtraction of the second term from the first yields K_{mm} and K_{mn}, which represent the kinetic energy of the internal coordinates computed with respect to the instantaneous position of the center of mass.

The set of atoms associated with the internal coordinate q_m will be defined to include those atoms which move with respect to the x,y,z-axes when the coordinate q_m varies. This set is not to be regarded as fundamental, because the atoms included in it depend, in general, on the definition of the axes. The vector $(\partial\mathbf{r}_i/\partial q_m)$ vanishes by definition for all atoms not in the set associated with q_m. As a result, the summations in eq 43 and 45 need extend only over the set of atoms associated with q_m. In eq 46 the two summations in brackets extend over the sets of atoms associated with q_m and q_n, respectively, whereas the first summation in eq 46 extends only over those atoms included in both of these sets.

The final reduced kinetic-energy matrix is obtained from the matrix 40 by applying the reduction process of eq 16 to the rotations, and to any internal coordinates that do not appear in the potential-energy expression. The elements of the matrix of eq 40 are not independent, in general, of the choice of the x,y,z-axes, but the reduced matrix is independent of the axes after the overall rotations have been removed. The reduced matrix is most easily obtained numerically, by applying the reduction process of eq 10 to one row and column of the matrix at a time (so that in each step S_{11} in eq 16 is a matrix with a single element). This procedure makes it unnecessary to reciprocate directly the submatrix for the coordinates that are to be removed.

(b) Equations for semirigid molecules

The equations for the calculation of the kinetic-energy matrix for generalized internal coordinates have been given in the preceding section. These equations may now be applied to the two types of internal coordinates which will be found useful in specifying the configuration of a semirigid molecule. These are coordinates that represent either a translation or a rotation of their associated sets of atoms with respect to the x,y,z-axes. Internal translational and rotational coordinates will be represented by q_t and q_r, respectively, where q_t is the distance of translation, and q_r is the angle of rotation, both measured from the equilibrium configuration.

Let $\bar{\mu}$ be a unit vector in the direction of translation for the coordinate q_t, with components μ_x, μ_y, and μ_z, and let $\bar{\xi}$ be a unit vector directed along the axis of rotation for the coordinate q_r, with components ξ_x, ξ_y, and ξ_z. Let $\bar{\rho}_i$ be the position vector of the ith atom associated with q_r, with respect to an arbitrary point on the axis of rotation for q_r. In terms of these vectors eq 38 becomes,

$$(\partial\mathbf{r}_i/\partial q_t)=\bar{\mu}, \quad (47)$$

and

$$(\partial\mathbf{r}_i/\partial q_r)=\bar{\xi}\times\bar{\rho}_i, \quad (48)$$

for translational and rotational coordinates, respectively. Equations 47 and 48 may now be substituted in eq 42 to 46, to obtain the elements

of the kinetic-energy matrix, eq 40, in vector form. These vector expressions may then be reduced by the usual methods to more useful scalar expressions involving the masses, moments of mass, and moments of inertia of the associated sets of atoms. The details of these reductions will be omitted and only the final formulas stated.

Some additional definitions will be necessary. The total mass of the set of atoms associated with a coordinate q_m ($m=t$ or r) will be denoted by M_m, and the coordinates of the center of mass of the set of atoms by x_{Mm}, y_{Mm}, and z_{Mm}. The corresponding quantities for the entire molecule are M, and x_M, y_M, and z_M.

For each rotational coordinate, q_r, define a set of orthogonal right-handed ξ, η, ζ-axes, with the origin at a point x_{or}, y_{or}, z_{or}, on the axis of rotation, but otherwise aribtrary, and the ξ-axis coinciding with the axis of rotation. The direction cosines of the ξ, η, ζ-axes with respect to the x, y, z-axes, written in matrix form, are

$$\begin{bmatrix} \xi_x & \eta_x & \zeta_x \\ \xi_y & \eta_y & \zeta_y \\ \xi_z & \eta_z & \zeta_z \end{bmatrix} \tag{49}$$

The determinant of this matrix will be $+1$ if both the x, y, z-, and ξ, η, ζ-axes are right-handed.

The following moments and products of inertia of the set of atoms associated with q_r will be required,

$$\left.\begin{aligned} I_\xi &= \sum_i m_i(\eta_i^2+\zeta_i^2) \\ I_{\xi\eta} &= \sum_i m_i\xi_i\eta_i \\ I_{\zeta\xi} &= \sum_i m_i\zeta_i\xi_i \end{aligned}\right\} \tag{50}$$

I_ξ is the moment of inertia about the axis of rotation. The products of inertia, $I_{\xi\eta}$ and $I_{\zeta\xi}$, vanish if (1) the ξ-axis is a twofold, or higher, axis of symmetry for the associated set of atoms; (2) the η, ζ-plane is a plane of symmetry; or (3) if a threefold, or higher, axis of symmetry lies in the η, ζ-plane, and intersects the ξ-axis. $I_{\xi\eta}$ (but not necessarily $I_{\zeta\xi}$) vanishes if (1) the ζ,ξ-plane is a plane of symmetry or (2) the η-axis is a twofold axis of symmetry.

Let d_r be the perpendicular distance from the center of mass of the set of atoms associated with q_r to the axis of rotation, or ξ-axis, and let λ_x, λ_y, and λ_z be the direction cosines, with respect to the x,y,z-axes, if the line along which this center of mass moves when q_r increases from zero to a small positive value.
That is,

$$d_r=(\eta_M^2+\zeta_M^2), \tag{51}$$

and

$$\left.\begin{aligned} \lambda_x &= (\eta_{Mr}\zeta_x-\zeta_{Mr}\eta_x)/d_r \\ \lambda_y &= (\eta_{Mr}\zeta_y-\zeta_{Mr}\eta_y)/d_r \\ \lambda_z &= (\eta_{Mr}\zeta_z-\zeta_{Mr}\eta_z)/d_r \end{aligned}\right\} \tag{52}$$

where,

$$\eta_{Mr}=M_r^{-1}\sum_i m_i\eta_i,\ \zeta_{Mr}=M_r^{-1}\sum_i m_i\zeta_i. \tag{53}$$

The sums in eq 50 and 53 extend over the atoms associated with q_r. Atoms on the axis of rotation are not associated with q_r, according to the definition given in the preceding section. It may be more convenient to calculate these quantities as follows. Define α_x, α_y, and α_z to be equal to their respective cofactors in the determinant,

$$\begin{vmatrix} \alpha_x & \alpha_y & \alpha_z \\ \xi_x & \xi_y & \xi_z \\ (x_{Mr}-x_{or}) & (y_{Mr}-y_{or}) & (z_{Mr}-z_{or}) \end{vmatrix} \tag{54}$$

Then

$$d_r=(\alpha_x^2+\alpha_y^2+\alpha_z^2), \tag{55}$$

and

$$\lambda_x=(\alpha_x/d_r),\ \lambda_y=(\alpha_y/d_r),\ \lambda_z=(\alpha_z/d_r). \tag{56}$$

The equations for the elements of the kinetic-energy matrix, eq 40, may now be stated. For a translational coordinate, q_t, H_{xt}, H_{yt}, and H_{zt} are equal to their respective cofactors in the determinant

$$\begin{vmatrix} H_{xt} & H_{yt} & H_{zt} \\ M_t\mu_x & M_t\mu_y & M_t\mu_z \\ (x_{Mt}-x_M) & (y_{Mt}-y_M) & (z_{Mt}-z_M) \end{vmatrix} \tag{57}$$

If the translation arises from the stretching of a bond, μ_x, μ_y, and μ_z are the direction cosines of the bond.

For a rotational coordinate, q_r,

$$\left.\begin{aligned} H_{xr} &= H^{(1)}_{xr} + H^{(2)}_{xr} \\ H_{yr} &= H^{(1)}_{yr} + H^{(2)}_{yr} \\ H_{zr} &= H^{(1)}_{zr} + H^{(2)}_{zr} \end{aligned}\right\}, \tag{58}$$

where $H^{(1)}_{xr}$, $H^{(1)}_{yr}$, and $H^{(1)}_{zr}$ are defined by the equations

$$\left.\begin{aligned} H^{(1)}_{xr} &= \xi_x I_\xi - \eta_x I_{\xi\eta} - \zeta_x I_{\xi\zeta} \\ H^{(1)}_{yr} &= \xi_y I_\xi - \eta_y I_{\xi\eta} - \zeta_y I_{\xi\zeta} \\ H^{(1)}_{zr} &= \xi_z I_\xi - \eta_z I_{\xi\eta} - \zeta_z I_{\xi\zeta} \end{aligned}\right\}, \tag{59}$$

and $H^{(2)}_{xr}$, $H^{(2)}_{yr}$, and $H^{(2)}_{zr}$ are equal to their respective cofactors in the determinant

$$\begin{vmatrix} H^{(2)}_{xr} & H^{(2)}_{yr} & H^{(2)}_{zr} \\ M_r d_r \lambda_x & M_r d_r \lambda_y & M_r d_r \lambda_z \\ (x_{or} - x_M) & (y_{or} - y_M) & (z_{or} - z_M) \end{vmatrix}. \tag{60}$$

In many cases, $I_{\xi\eta} = I_{\xi\zeta} = 0$, and eq 59 reduces to

$$H^{(1)}_{xr} = \xi_x I_\xi,\ H^{(1)}_{yr} = \xi_y I_\xi,\ H^{(1)}_{zr} = \xi_z I_\xi. \tag{61}$$

Before stating the formulas for the remaining elements, K_{mm}, and K_{mn}, of eq 40, it will be necessary to differentiate between connected and unconnected coordinates. If the sets of atoms associated with two coordinates q_m and q_n contain no atoms in common, the two coordinates will be said to be *unconnected*—otherwise they are *connected*. Whether two coordinates are connected or unconnected will be dependent, in general, on the way in which the x,y,z-axes are defined. The only types of connected coordinates that will be considered are those for which the set of atoms for one coordinate, say q_n, is completely contained within the set of atoms for the other coordinate, q_m. A special case is that in which the sets of atoms for q_m and q_n are identical. If q_m and q_n are unconnected, this fact will be indicated explicitly by writing $K_{mn} (= K_{nm})$ as $K_{m,n} (= K_{n,m})$. If q_m and q_n are connected, and the set of atoms for q_n is completely contained within the set of atoms for q_m, then $K_{mn} (= K_{nm})$ will be written $K_{m(n)} (= K_{(n)m})$. If the set of atoms for q_m and q_n are identical, $K_{m(n)} = K_{(m)n}$. Subscripts t and r will again be used to indicate translational and rotational coordinates, and a second coordinate of a given type will be distinguished by the use of primes. The equations for the several possible forms of K_{mm} and K_{mn} may now be written as

$$K_{tt} = M_t(1 - M^{-1}M_t) \tag{62}$$

$$K_{t,t'} = -M^{-1}M_t M_{t'}(\mu_x\mu'_x + \mu_y\mu'_y + \mu_z\mu'_z) \tag{63}$$

$$K_{t(t')} = M_{t'}(1 - M^{-1}M_t)(\mu_x\mu'_x + \mu_y\mu'_y + \mu_z\mu'_z) \tag{64}$$

$$K_{t,r} = -M^{-1}M_t M_r \Delta_{tr} \tag{65}$$

$$K_{t(r)} = M_r(1 - M^{-1}M_t)\Delta_{tr} \tag{66}$$

$$K_{r(t)} = M_t\Delta_{r(t)} - M^{-1}M_t M_r \Delta_{tr} \tag{67}$$

$$K_{rr} = I_\xi - M^{-1}M_r^2 d_r^2 \tag{68}$$

$$K_{r,r'} = -M^{-1}M_r M'_r d_r d'_r(\lambda_x\lambda'_x + \lambda_y\lambda'_y + \lambda_z\lambda'_z) \tag{69}$$

$$\begin{aligned} K_{r(r')} = {} & (\xi_x H^{(1)\prime}_{xr} + \xi_y H^{(1)\prime}_{yr} + \xi_z H^{(1)\prime}_{zr}) + M'_r d'_r \Delta_{r(r')} \\ & - M^{-1}M_r M'_r d_r d'_r(\lambda_x\lambda'_x + \lambda_y\lambda'_y + \lambda_z\lambda'_z) \end{aligned} \tag{70}$$

The symbols Δ_{tr}, $\Delta_{r(t)}$, and $\Delta_{r(r')}$, represent the following determinants:

$$\begin{aligned} \Delta_{tr} &= d_r(\mu_x\lambda_x + \mu_y\lambda_y + \mu_z\lambda_z) \\ &= \begin{vmatrix} \mu_x & \mu_y & \mu_z \\ \xi_x & \xi_y & \xi_z \\ (x_{Mt} - x_{or}) & (y_{Mt} - y_{or}) & (z_{Mt} - z_{or}) \end{vmatrix}, \end{aligned} \tag{71}$$

$$\Delta_{r(t)} = \begin{vmatrix} \mu_x & \mu_y & \mu_z \\ \xi_x & \xi_y & \xi_z \\ (x_{Mt} - x_{or}) & (y_{Mt} - y_{or}) & (z_{Mt} - z_{or}) \end{vmatrix}, \tag{72}$$

$$\Delta_{r(r')} = \begin{vmatrix} \lambda'_x & \lambda'_y & \lambda'_z \\ \xi_x & \xi_y & \xi_z \\ (x'_{or} - x_{or}) & (y'_{or} - y_{or}) & (z'_{or} - z_{or}) \end{vmatrix} \tag{73}$$

In eq 70, $H^{(1)\prime}_{xr}$, $H^{(1)\prime}_{yr}$, and $H^{(1)\prime}_{zr}$, are the quantities calculated from eq 59 (with $r = r'$). When eq 61 applies, the first term in parentheses in eq 70 reduces to,

$$(\xi_x\xi'_x + \xi_y\xi'_y + \xi_z\xi'_z)I'_\xi. \tag{74}$$

If the center of mass of the set of atoms associated with a rotation, q_r, lies on the axis of rotation, so that $d_r = 0$, q_r will be called a *balanced*

rotation. For a balanced rotation, $H^{(2)}_{\xi\tau}=H^{(2)}_{\eta\tau}=H^{(2)}_{\tau\tau}=0$, in eq 58, and there are obvious simplifications in eq 65 to 70, as $\Delta_{t\tau}=0$ (in addition to $d_\tau=0$). A balanced rotation may be called accidentally balanced if the ξ-axis is not an axis of symmetry of the associated set of atoms. Such cases are very unlikely to occur. As a rule, the ξ-axis for a balanced rotation will be a twofold or higher axis of symmetry. In this case, $I_{\xi\eta}=I_{\zeta\xi}=0$, and eq 59 is replaced by eq 61. However, it is not necessary that a rotation be balanced for $I_{\xi\eta}$ and $I_{\zeta\xi}$ to vanish.

III. Application to Propane, Toluene, and Ethylbenzene

1. Kinetic-Energy Matrices

The application of this method to certain vibrations in ethylbenzene will be described in this section. In order to obtain the necessary force constants for ethylbenzene, it also has been necessary to set up the kinetic-energy matrices for propane and toluene. In the semirigid model of ethylbenzene for which the calculation has been carried out, it is assumed that the benzene ring and the attached hydrogens move as a rigid body, and also that the methylene and methyl groups move as rigid bodies. That is, the force constants for all deformations of the benzene ring and attached hydrogens and for deformation of the H—C—H angles in the methylene and methyl groups have been set equal to infinity. The force constants for the stretching of the two C—C bonds in the ethyl group have also been assumed infinite.[7] In order that the force constants obtained from the observed frequencies of propane and toluene should be on a comparable basis, corresponding assumptions have been made for these molecules. The coordinates remaining in the problem are therefore the rocking and twisting motions of these rigid groups.

The total number of internal coordinators in ethylbenzene is 48; of these, 8 are retained in the present calculation, and 2 are assumed to have zero frequency. In calculating the kinetic-energy matrix by the present method it is necessary to consider only these 10 internal coordinates, plus the 3 over-all rotations, and then to remove the 5 coordinates of zero frequency, as discussed in section II,1. In order to obtain the reciprocal kinetic-energy matrix for the 8 internal coordinates, it would be necessary to set the matrix up for the 46 internal coordinates of nonzero frequency, and then to remove 38 coordinates, as discussed in section II,1.

Before enumerating the coordinates, the symmetry properties of the molecules will be reviewed briefly. The propane molecule has the symmetry C_{2v}, with the nondegenerate representations A_1, A_2, B_1, and B_2. Representations A and B are symmetric and antisymmetric, respectively, to rotation by 180 degrees about the twofold axis. Representations with subscripts 1 and 2 are symmetric and antisymmetric, respectively, to reflection in the symmetry plane. The toluene and ethylbenzene molecules have the symmetry C_{1h}, with nondegenerate representations A' and A'', which are symmetric and antisymmetric, respectively, to reflection in a plane perpendicular to the plane of the benzene ring.[8]

The notation adopted for the internal coordinates is as follows. In-plane and out-of-plane (with respect to the symmetry plane) rocking motions are denoted by σ_i and π_i, respectively. Internal rotational motions are denoted by ϕ_i. The subscript i indicates the group, as follows: Propane, methyl (1 and 2), and methylene (3); ethylbenzene, methyl (1), ethyl (2), and methylene (3); and toluene, methyl (1), and methyl group (2).[9] On this basis methylene twisting is represented by ϕ_3. The C—C—C angle bending (in propane and ethylbenzene) is denoted by α. The coordinates represent in each case the angular deformation from the equilibrium configuration. In addition the over-all rotations about the x,y,z-axes will be denoted by ϕ_x, ϕ_y, and ϕ_z, respectively.

[7] As no bond stretchings are included in the present calculations, they will not illustrate the use of the formulas for translational internal coordinates given in section II, 2b.

[8] The equilibrium configuration assumed for the ethylbenzene molecule is that in which the plane of the benzene ring is perpendicular to the plane of the C—C—C angle in the ethyl group. The angle of rotation of the methyl groups in these molecules does not affect the quantities entering into the calculations.

[9] The axes for methyl and methylene rocking pass through the carbon atoms of the CH_3 and CH_2 groups, respectively, so that these are motions of the hydrogen atoms only. The axis for ethyl rocking passes through the phenyl carbon atom, so that the entire C_2H_5 group moves as a unit. The motion in toluene of the entire CH_3 group as a unit about an axis through the phenyl carbon atom has been called "methyl group" rocking to distinguish it from methyl rocking. Methyl rocking may conveniently be denoted by CH_3 rocking, and methyl group rocking by $-CH_3$ rocking.

In the case of propane it is necessary to construct the following symmetry coordinates:

$$\left.\begin{aligned}
\sigma^+ &= (1/\sqrt{2})(\sigma_1+\sigma_2)\\
\sigma^- &= (1/\sqrt{2})(\sigma_1-\sigma_2)\\
\pi^+ &= (1/\sqrt{2})(\pi_1+\pi_2)\\
\pi^- &= (1/\sqrt{2})(\pi_1-\pi_2)\\
\phi^+ &= (1/\sqrt{2})(\phi_1+\phi_2)\\
\phi^- &= (1/\sqrt{2})(\phi_1-\phi_2)
\end{aligned}\right\} \qquad (75)$$

These transformations are orthogonal, with the matrix,

$$(1/\sqrt{2})\begin{bmatrix} 1 & 1 \\ 1 & -1 \end{bmatrix}.$$

From eq 26 there are obtained the relations

$$\left.\begin{aligned}
(\sigma^+,\sigma^+) &= (1/2)[(\sigma_1,\sigma_1)+(\sigma_2,\sigma_2)]+(\sigma_1,\sigma_2)\\
(\sigma^-,\sigma^-) &= (1/2)[(\sigma_1,\sigma_1)+(\sigma_2,\sigma_2)]-(\sigma_1,\sigma_2)\\
(\sigma^+,\sigma^-) &= (1/2)[(\sigma_1,\sigma_1)-(\sigma_2,\sigma_2)]=0\\
(\sigma^+,q) &= (1/\sqrt{2})[(\sigma_1,q)+(\sigma_2,q)]\\
(\sigma^-,q) &= (1/\sqrt{2})[(\sigma_1,q)-(\sigma_2,q)]
\end{aligned}\right\}, \qquad (76)$$

where (σ^+,σ^+) is the diagonal element in the kinetic-energy matrix for σ^+, (σ^+,σ^-) is the element connecting σ^+ and σ^- (equal to (σ^-,σ^+)), etc. q represents any coordinate other than σ_1, σ_2, σ^+, or σ^-. Similar relations hold for the π and ϕ coordinates. The elements for the internal coordinates are first calculated from the equations given in section II, 2b, and the elements for the symmetry coordinates are then calculated from eq 76.

The notation used for the coordinates, their symmetries or representations, and their conventional descriptions are summarized in table 1. Interaction terms in the kinetic- and potential-energy matrices between coordinates belonging to different representations vanish identically.

TABLE 1.—*Notation and symmetry for coordinates*

Symmetry	Coordinate [a]	Description
PROPANE (C_{3v})		
A_1	σ^-	CH_3 rocking
	α	C−C−C bending
A_2	φ_z	Over-all rotation
	φ^+	CH_3 rotation
	φ_2	CH_3 twisting
	π^+	CH_3 rocking
B_1	φ_y	Over-all rotation
	σ^+	CH_3 rocking
	σ_2	CH_3 rocking
B_2	φ_x	Over-all rotation
	φ^-	CH_3 rotation
	π^-	CH_3 rocking
	π_2	CH_3 rocking
ETHYLBENZENE (C_{1h})		
A'	φ_z	Over-all rotation
	σ_1	CH_3 rocking
	σ_2	C_2H_5 rocking
	σ_3	CH_3 rocking
	α	C−C−C bending
A''	φ_x	Over-all rotation
	φ_y	Over-all rotation
	φ_1	CH_3 rotation
	φ_2	C_2H_5 rotation
	φ_3	CH_3 twisting
	π_1	CH_3 rocking
	π_2	C_2H_5 rocking
	π_3	CH_3 rocking
TOLUENE (C_{1h})		
A'	φ_z	Over-all rotation
	σ_1	CH_3 rocking
	σ_2	$-CH_3$ rocking [b]
A''	φ_x	Over-all rotation
	φ_y	Over-all rotation
	φ_1	CH_3 rotation
	π_1	CH_3 rocking
	π_2	$-CH_3$ rocking [b]

[a] The coordinates above the dashed line in each representation were removed from the kinetic-energy matrices (see text).

The dimensions used in the calculations are as follows. The benzene ring was assumed to be a plane hexagon, with the length of the C—C bonds 1.39 angstrom units. The other bond lengths, in angstrom units, were 1.54 for the C—C bonds in propane and in the alkyl groups (including the bond joining the alkyl group to the ring [8]), 1.09 for the C—H bonds in propane and the alkyl groups, and 1.08 for the C—H bonds on the benzene ring. Tetrahedral angles were assumed in propane and in the alkyl groups. In every case the numerical values of the elements of the kinetic-energy matrices (tables 2 and 3) have the units of mass in atomic-weight units multiplied by the square of a length in angstrom units.

TABLE 2.—*Kinetic-energy matrices for propane before removal of over-all and internal rotations*

		σ^-	α
A_1	σ^-	1.960	−2.04
	α	−2.04	11.63

		ϕ_x	ϕ^+	ϕ_z	π^+
A_2	ϕ_x	58.44	2.61	1.60	4.26
	ϕ^+	2.61	3.194	0	0
	ϕ_z	1.60	0	1.597	0
	π^+	4.26	0	0	1.996

		ϕ_y	σ^+	σ_z
B_1	ϕ_y	66.66	4.67	1.57
	σ^+	4.67	1.978	0.026
	σ_z	1.57	0.026	.761

		ϕ_x	ϕ^-	π^-	π_z
B_2	ϕ_x	17.80	3.69	−2.07	3.16
	ϕ^-	3.69	3.194	0	0
	π^-	−2.07	0	1.941	−0.045
	π_z	3.16	0	−0.045	2.358

TABLE 3.—*Kinetic-energy matrices for propane, toluene, and ethylbenzene*

Propane (C_3)

		σ^-	α
A_1	σ^-	1.96	−2.04
	α	−2.04	11.6

		ϕ_z	π^+
A_2	ϕ_z	1.55	−0.120
	π^+	−0.120	1.67

		σ^+	σ_z
B_1	σ^+	1.65	−0.084
	σ_z	−0.084	.724

		π^-	π_z
B_2	π^-	1.63	0.44
	π_z	0.44	1.62

Toluene (C_7)

		σ_1	σ_2
A'	σ_1	1.87	−1.90
	σ_2	−1.90	14.4

		π_1	π_2
A''	π_1	1.91	−2.37
	π_2	−2.37	20.6

Ethylbenzene (C_8)

		σ_1	σ_2	σ_3	α
A'	σ_1	1.93	−1.85	−0.023	−2.77
	σ_2	−1.85	29.8	−.57	19.9
	σ_3	−0.023	−0.57	.764	−0.157
	α	−2.77	19.9	−.157	27.2

		ϕ_1	π_1	π_2	π_3
A''	ϕ_1	1.57	−0.089	−0.42	0.067
	π_1	−.089	1.66	.51	.25
	π_2	−.42	.51	22.4	−3.14
	π_3	.067	.25	−3.14	2.04

As stated previously, the intermediate steps in the calculation are dependent upon the choice of x,y,z-axes, but the final kinetic-energy matrices (after removal of over-all rotation) are not. The calculations for propane are described in some detail in order to illustrate the method, and the choice of axes for propane will therefore be stated. The x- and z-axes were taken in the plane of the C−C−C angle, with the origin at the vertex of the angle, and the z-axis bisecting the angle. The z-axis therefore remains a twofold axis of symmetry as the C−C−C angle is deformed. The origin is not at the center of mass of the molecule.

The coordinate α in propane is most easily treated as follows. By definition the z-axis bisects the C−C−C angle. Denote the changes in these two half-angles by α_1 and α_2. The kinetic-energy matrix is first set up for α_1 and α_2, and then the following transformation is carried out:

$$\left.\begin{aligned}\alpha&=(\alpha_1+\alpha_2)\\0&=(\alpha_1-\alpha_2)\end{aligned}\right\}. \tag{77}$$

The second equation is merely the condition that the z-axis bisect the C−C−C angle when the latter is deformed. The elements in the kinetic-energy matrix for $(\alpha_1-\alpha_2)$ are then ignored. The nonorthogonal matrix of this transformation is

$$\begin{bmatrix}1 & 1\\1 & -1\end{bmatrix}.$$

Equation 26 leads to the relations

$$(\alpha,\alpha)=(1/4)[(\alpha_1,\alpha_1)+2(\alpha_1,\alpha_2)+(\alpha_2,\alpha_2)] \tag{78}$$

$$(\alpha,q)=(1/2)[(\alpha_1,q)+(\alpha_2,q)],$$

where q is any coordinate other than α_1, α_2, or α.

The following remarks apply to the calculation of the elements of the unreduced kinetic-energy matrix, eq 40, for propane. If the origin of the ξ, η, ζ-axes (the point $x_{\sigma r}$, $y_{\sigma r}$, $z_{\sigma r}$) is located at the carbon atom on the ξ-axis (or at any point on the ξ-axis for the balanced rotations ϕ_1, ϕ_2, and ϕ_3), then $I_{\xi\eta}$ and $I_{\xi\zeta}$, vanish in each case, and $H^{(1)}_{xr}$, $H^{(1)}_{yr}$, and $H^{(1)}_{zr}$ may be calculated from eq 61. $H^{(2)}_{xr}$, $H^{(2)}_{yr}$, and $H^{(2)}_{zr}$ vanish for the balanced rotations ϕ_1, ϕ_2, and ϕ_3. The diagonal terms K_{rr} are obtained from eq 68. For balanced rotations $K_{rr}=I_{\xi}$. Coordinates with different subscripts (1, 2, or 3) are unconnected, and $K_{rr'}$ is calculated from eq 69. $K_{rr'}$ vanishes if either rotation is balanced (ϕ-coordinates), or if the directions of motion of the centers of mass are perpendicular (thus π-coordinates are perpendicular to σ- and α-coordinates). Coordinates with the same subscripts are connected, and $K_{r(r')}$ is obtained from eq 70 (the first term being given by eq 74). From a consideration of the directions of the ξ-axes, and the directions of motion of the centers of mass, for each coordinate, it is readily seen that the only terms that do not vanish are $K_{\alpha i(\sigma i)}$ $(i=1,2)$.

The numerical values of the elements of the matrices of eq 40 (one matrix for each representation) are given for propane in table 2.

The next step is the removal of the over-all rotations by the reduction process of eq 16. In the subsequent calculations the frequencies of the ϕ_1 and ϕ_2 internal coordinates (methyl rotations in propane and toluene, and methyl and ethyl rotations in ethylbenzene) have been assumed to be zero. This is justifiable because the potential barriers for these rotations[10] correspond to sufficiently low frequencies for small oscillations from the equilibrium configuration. The coordinates ϕ_1 and ϕ_2 have, therefore, also been removed by the reduction process of eq 16.

The final reduced kinetic-energy matrices, one for each representation, for each molecule, are shown in table 3.

2. Calculation of Frequencies

The force constants are now to be evaluated from the observed frequencies of propane and toluene. These force constants may then be substituted in the secular equation for ethylbenzene to yield calculated frequencies for the latter molecule.

The frequency assignment for propane has been taken from Pitzer [9], and the assignment for toluene from Pitzer and Scott [10]. The frequencies (ν) are summarized in table 4. The

[10] Propane, reference [9]; toluene and ethylbenzene, reference [11].

normal coordinates are mixtures of the coordinates in each representation, and when this mixing is appreciable it is not possible to assign the frequencies in each representation to the coordinates without some ambiguity. However, the pairing indicated is fairly certain. Previous investigators have assigned the two B_2 frequencies as π^- (748) and π_3 (1179), but the assignment of these frequencies in table 4 is supported by (1) the force constants obtained for ϕ_3, σ_3, and π_3, which should have approximately the proportions 2,1, and 1, respectively (these figures assume that interaction constants are negligible, and that the main constants arise from the constants for the four *C—C—H* angles), and (2) the approximate equality of the force constants obtained for π^- and σ^-.

TABLE 4.—*Frequencies and calculated force constants for propane and toluene*

Coordinate	Description	Symmetry	ν	λ	k
	PROPANE				
			cm^{-1}		
σ^-	CH_3 rocking	A_1	1155	1.334	2.08
α	C-C-C bending	A_1	375	0.1406	1.68
ϕ_3	CH_2 twisting	A_2	1,278	1.633	2.50
π^+	CH_3 rocking	A_2	940	0.884	1.49
σ^+	CH_3 rocking	B_1	922	.850	1.41
σ_3	CH_2 rocking	B_1	1,338	1.790	1.28
π^-	CH_3 rocking	B_2	1,179	1.390	1.97
π_3	CH_2 rocking	B_2	748	0.560	0.96
	TOLUENE				
σ_1	CH_3 rocking	A'	1,190	1.416	2.28
σ_2	$-CH_3$ rocking [a]	A'	216	0.0467	0.68
π_1	CH_3 rocking	A''	1,090	1.124	1.80
π_2	$-CH_3$ rocking [a]	A''	340	0.1156	2.43

The next column of table 4 gives the value of λ (eq 22 to 24) in the units

$$\lambda=[\nu(\text{cm}^{-1})/1000]^2.$$

The last column shows the calculated values for the force constants, k, as calculated from the secular equations. They are the diagonal elements in the potential energy, or F, matrix (off-diagonal elements have been set equal to zero as there are not sufficient data to determine them). The units of these force constants correspond to the units that have been used for λ and for the kinetic-energy matrices in table 3; in the reverse calculation for ethylbenzene the frequencies are again obtained in cm^{-1}.

Table 5 shows the force constants selected for the ethylbenzene molecule. Those derived from toluene are σ_2 from σ_2, and π_2 from π_2. Those derived from propane are σ_1 from $(\sigma^++\sigma^-)/2$, π_1 from $(\pi^++\pi^-)/2$, and σ_3,π_3, ϕ_3 and α from σ_3, π_3, ϕ_3, and α, respectively. The averaged force constants, $(\sigma^++\sigma^-)/2$ and $(\pi^++\pi^-)/2$, are the main force constants for methyl rocking in propane. The observed separation of the frequencies for σ^+, σ^-, and for π^+, π^-, in propane, is due to methyl-methyl interaction constants and the twofold symmetry.

TABLE 5.—*Force constants and calculated frequencies for ethylbenzene*

Coordinate	Description	Symmetry	k	λ	ν
	ETHYLBENZENE				
					cm^{-1}
σ_1	CH_3 rocking	A'	1.75	1.067	1,035
σ_2	C_2H_5 rocking	A'	0.68	0.0187	137
σ_3	CH_2 rocking	A'	1.28	1.721	1,310
α	C—C—C bending	A'	1.68	0.1437	380
ϕ_3	CH_2 twisting	A''	2.50	1.615	1,270
π_1	CH_3 rocking	A''	1.73	1.144	1,070
π_2	C_2H_5 rocking	A''	2.43	0.1025	320
π_3	CH_2 rocking	A''	0.96	.604	775

Substitution of these force constants in the secular equations for ethylbenzene then yields the values of λ, and the calculated frequencies, shown in the last two columns of table 5. The observed frequencies for ethylbenzene are discussed in the next section.

IV. Vibrational Frequencies of Ethylbenzene

The present calculations were undertaken as an aid to the assignment of the vibrational frequencies of ethylbenzene.* These frequencies were required for the calculation of the thermodynamic functions by statistical methods [11]. The frequencies have been assigned on a semiempirical basis which involved a detailed consideration of only the

*F. G. Brickwedde, M. Moskow, and R. B. Scott [24] have also presented an assignment of the vibrational frequencies of ethylbenzene.

lowest frequencies of vibration of the benzene ring and also of the frequencies associated with the vibration of the ethyl group. The remaining frequencies were taken from the assignment for toluene [10]. A complete frequency assignment for ethylbenzene at this time is impracticable.

Several workers have reported Raman spectra [13, 14, 15, 16, 17, 18] and infrared spectra [19, 20, 21, 22, 23] for ethylbenzene. The lowest observed frequencies in the Raman spectrum of ethylbenzene, are, approximately, 154, 305 (weak) 399 (weak), 452, 485, 538 (weak), 553 (weak), and 620 cm^{-1}. The frequencies 480, 567, and 617 cm^{-1} have been reported in the infrared spectrum in this region. It will be helpful to list the six lowest frequencies of toluene, as assigned by Pitzer and Scott [10]: 11, 216 (R); 18b, 340 (R); 16a, 405 (R); 16b, 467 (R); 6a, 521 (R); and 6b, 622 (R, IR). The first number designates the mode of vibration (see fig. 6, of Pitzer and Scott), the second is the frequency in cm^{-1}, and R and IR refer to the presence of the line in the Raman or the infrared spectrum, respectively.

The vibrations 11 and 18b correspond principally to the rocking of the alkyl group perpendicular to and parallel to the plane of the benzene ring, respectively. The frequencies of these modes in ethylbenzene were calculated as 137 cm^{-1} for 11 and 320 cm^{-1} for 18b by means of the approximate normal coordinate analysis of section III (these vibrations were denoted by σ_2 and π_2, respectively, in that section). The only possibility for the assignment of the 154 cm^{-1} frequency is therefore mode 11. The mode 18b was assigned the calculated frequency of 320 cm^{-1}. The frequency observed at 305 cm^{-1} may easily be the overtone of 154 cm^{-1}.

The mode 16a has a frequency of 400 cm^{-1} in benzene and 405 cm^{-1} in toluene. The observed frequency at 399 cm^{-1} in ethylbenzene may represent 16a, or an overlap of 16a with the carbon skeletal bending in the ethyl group, which should fall at about 380 cm^{-1}. The toluene value, 405 cm^{-1},was retained for ethylbenzene. The mode 16b has the frequency 467 cm^{-1} in toluene; the nearest observed frequency in the spectrum of ethylbenzene, 452 cm^{-1}, was assigned to this mode. The mode 6a in toluene gives rise to a relatively intense line at 521 cm^{-1}. The variation of the frequency of the mode 6a in other monosubstituted benzenes, as a function of the mass of the attached group [12], indicates that 6a should be lowered somewhat in ethylbenzene, since the effective mass of the ethyl group in this mode is considerably greater than that of a methyl group. Therefore, the frequency 485 cm^{-1}, which is the strongest observed line in this region, was assigned to 6a. The mode 6b has a frequency of 606 cm^{-1} in benzene, 622 cm^{-1} in toluene, and remains essentially unchanged in frequency in other monosubstituted benzene [12]. The frequency observed in ethylbenzene at 620 cm^{-1} was therefore assigned to 6b.

The mode 7a, which is principally the stretching of the C—C bond joining the alkyl group to the ring, has a frequency of 1,210 cm^{-1} in toluene. As a strong line appears at about 1,200 cm^{-1} in the ethylbenzene Raman spectrum, the toluene frequency was retained for 7a. The other C—C stretching mode in the ethyl group was assigned the frequency of the strong line at 965 cm^{-1} in the Raman spectrum of ethylbenzene as this is close to the average of the two carbon-carbon stretching frequencies of 868 and 1,053 cm^{-1} in propane [9]. The symmetry that splits these two components in propane is absent in ethylbenzene.

The symmetrical hydrogen bending in the methyl group was assigned the frequency 1,385 cm^{-1}, and the doubly degenerate unsymmetrical bending the frequency 1,460 cm^{-1}. The symmetrical hydrogen bending in the methylene group was assigned the value 1,460 cm^{-1}. The value 2,960 cm^{-1} was assigned the C—H stretchings in the methyl and methylene groups. These assignments were made on the basis of the frequencies of these modes in propane and toluene, and to some extent on the basis of the spectrum of ethylbenzene.

The remaining frequencies of vibration of the ethyl group were assigned values calculated by means of the approximate normal coordinate analysis of section III (see tables 1 and 5).

The complete frequency assignment for ethylbenzene is shown in table 6.

724217—47——2

TABLE 6.—*Vibration frequencies of the ethylbenzene molecule*

Type of Vibration	Symmetry	Frequency
Vibrations principally characteristic of the benzene ring or phenyl radical		
		cm^{-1}
11 (C_6H_5 rocking)	A'	154
18b (C_6H_5 rocking)	A''	320
16a	A''	405
16b	A'	452
6a	A'	485
6b	A''	620
4	A'	695
10b	A'	730
12	A'	785
10a	A''	842
17b	A'	890
5	A'	943
17a	A''	985
1	A'	1,002
18a	A'	1,030
15	A''	1,070
9b	A''	1,155
9a	A'	1,175
7a (C_6H_5-C_2H_5 stretching)	A'	1,210
3	A''	1,282
19b	A''	1,310
19a	A'	1,483
8b	A''	1,586
8a	A'	1,603
14	A''	1,630
13	A'	3,046
7b	A''	3,047
2 C-H stretching	A'	3,062
20a	A'	3,080
20b	A''	3,080
Vibrations principally characteristic of the ethyl group		
C_6H_5-CH_2-CH_3 angle bending	A'	380
CH_2 rocking	A''	775
CH_2-CH_3 stretching	A'	965
CH_3 rocking	A'	1,035
CH_2 rocking	A''	1,070
CH_2 twisting	A''	1,270
CH_2 rocking	A'	1,310
CH_3 symmetrical bending	A'	1,385
CH_2 symmetrical bending	A'	1,460
CH_3 unsymmetrical bending	A'	1,460
	A''	1,460
CH_2 symmetrical stretching	A'	2,960
CH_2 unsymmetrical stretching	A''	2,960
CH_3 symmetrical stretching	A'	2,960
CH_3 unsymmetrical stretching	A'	2,960
	A''	2,960

References

[1] L. S. Majantz, Compt. rend. URSS **32,** 119 (1941).
[2] A. Sayvetz, J. Chem. Phys. **7,** 383 (1939).
[3] B. L. Crawford, Jr., and E. B. Wilson, Jr., J. Chem. Phys. **9,** 323 (1941).
[4] E. B. Wilson, Jr., J. Chem. Phys. **7,** 1047 (1939); **9,** 76 (1941).
[5] A. G. Meister and F. F. Cleveland, Am. J. Phys. **14,** 13 (1946).
[6] J. E. Rosenthal and G. M. Murphy, Rev. Modern Phys. **8,** 317 (1936).
[7] S. Silver, J. Chem. Phys. **8,** 919 (1940).
[8] L. Pauling and L. O. Brockway, J. Am. Chem. Soc. **59,** 1223 (1937).
[9] K. S. Pitzer, J. Chem. Phys. **12,** 310 (1944).
[10] K. S. Pitzer and D. W. Scott, J. Am. Chem. Soc. **65,** 803 (1943).
[11] W. J. Taylor, D. D. Wagman, Mary G. Williams, K. S. Pitzer, and F. D. Rossini, J. Research NBS **37,** 95 (1946) RP1732.
[12] K. W. F. Kohlrausch, Der Smekal-Raman-Effekt, p. 163 (J. Springer, Berlin, 1938).
[13] A. Dadieu and K. W. F. Kohlrausch, Monatsh. **53-54,** 282 (1929).
[14] J. Soderqvist, Z. Physik **59,** 446 (1930).
[15] A. S. Ganesan and S. Venkateswaran, Indian J. Phys. **13,** 195 (1929).
[16] R. Signer and J. Weiler, Helv. Chim. Acta. **15,** 649 (1932).
[17] A. W. Reitz and W. Stockmair, Monatsh. **67,** 92 (1935).
[18] G. Dupont, R. Dulou, and V. Desreux, Bul. soc. chim. **3,** 1639 (1936).
[19] P. Lambert and J. Lecomte, Ann. phys. **18,** 329 (1932).
[20] R. Stair and W. W. Coblentz, J. Research NBS **15,** 295 (1935) RP830.
[21] P. Lambert and J. Lecomte, Ann. Phys. **10,** 503 (1938).
[22] American Petroleum Institute Research Project 44 at the National Bureau of Standards. Catalog of infrared absorption spectrograms. Ethylbenzene: Serial No. 53, contributed by the Phillips Petroleum Co. and University of Oklahoma Research Institute; Serial Nos. 123 and 194, contributed by the Texas Co.; Serial No. 135, contributed by the Mellon Institute of Industrial Research and Carnegie Institute of Technology; Serial No. 309, contributed by the U. S. Naval Research Laboratory.
[23] Shell Development Co., Emeryville, Calif., Unpublished data, made available by Otto Beeck.
[24] F. G. Brickwedde, M. Moskow, and R. B. Scott, J. Chem. Phys. **13,** 547 (1945).

Appendix 1 [11]

Let the coordinates q_i be divided into two groups, q_a and q_b, and partition S_{ij} into the corresponding submatrices. Then the kinetic energy matrix, eq 4, becomes

$$\begin{bmatrix} S_{aa} & S_{ab} & S_{a2} \\ \tilde{S}_{ab} & S_{bb} & S_{b2} \\ \tilde{S}_{a2} & \tilde{S}_{b2} & S_{22} \end{bmatrix}. \tag{79}$$

The removal of the cross terms in the kinetic energy that contain $\dot{q}_a$ leads to the reduced matrix

$$\begin{bmatrix} (S_{bb}-\tilde{S}_{ab}S_{aa}^{-1}S_{ab}) & (S_{b2}-\tilde{S}_{ab}S_{aa}^{-1}S_{a2}) \\ (\tilde{S}_{b2}-\tilde{S}_{a2}S_{aa}^{-1}S_{ab}) & (S_{22}-\tilde{S}_{a2}S_{aa}^{-1}S_{a2}) \end{bmatrix}, \tag{80}$$

and the removal of the remaining cross terms that contain $\dot{q}_b$ leads to the final reduced matrix for the coordinates q_b

[11] See section II, 1 (following eq. 16).

$$S'_{22}=(S_{22}-\tilde{S}_{a2}S_{aa}^{-1}S_{a2})-(\tilde{S}_{b2}-\tilde{S}_{a2}S_{aa}^{-1}S_{ab})(S_{bb}-\tilde{S}_{ab}S_{aa}^{-1}S_{ab})^{-1}(S_{b2}-\tilde{S}_{ab}S_{aa}^{-1}S_{a2}). \tag{81}$$

Equation 81 may be rewritten in the form

$$S'_{22}=S_{22}-[\tilde{S}_{a2}\tilde{S}_{b2}]\begin{bmatrix}(S_{aa}^{-1}+S_{aa}^{-1}S_{ab}G'_{bb}\tilde{S}_{ab}S_{aa}^{-1}) & -G'_{bb}\tilde{S}_{ab}S_{aa}^{-1}\\ -S_{aa}^{-1}S_{ab}G'_{bb} & G'_{bb}\end{bmatrix}\begin{bmatrix}S_{a2}\\S_{b2}\end{bmatrix}, \tag{82}$$

where

$$G'_{bb}=(S_{bb}-\tilde{S}_{ab}S_{aa}^{-1}S_{ab})^{-1}. \tag{83}$$

On the other hand, the simultaneous removal of the cross terms that involve $\dot{q}_a$ and $\dot{q}_b$ leads to the reduced matrix

$$S'_{22}=S_{22}-[\tilde{S}_{a2}\ \tilde{S}_{b2}]\begin{bmatrix}S_{aa} & S_{ab}\\ \tilde{S}_{ab} & S_{bb}\end{bmatrix}^{-1}\begin{bmatrix}S_{a2}\\S_{b2}\end{bmatrix} \tag{84}$$

The matrices S'_{22} calculated from eq 82 and 84 are identical, provided that

$$\begin{bmatrix}(S_{aa}^{-1}+S_{aa}^{-1}S_{ab}G'_{bb}\tilde{S}_{ab}S_{aa}^{-1}) & -S_{aa}^{-1}S_{ab}G'_{bb}\\ -G'_{bb}\tilde{S}_{ab}S_{aa}^{-1} & G'_{bb}\end{bmatrix}\cdot\begin{bmatrix}S_{aa} & S_{ab}\\ \tilde{S}_{ab} & S_{bb}\end{bmatrix}=\begin{bmatrix}E_{aa} & 0\\ 0 & E_{bb}\end{bmatrix} \tag{85}$$

where E_{aa} and E_{bb} are unit matrices. But the last relation is easily verified by multiplying out the matrices on the left. This establishes the theorem when q_i is divided into two groups; the truth of the theorem for any number of groups follows by induction.

Appendix 2 [12]

From the relation that $SG=E$, where E is the unit matrix, and eq 3, there are obtained the relations

$$\tilde{S}_{12}G_{12}+S_{22}G_{22}+S_{23}\tilde{G}_{23}=E \tag{86}$$

$$S_{11}G_{12}+S_{12}G_{22}+S_{13}\tilde{G}_{23}=0 \tag{87}$$

$$S_{12}G_{13}+S_{22}G_{23}+S_{23}G_{33}=0 \tag{88}$$

$$S_{11}G_{13}+S_{12}G_{23}+S_{13}G_{33}=0 \tag{89}$$

Now multiply eq 89 from the left by $\tilde{S}_{12}S_{11}^{-1}$, and from the right by $G_{33}^{-1}\tilde{G}_{23}$, and add the resulting equation to eq 86; next multiply eq 87 from the left by $\tilde{S}_{12}S_{11}^{-1}$ and eq 88 from the right by $G_{33}^{-1}\tilde{G}_{23}$, and subtract both of the resulting equations from the previous sum. The resulting equation may be factored as follows:

$$(S_{22}-\tilde{S}_{12}S_{11}^{-1}S_{12})(G_{22}-G_{23}G_{33}^{-1}\tilde{G}_{23})=E_{22}. \tag{90}$$

Equation 21 follows immediately from eq 16, 20, and 90.

WASHINGTON, September 24, 1946.

[12] See section II, 1 (eq 20 and 21).

U. S. Department of Commerce
National Bureau of Standards

Research Paper RP1759
Volume 38, January 1947

Part of the Journal of Research of the National Bureau of Standards

Analysis of a Standard Sample of Natural Gas by Laboratories Cooperating with the American Society for Testing Materials

By Martin Shepherd [1,2]

This is a report of the analysis of a standard sample of natural gas by 30 laboratories cooperating with Subcommittee VII of Committee D–3 of the American Society for Testing Materials. The data are presented in a series of frequency distribution plots that show at a glance how the analyses from all laboratories compare with respect to each component determined, as well as calculated heating value and specific gravity. The heating value and specific gravity determined by analysis are compared with values carefully measured at the National Bureau of Standards. The analyses were performed volumetrically by the absorption and combustion methods, and the plots form a clear picture of this type of gas analysis in this country. Although some very creditable work is reported, the need for standardization is evident.

I. Introduction

Subcommittee VII of Committee D–3 of the American Society for Testing Materials has been assigned the task of standardizing the analysis of gaseous fuels. This is the second of a series of reports concerned with work preliminary to actual standardization. In the first of these reports[2] it was stated that the subcommittee was approaching their assigned task with certain reservations derived from an acquaintance with gas analysis methods, gas analysis apparatus, and gas analysts. The reason for such reservations usually becomes apparent when a gas analyst is asked to substitute a new reagent, pipette, procedure, method—or a whole new apparatus or system of analysis—for one that he has been using satisfactorily. Such a request is unamiable and might very often be unreasonable. Indeed, if it can be demonstrated by actual measurement that an apparatus or method now in use will give satisfactory results, there is no real justification for insisting that it be discarded in favor of another that may be sponsored as the official instrument of some group.

As it seems reasonable and fair to approve any apparatus and method capable of giving satisfactory analytical results, it remains only to decide what are satisfactory analytical results and which methods and apparatus will yield these results. To reach these decisions, two steps are being taken.

First, the various purposes to be served by the analytical data are listed, and the necessary accuracy with which each component of each type of fuel gas must be known in order to serve each specific purpose is then estimated. These estimates afford the first criterion by means of which the suitability of analytical methods and apparatus may be judged, but they are subject to revision when more is known about the limiting attainable

[1] Chairman of Subcommittee VII (Analysis of Gaseous Fuels) of Committee D-3 (Gaseous Fuels), American Society for Testing Materials.

[2] Martin Shepherd, Analysis of a standard sample of the carburetted water-gas type by laboratories cooperating with the American Society for Testing Materials, J. Research NBS **36**, 313 (1946) RP1704.

accuracies of the analytical methods and also when the significance of the term "necessary" in the phrase "necessary accuracy" has been evaluated with more realism than enthusiasm.

Second, the accuracy and reproducibility of existing apparatus and methods are being measured by the direct procedure of conducting a series of cooperative analyses of standard gas samples of various types. (Although these samples are being prepared at the National Bureau of Standards, they are not to be confused with the Bureau's series of Standard Samples available for purchase. These gas samples are being prepared for free distribution to laboratories cooperating with ASTM D–3 in this project).

The cooperative analytical results obtained so far represent the first clear picture of the actual state of gas analysis in this country.

II. Cooperating Laboratories

These analyses are being conducted on a considerable scale. Cooperating laboratories include those of State and Federal agencies and of colleges, but the greatest contribution has come from the laboratories of the gas, petroleum, steel, and chemical industries. The laboratories are located throughout the United States. They are equipped with many types of apparatus, almost entirely modern, and employ different analytical methods. The type of apparatus used in the analysis of this sample is noted with the presentation of the analytical data. Of the 30 laboratories which analyzed the natural-gas sample, all but one (a college) employed chemists specifically trained in gas analysis. Taken as a whole, the work represents the best present-day American practice.

III. Preparation of Standard Gas Sample ASTM D–3–VII–2

Standard sample ASTM D–3–VII–2, natural gas type, was prepared to conform with the range of composition accepted for this test sample by Subcommittee VII:

	Percent by volume
CO_2	0 to 15
O_2	0 to 2
N_2	0 to 50
CH_4	32 to 99
C_2H_6+	0 to 50
C_3H_8	0 to 3
Heating value	1,080 to 1,140 Btu/ft [3]
Specific gravity	0.630 to 0.750

The sample was made up from the following compressed gases obtained from commercial sources:

	Approximate purity	Chief impurity
	Percent	
CO_2	99.98	Air
N_2	99.9	O_2
CH_4	98	N_2 and C_2H_6+
C_2H_6	98	C_2H_4 and C_3H_8
C_3H_8	98	C_4H_{10}

As this sample was not prepared from gases of known high purity, its actual composition with respect to all components is not known. It was definitely established that no significant amount of oxygen (i. e., less than 0.02 percent by volume) occurred in the sample. In addition, its heating value and specific gravity were carefully measured. The sample, therefore, has four definite purposes, as it serves to measure (1) reproducibility,[3] (2) accuracy of the computed specific gravity, (3) relation between the measured and the computed heating value, (4) ability to determine correctly absence of oxygen in gas mixtures of this type. It will not serve as a final criterion of accuracy (see footnote 3), since its exact composition is not known.[4]

The sample was prepared under a pressure of 300 lb/in.[2] in the large storage and mixing tank used to prepare the mixtures for the Bureau's study of specific gravity instruments.[5] After very thorough mechanical mixing, the uniformity of the

[3] Lest there be any confusion as to the meaning of the terms accuracy and reproducibility, it should be stated that the conventional concepts are here implied. Accuracy is measured in terms of agreement with a true value; reproducibility is measured in terms of the mutual agreement of a series of measurements of the same property of a substance. As a matter of convenience, reproducibility has long served the gas analyst in lieu of a definite measurement of accuracy. Eventually this situation will be corrected.

[4] Such terms as "known mixture" or "synthetic sample" are rather too lightly used in the literature. Unless the composition of a mixture is known to one order of magnitude better than may be expected from an analytical method, analysis of the mixture cannot be considered a measurement of the accuracy of the analytical method. If a mixture is "known," the purity (exact composition) of each component must have been measured to a greater significance than the method used for its analysis will yield, and the portioning of each component to form the mixture must have been done in such a way that the relative amounts of all present are known again to a greater significance than they can be resolved by analysis. To make such a mixture usually seems too difficult, and the "synthetic sample" usually invoked may not be truly definitive.

[5] F. A. Smith, J. H. Eiseman, and E. C. Cretiz, Tests of instruments for the determination, indication, or recording of the specific gravities of gases, NBS Miscellaneous Publication M177. (1947.)

whole sample was definitely established by sampling from various parts of the tank and intercomparing these portions by means of a 1–m Zeiss gas interferometer to detect any difference in composition. This interferometer is sensitive to changes of 0.01 percent or less of carbon dioxide and methane which were part of the standard sample. The sample was then transferred to small sample cylinders as follows:

1. The sample cylinders, equipped with needle valves having vacuum-tight packing, were connected to a single welded manifold by means of high-pressure unions. The large mixing tank and a vacuum pump were connected to this same manifold. The manifold and opened sampling cylinders were evacuated to 0.0001 mm Hg pressure overnight. Thereafter, with vacuum pump disconnected, the increase of pressure within this system was less than 0.0005 mm during the first hour. Only a few minutes were required to transfer the gas sample from the mixing tank to the sample cylinders. No significant contamination from leakage was possible under these conditions.

2. The small cylinders were flushed with the sample from the mixing tank by alternate filling to 2 atmospheres and evacuating to 1 mm Hg. After the third flushing, the sample cylinders were filled to 300 lb/in^2. With full pressure on the manifold, the sample cylinders were then closed. The manifold was then opened to a water seal, and no leakage from the cylinders was observed overnight.

3. All of the sample cylinders issued for the cooperative analysis of this sample were thus filled simultaneously from the manifold connected to the single uniform source of supply. The samples were, therefore, identical at the date of issue.

To avoid contamination while transferring the sample to the burette, the following illustrated instructions for a definite procedure were furnished the laboratories.

INSTRUCTIONS REGARDING SAMPLER AND SAMPLING

1. The cylinder containing the sample is shipped in a metal case made from standard pipe fittings. Save this for return of the cylinder, which must be returned immediately upon completion of your analyses.

2. The cylinder is equipped with a very special vacuum-type needle valve. DO NOT close this valve with anything but the thumb and one finger. DO NOT force the valve shut. If too much twist is applied to the valve handle, the seat will be ruined.

3. Remove the dust cap from the valve and attach the sampling fitting, which terminates in a thin brass tapered sleeve. This sleeve fits a standard glass interchangeable joint, male part, size $\overline{\S}$ 10/30. This glass joint should be sealed to the brass sleeve by a thermoplastic cement of the DeKhotinsky type, or other cement capable of making a gas-tight joint. We find the arrangement sketched below desirable.

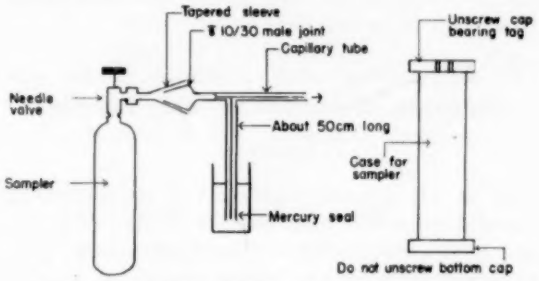

FIGURE 1.—*Flow diagram for sampling assembly.*

With cock of burette closed, gently open needle valve until gas bubbles out through mercury seal. When this line is flushed, take gas into burette and discard until horizontal portion of sampling line is flushed. About 50 ml in all is adequate for flushing capillary lines. Leave connected to burette for next sample to be taken. Use mercury seal as manometer to avoid sampling under reduced pressure. If direct glass seal or interchangeable joint is not used in connecting to burette, flush sampling line each time with about 20 ml of gas. For convenience and safety, we prefer interchangeable joints secured with DeKhotinsky or a heavy lubricant.

In no case did any analyst who made any of these determinations have any other knowledge of the properties of this sample, nor was any information other than that given above imparted to anyone until all of the laboratories represented in this account had reported. During 1941, the specific gravity was measured by E. C. Creitz and the heating values by J. H. Eiseman, both of the National Bureau of Standards. These values were turned over to the author, who, as chairman of Subcommittee VII, did not engage in the analyses conducted at this Bureau, nor did he consult these values until the Bureau's analyses, performed by Shuford Schuhmann, had been reported to him.

In July 1944, R. S. Jessup, of this Bureau, redetermined the heating value. Also, during 1944, there were three determinations of composition made with the Bureau's mass spectrometer (manufactured by the Consolidated Engineering

Co.) under the charge of A. Keith Brewer. As the cooperative analyses had not then been reported, the first two measurements by the mass spectrometer could not have been made with a knowledge of the previously obtained results. The third analysis was made by Vernon H. Dibeler after all the other results from all sources had been reviewed by him, and proper corrections had been made for hydrogen. (See discussion in section V, 12.)

IV. Apparatus and Methods Used for Analysis of Standard Gas Sample

1. Apparatus

It has been stated that most of the analytical apparatus used in this cooperative investigation was of the modern type. The apparatus may be classified with respect to the system of volume measurement, the arrangement of pipettes or reaction tubes, and the confining fluid. For convenience, a set of abbreviations may be used.

V_1—Volumes are made comparable by means of a pressure-temperature compensator with manometer interposed between the compensating tube and the burette.

V_2—Pressure within the burette is balanced against existing barometric pressure, and gas volumes are corrected from the observed pressure and temperature to a common basis, including a correction for changes in the saturation pressure of water.

V_3—Pressure in burette is balanced against atmospheric pressure but no correction is made for changes in pressure or temperature during analysis.

V_4—Volumes are measured by observing the pressure exerted within a constant volume.

R_1—Pipettes are connected to the burette by a manifold.

R_2—A single pipette, connected to the burette, serves for all reactions.

R_3—Pipettes are temporarily connected in succession to the burette as the different reactions are progressively conducted.

R_4—The burette itself serves as a reaction tube.

Hg—Mercury is used as the confining fluid.

H_2O (with appropriate subscript)—An aqueous solution serves as the confining fluid.

Thus the abbreviation V_1R_1Hg designates an apparatus equipped with pressure-temperature compensator and manometer, manifold connecting pipettes to burette, with mercury serving as the confining fluid; 23 of the 30 laboratories used this type of apparatus. Three laboratories used a V_2R_1Hg type of apparatus, two used a $V_2R_1H_2O$ type, another a Hemple apparatus (V_2R_2Hg), another a $V_3R_2H_2O$ type, and finally one used a Bone and Wheeler apparatus, widely employed in Great Britain (V_4R_2Hg).

2. Methods of Analysis

In general, the method of analysis used involved the conventional four steps, as follows:

Method A:

1. Absorption of carbon dioxide in an aqueous solution of potassium hydroxide.
2. Absorption of oxygen in alkaline pyrogallol or in a chromous solution.
3. A single combustion over hot paltinum in the presence of excess oxygen, measurement of the contraction and carbon dioxide produced, and computation of all hydrocarbons present as CH_4 and C_2H_6, using the conventional formulas:

$$CH_4 = 1/3\ (4TC - 5CO_2)$$

$$C_2H_6 = 1/3\ (4CO_2 - 2TC),$$

where TC is the total contraction on burning, and CO_2 is the carbon dioxide produced by the combustion.

4. Nitrogen by difference.

Although 23 of the laboratories used this method, there were a few notable exceptions. Four of the laboratories employed the following method:

Method B:

1 and 2 as in method *A*.

(One of the four laboratories then took fresh portions of the sample for combustion, correcting the combustion data for the CO_2 and O_2 originally found. The other three used the general procedure of combustion of a portion of the sample taken for absorption.)

3. A single combustion over hot platinum in the presence of excess oxygen, measurement of the contraction, carbon dioxide produced, oxygen consumed, and the unreacted residue, and computation of all hydrocarbons as CH_4 and C_2H_6 using the formulas:

$$CH_4 = 1/3\ [7(TC + CO_2) - 9O_2]$$

$$C_2H_6 = 1/3[6O_2 - 4(TC + CO_2)]$$

4. Nitrogen reported as the measured unreacted residue.

Method *B* has the advantage of eliminating from the combustion data the additive errors caused by the deviation of CO_2 from ideality, the loss of CO_2 by solution in water formed or originally present, and the loss of CO_2 in any rubber connections. All of these errors result in too high a contraction and too low a produced carbon dioxide.[6] It will be shown that the few laboratories using this method reported more consistent results than the group as a whole. Whether or not this consistency would persist if the method were used by all of the laboratories is yet to be determined.

In addition to the two chemical methods just outlined, there were a few departures. One laboratory employed one of the procedures ordinarily used for the analysis of a fuel of the carburetted water-gas type. This procedure, method II described in a previous report (see footnote 2), included absorption of unsaturated hydrocarbons in fuming sulfuric acid and a fractional combustion over copper oxide, both preceding the combustion over hot platinum in the presence of excess oxygen.

In addition to these chemical methods, two laboratories used procedures involving distillation as follows:

Method X:

1. CO_2 and O_2 by absorption in a separate sample.
2. A single combustion of the hydrocarbons, with measurement of contraction and carbon dioxide produced.
3. A separation of the hydrocarbons by distillation in one of the usual rectifying columns.
4. Correction of the combustion data to take account of hydrocarbons heavier than C_2H_6.

Also, one laboratory employed only distillation for the analysis of the hydrocarbon fraction:

Method Y:

1. CO_2 and O_2 separately by absorption.
2. Other components by distillation.

Finally, this sample was analyzed by the Consolidated mass spectrometer, under the direction of A. Keith Brewer at the National Bureau of Standards.

It will be shown that two of the laboratories employing these special methods contributed the maximum and minimum calculated heating values—respectively about 50 and 40 Btu on either side of the measured values.

V. Results of Cooperative Analysis of Standard Gas Sample

1. Manner of Presenting the Analytical Data

All the analytical data submitted have been tabulated, together with the average values derived from each series of analyses, but contemplation of these tabulated data for some hours would not serve to reveal what may be seen at a glance when the same data are presented in a series of frequency-distribution plots. Accordingly, these plots, which amount to actual pictures of the analytical data, are presented first, and the discussion is centered around them. The tabulated data are given in an appendix, without discussion, but with sufficient explanation concerning their arrangement to permit their detailed study by those interested. (See table 1, page 40.)

Each circle appearing on the frequency-distribution plots represents a value derived from a single analysis. The circles are plotted equidistant on

[6] This has been repeatedly demonstrated. See Martin Shepherd, An improved apparatus and method for the analysis of gas mixtures by combustion and absorption, BS J. Research **6**, 121–167 (1931) RP266; Martin Shepherd and Joseph R. Branham, Critical study of the determination of ethane by combustion over platinum in the presence of excess oxygen, BS J. Research **10**, 783 (1933) RP625; Joseph R. Branham and Martin Shepherd, Critical study of the determination of ethane by explosion with oxygen or air, J. Research NBS **13**, 377 (1934) RP715; Joseph R. Branham, Martin Shepherd, and Shuford Schuhmann, Critical study of the determination of carbon monoxide by combustion over platinum in the presence of excess oxygen, J. Research NBS **26**, 571 (1941) RP1396.

the ordinate corresponding to their value. Thus the abscissas are values derived from the analyses, and the ordinates indicate the frequency with which these values occur. For example, in the plot showing the distribution of the results of the analyses for carbon dioxide (fig. 2) it will be seen

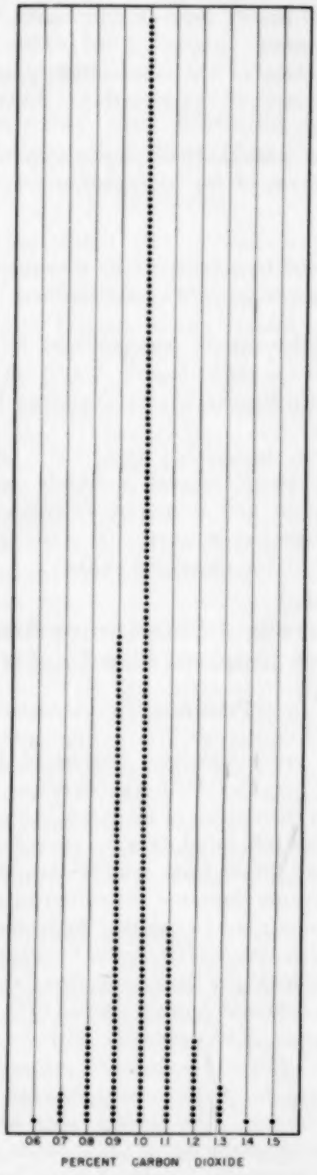

FIGURE 2.—*Frequency-distribution plot for carbon dioxide-0.1 percent interval.*

that 1 analysis gave 0.6 percent CO_2, 5 analyses gave 0.7 percent, 15 analyses gave 0.8 percent, and so on. This manner of plotting shows the distribution of all of the results at a glance, and forms the basis of a probability curve, of which the maxima are the most probable values. These graphical pictures not only save hours of study of the tabulated data, but actually make the significance of the data so self-evident that lengthy and detailed discussion of each plot is hardly necessary.

2. Carbon Dioxide

All the analyses reported for carbon dioxide are given in this plot (fig. 2). Analyses reported to hundredths of a percent were rounded off to the nearest tenth percent. Figure 3 is a separate plot

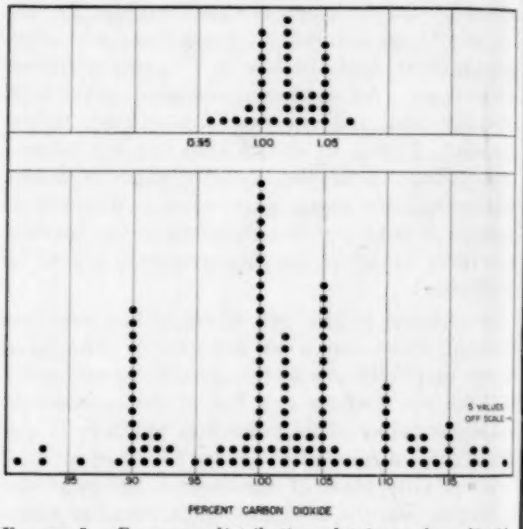

FIGURE 3.—*Frequency-distribution plot for carbon dioxide-0.01 percent interval.*

of those analyses which were reported to hundredths of a percent. (The tendency to round off to the nearest 0.05 percent is apparent.) The upper section of this plot gives the results of four laboratories that have generally been in agreement during this series of cooperative analyses, and probably represents the best reproducibility to be hoped for between laboratories with this type of sample. The total spread in this group is less than that noted for the whole group and suggests the desirability of taking the little extra trouble to adjust pressures and read volumes rather carefully.

The greatest frequency occurs at 1.0 percent. Of the 313 analyses reported for this constituent, 271 are between 0.9 and 1.1 percent. These results are not unsatisfactory, but can be improved.

3. Oxygen

The analyses for oxygen are plotted in figure 4. These are particularly interesting as there was no significant amount of oxygen in the sample. One or two-tenths of a percent of oxygen is usually reported in the analysis of a natural gas, and the extent to which oxygen really does occur has long been a question. Other constituents of the gas will dissolve in the reagents used to remove oxygen, and it is accordingly necessary to saturate these reagents with respect to the other gases and to maintain this equilibrium throughout the analysis. If this is correctly done, the error of solubility, leading to an erroneously high value for oxygen, should be minimized or eliminated. The present analyses show the extent to which this procedure has been successfully applied. Of the 294 analyses reported, 124 (only 42 percent) correctly indicated no oxygen; 58 (about 20 percent) indicated 0.1 percent oxygen, which may be considered the average error of solubility that experience has shown may be expected; and 69 (about 23 percent) indicated 0.2 percent oxygen, which should have been the maximum error caused by solubility alone. However, 24 and 19 analyses indicated 0.3 and 0.4 percent, respectively, and these values round off the probability curve. Beyond this, there are 20 values between 0.5 and 1.5 percent, which probably were the result of air contamination during the transfer of the sample to the analytical apparatus.

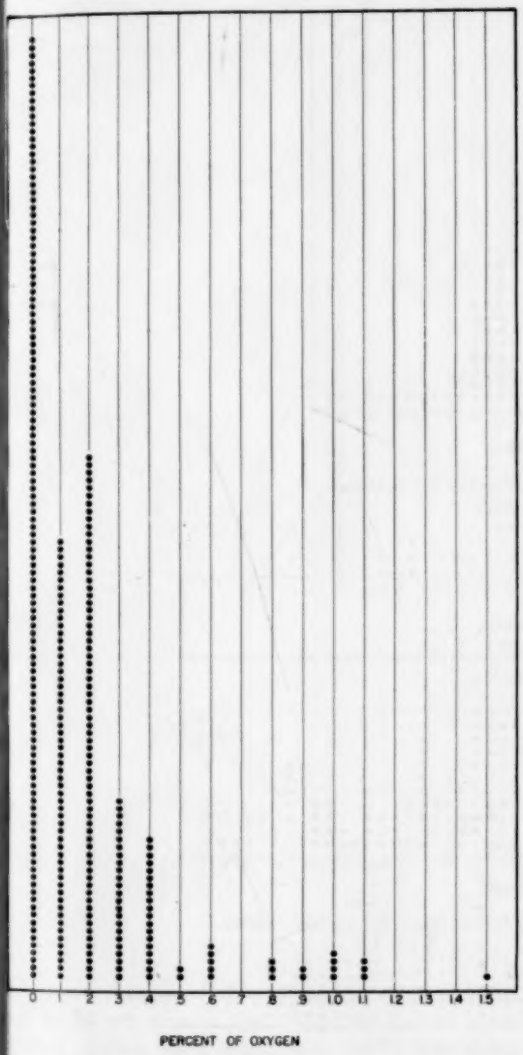

FIGURE 4.—*Frequency-distribution plot for oxygen-0.1 percent interval.*

It will be shown later that the heating values computed from the analyses indicating no oxygen are in general higher than those reported by the whole group.

4. Methane

The data for methane are given in two plots, figures 5 and 6. In the first of these, methane is plotted to the nearest half percent; in the second plot, 36 values have been eliminated before plotting to the nearest tenth percent.

Referring to the first plot (fig. 5), the greatest frequency appears at 77 percent, with an average of 76.5 percent if values lower than 73.5 and higher than 80.0 are discarded. The range 73.5 to 80.0, which includes about 94 percent of all the analyses, is rather wider than could be desired. The analyses were generally reported to the nearest tenth percent, although some were noted to hundredths. When plotted to the nearest tenth (fig. 6, section $A+B$) the whole group loses the sharp peak near 77 percent, and the distribution becomes widespread. This plot has been separated into two sections, and the letters A and B, correspond to the two methods previously

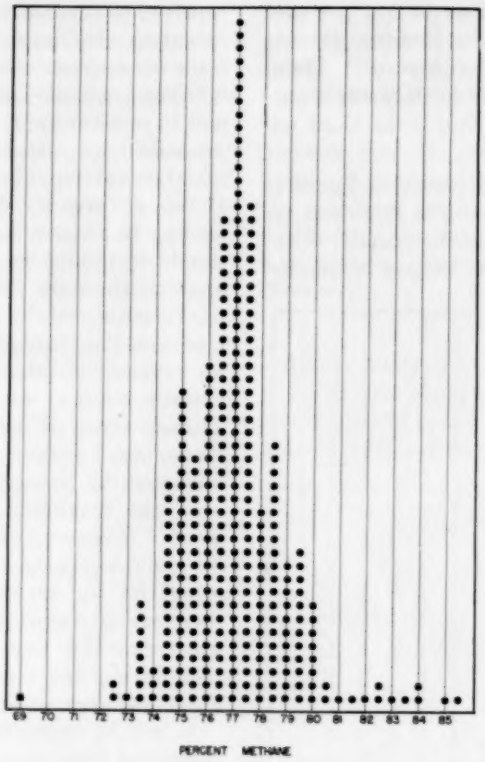

FIGURE 5.—*Frequency-distribution plot for methane—0.5 percent interval.*

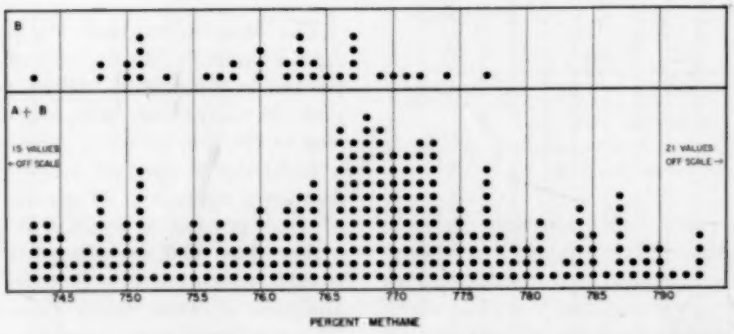

FIGURE 6.—*Frequency-distribution plot for methane—0.1 percent interval.*

noted. The upper section gives the analyses reported by the four laboratories that used method *B*, which takes account of oxygen consumed during the combustion as well as the contraction and carbon dioxide produced. Although these values are still widely spread, they are more closely grouped than is true for all of the analyses. (Note that none is off scale.) Group *B* indicates a somewhat lower average value, 76.1 percent, for methane.

5. Ethane

The analyses for ethane are given in two plots, figures 7 and 8, which follow the same scheme used for plotting methane. The first plot (fig. 7) shows the greatest frequency to be at 18.5 percent. About 89 percent of the analyses lie in the range 17.0 to 21.5 percent, with an average value of 19 percent. The analyses are plotted to the nearest tenth percent in section $A+B$ of figure 8. The distribution is again wide, even more so than is shown, for 31 values have been

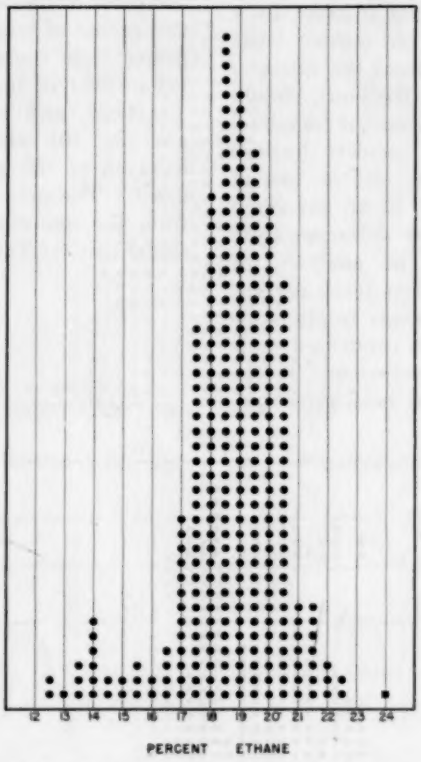

FIGURE 7.—*Frequency-distribution plot for ethane—0.5 percent interval.*

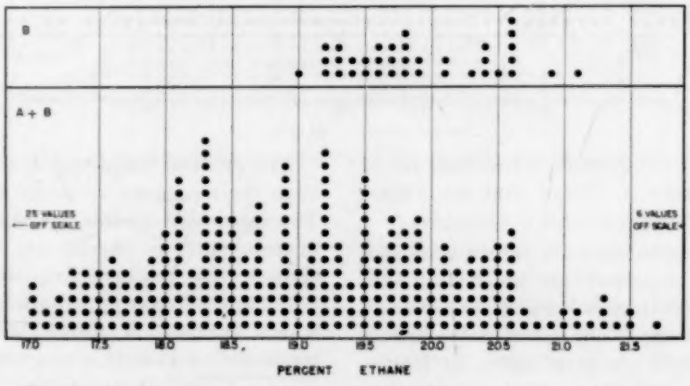

FIGURE 8.—*Frequency-distribution plot for ethane—0.1 percent interval.*

dropped. The values noted in the upper section of this plot, yielded by method *B*, are more closely clustered and are higher than the whole group. The average is 19.9.

6. Nitrogen

Nitrogen is always of especial interest in a combustion analysis, because no matter what method is used for the combustion the nitrogen (or more properly, the inert fraction), should always be the same. It is a measure of completeness of combustion and may indicate leakage during sampling or the analysis. In the case of method *B*, nitrogen is measured as an unreacted residue, while it is computed by difference from 100 percent in method *A*. The analyses for nitrogen are plotted to the nearest tenth percent in figure 9. This scale corresponds to the scale used in figures 4, 6, and 8. A condensed scale (0.5 percent) for nitrogen, to correspond to the scale of figures 5 and 7, has not been presented, even though it was not possible to include all of the analyses in figure 9. Note that six values are off scale to the left.

The plot for nitrogen shows a rather wide distribution. Values reported for method *B* are more closely grouped than is found in the over-all picture, but the average, 3.0, differs only slightly from that of the whole group, which is 3.1 for the range 1.5 to 5.0 percent.

7. Calculated and Measured Specific Gravity

The accuracy with which the specific gravity was computed from these analyses has been directly determined, since the specific gravity of this standard sample was measured by E. C. Creitz of the National Bureau of Standards.[7] The measured value was definitely known to one or two orders of magnitude more than could be expected from the analytical data. The measured value (referred to dry CO_2-free air=1) was 0.6820 $\pm$0.00005, and this has been indicated on the plot (fig. 10), which shows the values calculated from all of the analyses, plotted to the nearest 0.002. The calculated values were all computed from the following values given in the International Critical Tables:

CO_2	1.5290
O_2	1.1053
N_2	0.97208
CH_4	.5544
C_2H_6	1.0493
C_3H_8	1.5624

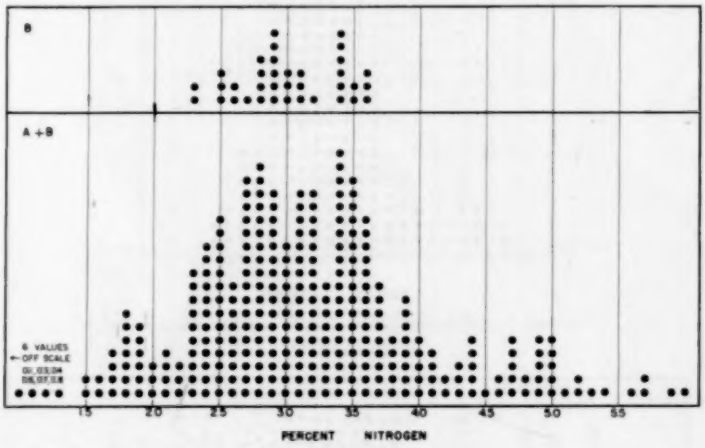

FIGURE 9.—*Frequency-distribution plot for nitrogen—0.1 percent interval.*

The greatest frequency is noted at 0.672, lower than the measured value by 0.01C or 1.5 percent. The calculated specific gravities are plotted to the nearest 0.001 in figure 11, section *A+B*. Although the greatest frequency is still seen at 0.671 to 0.672, the distribution now appears rather wide. Section *B* shows the values given by method *B*, and in this case the distribution is still

[7] See footnote 5.

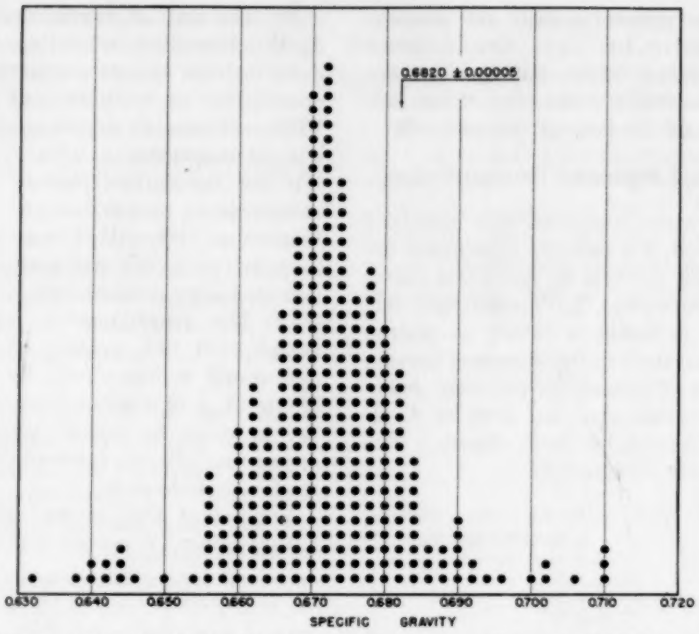

FIGURE 10.—*Frequency-distribution plot for calculated specific gravity-0.002 interval.*

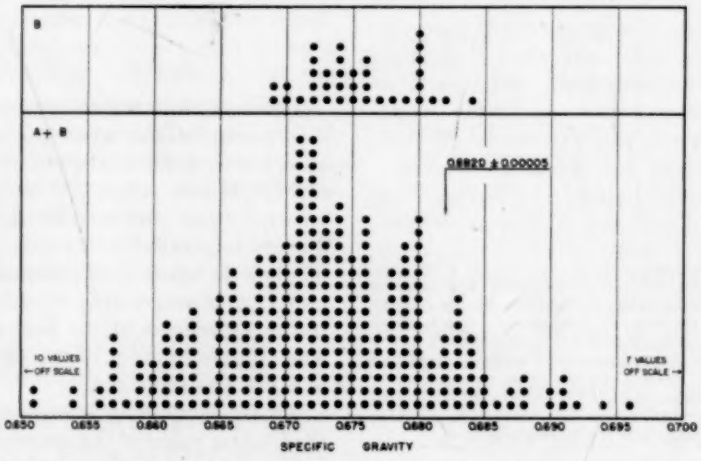

FIGURE 11.—*Frequency-distribution plot for calculated specific gravity-0.001 interval.*

wide, although the range is considerably improved. If 37 of the 272 values are eliminated, the average of the whole group from 0.657 to 0.685 (about 88 percent of all values reported) is 0.672, or 1.5 percent too low. The average of the *B* group is 0.675, somewhat closer to the measured value, although 1 percent too low.

A comparison with the specific gravity measured by the various instruments ordinarily used for this determination shows a generally better score for laboratory type instruments designed for this measurement, but a somewhat spotty score for recording instruments. Three specific-gravity balances yield average values of 0.680, 0.682, and

0.681. An effusion apparatus gave the average value 0.689, 1 percent too high. One recorder gave the correct value, 0.682, but three others recorded the values 0.690, 0.687, and 0.696, too high, by 1.2, 0.7, and 2.0 percent, respectively.

8. Calculated and Measured Heating Value

Because the heating value of this standard sample was measured, it is possible to estimate the accuracy with which the heating value was calculated from the analyses. Unfortunately, this estimation cannot be made as closely as desired because of the uncertainty in the measured heating value. Two series of measurements were made with the Junkers calorimeter, the first by J. H. Eiseman and the second by R. S. Jessup. The following values were obtained:

	Btu/ft³, 60° C, 30 in. Hg	
	1100. 7	[a] (1102. 4)
	1097. 4	(1099. 1)
	1098. 5	(1100. 2)
Average	1098. 9	(1100. 6)
	1106. 6	(1107. 8)
	1108. 5	(1109. 5)
	1107. 9	(1109. 1)
Average	1107. 9	(1109. 1)
Average of the two series	1103	(1105)

[a] Since this report was first issued for study by the ASTM Committees involved, Mr. Jessup has recomputed the measured heating values according to the new procedures of ASTM Tentative Method of Test for Calorific Value of Gaseous Fuels by the Water-Flow Calorimeter. This tentative method has been approved by Committees ASTM D-3 and D-3-III, ASTM designation D-900-46T. The values in parentheses are those obtained by the new computation, which makes a correction of the measured heat of combustion to the standard temperature of 60° F. The original values noted on the frequency distribution plots have not been altered, although official action of the ASTM will probably make this desirable eventually.

In addition to the Junkers determinations, other independent measurements were made. The Thomas recording calorimeter gave the value 1,100 Btu/ft³ at the time the first Junkers series yielded the value 1,099. In addition, the values 1,099 and 1,102 were obtained from a measurement of the heat of combustion of this sample and a measurement of the carbon dioxide produced on combustion. These values were derived as follows:

(1) The heat of combustion was measured by J. W. Knowlton according to the procedures described for the determination of the heats of combustion of methane and carbon monoxide.[8] Three calorimetric experiments were performed at a mean temperature of 25° C, with the water vapor, but not the carbon dioxide, removed from the sample prior to combustion. The heat of combustion so determined was 842.68±0.20 international kilojoules per mole (44.010 g) of CO_2 collected after combustion.

(2) The stoichiometric relationship between sample and CO_2 present after combustion was determined volumetrically by burning the sample (containing its original CO_2) over hot platinum in the presence of excess oxygen in an all-glass apparatus.[9] Seven determinations were made by Shuford Schuhmann.

Volume of CO_2 present after combustion of 1.0000 volume of sample ASTM–2:

1. 1679
1. 1677
1. 1672
1. 1678
1. 1665
1. 1681
1. 1669
Average 1. 1674±0. 0005

The tabulated values represent the measured decrease in volume when the carbon dioxide was absorbed from the mixture of oxygen, nitrogen, and carbon dioxide after the combustion of 1.0000 volume of gas, corrected for the measured carbon dioxide originally in the sample. The measurements were made at approximately 25°C and 760 mm Hg, corresponding to the conditions during the measurement of the heat of combustion (1). The volume fraction of the carbon dioxide in the mixture was about 0.6.

(3) By combining measurements (1) and (2) the heating value of the sample may be calculated.

Converting int. kj/mole of CO_2 to Btu/mole of CO_2: $\frac{842.68}{1.05460}$=799.05 Btu/mole of CO_2 present after combustion.

[8] Frederick D. Rossini, The heat of formation of water, BS J. Research 6 (1931) RP259; The heats of combustion of methane and carbon monoxide, 6 37 (1931) RP260; The heat of formation of water and the heats of combustion of methane and carbon monoxide, A correction, 7, 329 (1931) RP343.

[9] A modification of the analytical apparatus described in BS J. Research 6 121 (1931) RP266, with the manometer-compensator described in J. Research NBS 26, 351 (1941) RP1382, and all rubber connections eliminated.

Converting Btu/mole of CO_2 to Btu/ft³ of CO_2 (in the ideal gas state at 0° C and 760 mm of mercury): 799.05 Btu/22.4140 liters=1009.46 Btu/28.3162 liters or per ft³ of CO_2.

Converting this expression to the condition 30 in Hg, 60° F, saturated: $\frac{273.16}{288.71}\ \frac{762-13.25}{760}1009.46$ =940.95 Btu/ft³ of CO_2 (ideal gas) present after burning this sample, at 30 in Hg, 60° F, saturated.

It now remains to correct the carbon dioxide measured volumetrically after combustion for deviation from ideality. This correction introduces the greatest uncertainty in the present calculation:

The partial pressure of CO_2 in the residual volume after combustion was approximately 0.6. Under the conditions of the experiment (nearly 25° C and 1 atm), the deviation of CO_2 from ideality is 0.0051, which is to say that it occupies only 0.9949 of the volume 1.0000, which represents the ideal condition. However, the actual deviation of CO_2 mixed with the oxygen and nitrogen in the products of combustion is not equally well known. Some rough measurements made under essentially the same experimental conditions [10] indicate a partial deviation of 0.0004; and if this is accepted, 1 volume of sample is equivalent to 1.1679 volumes of CO_2 in the products of combustion. On the other hand, the conventional assumption, that the deviation of CO_2 is proportional to its partial pressure, would fix the partial deviation as 0.0030, and the corresponding relation would be altered, 1 volume of sample now being equivalent to 1.1709 volumes of CO_2 after combustion. The two heating values calculated from these two stoichiometric relations are

$$(940.95)\ (1.1679)=1{,}099\ \text{Btu/ft}^3\ (1{,}100)\ ^{11}$$
$$(940.95)\ (1.1709)=1{,}102\ \text{Btu/ft}^3\ (1{,}103)$$

Thus the uncertainty in the deviation of CO_2 from ideality corresponds to 3 Btu, whereas the uncertainty in the stoichiometric determination itself was only 0.7 Btu/ft³, and the uncertainty in the determination of the heat of combustion was reported by Rossini as the equivalent of 0.2 Btu/ft³.

An attempt was made to take advantage of the accuracy of the determination of the heat of combustion by a gravimetric measurement of the CO_2 present after the combustion of a known volume of the sample. A number of such determinations were made by E. C. Creitz, of the National Bureau of Standards. The heating values calculated from these determinations and the measured heat of combustion were

Btu/ft³
1101.7
1100.3
1101.7
1101.6
1100.7
1099.4
1104.2
1104.1
1102.3
1103.0
1101.9 ±1.2 (1102.8)

Several determinations obviously out of line, and all much lower, have been omitted from this average. There was no direct evidence that all of the gas had always been burned. However, some support is given the value 1,102 (1,103) Btu/ft³, derived from the stoichiometric experiment. These values are within 1 Btu of the average determinations with the Junkers calorimeter.[12]

For the present, the average heating value, 1,103 ±4 Btu (1,105), obtained with the Junkers instrument will be accepted for comparison with the analyses. This value is noted in the two frequency-distribution plots that give the data for heating values calculated from analyses. All the data are plotted to the nearest 2 Btu/ft³ in figure 12. The greatest frequency is noted at 1,104 Btu. The data are plotted to the nearest 1 Btu in figure 13, with 25 values (8 percent of those reported) omitted. Section *B* of this plot gives the values calculated from analyses performed by method *B*. These values are more closely grouped than the whole and are higher.

[10] Joseph R. Branham and Martin Shepherd, Gasometric method and apparatus for the analysis of mixtures of ethylene oxide and carbon dioxide, J. Research NBS **22**, 171 (1939) RP1175. (See p. 185.) Joseph R. Branham, Martin Shepherd, and Shuford Schuhmann, Critical study of the determination of carbon monoxide by combustion over platinum in the presence of excess oxygen, J. Research NBS **26**, 571 (1941) RP1396. (See p. 586.)

[11] See footnote "a," p. 30. Parenthetical values given hereafter refer to this same footnote.

[12] A standard sample of this type for the cooperative determination of heating value, using the procedure given in the new tentative standard proposed by Subcommittee D-3-III of ASTM on Determination of Calorific Value of Gaseous Fuels, might well be distributed. It would then be possible to compare the reproducibility of the measured heating value with that calculated from analysis. Another profitable excursion would be the accurate determination of heating value, either by improving the gravimetric measurement of carbon dioxide present after combustion, or by means of a more accurate calorimeter.

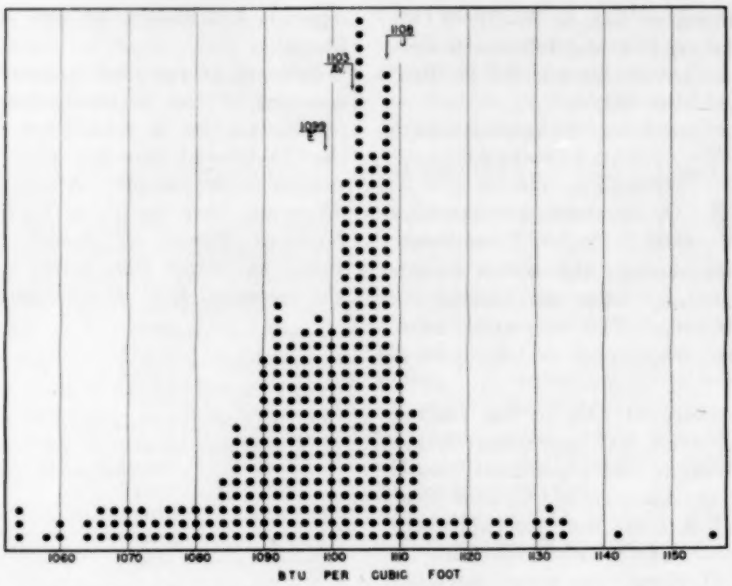

FIGURE 12.—*Frequency-distribution plot for calculated heating value—2.0 Btu interval.*

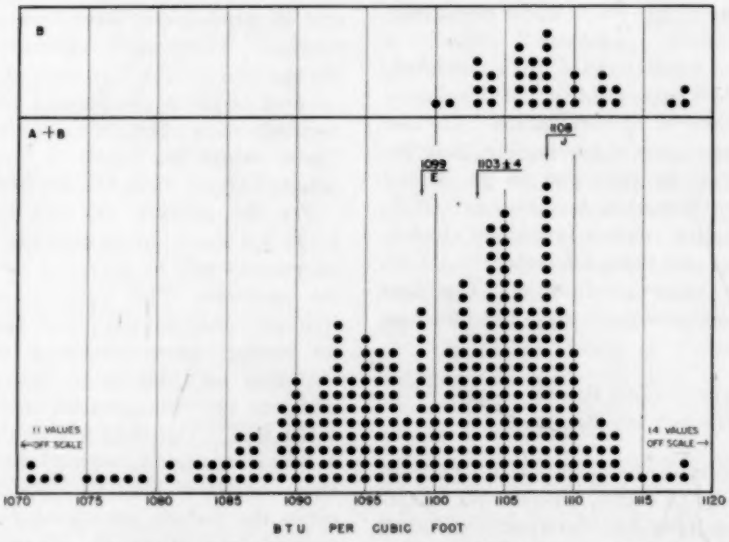

FIGURE 13.—*Frequency-distribution plot for calculated heating value—1.0 Btu interval.*

The average of the *B* group is 1,108 Btu/ft³. The average of all the computed values taken from 1,086 to 1,113 Btu (about 85 percent of all values reported) is 1,101 Btu/ft³. These averages for the calculated values are within 0.5 and 0.2 percent, respectively, of the average measured value, which is itself expressed within ±0.4 percent. The thing desired of the calculated values is greater frequency at and near the true heating value. The thing desired of the measured value is a closer approach to whatever the true value may be.

9. Laboratory Averages

So far the picture has included all of the determinations made by all of the laboratories. A picture of each laboratory with relation to the others may now be presented. Figure 14 is a plot showing the average values obtained by each laboratory for each of the constituents determined. Several of the laboratories reported more than one average value, and these have been included as separate points on the plots. Points with a slight tail to the right indicate average values derived from method *B*. All others were derived from method *A*, with the very few exceptions to be noted in the next section of this report, which will give results obtained by the three special methods previously noted.

The plot for methane has not included four values higher than 78.8 percent, and that for ethane has omitted four values lower than 17.0 percent. In general, the spread of the averages is too wide, and a need for standardization is indicated.

The average calculated specific gravities and heating values reported by each laboratory are plotted in figure 15. All values reported are given in the lower sections, marked $A+B+C$. As before, the sections marked *B* give values obtained by the laboratories using method B. The section marked *C* gives the results of the laboratories which reported no oxygen in the sample. Apparently there is no correlation between "no oxygen" and calculated specific gravity. However, those who found no oxygen reported heating values which were more consistently grouped around the measured value. This suggests the removal of some hydrocarbons during the absorption analysis, and again the inclusion of some air in the samples transferred for analysis—an effect seen in the tendency for these values to wander to the left of center, in comparison with the C group.

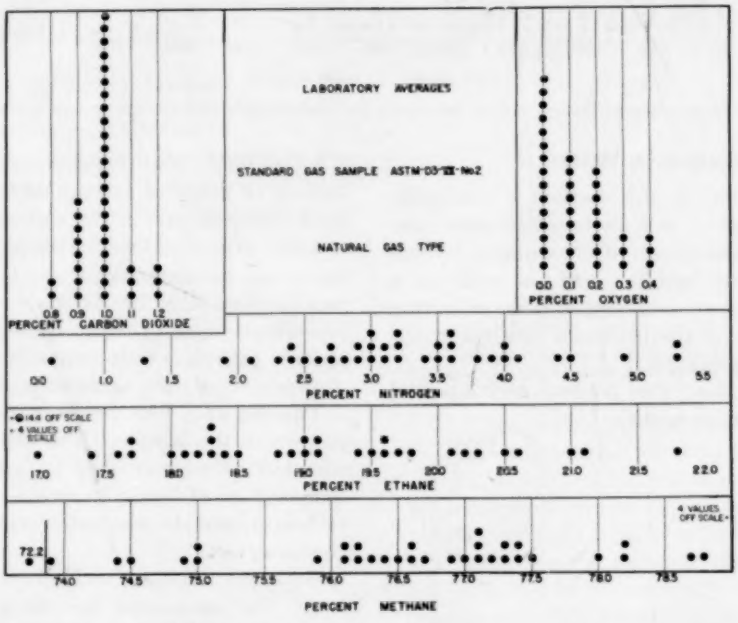
LABORATORY AVERAGES
STANDARD GAS SAMPLE ASTM-D3-BB-No2
NATURAL GAS TYPE
0.8 0.9 1.0 1.1 1.2
PERCENT CARBON DIOXIDE
0.0 0.1 0.2 0.3 0.4
PERCENT OXYGEN
0.0 1.0 1.5 2.0 2.5 3.0 3.5 4.0 4.5 5.0 5.5
PERCENT NITROGEN
1.70 1.75 1.80 1.85 1.90 1.95 2.00 2.05 2.10 2.15 2.20
PERCENT ETHANE
72.2 7.40 7.45 7.50 7.55 7.60 7.65 7.70 7.75 7.80 7.85
PERCENT METHANE

FIGURE 14.—*Frequency-distribution plot for laboratory averages of all constituents.*

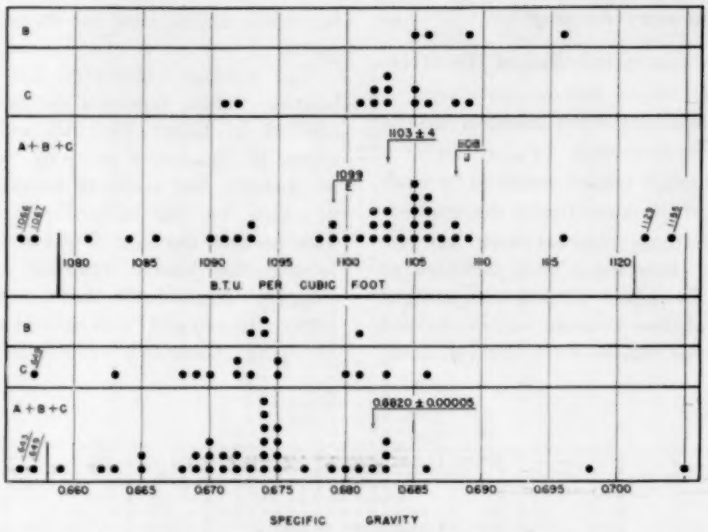

FIGURE 15.—*Frequency-distribution plot for laboratory averages of calculated specific gravity and heating value.*

10. Analysis by Method II

As previously stated, this method is ordinarily used for the analysis of a carburetted-water gas and involves an absorption of unsaturated hydrocarbons in fuming sulfuric acid, as well as a fractional combustion over copper oxide preceding the combustion over the platinum catalyst in the presence of excess oxygen.

Laboratory 21 used this method and reported the following average results:

	Percent
CO_2	1.0
O_2	0.0
N_2	5.3
C_2H_4	0.6
H_2	0.5
C_0	0.5
CH_4	74.5
C_2H_6	17.6
Specific gravity	0.6754
Btu/ft^3	1,065.9

The analysis is interesting for many reasons. The CO_2 and O_2 are correctly reported. The high nitrogen is not explained by air contamination, and probably resulted from incomplete combustion or a faulty exchange of atmospheric inerts in the reaction tubes.

The amount of C_2H_4 found was high, and indicated loss of other constituents in the fuming sulfuric acid. Actually, there was about 0.2 percent of propylene in this sample. Laboratory 1 determined unsaturated compounds by absorption in 10 drops of fuming sulfuric acid on glass wool, using as part of the volumetric apparatus a reaction tube described by Shepherd.[13] The average of six determinations was 0.19 ±0.04. This was checked later by the mass spectrometer (see following section "Analysis by Mass Spectrometer" of this paper), which indicated the presence of .0.18 percent of C_3H_6 as the only unsaturate present.

The H_2 and CO reported were actually not present in the sample. The absence of hydrogen was definitely established by a separation at the temperature of liquid hydrogen. The absence of carbon monoxide was established by a sensitive chemical test.[14]

Both the methane and ethane found were too low. The calculated specific gravity was low. The calculated heating value, however, was the minimum noted for the whole group, 37 Btu lower than the average measured value.

These results taken alone afford no recommendation for the double combustion method. On the contrary, this refinement of the single combustion method has not yielded the desired results.

Laboratory 24 did not follow method II but did make an absorption in fuming sulfuric acid

[13] Modification of apparatus for volumetric gas analysis, J. Research NBS **26**, 351 (1941) RP1382. See page 354, figure 2, tube number 2.

[14] Martin Shepherd, A preliminary report on the NBS colorimetric indicating gel for the rapid determination of small amounts of carbon monoxide, Anal. Chem. **19**, 77 (1947).

reporting the contraction as C_3H_8. The averages found for two series of 10 analyses each were 0.6 and 0.5 percent. The complete results follow:

	Series 1 *Percent*	Series 2 *Percent*
CO_2	1. 0	1. 0
O_2	0. 0	0. 0
CH_4	76. 7	77. 3
C_2H_6	18. 5	18. 1
C_3H_8	0. 6	0. 5
N_2	3. 2	3. 1
Specific gravity	0. 675	0. 672
Btu/ft ^{3}	1106	1103

Correct values for CO_2 and O_2 are reported. The C_2H_6 is apparently lowered at the expense of the "C_3H_8." The specific gravities are a bit low, but the heating values are very good.

11. Analysis by Distillation Methods *X* and *Y*

Laboratory 28 analyzed the sample by method *A*, but in addition separated the sample by fractional distillation and noted in a secondary report the result of the correction for propane found by the distillation method. The data are

	Average values by method *A*	Average values by Method *A* corrected for C_3H_8
CO_2	1. 05	1. 05
N_2	3. 95	3. 95
O_2	0. 05	0. 05
CH_4	74. 40	77. 55
C_2H_6	20. 55	14. 25
C_3H_8	----------	3. 15
Specific gravity	0. 683	0. 683_7
Btu/ft ^{3}	1103. 0	1103. 8

This is very satisfactory work. The slight corrections applied did not materially alter the calculated specific gravity or heating value—and did not improve the calculated specific gravity.

Laboratory 29 employed method *X*. The combustion data were thus not calculated as such but corrected for C_3H_8 found by fractional distillation. The average values obtained by this laboratory are

	Percent
CO_2	0. 8
O_2	. 24
CH_4	76. 98
C_2H_6	14. 1
C_3H_8	3. 0
N_2	4. 88
Specific gravity	0. 6838
Btu/ft ^{3}	1091. 6

Carbon dioxide is a bit too low, oxygen is high, and nitrogen is higher than the average value by a large enough amount to suggest air contamination. The calculated heating value is low. The calculated specific gravity is within 0.002 of the measured value. The method should have improved the accuracy of the calculated heating value, and did not.

Laboratory 30 employed method *Y*, which depended upon distillation for all constituents except CO_2 and O_2. These average results were reported:

	Percent
CO_2	1. 00
O_2	0. 00
CH_4	80. 6
C_2H_6	14. 8
C_3H_8	* 3. 6
N_2	0. 0
Specific gravity	0. 6736
Btu/ft ^{3}	1155. 2

* Actually, the distillation indicated 2.4 percent heavier than C_3H_8, but this was called C_3H_8 in the computation of specific gravity and heating value.

The distillation method has long been favored over the combustion method for the analysis of natural gases, and it is well understood that the latter method cannot yield the true composition. It is accordingly surprising to find the maximum calculated heating value of the present series of analyses has been derived from the distillation procedure. This heating value is about 50 Btu/ft^3 too high. The specific gravity is 0.008 too low. The absorption analysis has reported the correct values for carbon dioxide and oxygen.

12. Analysis by Mass Spectrometer

The first two analyses by the Consolidated mass spectrometer were made under the direction of A. Keith Brewer. Notable amounts of hydrogen were reported, and the results were not concordant. The calculated heating value and specific gravity were not in agreement with the measured values

for the first analysis, but in good agreement in case of the second analysis.

Because of the apparent presence of hydrogen, which is not to be expected in a natural gas in anything like the amount found, a separation of this sample was made at the temperature of liquid hydrogen. This experiment definitely proved the absence of hydrogen (i. e., the amount present could not have exceeded 0.001 percent). Accordingly, the original fragmentation patterns of the hydrocarbons used in the analyses by mass spectrometer were redetermined, and the corrected patterns were then used in computing the mass spectrogram obtained in a third analysis. This analysis and computation were made by Vernon Dibeler. The three analyses are

	First analysis	Second analysis	Third analysis
	Percent	*Percent*	*Percent*
H_2	0. 34	0. 74	0
CH_4	68. 02	76. 7	77. 5
N_2	13. 93	3. 90	4. 09
C_2H_6	13. 55	14. 7	14. 4
C_2H_4	0. 22	0. 17	0. 18
CO_2	1. 22	. 94	. 96
C_3H_8	2. 72	2. 90	2. 82
Other hydrocarbons	0	0	0
Specific gravity	0. 719	0. 680	0. 682
Btu/ft³	992	1, 102	1, 102

Although the first analysis is out of line, the second and third are in good agreement (with H_2 dropped from the second), and both yield excellent values for specific gravity and heating value. The C_3H_8 found checks the chemical determination of unsaturated hydrocarbons made by laboratory 1. The correct value for CO_2 was reported, and no oxygen was found. The nitrogen is somewhat higher than the value indicated by chemical analysis. The 2.82 percent of C_3H_8 found compares reasonably with the values 3.0, 3.1, and 3.6, reported by three laboratories using distillation. For ready comparison, the values obtained by the mass spectrometer (third analysis) are plotted in figures 14 and 15 as open circles. Methane and ethane are not directly comparable to the amounts found by combustion; and the propane and propylene do not appear.

13. Errors in Calculated Specific Gravity and Heating Value

In view of the additional data furnished by the special methods just discussed, it will be well to reexamine the specific gravity and heating values calculated from the analyses. The presence of 3.0 percent of C_3H_8 and 0.2 percent C_3H_6 in this sample seems well established. (The figures have been rounded off to the needed significance.) As these C_3 hydrocarbons were computed as CH_4 and C_2H_6, it is well to check the errors thus introduced in the calculated values.

Propane is calculated thus in the analysis:

$$C_3H_8 \rightarrow 2C_2H_6 - CH_4.$$

Accordingly, the calculated specific gravity was too high by 0.002:

$$1.5624 \rightarrow 2(1.0493) - 0.5544$$

$$(0.03)\ (1.6442 \text{ calculated} - 1.5624 \text{ actual}) = 0.0024$$

Similarly, the calculated heating value was too low by 0.2 Btu/ft³:

$$2528 \rightarrow 2(1759) - 997$$

$$0.03(2528 - 2521) = 0.21.$$

The calculation for the propylene depends in turn on the manner in which methane and ethane were calculated.

(1) When CH_4 and C_2H_6 are calculated from total contraction and carbon dioxide formed, these stoichiometric relations are used:

$$CH_4 = 1/3(4TC - 5CO_2)$$

$$C_2H_6 = 1/3(4CO_2 - 2TC).$$

With propylene injected, TC and CO_2 are expressed thus:

$$TC = 2CH_4 + 2.5C_2H_6 + 2.5C_3H_6$$
$$CO_2 = CH_4 + 2C_2H_6 + 3C_3H_6.$$

Accordingly, CH_4 and C_2H_6, calculated as above, are in error:

$$CH_4 \rightarrow CH_4 - 5/3C_3H_6$$
$$C_2H_6 \rightarrow C_2H_6 + 7/3C_3H_6.$$

The 0.2-percent propylene thus makes the calculated CH_4 too low by (5/3) (0.2)=0.33, and the C_2H_6 too high by (7/3) (0.2)=0.47 percent.

(2) Similarly, when CH_4 and C_2H_3 are calculated from the total contraction plus carbon dioxide and the oxygen consumed, according to the relations

$$CH_4 = 1/3[7(TC + CO_2) - 9O_2]$$
$$C_2H_6 = 1/3[6O_2 - 4(TC + CO_2)],$$

and the $(TC + CO_2)$ and O_2 are expressed

$$(TC + CO_2) \rightarrow 3CH_4 + 4.5C_2H_6 + 5.5C_3H_6$$
$$O_2 \rightarrow 2CH_4 + 3.5C_2H_6 + 4.5C_3H_6,$$

the calculated CH_4 and C_2H_3 are in error thus:

$CH_4 \rightarrow CH_4 - 2/3C_3H_6 = 0.13$ percent (in this case)
$C_2H_6 \rightarrow C_2H_6 + 5/3C_3H_6 = 0.33$ percent (in this case).

The errors can now be evaluated:

(1) When CH_4 and C_2H_6 are calculated from TC and CO_2 alone, the presence of 0.2 percent of C_3H_6 causes the calculated specific gravity to be too high by 0.0002 (which is not significant): $(0.0047)(1.049) - (0.0033)(0.5544) - 0.002(1.45) = 0.0002$.

The calculated heating value is 0.3 Btu/ft³ too high: $(0.0047)\ (1759) - (0.0033)\ (997.4) - (0.002)\ (2339)$.

(2) When CH_4 and C_2H_6 are calculated from $(TC + CO_2)$ and O_2, 0.2 percent of C_3H_6 makes the calculated specific gravity too low by 0.001 (not significant): $(0.002)\ (1.45) - [(0.0033)\ (1.049) - (0.0013)\ (0.5544)]$ and the calculated heating value too low by 0.2 Btu/ft³: $(0.002)\ (2339) - [(0.0033)\ (1759) - (0.0013)\ (997.4)]$.

The errors for propane and propylene may now be combined:

(1) The calculation from TC and CO_2 makes the calculated specific gravity too high by 0.002, and the calculated heating value too high by 0.1 Btu/ft³.

(2) The calculation from $(TC + CO_2)$ and O_2 makes the calculated specific gravity too high by 0.002 and the calculated heating value too low by 0.4 Btu/ft³.

The errors in calculated heating value are of no interest, once they are known. The error in specific gravity does not improve the situation, since the correction would move the calculated value further from the observed one.

14. Comparison of Analysts in Same Laboratory

The extent to which the different analysts using the same apparatus and method will achieve concordant results has often been discussed and with varying opinions. One school holds that analysts are born and not made; while a second and more optimistic group believe that any high-school child can be quickly converted to the desired robot. The analyses submitted in this cooperative series prove nothing conclusively, but offer interesting comparisons to show that analysts using the same apparatus and procedure can be together or apart, which was to be expected.

Two frequency distribution plots have been prepared to give this picture. It was not worthwhile to plot each component of the mixture. Nitrogen and the calculated heating value were selected to illustrate these agreements and disagreements; nitrogen because it is a measure of the over-all behavior of the chemical analysis, and is comparable no matter what procedure has been used; and heating value because it is another measure of the over-all success of the analysis, and of especial engineering interest.

The plots showing the comparative results of analyst versus analyst are shown in figures 16 and 17. Each laboratory that contributed to this competition is numbered and separated by heavy horizontal boundaries. The analysts who entered each laboratory competition are lettered, and their individual efforts are separated by lighter horizontal boundaries.

By reading these plots we find, for example, that analysts *A* and *D* in laboratory 2 were on good terms. Figure 16 for nitrogen shows no evidence for great concern until laboratories 22 and 23 are examined. It is obvious that in both laboratories an analyst, *M*, had some difficulty in deciding upon a suitable value. Figure 17 shows in general a somewhat greater disagreement. There are differences between analysts *A* and *B* of laboratory 5, *A* and *B* of laboratory 14, and *M* and *N* of laboratory 22, which might well be straightened out. Laboratories 2, 17, 18, 20, and 24 appear to have arrived at agreement with themselves if not always with each other. Here then is a brief picture showing the expected differences in talent.

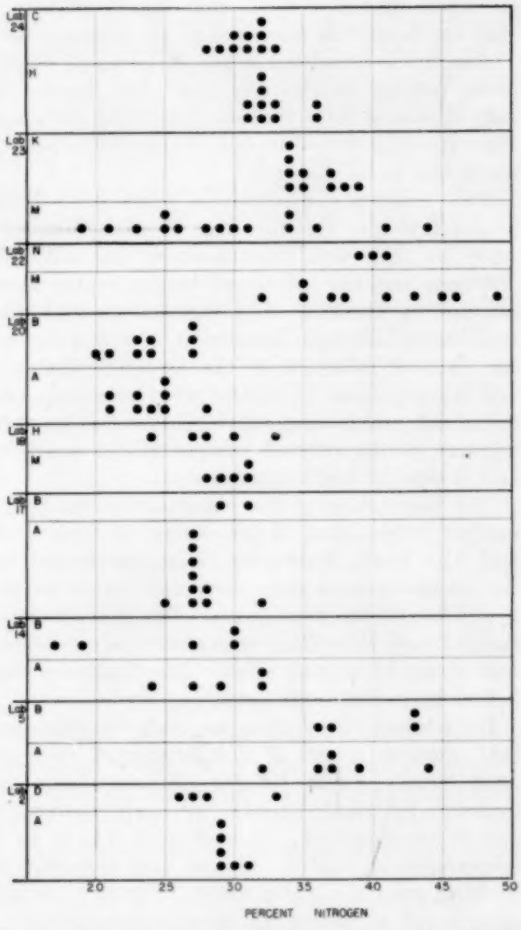

FIGURE 16.—*Frequency-distribution plot comparing different analysts in the same laboratory with percent nitrogen as the basis for comparison.*

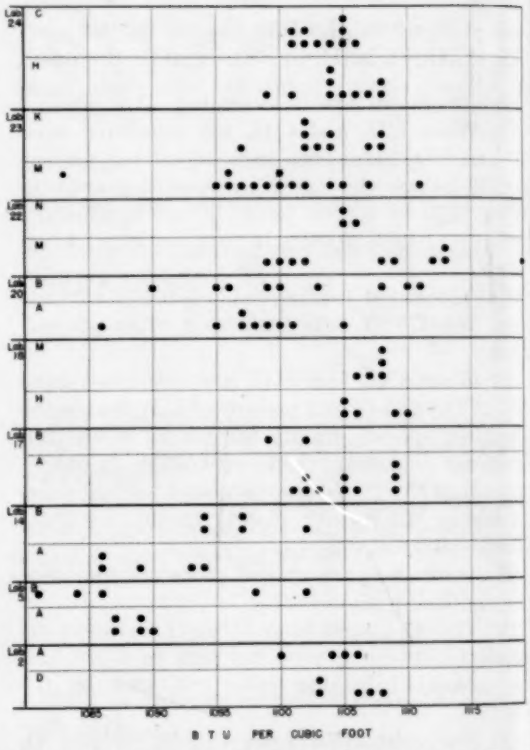

FIGURE 17.—*Frequency-distribution plot comparing different analysts in the same laboratory, with calculated heating value as the basis for comparison.*

15. Comparison of Laboratories Within Same Organization

It might logically be expected that laboratories within th e same organization would have compared results and composed their differences, but the story seems to be much the same as for the individual analysts. The data available offer no other information than this, for their number is not sufficient to tempt a statistical statement as to the proportion of agreement and disagreement within companies.

These data, again for nitrogen and heating value, have been plotted in figures 18 and 19.

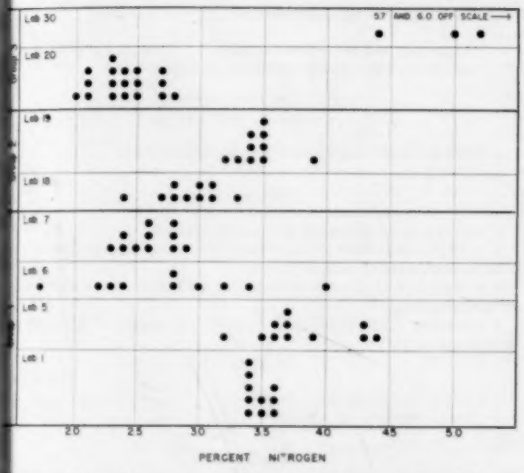

FIGURE 18.—*Frequency-distribution plot comparing different laboratories in the same organization, with percent nitrogen as the basis for comparison.*

There are three groups or organizations represented, divided on the plots by heavy horizontal boundaries; the laboratories within each group are separated by lighter horizontal boundaries.

Perhaps there is less reason to expect agreement among the four laboratories in group 1 than in the other two cases, for this is a group of Government laboratories. Laboratories 5, 6, and 7 are in the same Bureau, and 5 and 6 are in the same building; but each laboratory employs different apparatus and methods. Laboratory 1 is in another Bureau. The agreement between laboratories 1 and 5 in the matter of percentage of nitrogen is not extended to laboratories 6 and 7. The agreement between laboratories 1 and 7 in the calculated heating value is not extended to laboratories 5 and 6.

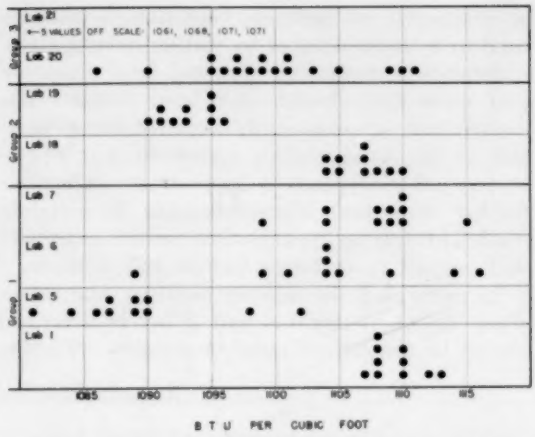

FIGURE 19.—*Frequency-distribution plot comparing different laboratories in the same organization, with computed heating value as the basis for comparison.*

In the case of laboratories 18 and 19 of group 2, both in the same company, and both operating in connection with different phases of the same general project and in the same location, there is only fair agreement on the percentage of nitrogen, and no good agreement on heating value. Both laboratories employed like apparatus and methods. In the case of laboratories 20 and 21 of group 3, both laboratories were in the same company, but were widely separated geographically, and used different methods. There is no agreement between these laboratories. Indeed, it was not found possible to plot the results of laboratory 21 on the scale selected to include the other laboratories.

These cases pictured in the last four plots serve to emphasize the need for standardization, and the further need for equally expert analysts.

VI. Conclusions

The data presented here give the first clear picture so far available of the actual status of gas analysis of this particular type in this country. As such they are worthy of considerable reflection on the part of gas chemists and plant engineers. In view of the considerable effort expended by everyone who took part in the analyses, and because of the importance of the data, the committee believes that the results should be released for study by all laboratories engaged in this type

of volumetric gas analysis, even though the data need to be supplemented by further investigation.

Some very creditable work has been presented and some that should have been better. The data indicate a considerable degree of standardization in the use of modern equipment, but, nevertheless, offer evidence to support the claim that further important standardization is certainly needed to clear up the analytical picture, especially with respect to operating technic and methods.

In particular, the relative accuracy and reproducibility of methods *A* and *B* herein described should be determined more thoroughly. Further correlation of the results obtained by the absorption-combustion and the distillation methods is an indicated need. An investigation of the accuracy and reproducibility of that important new analytical tool, the mass spectrometer, is another indicated need. And quite aside from the analytical one or two standard samples might well be distributed to cooperating laboratories for the determination of heating value, using the recently proposed ASTM Tentative Standard. In this connection, the need for a very accurate method to determine heating value is becoming more apparent.

TABLE 1.—*Analytical data reported by the cooperating laboratories*

Each laboratory has been assigned a number, and the reports are arranged in the order of these numbers. At the left hand, just under the laboratory number, the method used is designated by the proper key letter. At the right hand, under the laboratory number, is the key designating the apparatus used. These keys are given below.

Referring to the tabulated data, column 1 gives the analysis number, column 2 the analyst, columns 3, 4, 5, 6, 7 give in order the percentage by volume of CO_2, O_2, CH_4, C_2H_6, and N_2. Column 8 is used to report other hydrocarbons, or other gases, which may have been determined by special methods. Column 9 gives the total for all the constituents determined. Columns 10 and 11 give, respectively, the heating value (in Btu/ft^3_{ASTM}) and specific gravity calculated from the analyses. The measured heating value was 1,103 ±4 Btu/ft^3 (30 in. Hg, 60° F, saturated), and the measured specific gravity was 0.6820 ±0.0005, referred to dry CO_2-free air.

The keys to methods and apparatus follow.

Method A

1. Absorption of carbon dioxide in an aqueous solution of potassium hydroxide.
2. Absorption of oxygen in alkaline pyrogallol or in a chromous solution.
3. A single combustion over hot platinum in the presence of excess oxygen, measurement of the contraction and carbon dioxide produced, and computation of all hydrocarbons present as CH_4 and C_2H_6, using the conventional formulas:

$$CH_4 = 1/3(4TC - 5CO_2)$$
$$C_2H_6 = 1/3(4CO_2 - 2TC),$$

where TC is the total contraction on burning, and CO_2 is the carbon dioxide produced by the combustion.

4. Nitrogen by difference.

Method B

1. Absorption of carbon dioxide in a solution of potassium hydroxide.
2. Absorption of oxygen in alkaline pyrogallol.
   (One of the four laboratories then took fresh portions of the sample for combustion, correcting the combustion data for the CO_2 and O_2 originally found. The other three used the general procedure of combustion of a portion of the sample taken for absorption.)
3. A single combustion over hot platinum in the presence of excess oxygen, measurement of the contraction, carbon dioxide produced, oxygen consumed, and the unreacted residue. Computation of all hydrocarbons as CH_4 and C_2H_6 using the formulas:

$$CH_4 = 1/3[7(TC + CO_2) - 9O_2]$$
$$C_2H_6 = 1/3[6O_2 - 4(TC + CO_2)].$$

4. Nitrogen reported as the measured unreacted residue.

Method X

1. CO_2 and O_2 by absorption in a separate sample.
2. A single combustion of the hydrocarbons, with measurement of contraction and carbon dioxide produced.
3. A separation of the hydrocarbons by distillation in one of the usual rectifying columns.
4. Correction of the combustion data to take account of hyrdocarbons heavier than C_2H_6.

Method Y

1. CO_2 and O_2 separately by absorption.
2. Other components by distillation.

Apparatus

V_1—Volumes are made comparable by means of a pressure-temperature compensator with manometer interposed between the compensating tube and the burette.

V_2—Pressure within the burette is balanced against existing barometric pressure, and gas volumes are corrected from the observed pressure and temperature to a common basis, including a correction for changes in the saturation pressure of water.

V_3—Pressure in burette is balanced against atmospheric pressure but no correction is made for changes in pressure or temperature during analysis.

V_4—Volumes are measured by observing the pressure exerted within a constant volume.

R_1—Pipettes are connected to the burette by a manifold.

R_2—A single pipette, connected to the burette, serves for all reactions.

R_3—Pipettes are temporarily connected in succession to the burette as the different reactions are progressively conducted.

R_4—The burette itself serves as a reaction tube.

Hg—Mercury is used as the confining fluid.

H_2O—(with appropriate subscript)—An aqueous solution serves as the confining fluid.

TABLE 1.—*Analytical data reported by the cooperating laboratories*—Continued

LABORATORY NUMBER 1

Method *B* — Apparatus V_1R_1Hg-Shepherd

Anal. No.	Analyst	Percentage by volume							Calculated	
		CO_2	O_2	CH_4	C_2H_6	N_2	(C_nH_{2n})	Total	Btu/ft ^{3}	sp gr
1	SS	0.99	0.01	.....	.....	.....	0.22	.....	.....	.....
2	SS	.96	.00	.....	.....	.....	.17	.....	.....	.....
3	SS	.98	02	.....	.....	.....	.19	.....	.....	.....
4	SS	1.02	.00	.....	.....	.....	.21	.....	.....	.....
5	SS	1.00	−.04	.....	.....	.....	.20	.....	.....	.....
6	SS	0.97	−.01	.....	.....	.....	.17	.....	.....	.....
7	SS	1.02	.....	.....	.....	.....	.....	.....	.....	.....
8	SS	1.02	.....	.....	.....	.....	.....	.....	.....	.....
9	SS	1.04	.....	.....	.....	.....	.....	.....	.....	.....
10	SS	1.03	.....	.....	.....	.....	.....	.....	.....	.....
Avg	.....	1.00	0.00	.....	.....	.....	0.19	.....	.....	.....
1	SS	1.00	0.00	74.77	20.88	3.36	0.19	100.01	1,113	0.682
2	SS	1.00	.00	75.06	20.55	3.39	.19	100.00	1,110	.680
3	SS	1.00	.00	74.30	21.08	3.62	.19	100.00	1,112	.684
4	SS	1.00	.00	75.15	20.36	3.49	.19	100.00	1,108	.680
5	SS	1.00	.00	75.27	20.33	3.41	.19	100.01	1,108	.679
6	SS	1.00	.00	74.81	20.59	3.60	.19	100.00	1,108	.681
7	SS	1.00	.00	75.01	20.57	3.41	.19	99.99	1,110	.680
8	SS	1.00	.00	75.07	20.44	3.49	.19	100.00	1,108	.680
9	SS	1.00	.00	75.03	20.38	3.59	.19	100.00	1,107	.680
10	SS	1.00	.00	75.06	20.53	3.41	.19	100.00	1,110	.680
Avg	.....	.....	.....	74.95	20.57	3.48	.....	100.00	1,109	0.681

LABORATORY NUMBER 2

Method *B* — Apparatus V_1R_1Hg-Shepherd

Anal. No.	Analyst	Percentage by volume							Calculated	
		CO_2	O_2	CH_4	C_2H_6	N_2	(C_3H_8)	Total	Btu/ft ^{3}	sp gr
1	D	1.13	0.12	76.05	19.60	3.11	.....	100.01	1103.28	0.6761
2	D	1.13	.07	76.02	19.85	2.91	.....	99.98	1107.38	.6762
3	D	1.15	.12	76.26	19.62	2.86	.....	100.01	1105.74	.6754
4	D	1.05	.05	76.24	19.75	2.92	.....	100.01	1107.82	.6750
5	D	0.99	.12	76.35	19.64	2.90	.....	100.00	1106.98	.6740
6	D	1.02	.22	76.67	19.26	2.84	.....	100.01	1103.49	.6728
7	A	0.89	.10	77.24	18.96	2.82	.....	100.01	1103.90	.6093
8	A	1.08	.10	77.01	19.25	2.57	.....	100.01	1107.60	.6722
9	A	0.98	.10	76.45	19.73	2.75	.....	100.01	1100.00	.6736
10	A	.83	.18	75.80	19.88	3.36	.....	100.05	1106.00	.6762
Avg	.....	1.03	0.12	76.41	19.55	2.90	.....	100.01	1106.16	0.6741

LABORATORY NUMBER 3

Method *B* — Apparatus V_1R_1-Shepherd

1	PS	1.05	0.06	75.96	20.15	2.79	.....	100.01	1,112	0.676
2	PS	1.07	.08	75.73	20.59	2.53	.....	100.00	1,118	.678
3	PS	1.05	.06	75.80	20.58	2.52	.....	100.01	1,118	.677
4	PS	0.99	.06	76.56	19.87	2.53	.....	100.01	1,113	.673
5	PS	1.03	.08	76.45	20.14	2.31	.....	100.01	1,117	.674
6	PS	[a] 1.02	[a] .02	77.69	19.82	1.47	.....	100.02	1,124	.669
7	PS	[a] 1.02	[a] .02	77.37	19.35	2.27	.....	100.03	1,112	.670
Avg	.....	1.03	.05	76.51	20.07	2.35	.....	.....	1,116	0.674

TABLE 1.—*Analytical data reported by the cooperating laboratories*—Continued

LABORATORY NUMBER 4

Method *B* — Apparatus V_1R_1Hg-Sherlock

Anal. No.	Analyst	Percentage by volume							Calculated	
		CO_2	O_2	CH_4	C_2H_6	N_2	(C_3H_8)	Total	Btu/ft³	sp gr
1	SC	1.02	0.00	77.09	19.29	2.60	.....	100.0	1,108	0.671
2	SC	1.02	.00	76.70	19.41	2.87	.....	100.0	1,106	.672
3	SC	1.04	.00	76.31	19.80	2.85	.....	100.0	1,109	.674
4	SC	1.03	.00	77.22	18.82	2.93	.....	100.0	1,101	.670
5	SC	1.04	.00	76.25	19.66	3.05	.....	100.0	1,106	.675
6	SC	1.00	.00	76.63	19.27	3.10	.....	100.0	1,103	.672
7	SC	1.02	.00	76.74	19.18	3.06	.....	100.0	1,103	.672
8	SC	1.05	.00	76.74	19.19	3.02	.....	100.0	1,103	.672
9	SC	1.00	.00	76.47	19.50	3.03	.....	100.0	1,106	.673
10	SC	1.01	.00	76.30	19.52	3.17	.....	100.0	1,104	.674
Avg	.....	1.02	0.00	76.65	19.36	2.97	.....	100.0	1,105	0.673

LABORATORY NUMBER 5

Method *A* — Apparatus V_1R_1Hg-Bureau of Mines

1	A	1.1	0.2	77.6	17.9	3.2	.....	100.0	1,089	0.668
2	A	1.0	.3	76.7	18.3	3.7	.....	100.0	1,087	.672
3	A	1.0	.3	76.6	18.5	3.6	.....	100.0	1,089	.672
4	A	1.0	.1	76.7	18.5	3.7	.....	100.0	1,090	.672
5	B	1.0	.1	77.0	17.6	4.3	.....	100.0	1,078	.670
6	B	1.0	[a] 1.4	75.6	17.9	.....	.....	.....	1,069	.....
7	B	0.9	0.6	77.3	17.6	3.6	.....	100.0	1,081	.669
8	B	1.0	.4	76.8	18.1	3.7	.....	100.0	1,084	.671
9	A	1.1	.8	75.0	18.7	4.4	.....	100.0	1,077	.669
10	A	1.0	.3	76.2	18.6	3.9	.....	100.0	1,087	.674
11	C	0.9	.2	77.1	18.3	3.5	.....	100.0	1,091	.669
12	B	1.0	.2	75.7	18.8	4.3	.....	100.0	1,086	.676
13	B	.....	.....	76.8	19.1	.....	.....	.....	1,102	.....
14	B	.....	.....	77.8	18.3	.....	.....	.....	1,098	.....
Avg	.....	1.0	0.3	76.6	18.3	3.8	.....	.....	1,086	0.672

LABORATORY NUMBER 6

Method *A* — Apparatus V_1R_2Hg-Bone and Wheeler

1	.....	0.9	0.0	76.8	19.5	2.8	.....	100.0	1,104	0.671
2	.....	.9	.2	77.8	18.7	2.4	.....	100.0	1,105	.667
3	.....	.9	.1	77.9	18.3	2.8	.....	100.0	1,099	.666
4	.....	.9	.2	78.5	18.1	2.3	.....	100.0	1,101	.663
5	.....	1.0	.0	77.0	19.8	2.2	.....	100.0	1,116	.671
6	.....	1.0	.0	78.7	17.3	3.0	.....	100.0	1,089	.662
7	.....	0.9	.0	78.7	18.7	1.7	.....	100.0	1,114	.663
8	.....	1.0	.1	76.1	19.6	3.2	.....	100.0	1,104	.675
9	.....	1.0	.1	74.3	20.6	4.0	.....	100.0	1,104	.683
10	.....	0.9	.1	75.1	20.5	3.4	.....	100.0	1,109	.679
Avg	.....	0.9	0.1	77.1	19.1	2.8	.....	100.0	1,105	0.670

TABLE 1.—*Analytical data reported by the cooperatiing laboratories*—Continued

LABORATORY NUMBER 7

Method *A* — Apparatus V_1R_1Hg-Allen

Anal. No.	Analyst	Percentage by volume							Calculated	
		CO_2	O_2	CH_4	C_2H_6	N_2	(C_3H_8)	Total	Btu/ft³	sp gr
	F	1.05	0.28	76.07	20.26	2.34	.....	100.0	1115.1	0.6762
				75.93	19.93	2.81	.....	100.0	1107.9	.6765
				76.88	19.19	2.60	.....	100.0	1104.4	.6720
	F	1.06	.40	75.77	20.16	2.61	.....	100.0	1110.3	.6776
				76.43	19.72	2.39	.....	100.0	1109.2	.6745
				76.26	19.84	2.44	.....	100.0	1109.6	.6753
	F	1.02	.39	75.42	20.35	2.82	.....	100.0	1110.2	.6790
				75.43	20.21	2.95	.....	100.0	1107.8	.6788
				76.39	19.43	2.77	.....	100.0	1103.7	.6742
	F	1.13	.60	75.64	20.14	2.49	.....	100.0	1108.7	.6788
				76.54	19.09	2.64	.....	100.0	1099.2	.6742
Avg	.....	1.06	0.40	76.07	19.85	2.62	.....	100.0	1107.8	0.6761

LABORATORY NUMBER 8

Method *A* — Apparatus V_1R_1Hg-Burrell

1	RJG	1.10	0.10	78.50	18.35	1.95	.....	100.00	1,105	0.665
2	RJG	1.10	.20	77.75	18.90	2.05	.....	100.00	1,108	.668
3	RJG	1.05	.20	78.40	18.50	1.85	.....	100.00	1,107	.665
4	RJG	1.15	.20	78.75	18.15	1.75	.....	100.00	1,106	.664
5	RJG	1.10	.20	78.40	18.40	1.90	.....	100.00	1,105	.665
Avg	.....	1.10	0.20	78.35	18.45	1.90	.....	100.00	1,106	0.665

LABORATORY NUMBER 9

Method *A* — Apparatus V_2R_2Hg-Hempel

1	MLN	0.8	0.1	76.2	19.1	3.8	.....	100.0	1,096	0.673
2	MLN	.9	.2	75.3	20.1	3.5	.....	100.0	1,105	.678
3	MLN	.7	.2	75.5	20.1	3.5	.....	100.0	1,107	.676
4	MLN	.7	.1	74.9	20.6	3.7	.....	100.0	1,109	.679
5	MLN	.9	.2	76.8	19.2	2.9	.....	100.0	1,104	.679
6	MLN	.9	.2	76.3	19.5	3.1	.....	100.0	1,104	.674
7	MLN	1.0	.2	75.6	20.1	3.1	.....	100.0	1,108	.678
8	MLN	0.7	.1	77.7	19.0	2.5	.....	100.0	1,109	.666
9	MLN	.6	.2	76.6	19.5	3.1	.....	100.0	1,107	.671
10	MLN	.9	.1	77.3	18.9	2.8	.....	100.0	1,104	.663
Avg	.....	0.81	0.16	76.22	19.61	3.10	.....	.....	1,105	0.674

LABORATORY NUMBER 10

Method *A* — Apparatus V_1R_1Hg-Burrell

1	.....	1.17	0.53	74.34	18.10	5.86	.....	100.00	1,060	0.683
2	.....	1.18	.54	75.53	18.10	4.65	.....	100.00	1,072	.678
3	.....	1.18	.43	75.49	19.46	3.44	.....	100.00	1,095	.679
4	.....	1.12	.41	77.16	18.28	3.03	.....	100.00	1,091	.671
5	.....	1.28	.43	79.42	17.07	1.80	.....	100.00	1,092	.661
6	.....	1.12	.41	78.16	16.83	3.48	.....	100.00	1,076	.665
7	.....	1.25	.42	78.70	17.05	2.58	.....	100.00	1,085	.669
8	.....	1.14	.41	77.13	17.83	3.49	.....	100.00	1,083	.671
9	.....	1.17	.43	79.57	16.96	1.87	.....	100.00	1,092	.660
10	.....	1.06	.42	78.88	17.40	2.24	.....	100.00	1,093	.662
Avg	.....	1.17	0.44	77.44	17.71	3.24	.....	100.00	1,084	0.670

TABLE 1.—*Analytical data reported by the cooperating laboratories*—Continued

LABORATORY NUMBER 11

Method *A* — Apparatus V_1R_1Hg.

Anal. No.	Analyst	Percentage by volume							Calculated	
		CO_2	O_2	CH_4	C_2H_6	N_2	(C_3H_8)	Total	Btu/ft³	sp. gr
1	HFB	1.00	0.30	16.70	80.00	2.00	.....	100.00	1,092	0.657
2	HFb	1.00	.30	17.20	78.80	2.70	.....	100.00	1,088	.662
3	HFB	1.00	.40	17.00	79.30	2.30	.....	100.00	1,090	.660
4	HFB	1.05	.35	17.50	78.30	2.80	.....	100.00	1,089	.663
5	HFB	1.05	.40	16.80	79.90	1.85	.....	100.00	1,092	.657
6	HFB	1.05	.35	17.00	79.95	1.65	.....	100.00	1,096	.657
7	HFB	1.00	.40	16.80	80.10	1.70	.....	100.00	1,095	.656
8	HFB	1.00	.30	17.10	79.80	1.80	.....	100.00	1,096	.657
9	HFB	1.00	.40	17.40	78.70	2.50	.....	100.00	1,092	.661
10	HFB	1.05	.35	16.90	79.90	1.80	.....	100.00	1,094	.657
Avg	.....	1.02	0.35	17.04	79.48	2.11	.....	100.00	1,092.4	0.659

LABORATORY NUMBER 12

Method *A* — Apparatus V_1R_1—Fischer

1	R	0.9	0.1	85.2	13.7	0.1	.....	100.0	1,091	0.632
2	R	1.0	.1	82.2	16.4	.3	.....	100.0	1,108	.647
3	R	0.9	.1	79.7	17.7	1.6	.....	100.0	1,106	.658
4	R	.9	.1	82.8	15.5	0.7	.....	100.0	1,098	.643
5	R	.9	.1	83.9	14.7	.4	.....	100.0	1,095	.639
Avg	.....	0.9	0.1	82.8	15.6	0.6 (by diff.)	.....	100.0	1,100	0.643

LABORATORY NUMBER 13

Method *A* — Apparatus V_1R_1Hg—Burrell—U. S. Steel

1	H	1.10	1.10	78.15	18.35	5.75	.....	104.45	1,102	0.711
2	H	1.25	1.00	79.60	17.55	5.60	.....	105.00	1,102	.710
3	H	1.10	1.05	79.50	17.60	5.10	.....	104.35	1,103	.703
4	H	1.15	1.10	77.60	18.85	5.35	.....	104.05	1,106	.710
5	H	1.20	1.00	75.85	18.95	5.40	.....	102.40	1,090	.701
6	H	1.25	1.00	78.00	18.30	5.00	.....	103.55	1,100	.703
7	H	1.25	1.15	77.25	18.10	4.75	.....	102.50	1,089	.696
Avg	.....	1.19	1.06	77.99	18.24	5.28	.....	103.76	1,099	0.705

LABORATORY NUMBER 14

Method *A* — Apparatus V_1R_1Hg—Elliott—Burrell

1	A	0.8	0.4	79.0	17.4	2.4	.....	100.0	1,094	0.661
2	A	.9	.4	78.8	17.2	2.7	.....	100.0	1,089	.662
3	A	.8	.3	78.4	17.3	3.2	.....	100.0	1,086	.663
4	A	1.0	.2	78.0	17.9	2.9	.....	100.0	1,093	.666
5	A	0.8	.3	78.4	17.3	3.2	.....	100.0	1,086	.663
6	B	1.1	.3	79.3	17.4	1.9	.....	100.0	1,097	.661
7	B	1.0	.4	77.9	18.0	2.7	.....	100.0	1,094	.667
8	B	1.0	.4	77.2	18.4	3.0	.....	100.0	1,094	.670
9	B	1.1	.3	76.7	18.9	3.0	.....	100.0	1,097	.673
10	B	1.0	.3	79.4	17.6	1.7	.....	100.0	1,102	.660
Avg	.....	1.0	0.3	78.3	17.7	2.7	.....	100.0	1,093	0.665

TABLE 1.—*Analytical data reported by the cooperating laboratories*—Continued

LABORATORY NUMBER 15

Method *A*

Apparatus $V_3R_1R_2H_2O$-$Na_2SO_4H_2SO_4$ Modified Williams

Anal. No.	Analyst	Percentage by volume							Calculated	
		CO_2	O_2	CH_4	C_2H_6	N_2	(C_3H_8)	Total	Btu/ft³	sp gr
1	RWG	1.2	0.2	76.9	20.4	1.3	Not Detd.	100.0	1125.8	0.6735
2	RWG	1.2	.2	77.3	20.2	1.1	...do....	100.0	1126.3	.6718
3	RWG	1.5	.2	73.8	22.7	1.8	...do....	100.0	1135.4	.6899
4	RWG	1.0	.2	78.3	20.0	0.5	...do....	100.0	1132.8	.6664
5	RWG	1.4	.2	77.3	20.1	1.0	...do....	100.0	1124.6	.6728
6	RWG	1.0	.2	76.0	21.3	1.5	...do....	100.0	1132.7	.6769
7	RWG	1.3	.2	73.3	22.7	2.5	...do....	100.0	1130.4	.6910
8	RWG	1.1	.2	74.8	22.1	1.8	...do....	100.0	1134.8	.6831
9	RWG	1.1	.2	76.7	20.8	1.2	...do....	100.0	1130.9	.6742
10	RWG	1.3	.2	78.4	19.3	0.8	...do....	100.0	1121.5	.6670
Avg	------	1.2	0.2	76.3	21.0	1.3	------	------	1129.5	0.6767
1	RWG	1.2	0.3	------	------	------	------	------	------	------
2	------	0.9	.2	------	------	------	------	------	------	------
3	------	1.0	.2	------	------	------	------	------	------	------
4	------	1.0	.1	------	------	------	------	------	------	------
5	------	1.2	.3	------	------	------	------	------	------	------
6	------	1.0	.0	------	------	------	------	------	------	------
7	------	1.2	.0	------	------	------	------	------	------	------
Avg	------	1.1	0.2	------	------	------	------	------	------	------

LABORATORY NUMBER 16

Method *A*

Apparatus V_1R_1Hg—U. S. Steel, Modified

1	U	1.0	0.0	74.5	20.5	4.0	------	100.0	1,104	0.682
2	U	1.0	.0	75.1	19.9	4.0	------	100.0	1,099	.679
3	U	0.9	.0	76.7	18.9	3.5	------	100.0	1,097	.671
4	U	1.0	.0	76.4	19.9	2.7	------	100.0	1,112	.674
5[b]	U	.9	.0	76.6	18.9	3.6	------	100.0	1,096	.671
Avg	------	1.0	0.0	75.9	19.6	3.5	------	100.0	1,102	0.675

LABORATORY NUMBER 17

Method *A*

Apparatus V_1R_1Hg-U. S. Steel

1	A	1.0	0.1	76.9	19.2	2.8	------	100.0	1,105	0.671
2	A	1.0	.1	76.5	19.2	3.2	------	100.9	1,101	.673
3	A	1.0	.1	77.5	18.7	2.7	------	100.0	1,102	.669
4	A	0.9	.1	77.6	18.7	2.7	------	100.0	1,103	.668
5	A	1.0	.1	77.5	18.7	2.7	------	100.0	1,102	.669
6	A	1.0	.0	76.8	19.5	2.7	------	100.0	1,109	.672
7	A	1.0	.0	77.6	18.9	2.5	------	100.0	1,106	.668
8	A	0.9	.1	76.8	19.5	2.7	------	100.0	1,109	.672
9	A	1.0	.1	76.9	19.2	2.8	------	100.0	1,105	.671
10	A	1.0	.0	76.8	19.5	2.7	------	100.0	1,109	.672
Avg	------	0.98	0.07	77.09	19.11	2.75	------	------	1,105	0.671
1	B[1]	1.0	0.0	77.2	18.9	2.9	------	100.0	1,102	0.670
2	B	1.0	0	77.2	18.7	3.1	------	100.0	1,099	.670
Avg	------	1.0	0.0	77.2	18.8	3.0	------	------	1,101	0.670

See footnotes at end of table.

TABLE 1.—*Analytical data reported by the cooperating laboratories*—Continued

LABORATORY NUMBER 18

Method *A*

Apparatus V_1H_1Hg-Bureau of Mines

Anal. No.	Analyst	Percentage by volume							Calculated	
		CO_2	O_2	CH_4	C_2H_6	N_2	(C_3H_8)	Total	Btu/ft³	sp gr
1	H	1.0	0.2	77.5	18.9	2.4	.....	100.0	1105.5	0.6688
2	H	1.3	.0	76.9	19.2	2.6	.....	100.0	1104.7	.6730
3	H	1.0	.0	77.1	19.2	2.7	.....	100.0	1106.7	.6701
4	H	1.0	.2	77.7	18.7	2.7	.....	100.0	1103.9	.6678
5	H	1.0	.0	77.3	19.3	2.4	.....	100.0	1110.5	.6697
6	M	0.7	.2	77.7	18.9	2.5	.....	100.0	1107.5	.6663
7	M	1.3	.0	77.3	19.0	2.4	.....	100.0	1105.2	.6711
8	M	1.1	.0	76.8	19.2	2.9	.....	100.0	1103.7	.6723
9	M	1.0	.3	77.3	19.0	2.4	.....	100.0	1105.2	.6699
10	M	1.0	.3	78.1	18.7	1.9	.....	100.0	1107.9	.6663
Avg	.....	1.04	0.12	77.37	19.01	2.46	.....	100.0	1106.1	0.6696
		Same experimental data as above, but corrected for 0.14 ml of water in burette								
1	H	1.0	0.2	76.3	19.6	2.9	.....	100.0	1105.8	0.6744
2	H	1.3	.0	75.7	19.9	3.1	.....	100.0	1105.0	.6785
3	H	1.0	.0	75.9	20.0	3.1	.....	100.0	1108.8	.6761
4	H	1.0	.2	76.6	19.4	2.8	.....	100.0	1105.2	.6730
5	H	1.0	.0	76.0	20.0	3.0	.....	100.0	1109.8	.6757
6	M	0.7	.2	76.5	19.6	3.0	.....	100.0	1107.8	.6719
7	M	1.3	.0	76.1	19.8	2.8	.....	100.0	1107.3	.6768
8	M	1.1	.0	75.6	20.0	3.3	.....	100.0	1105.8	.6779
9	M	1.0	.3	76.2	19.8	2.7	.....	100.0	1108.3	.6751
10	M	1.0	.3	76.9	19.4	2.4	.....	100.0	1108.2	.6718
Avg	.....	1.04	0.12	76.18	19.75	2.91	.....	100.0	1107.2	0.6751

LABORATORY NUMBER 19

Method *A*

Apparatus V_1R_1Hg-U. S. Steel

1	SCG	0.95	0.0	77.57	18.28	3.20	.....	100.0	1095.2	0.6673
2	SCG	.93	.0	77.25	18.29	3.53	.....	100.0	1092.2	.6667
3	SCG	.93	.0	77.12	18.51	3.44	.....	100.0	1094.8	.6694
4	SCG	.92	.0	77.48	18.22	3.38	.....	100.0	1093.3	.6676
5	SCG	.92	.0	77.46	18.13	3.49	.....	100.0	1091.5	.6677
6	SCG	.91	.0	77.55	18.16	3.38	.....	100.0	1092.9	.6673
7	SCG	.90	.0	76.75	18.45	3.90	.....	100.0	1090.0	.6708
8	SCG	.92	.0	77.32	18.48	3.28	.....	100.0	1096.3	.6685
9	SCG	.91	.0	77.67	17.96	3.46	.....	100.0	1090.6	.6666
10	SCG	.91	.0	76.98	18.63	3.48	.....	100.0	1095.5	.6700
Avg	.....	0.92	0.0	77.32	18.31	3.45	.....	100.0	1093.2	0.6684

TABLE 1.—*Analytical data reported by the cooperating laboratories*—Continued

LABORATORY NUMBER 20

Method *A*

Apparatus V_1R_1Hg–U. S. Steel

Anal. No.	Analyst	Percentage by volume							Calculated	
		CO_2	O_2	CH_4	C_2H_6	N_2	(C_3H_8)	Total	Btu/ft³	sp gr
1	A	0.9	0.1	78.9	17.6	2.5	Not detd.	100.0	1,097	0.6613
2	A	.9	.1	78.7	18.2	2.1	do	100.0	1,105	.6626
3	A	1.0	.1	81.1	15.7	2.1	do	100.0	1,086	.6512
4	A	1.0	.1	79.1	17.5	2.3	do	100.0	1,097	.6609
5	A	0.9	.1	78.7	17.8	2.5	do	100.0	1,098	.6623
6	A	.9	.1	79.3	17.3	2.4	do	100.0	1,095	.6594
7	A	1.0	.2	78.5	18.0	2.3	do	100.0	1,100	.6639
8	A	1.0	.2	77.1	18.9	2.8	do	100.0	1,101	.6705
9	A	1.0	.2	78.1	18.2	2.5	do	100.0	1,099	.6658
Avg	------	1.0	0.1	78.8	17.7	2.4	------	100.0	1,098	0.6620
1	B	0.9	0.0	78.9	17.5	2.7	Not detd.	100.0	1,095	0.6615
2	B	.9	.0	80.2	16.5	2.4	do	100.0	1,090	.6549
3	B	.9	.0	76.9	19.5	2.7	do	100.0	1,109	.6714
4	B	.9	.0	79.3	17.5	2.3	do	100.0	1,099	.6594
5	B	.9	.1	77.4	19.2	2.4	do	100.0	1,110	.6688
6	B	.9	.1	79.2	17.8	2.0	do	100.0	1,103	.6602
7	B	.9	.0	78.7	17.7	2.7	do	100.0	1,096	.6624
8	B	.9	.0	79.0	17.8	2.3	do	100.0	1,101	.6609
9	B	.9	.1	78.0	18.9	2.1	do	100.0	1,111	.6660
Avg	------	0.9	0.0	78.7	18.0	2.4	------	100.0	1,102	0.6628

LABORATORY NUMBER 21

Method *II*

Apparatus V_2R_1Hg-Burrell

Anal. No.	Analyst	Percentage by volume								Calculated	
		CO_2	O_2	CH_4	C_2H_6	N_2	C_2H_4	CO	H_2	Btu/ft³	sp gr
1	1	1.0	0.0	75.5	17.3	4.4	0.6	0.4	0.8	1070.6	0.6684
2	1	1.0	.0	73.4	18.1	6.0	.5	.5	.5	1061.5	.6805
3	1	1.0	.0	74.3	17.7	5.2	.8	.5	.5	1068.2	.6765
4	1	1.0	.0	74.6	17.2	5.7	.5	.5	.5	1057.7	.6748
5	1	1.0	.0	74.7	17.7	5.0	.8	.5	.3	1071.5	.6766
Avg	------	1.0	.0	74.5	17.6	5.3	.6	.5	.5	1065.9	.6754

TABLE 1.—*Analytical data reported by the cooperating laboratories*—Continued

LABORATORY NUMBER 22

Method *A* — Apparatus V_1R_1Hg and V_2R_1H-O-Na

Anal. No.	Analyst	Percentage by volume							Calculated	
		CO_2	O_2	CH_4	C_2H_6	N_2	(C_3H_8)	Total	Btu/ft³	sp gr
1	M	1.0	0.0	72.8	21.7	4.5	.....	100.0	1,108	0.690
2	M	1.1	.1	75.1	19.9	3.8	.....	100.0	1,099	.680
3	M	1.9	.0	73.6	21.3	4.1	.....	100.0	1,109	.687
4	M	1.0	.0	73.4	22.1	3.5	.....	100.0	1,121	.688
5	M	1.0	.1	73.3	21.0	4.6	.....	100.0	1,101	.688
6	M	1.0	.1	76.6	19.1	3.2	.....	100.0	1,100	.671
7	M	1.0	.0	72.7	21.4	4.9	.....	100.0	1,102	.691
8	M	1.0	.0	72.7	22.0	4.3	.....	100.0	1,112	.691
9	M	1.0	.0	74.0	21.3	3.7	.....	100.0	1,113	.685
10	M	1.0	.0	74.4	21.1	3.5	.....	100.0	1,113	.684
Avg	.....	1.0	0.0	73.9	21.1	4.0	.....	100.0	1,108	.686
1	N	0.9	0.1	74.4	20.7	4.1	.....	100.2	1,106	0.684
2	N	.9	.0	74.8	20.4	4.0	.....	100.1	1,105	.681
3	N	1.0	.0	75.9	19.8	3.9	.....	100.6	1,105	.676
Avg	.....	0.9	0.0	75.0	20.3	4.0	.....	100.3	1,105	.680

LABORATORY NUMBER 23

Method *A* — Apparatus V_1R_1Hg-Burr

1	M	1.0	0.2	76.6	18.8	3.4	.....	100.0	1,095	0.672
2	M	1.0	.2	75.5	19.7	3.6	.....	100.0	1,100	.678
3	M	1.0	.1	77.8	18.4	2.6	.....	100.0	1,100	.666
4	M	1.0	.2	77.8	18.5	2.5	.....	100.0	1,101	.667
5	M	1.0	.2	77.3	18.5	3.0	.....	100.0	1,096	.669
6	M	1.0	.2	77.0	18.7	3.1	.....	100.0	1,097	.671
7	M	1.0	.2	74.5	20.2	4.1	.....	100.0	1,098	.682
8	M	1.0	.2	78.4	18.3	2.1	.....	100.0	1,104	.663
9	M	1.0	.2	78.6	17.9	2.3	.....	100.0	1,099	.663
10	M	1.0	.2	76.4	19.0	3.4	.....	100.0	1,096	.673
11	M	1.0	.2	76.1	18.3	4.4	.....	100.0	1,081	.674
12	M	1.0	.2	75.8	18.6	4.4	.....	100.0	1,083	.676
13	M	1.0	.2	77.0	19.3	2.5	.....	100.0	1,107	.671
14	M	1.0	.2	76.4	19.5	2.9	.....	100.0	1,105	.674
15	M	1.0	.2	76.9	19.1	2.8	.....	100.0	1,102	.671
16	M	1.0	.2	77.9	19.0	1.9	.....	100.0	1,111	.668
Avg	.....	1.0	0.2	76.9	18.9	3.1	.....	100.0	1,099	0.671
1	K	1.0	0.2	75.1	20.2	3.5	.....	100.0	1,104	0.679
2	K	1.0	.2	74.7	20.4	3.7	.....	100.0	1,104	.682
3	K	1.0	.2	74.8	20.3	3.7	.....	100.0	1,103	.680
4	K	1.0	.2	75.7	19.7	3.4	.....	100.0	1,102	.673
5	K	1.0	.2	75.2	19.7	3.9	.....	100.0	1,097	.679
6	K	1.0	.2	74.7	20.3	3.8	.....	100.0	1,102	.681
7	K	1.0	.2	74.9	20.5	3.4	.....	100.0	1,108	.680
8	K	1.0	.2	75.7	19.7	3.4	.....	100.0	1,102	.676
9	K	1.0	.2	74.8	20.5	3.5	.....	100.0	1,107	.681
10	K	1.0	.2	74.8	20.6	3.4	.....	100.0	1,108	.680
Avg	.....	1.0	0.2	75.0	20.2	3.6	.....	100.0	1,104	0.679

TABLE 1.—*Analytical data reported by the cooperating laboratories*—Continued

LABORATORY NUMBER 24

Method *A* — Apparatus V_1R_1Hg-Burrell

Anal. No.	Analyst	Percentage by volume							Calculated	
		CO_2	O_2	CH_4	C_2H_6	N_2	(C_3H_8)	Total	Btu/ft³	sp gr
1	H	0.9	0.0	77.2	18.1	3.3	0.5	100.0	1,101	0.6714
2	H	1.0	.0	77.2	18.1	3.1	.6	100.0	1,104	.6723
3	H	1.0	.0	76.7	18.5	3.2	.6	100.0	1,106	.6751
4	H	0.9	.0	77.0	18.4	3.2	.5	100.0	1,104	.6727
5	H	1.0	.0	76.8	18.4	3.2	.6	100.0	1,105	.6749
6	H	1.0	.0	76.6	18.3	3.6	.5	100.0	1,099	.6749
7	H	1.0	.0	76.5	18.7	3.2	.6	100.0	1,107	.6762
8	H	1.0	.0	76.0	19.1	3.3	.6	100.0	1,108	.6779
9	H	1.0	.0	75.9	18.9	3.6	.6	100.0	1,104	.6785
10	H	1.0	.0	76.8	18.4	3.1	.7	100.0	1,108	.6754
Avg		1.0	0.0	76.7	18.5	3.2	0.6	100.0	1,106	0.6751
1	C	0.9	0.0	77.1	18.1	3.2	0.7	100.0	1105.1	0.6731
2	C	.9	.0	77.4	18.0	3.2	.5	100.0	1101.2	.6707
3	C	1.0	.0	76.9	18.3	3.3	.5	100.0	1101.5	.6735
4	C	1.0	.0	77.4	17.9	3.0	.7	100.0	1104.6	.6723
5	C	.9	.0	77.3	18.1	3.2	.5	100.0	1102.0	.6712
6	C	1.0	.0	77.2	18.2	3.1	.5	100.0	1102.7	.6722
7	C	.9	.1	77.5	18.0	3.0	.5	100.0	1102.3	.6705
8	C	1.0	.0	77.0	18.3	3.1	.6	100.0	1105.1	.6737
9	C	1.0	.0	77.7	18.0	2.8	.5	100.0	1104.3	.6685
10	C	1.0	.0	77.2	18.4	2.9	.5	100.0	1106.3	.6724
Avg		1.0	0.0	77.3	18.1	3.1	0.5	100.0	1103.5	0.6718

LABORATORY NUMBER 25

Method *A* — Apparatus V_1R_1Hg-Burrell

1	HRH	0.90	0.00	75.41	19.74	3.95	------	100.0	1099.4	0.6774
2	HRH	1.00	.10	77.71	18.05	3.14	------	100.0	1092.6	.6671
3	HRH	1.00	.00	76.12	19.20	3.68	------	100.0	1096.9	.6745
4	HRH	0.90	.00	78.09	17.71	3.30	------	100.0	1090.4	.6646
5	HRH	.90	.00	77.30	17.98	3.82	------	100.0	1087.3	.6681
6	HRH	.90	.00	76.90	18.57	3.63	------	100.0	1093.6	.6702
7	HRH	.90	.00	77.66	17.57	3.87	------	100.0	1083.6	.6663
8	HRH	1.00	.00	78.10	17.39	3.51	------	100.0	1084.9	.6649
9	HRH	.90	.00	77.42	17.88	3.80	------	100.0	1086.7	.6675
10	HRH	.90	.00	76.82	18.65	3.63	------	100.0	1094.3	.6706
Avg		0.93	0.01	77.15	18.28	3.63	------	100.0	1091.0	0.6691

LABORATORY NUMBER 26

Method *A* — Apparatus V_1R_1Hg-Burrell

1	------	0.90	0.0	82.74	13.72	2.94	------	100.30	1,066	0.645
2	------	.81	.0	80.70	14.85	3.60	------	99.96	1,066	.645
3	------	.90	.0	78.99	15.71	4.38	------	99.98	1,064	.659
4	------	1.00	.0	79.80	16.15	3.27	------	100.22	1,079	.659
5	------	1.00	.0	84.00	13.38	2.26	------	100.64	1,073	.643
6	------	0.83	.0	85.50	12.60	2.60	------	101.53	1,075	.644
7	------	.90	.0	82.75	13.06	3.27	------	99.98	1,055	.641
8	------	.90	.0	83.50	12.64	3.27	------	100.31	1,054	.641
9	------	1.12	.0	80.30	15.80	2.92	------	100.14	1,054	.656
10	------	0.90	.0	79.60	16.36	3.15	------	100.01	1,081	.657
Avg	------	0.93	------	81.79	14.43	3.17	------	100.32	1,067	0.649

TABLE 1.—*Analytical data reported by the cooperating laboratories*—Continued

LABORATORY NUMBER 27

Method *A*

Apparatus V_1R_1Hg-Bur

Anal. No.	Analyst	Percent by volume							Calculated	
		CO_2	O_2	CH_4	C_2H_6	N_2	(C_3H_8)	Total[c]	Btu/ft³	sp gr
1	CMD	0.9	1.5	74.3	20.0	3.3	.....	93.4	1092.86	0.694
2	CMD	.9	0.9	73.3	21.5	3.4	.....	94.2	1109.27	.691
3	CMD	.9	.9	69.1	23.9	5.2	.....	93.7	1107.84	.707
4	CMD	.9	.0	.....	.....	4.7	.....	94.4	.....	.....
5	CMD	1.0	.0	.....	.....	4.9	.....	94.1	.....	.....
6	CMD	0.9	.3	.....	.....	4.8	.....	94.0	.....	.....
7	CMD	.9	.0	.....	.....	4.9	.....	94.2	.....	.....
8	CMD	1.1	.0	.....	.....	4.7	.....	94.2	.....	.....
Avg	.....	0.94	0.45	72.2	21.8	4.5	.....	94.0	1103.32	0.697

LABORATORY NUMBER 28

Methods *A* and *X*

Apparatus V_1R_1Hg-Burrell-Oberfell and Distillation Appara

Anal. No.	Analyst	Percent by volume							Calculated	
		CO_2	O_2	CH_4[e]	C_2H_6	N_2	(C_3H_8)	Total	Btu/ft³	sp gr
1	FWM	1.00	0.05	73.30	21.55	4.10	[d]	100.00	1110.2	0.682
2	FWM	1.05	.00	73.20	21.00	4.45	[d]	100.00	1102.5	.687
3	FWM	1.00	.05	74.45	20.75	3.75	[d]	100.00	1107.6	.683
4	FWM	1.05	.10	74.60	20.60	3.65	[d]	100.00	1106.4	.682
5	FWM	1.05	.05	75.10	19.90	3.90	[d]	100.00	1099.1	.676
6	FWM	1.10	.05	74.00	21.20	3.65	[d]	100.00	1111.0	.686
7	FWM	1.10	.10	74.40	20.50	3.90	[d]	100.00	1102.7	.683
8	FWM	1.05	.00	75.00	19.95	4.00	[d]	100.00	1099.0	.680
9	FWM	1.00	.10	75.10	19.55	4.25	[d]	100.00	1092.9	.676
10	FWM	1.00	.10	74.40	20.30	4.20	[d]	100.00	1099.1	.682
Avg	.....	1.05	0.05	74.40	20.55	3.95	[d]	100.00	1103.0	0.683

LABORATORY NUMBER 29

Method *X*

Apparatus V_2R_1—Gockel and Distillation Apparatus

1	E	[f] 0.8	0.2	77.1	[g] 14.1	4.8	[g] 3.0	100.0	1092.8	0.682
2	E	.8	.3	76.8	14.1	5.0	3.0	100.0	1089.8	.684
3	E	.8	.2	77.0	14.1	4.9	3.0	100.0	1091.8	.683
4	E	.8	.2	76.9	14.1	5.0	3.0	100.0	1090.8	.684
5	E	.8	.3	77.1	14.1	4.7	3.0	100.0	1092.8	.680
6	.....	.....	.....	.....	.....	4.88	.....	.....	.....	.....
7	.....	.....	.....	.....	.....	5.0	.....	.....	.....	.....
8	.....	.....	.....	.....	.....	4.7	.....	.....	.....	.....
Avg	.....	0.8	0.24	76.98	14.1	4.88	3.0	100.0	1091.6	0.682
Maximum	.....	.9	.30	77.1	.....	5.0	.....	.....	1092.8	0.684
Minimum	.....	.7	.20	76.8	.....	4.7	.....	.....	1089.8	0.680

See footnote at end of table.

TABLE 1.—*Analytical data reported by the cooperating laboratories*—Continued

LABORATORY NUMBER 30

Method Y

Apparatus V_1R_1 Hg and distillation apparatus

Anal. No.	Analyst	Percentage by volume							Calculated	
		CO_2	O_2	CH_4	C_2H_6	N_2	(C_3H_8)	Total	Btu/ft ^{3}	sp gr
1	JHS	1.05	0.05	.....	.....	.....	.....	.....	.....	.....
2	JHS	1.00	.00	79.7	15.0	0.0	4.3	100.00	[b] 1157.4	0.6817
3	JHS	1.00	.05	.....	.....	.....	.....	.....	.....	.....
4	JHS	1.00	.00	81.6	14.5	.0	2.9	100.00	1142.3	.6651
5	JHS	1.00	.00	.....	.....	.....	.....	.....	.....	.....
6	JHS	1.02	.00	.....	.....	.....	.....	.....	.....	.....
7	JHS	1.00	.00	.....	.....	.....	.....	.....	.....	.....
8	JHS	0.86	.00	.....	.....	.....	.....	.....	.....	.....
9	JHS	0.97	.00	.....	.....	.....	.....	.....	.....	.....
10	JHS	1.01	.00	.....	.....	.....	.....	.....	.....	.....
Avg	.....	1.00	0.00	80.6	14.8	0.0	3.6	100.00	1155.2	0.6736

[a] Erroneous result; apparatus not completely flushed with nitrogen in preparing for analysis.
[b] Gas sample exhausted after this analysis.
[c] Total combustibles; numbers 1, 2, and 3—wet manifold; numbers 5, 6, 7, and 8—dry manifold.
[d] Propane assumed absent.
[e] Total hydrocarbon volume determined by difference, nitrogen directly determined.
[f] Obtained from average of absorption analyses.
[g] Obtained from fractionation analysis of small sample.
[h] Heating value computed, using given factors and analysis on dry basis. Average heating value and specific gravity computed from average composition.
[i] Analyst *B* did not have enough time to complete any more of the analyses.

WASHINGTON, June 20, 1946.

U. S. Department of Commerce
National Bureau of Standards

Research Paper RP1760
Volume 38, January 1947

Part of the Journal of Research of the National Bureau of Standards

Purification, Purity, and Freezing Points of 8 Nonanes, 11 Alkylcyclopentanes, 6 Alkylcyclohexanes, and 4 Butylbenzenes of the API-Standard and API-NBS Series*[1]

By Anton J. Streiff,[2] Evelyn T. Murphy,[2] Janice C. Cahill,[2] Helen F. Flanagan,[2] Vincent A. Sedlak,[2] Charles B. Willingham, and Frederick D. Rossini

This report describes the purification and determination of freezing points and purity of 29 hydrocarbons of the API-Standard and API–NBS series, including 8 nonanes, 11 alkylcyclopentanes, 6 alkylcyclohexanes, and 4 butylbenzenes.

I. Introduction

A previous report described the purification, and determination of freezing points and purity of 37 hydrocarbon compounds of the API-Standard and API–NBS series, which were produced as part of the cooperative program on standard samples of hydrocarbons of the National Bureau of Standards and the American Petroleum Institute. This report describes the purification and determination of freezing points and purity of an additional 29 hydrocarbon compounds under this cooperative program, including 8 nonanes, 6 alkylcyclohexanes, 11 alkylcyclopentanes, and 4 butylbenzenes.[3]

The final lots of the material labeled API-Standard are sealed "in vacuum" in glass ampoules and made available as NBS standard samples of hydrocarbons [4].** The material labeled API–NBS is made available in appropriate small lots on loan to qualified investigators for the measurement of needed properties.[4]

II. Materials

The starting materials were supplied as follows:[5]

By the API Research Project 45 on the "Synthesis and Properties of Hydrocarbons of Low Molecular Weight" at the Ohio State University, Columbus, Ohio, under the supervision of C. E. Boord:

3,3-Diethylpentane.
2,2,3,3-Tetramethylpentane.
Ethylcyclohexane (*B*).
1,1-Dimethylcyclohexane.
cis-1,2-Dimethylcyclohexane.
trans-1,2-Dimethylcyclohexane.
Ethylcyclopentane (one-half) (*B*).
trans-1,3-Dimethylcyclopentane.
n-Propylcyclopentane.
Isopropylcyclopentane.
1,1,3-Trimethylcyclopentane (three-fourths).

*Presented before the Division of Petroleum Chemistry of the American Chemical Society, Chicago, Ill., September 1946.

**Figures in brackets indicate the literature references at the end of this paper.

[1] This investigation was performed at the National Bureau of Standards as part of the work of the American Petroleum Institute Research Project 6 on the Analysis, Purification, and Properties of Hydrocarbons.

[2] Research Associate on the American Petroleum Institute Research Project at the National Bureau of Standards.

[3] The cooperative program was carried on under the API Research Project 46 Committee on Hydrocarbons for Spectrometer Calibration (W. J. Sweeney, chairman). Further details are given in references [1, 2, 3].

[4] The allocation of the API-NBS samples of hydrocarbons is handled by the Advisory Committee for the API Research Project 44 on the "Collection, Analysis, and Calculation of Data on the Properties of Hydrocarbons" (W. E. Kuhn, chairman).

[5] (*B*) following the name of a compound indicates that, for the API–NBS series, it is a second (and usually slightly purer) sample of the given compound, the first sample of which is labeled (*A*). (See reference [5]).

By the Hydrocarbon Laboratory at the Pennsylvania State College, State College, Pa., under the supervision of F. C. Whitmore:

2,4,4-Trimethylhexane.
Ethylcyclopentane (one-half) (*B*).
1,1-Dimethylcyclopentane.
cis-1,2-Dimethylcyclopentane.
trans-1,2-Dimethylcyclopentane.
1,1,2-Trimethylcyclopentane.
cis, cis, trans-1,2,4-Trimethylcyclopentane.
cis, trans, cis-1,2,4-Trimethylcyclopentane.

By the National Advisory Committee for Aeronautics, through its Aeronautical Engine Research Laboratory at Cleveland, Ohio, and the Automotive Section at the National Bureau of Standards:

n-Butylbenzene (*B*).
Isobutylbenzene (*B*).
sec-Butylbenzene (*B*).
tert-Butylbenzene (*B*).
2,2,3,4-Tetramethylpentane.
2,2,4,4-Tetramethylpentane.
2,3,3,4-Tetramethylpentane.

By the Standard Oil Development Co., Elizabeth, N. J., through W. J. Sweeney:

cis-1,4-Dimethylcyclohexane. *trans*-1,4-Dimethylcyclohexane.

By the Gulf Oil Co. Fellowship at the Mellon Institute of Industrial Research, Pittsburgh, Pa., through W. A. Gruse:

1,1,3-Trimethylcyclopentane (one-fourth).

By the API Research Project 6 at the National Bureau of Standards, under the supervision of F. D. Rossini:

n-Nonane. 2,2,5-Trimethylhexane.

Table 1 summarizes the amounts of the starting materials and gives some additional information as to the source and purity.

TABLE 1.—*Information on the purification of 29 API-Standard and API-NBS hydrocarbons*

Compound [a]	Starting material [b] provided by—	Hydrocarbon charged for distillation		Distillation [f]								Volume of selected sample	
		Volume	Purity	Kind [c]	Azeotrope-forming substance [d]	Amount of hydrocarbon in the azeotropic distillate [e]	Distilling column number [f]	Number of theoretical plates [f] (approx.)	Reflux ratio [f] (approx.)	Rate of collection of distillate	Results plotted in figure	API-Standard	API-NBS
PARAFFINS													
		Liters	*Mole %*			*% by volume*				*ml/hr*		*ml*	*ml*
n-Nonane	APIRP6 [g]	5.20	99.05	Reg			14	125	130/1	12.0	1		
		2.75	99.75	Azeo	Cell	49	13	130	145/1	8.5	2	1350	
2,2,5-Trimethylhexane	APIRP6 [h]	2.40	99.50	Reg			3	100	120/1	2.5	3	1550	
2,4,4-Trimethylhexane	Penn State	2.62	99.26	Azeo	Cell	70	13	130	145/1	8.5	4		
		2.08	99.54	Reg			12	135	185/1	4.0	5	1065	
2,2,3,3-Tetramethylpentane	APIRP45	2.00		Azeo	Cell	61	10	135	165/1	4.5	6		
		1.38	99.90	Reg			11A	200	180/1	4.0	7	818	
2,2,3,4-Tetramethylpentane	NACA	11.89	(i)	do			6	125	125/1	12.5	8		
		2.85		Azeo	Me. Cell	58	10	135	165/1	4.5	9	598	
2,2,4,4-Tetramethylpentane	do	1.32	98.62	do	Cell	76	4	200	145/1	5.0	10	855	
2,3,3,4-Tetramethylpentane	do	4.83	94.61	Reg			8	130	155/1	8.0	11		
		2.35	99.86	Azeo	Cell	58	8	130	155/1	8.0	12	1100	
3,3-Diethylpentane	APIRP45	3.05	[j] 99.31	Reg			13	130	155/1	8.0	13		
		1.75	99.89	Azeo	Cell	55	13	130	145/1	8.5	14	895	
ALKYLBENZENES													
n-Butylbenzene (*B*)	NACA	3.75		Reg			9	135	165/1	4.5	15	1415	
Isobutylbenzene (*B*)	do	3.69	99.75	do			8	130	155/1	8.0	16	1190	
sec-Butylbenzene (*B*)	do	2.47	99.09	Azeo	Me Carb	83	8	130	145/1	8.5	17		
		1.53	99.73	do	do	83	13	130	150/1	8.25	18		
		1.32	99.73	Reg			12	135	165/1	4.5	19	1000	
tert-Butylbenzene (*B*)	do	3.23	99.87	Azeo	Me Carb	86	8	130	145/1	8.5	20	1225	

Footnotes on page 56.

TABLE 1.—*Information on the purification of 29 API-Standard and API-NBS hydrocarbons*—Continued

Compound [a]	Starting material [b] provided by—	Hydrocarbon charged for distillation		Distillation [f]								Volume of selected sample	
		Volume	Purity	Kind [e]	Azeotrope-forming substance [d]	Amount of hydrocarbon in the azeotropic distillate [e]	Distilling column number [f]	Number of theoretical plates [f] (approx.)	Reflux ratio [f] (approx.)	Rate of collection of distillate	Results plotted in figure	API-Standard	API-NBS
		Liters	*Mole %*			*% by volume*				*ml/hr*		*ml*	*ml*
ALKYLCYCLOPENTANES													
Ethylcyclopentane (B)	APIRP45	3.47	99.47	Reg			15	125	110/1	14.0	21		
	Penn State	2.90	96.29										
		2.80	99.66	Azeo	Ethanol	52	13	130	155/1	8.0	22	1400	375
1,1-Dimethylcyclopentane	Penn State	1.82	99.958	do	do	64	9	135	165/1	4.5	23	1126	260
cis-1,2-Dimethylcyclopentane	do	1.36	99.90	do	do	53	9	135	165/1	4.5	24	780	120
trans-1,2-Dimethylcyclopentane	do	1.46	99.68	do	do	61	4	200	160/1	4.5	25	906	138
trans-1,3-Dimethylcyclopentane	APIRP45	3.00	73.6	Reg			4	200	145/1	5.0	26		
		1.83	90.0	Azeo	Methanol	55	10	135	165/1	4.5	27		
		1.13	94.6	do	Ethanol	63	4	200	180/1	4.0	28	579	102
n-Propylcyclopentane	do	1.30		Reg			4	200	145/1	5.0	29	[h] 333	[i] 75
		0.30	95.1										
	do	[g] 2.70	97.06	do			13	130	155/1	8.0	30	972	275
	do	[g] 0.44	98.67										
Isopropylcyclopentane	do	5.71		do			10	135	145/1	5.0	31	1180	370
1,1,2-Trimethylcyclopentane	Penn State	1.32		Azeo	Isoprop	33	9	135	165/1	4.5	32		
		1.07		Reg			3	100	150/1	2.0	33	680	115
1,1,3-Trimethylcyclopentane	Gulf-Mellon	0.60		do			3	100	120/1	2.5	34		
	APIRP45	0.50											
		[g] 1.80		do			12	135	185/1	4.0	35		
		1.57		Azeo	Me. Cell	80	12	135	165/1	4.5	36		
		0.80		do	Isoprop	46	7	130	145/1	8.5	37		
		0.51											
		[g] 0.52		do	do	46	4	200	180/1	4.0	38	460	65
cis, cis, trans-1,2,4-Trimethylcyclopentane	Penn State	3.00		Reg			4	200	180/1	4.0	39		
		1.86	98.5	Azeo	Isoprop	30	11	(*)	160/1	4.5	40		
cis, trans, cis-1,2,4-Trimethylcyclopentane	do	1.28	98.9	do	do	30	4	200	145/1	5.0	41	515	81
		1.80	98.5	Reg			2	100	150/1	2.0	42		
		1.42	99.66	Azeo	Ethanol	48	9	135	165/1	4.5	43	700	125
ALKYLCYCLOHEXANES													
Ethylcyclohexane	APIRP45	5.06		Reg			8	130	145/1	8.5	44		
		2.37	99.78										
	do	[g] 0.29	99.81	Azeo	Cell	63	15	125	125/1	12.5	45	2360	
	do	[g] 0.27	99.50										
1,1-Dimethylcyclohexane	do	1.50	98.95	Reg			12	135	185/1	4.0	46		
		1.36		Azeo	Ethanol	64	9	135	165/1	4.5	47	732	131
cis-1,2-Dimethylcyclohexane	do	[g] 9.16		Reg			5	125	125/1	12.5	48		
		2.84		do			9	135	165/1	4.5	49	1060	243
trans-1,2-Dimethylcyclohexane	do	[g] 9.16		do			5	125	125/1	12.5	48		
		5.21		do			7	130	155/1	8.0	50		
		2.39	99.84	Azeo	[j] Isoprop Cell	21 73	13	130	145/1	8.5	51	1034	330
cis-1,4-Dimethylcyclohexane	Std. Oil Dev	1.70	99.90	do	Ethanol	30	9	135	165/1	4.5	52	1000	215
trans-1,4-Dimethylcyclohexane	do	1.90	99.66	do	do	36	10	135	165/1	4.5	53	1160	260

Footnotes on page 56.

TABLE 1.—*Information on the purification of 29 API-Standard and API-NBS hydrocarbons*—Continued

[a] (*B*) following the name of a compound indicates that for the API-NBS series, it is a second (and usually slightly purer) sample of the given compound, the first sample of which is labeled (*A*). See reference [6].

[b] The abbreviations represent the following laboratories: APIRP45; American Petroleum Institute Research Project 45 (formerly the American Petroleum Institute Hydrocarbon Research Project) at the Ohio State University, Columbus, Ohio. Penn State; Hydrocarbon Laboratory at the Pennsylvania State College, State College, Pa. NACA; National Advisory Committee for Aeronautics, Aeronautical Engine Research Laboratory, Cleveland, Ohio, and the Automotive Section, National Bureau of Standards Washington, D. C. Std. Oil Dev.; Standard Oil Development Co., Elizabeth, New Jersey. Gulf-Mellon; Gulf Oil Co. Fellowship at the Mellon Institute of Industrial Research, Pittsburgh, Pennsylvania. APIRP6; American Petroleum Institute Research Project 6 at the National Bureau of Standards, Washington, D. C.

[c] The abbreviations are Azeo., azeotropic; Reg., regular.

[d] The abbreviations are Cell., Cellosolve (ethylene glycol monoethyl ether); Me. Cell., methyl Cellosolve (ethylene glycol monomethyl ether); Me. Carb., methyl Carbitol (diethylene glycol monomethyl ether); Isoprop., isopropanol.

[e] Approximate value obtained from the actual volume of hydrocarbon recovered by extracting the azeotrope-forming substance with water in separatory funnels.

[f] See reference [4] for further details.

[g] Obtained by distillation from an Oklahoma petroleum.

[h] Obtained by distillation from commercial "pentenes" alkylates (pentene + isobutane).

[i] This starting material consisted of a blend of 2,2,3,4-tetramethylpentane (approximately 25%), "S-4" reference fuel ("isooctane") (approximately 66%), and *n*-heptane (approximately 9%).

[j] Calculated from the measured freezing points of two separate lots which were blended together for this charge.

[k] The total volume of the API-Standard sample was 1,305 ml.

[l] The total volume of the API-NBS sample was 350 ml.

[m] This is a second lot of *n*-propylcyclopentane supplied by API Research Project 45.

[n] Fractions 272 to 292 from the distillation of isopropylcyclopentane in column 10 (see figure 31).

[o] This second lot of 1,1,3-trimethylcyclopentane was supplied by the API Research Project 45.

[p] Fractions 41 to 60 from the azeotropic distillation in column 12 (see fig.

[q] This is a second lot of ethylcyclohexane supplied by the API Research Project 45.

[r] This is a third lot of ethylcyclohexane supplied by the API Research Project 45.

[s] Both *cis* and *trans* 1,2-dimethylcyclohexane were obtained from the material (see fig. 48).

[t] The distillation was begun with isopropanol as the azeotrope-forming substance, but because of the relatively small percentage of hydrocarbon in the azeotropic distillate, cellosolve was added to complete the distillation.

[u] The number of theoretical plates for this column was not determined.

III. Purification

The procedure followed in the process of purification and determination of purity was the same as that described in the previous report [1].

In addition to the name of the laboratory supplying the starting materials, table 1 and its footnotes give complete information for each distillation for each of the compounds.

Details of the distillation apparatus and operations are described in reference [4].

Figures 1 to 53, inclusive, show graphically the results of the distillations listed in table 1. These figures give, as a function of volume of hydrocarbon distillate, the refractive index (n_D at 25° C, to ±0.0001°), the boiling point of the distillate (at the controlled pressure of 724.5 mm Hg, to ±0.01° C), the freezing point of selected fractions of hydrocarbon distillate (in air at 1 atm, usually with a precision near ±0.003° C), and the purity of the hydrocarbon distillate. The letters *W*, *X*, *Y*, and *Z* indicate the disposition of the material, as follows: *W*, returned to the laboratory supplying the material; *X*, blended for redistillation; *Y*, used for the API-Standard material; *Z*, used for the API-NBS material.

As demonstrated in the previous report, the blending of fractions of distillate for the preparation of material of the highest purity can be done safely only on the basis of freezing points of selected fractions. An example of a case where the purest material is at the very beginning of distillation is shown in figure 27 on *trans*-1,2-dimethylcyclopentane, and an example of a case where the purest material is at the end of the distillation is shown in figure 17 for *sec*-butylbenzene.

IV. Freezing Points, Cryoscopic Constants and Purity

Table 2 gives the following information for each of the 29 compounds, except as otherwise indicated: The kind of time-temperature curve, whether freezing or melting, used to determine the freezing point [7]; the freezing point of the actual sample, in air at 1 atm [7], for both the API-Standard and API-NBS lots; the calculated value of the freezing point for zero impurity [7]; the value of the cryoscopic constant, determined from the lowering of the freezing point on the addition of a known amount of an appropriate impurity [7]; and the resulting calculated amount of impurity in the API-Standard and the API-NBS material.

TABLE 2.—*Freezing points and purity of 29 API-Standard and API-NBS hydrocarbons*

Compound [a]	Kind of time-temperature observations used to determine the freezing point [b]	Freezing point of the actual selected sample, in air at 1 atm		Freezing point for zero impurity in air at 1 atm	Cryoscopic constant, A	Calculated amount of impurity in the actual selected sample [c]	
		API-Standard	API-NBS			API-Standard	API-NBS
PARAFFINS							
		°C	°C	°C	deg⁻¹	Mole %	Mole %
n-Nonane	F	−53.555	−53.550	−53.535±0.010	0.0388	0.08 ±0.04	0.06 ±0.04
2,5-Trimethylhexane	F and M	−105.856	−105.834	−105.780±0.015	[d].0265	.20 ±0.04	.14 ±0.04
2,4-Trimethylhexane	M	−113.434	−113.430	−113.380±0.020	.0535	.29 ±0.11	.27 ±0.11
2,2,3-Tetramethylpentane	F	−10.06	−10.05	−9.90 ±0.05	.0040	.064±0.020	.060±0.020
2,3,4-Tetramethylpentane	F	−121.221	−121.178	−121.09 ±0.05	.0027	.035±0.014	.024±0.014
2,2,4-Tetramethylpentane	F and M	−66.599	−66.580	−66.54 ±0.05	.0273	.16 ±0.08	.11 ±0.08
2,3,4-Tetramethylpentane	F and M	−102.137	−102.135	−102.123±0.010	.0309	.051±0.037	.044±0.037
3,3-Diethylpentane	M	−33.118	−33.116	−33.110±0.005	.0223	.018±0.011	.013±0.011
ALKYLBENZENES							
n-Butylbenzene (*B*)	M	−88.009	−87.993	−87.970±0.020	[d](0.0385)	0.12±0.08	0.09 ±0.08
Isobutylbenzene (*B*)	M	−51.523	−51.520	−51.48 ±0.03	.0306	.13±0.09	.112±0.09
sec-Butylbenzene (*B*)	M	−75.511	−75.493	−75.470±0.020	.0303	.12±0.06	.07 ±0.06
tert-Butylbenzene (*B*)	M	−57.876	−57.876	−57.850±0.015	.0218	.06±0.03	.06 ±0.03
ALKYLCYCLOPENTANES							
Ethylcyclopentane	M	−138.454	−138.452	−138.435±0.010	0.0303	0.06 ±0.03	0.05 ±0.03
1,1-Dimethylcyclopentane	F	−69.802	−69.802	−69.73 ±0.04	[d].004	.03 ±0.02	.03 ±0.02
cis-1,2-Dimethylcyclopentane	F	−53.927	−53.910	−53.85 ±0.04	.0042	.031±0.016	.025±0.016
trans-1,2-Dimethylcyclopentane	M	−117.63	−117.61	−117.57 ±0.03	[d](.0320)	.19 ±0.10	.13 ±0.10
trans-1,3-Dimethylcyclopentane	M	−133.767	−133.758	−133.680±0.020	.0455	.39 ±0.09	.35 ±0.09
n-Propylcyclopentane	M	−117.379	−117.378	−117.340±0.020	.0511	.20 ±0.10	.19 ±0.10
Isopropylcyclopentane	M	−111.433	−111.431	−111.375±0.020	.0346	.20 ±0.07	.19 ±0.07
1,1,2-Trimethylcyclopentane	F	−21.69	−21.68	−21.64 ±0.03	.0030	.015±0.009	.012±0.009
1,1,3-Trimethylcyclopentane	M	−142.56	−142.55	−142.44 ±0.08	.040	.48 ±0.32	.44±0.32
cis, trans-1,2,4-Trimethylcyclopentane	M	−132.66	−132.64	−132.55 ±0.06	.0385	.42 ±0.23	.35±0.23
trans, cis-1,2,4-Trimethylcyclopentane	M	−130.85	−130.84	−130.78 ±0.03	.0343	.24 ±0.10	.21±0.10
ALKYLCYCLOHEXANES							
Ethylcyclohexane	M	−111.335	----------	−111.300±0.020	0.0384	0.13±0.08	----------
1,1-Dimethylcyclohexane	F and M	−33.839	−33.654	−33.54 ±0.05	.0065	.19 ±0.03	0.07 ±0.03
cis-1,2-Dimethylcyclohexane	M	−50.047	−50.034	−50.00 ±0.03	.0051	.024±0.015	.017±0.015
trans-1,2-Dimethylcyclohexane	M	−88.203	−88.203	−88.180±0.020	.0365	.08 ±0.07	.08 ±0.07
cis-1,4-Dimethylcyclohexane	M	−87.445	−87.445	−87.425±0.015	.0283	.06 ±0.04	06 ±0.04
trans-1,4-Dimethylcyclohexane	F and M	−36.976	−36.964	−36.92 ±0.03	.0259	.14 ±0.08	.11 ±0.08

[a] (*B*) following the name of a compound indicates that, for the API-NBS series, it is a second (and usually slightly purer) sample of the given compound, the first sample of which is labeled (*A*). See reference [6].

[b] F indicates freezing and M indicates melting. See reference [7] for experimental details and the definition of the cryoscopic constant.

[c] The values in this column were calculated as described in reference [7], using the values of the cryoscopic constants and freezing points for zero impurity given in the preceding columns.

[d] This cryoscopic constant was determined by the procedure given on page 371 of reference [7].

[e] Not determined in this investigation. From the "z" tables of the American Petroleum Institute Research Project 44 [8].

Grateful acknowledgment is made to the organizations and individuals listed in section II of this report for their contributions of materials for use in this work.

References

[1] A. J. Streiff, E. T. Murphy, V. A. Sedlak, C. B. Willingham, and F. D. Rossini, J. Research NBS **37,** 331 (1946) RP1752.
[2] R. L. Denmerle. Chem. Eng. News **15,** (1946).
[3] Tech. News Bul. NBS No. 350 (June 1946).
[4] B. J. Mair, D. J. Termini, C. B. Willingham, and F. D. Rossini, J. Research NBS **37,** 229 (1946) RP1744.
[5] A. R. Glasgow, Jr., E. T. Murphy, C. B. Willingham, and F. D. Rossini, J. Research NBS **37,** 141 (1946) RP1734.
[6] C. B. Willingham and F. D. Rossini, J. Research NBS **37,** 15 (1946) RP1724.
[7] A. R. Glasgow, Jr., A. J. Streiff, and F. D. Rossini, J. Research NBS **35,** 355 (1945) RP1676.
[8] American Petroleum Institute Research Project 44 at the National Bureau of Standards. Selected values of properties of hydrocarbons. Heat and entropy of fusion, freezing points, and cryoscopic constants. Tables 1z, 2z, 3z, 5z, and 6z.

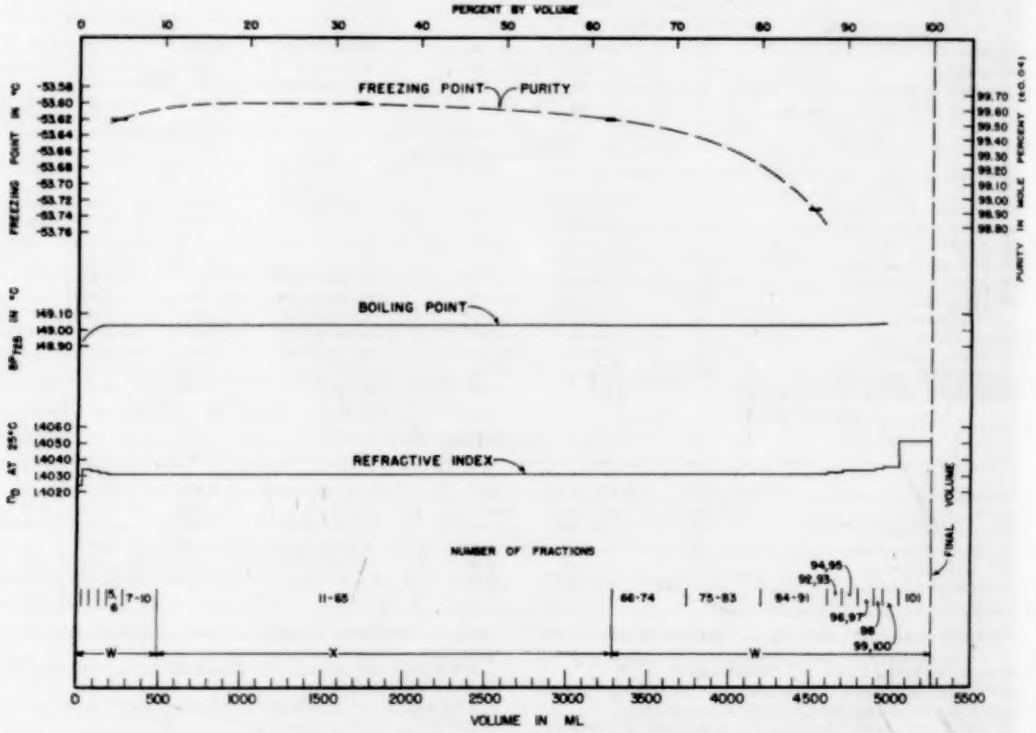

FIGURE 1.—*Results of the first distillation of n-nonane.*

Regular distillation at 725 mm Hg in still 14 (8/28/45 to 9/15/45).

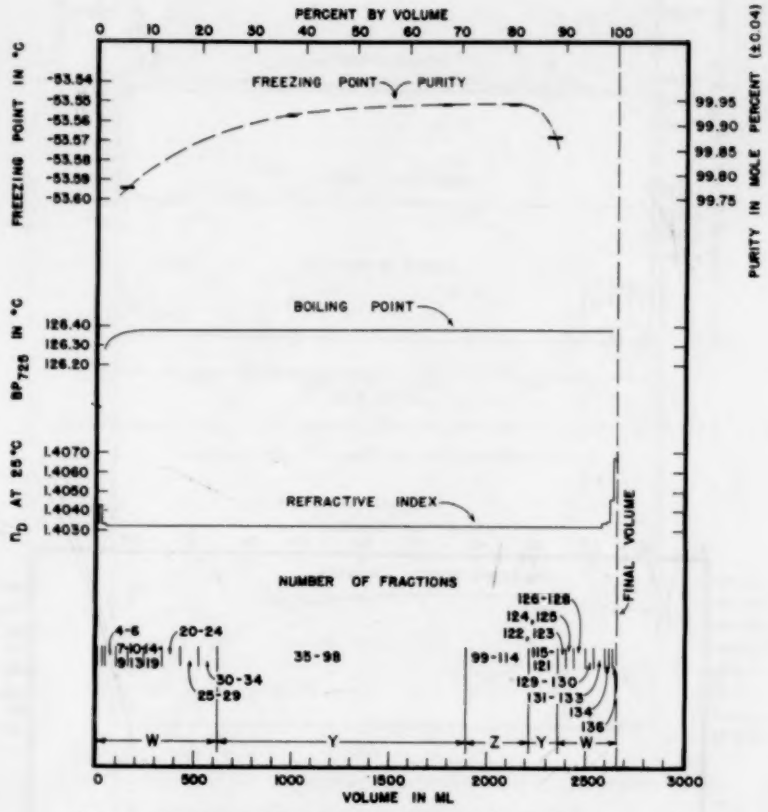

FIGURE 2.—*Results of the second and final distillation of n-nonane.*

Azeotropic distillation with ethylene glycol monoethyl ether at 725 mm Hg in still 13 (10/13/45 to 11/14/45).

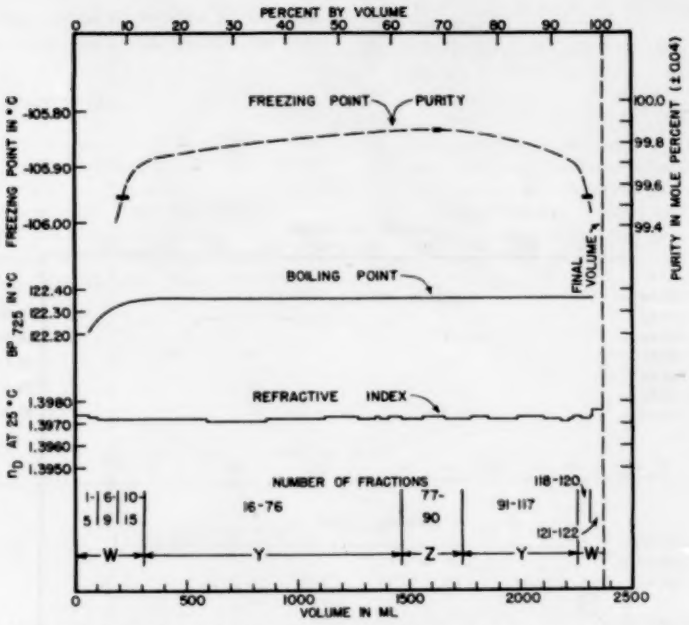

FIGURE 3.—*Results of the first and only distillation of 2,2,5-trimethylhexane.*

Regular distillation at 725 mm Hg in still 3 (6/26/44 to 8/6/44).

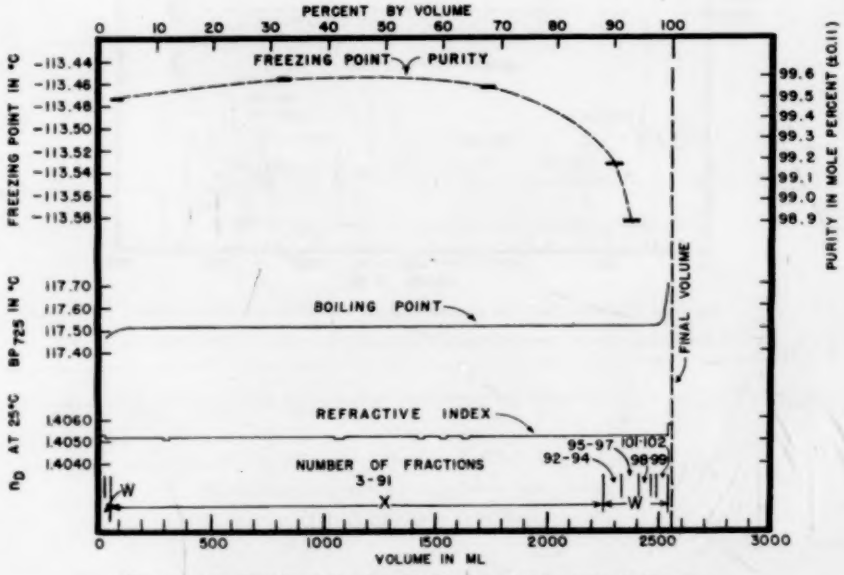

FIGURE 4.—*Results of the first distillation of 2,4,4-trimethylhexane.*

Azeotropic distillation with ethylene glycol monoethyl ether at 725 mm Hg in still 13 (11/16/44 to 12/6/44).

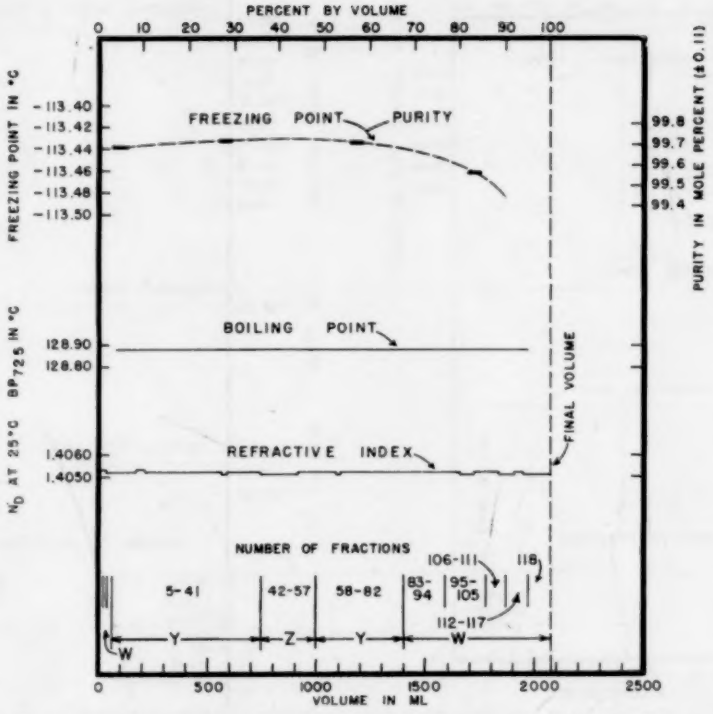

FIGURE 5.—*Results of the second and final distillation of 2,4,4-trimethylhexane.*

Regular distillation at 725 mm Hg in still 12 (6/21/45 to 7/13/45).

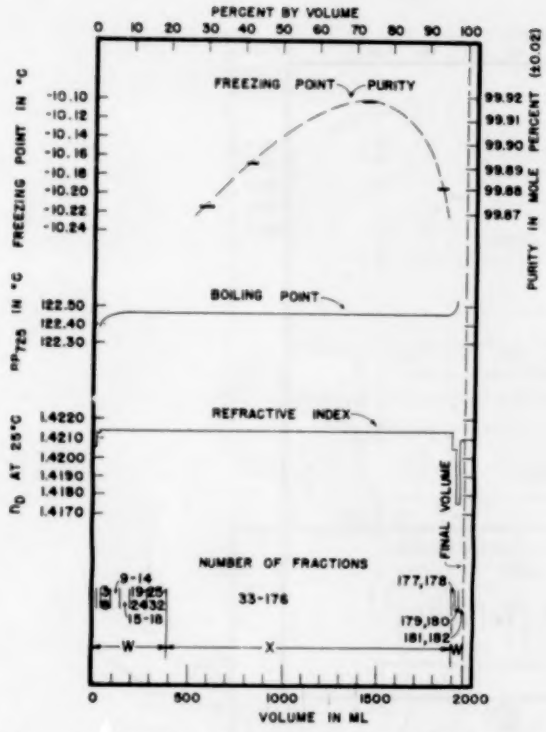

FIGURE 6.—*Results of the first distillation of 2,2,3,3-tetramethylpentane.*

Azeotropic distillation with ethylene glycol monoethyl ether at 725 mm Hg in still 10 (11/23/45 to 12/31/45).

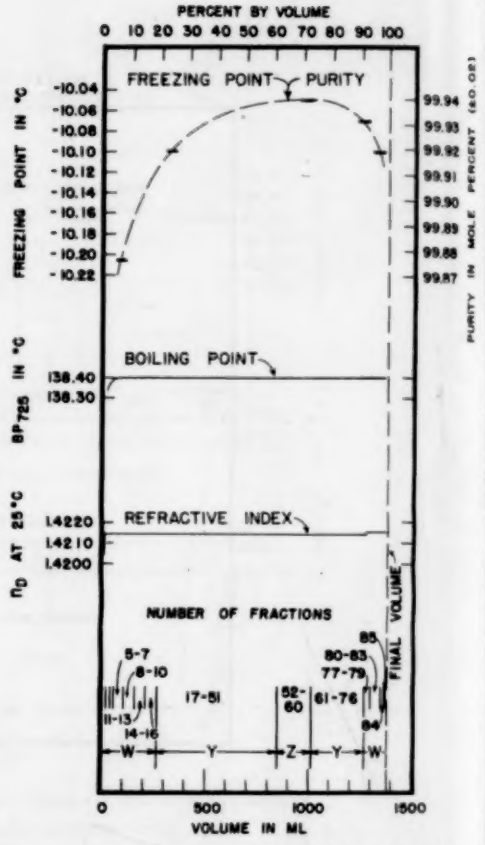

FIGURE 7.—*Results of the second and final distillation of 2,2,3,3-tetramethylpentane.*

Regular distillation at 725 mm Hg in still 11A (2/20/46 to 3/14/46)

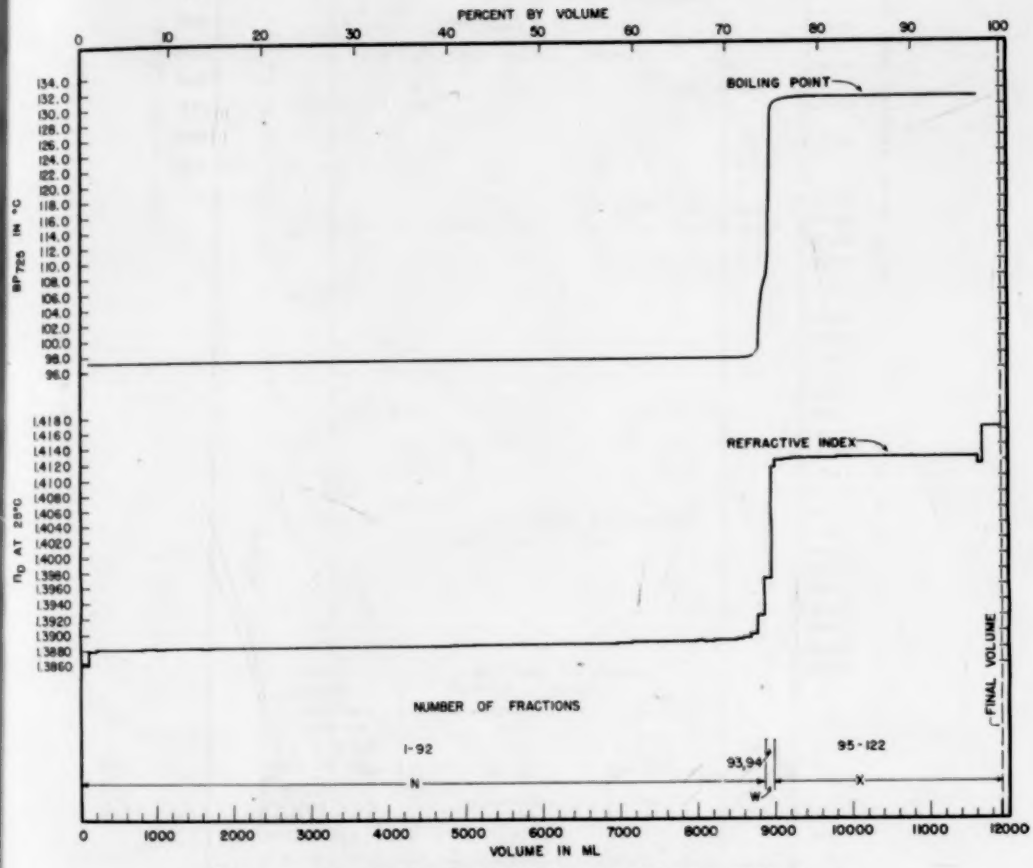

FIGURE 8.—*Results of the first distillation of 2,2,3,4-tetramethylpentane.*

Regular distillation at 725 mm Hg in still 6 (7/27/45 to 9/11/45).
The portion marked "N" was discarded. See footnote *i* of table 1.

724217—47——5

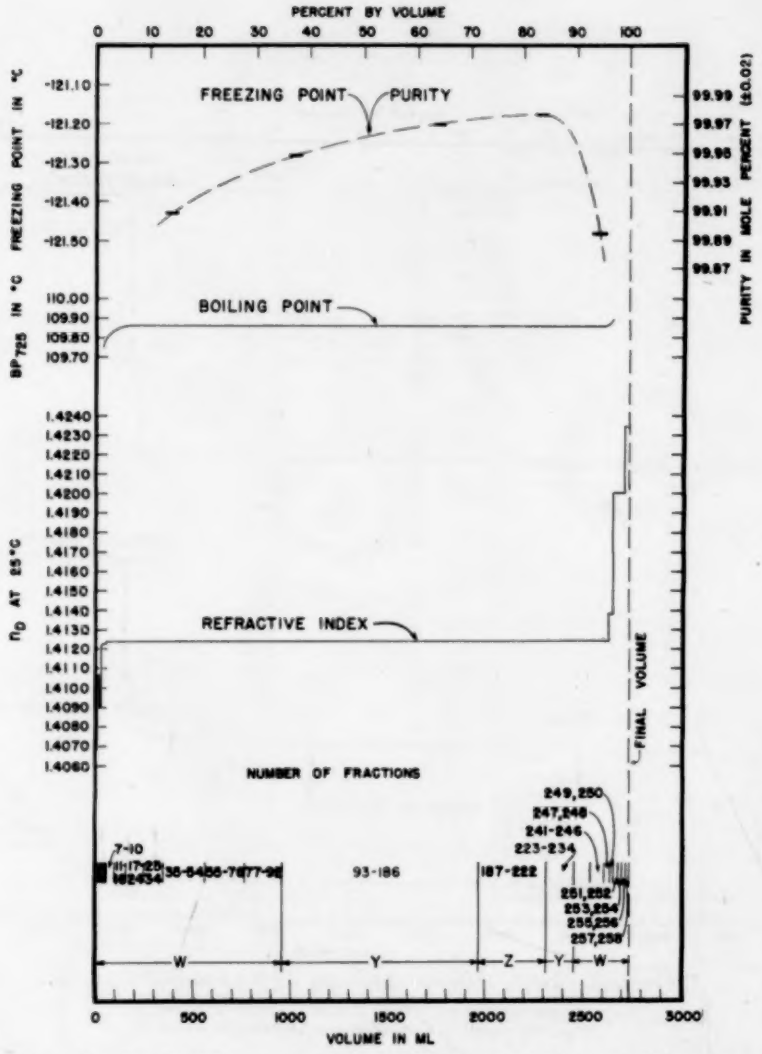

FIGURE 9.—*Results of the second and final distillation of 2,2,3,4-tetramethylpentane.*
Azeotropic distillation with ethylene glycol monomethyl ether at 725 mm Hg in still 10 (9/27/45 to 11/19/45).

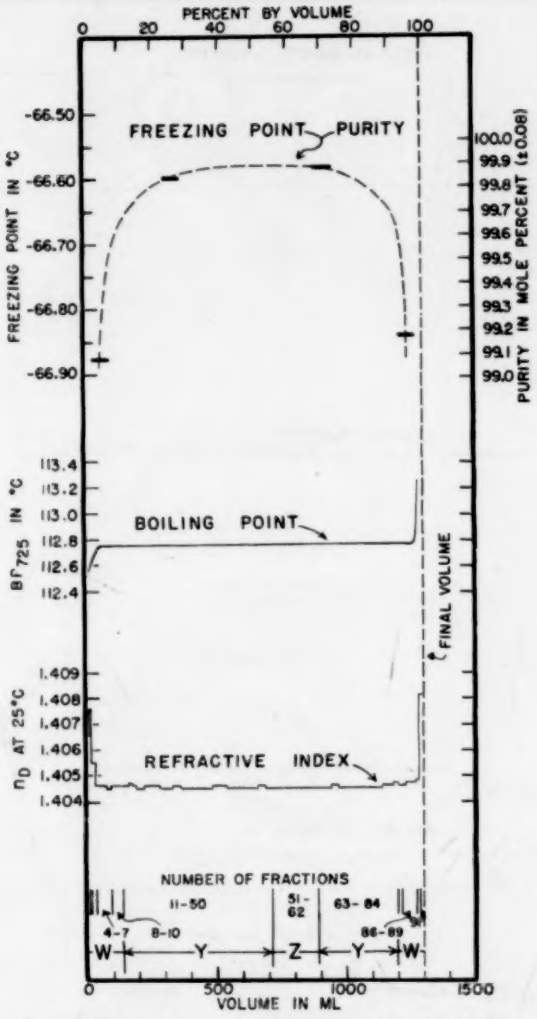

FIGURE 10.—*Results of the first and only distillation of 2,2,4,4-tetramethylpentane.*

Azeotropic distillation with ethylene glycol monoethyl ether at 725 mm Hg in still 4 (9/11/44 to 9/29/44).

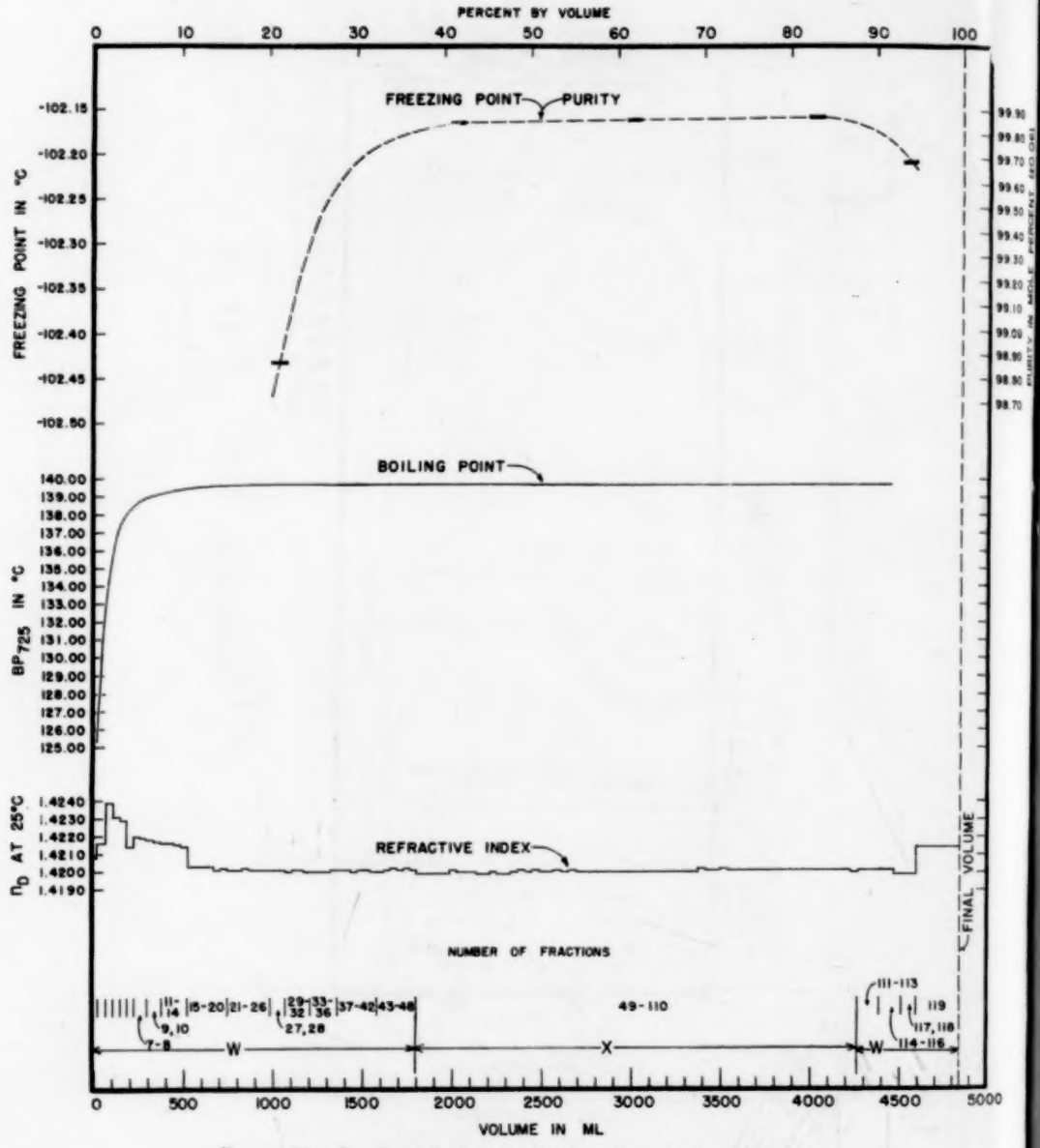

FIGURE 11.—*Results of the first distillation of 2,3,3,4-tetramethylpentane*

Regular distillation at 725 mm Hg in still 8 (7/4/45 to 7/31/45).

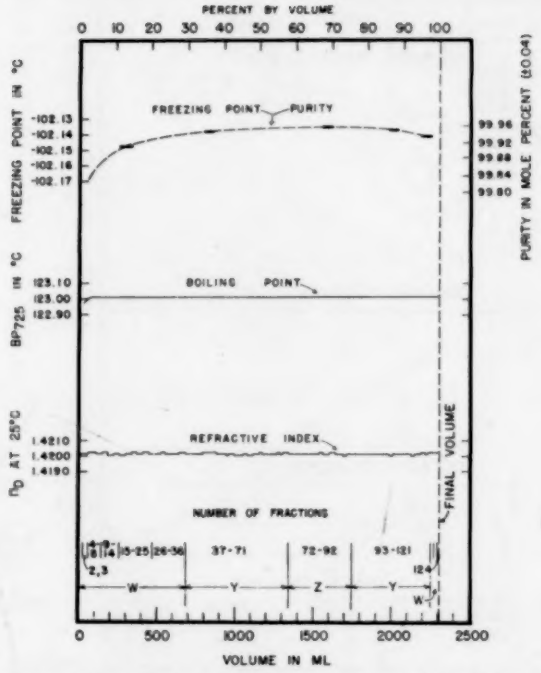

FIGURE 12.—*Results of the second and final distillation of 2,3,3,4-tetramethylpentane.*

Azeotropic distillation with ethylene glycol monoethyl ether at 725 mm Hg in still 8 (9/18/45 to 10/16/45).

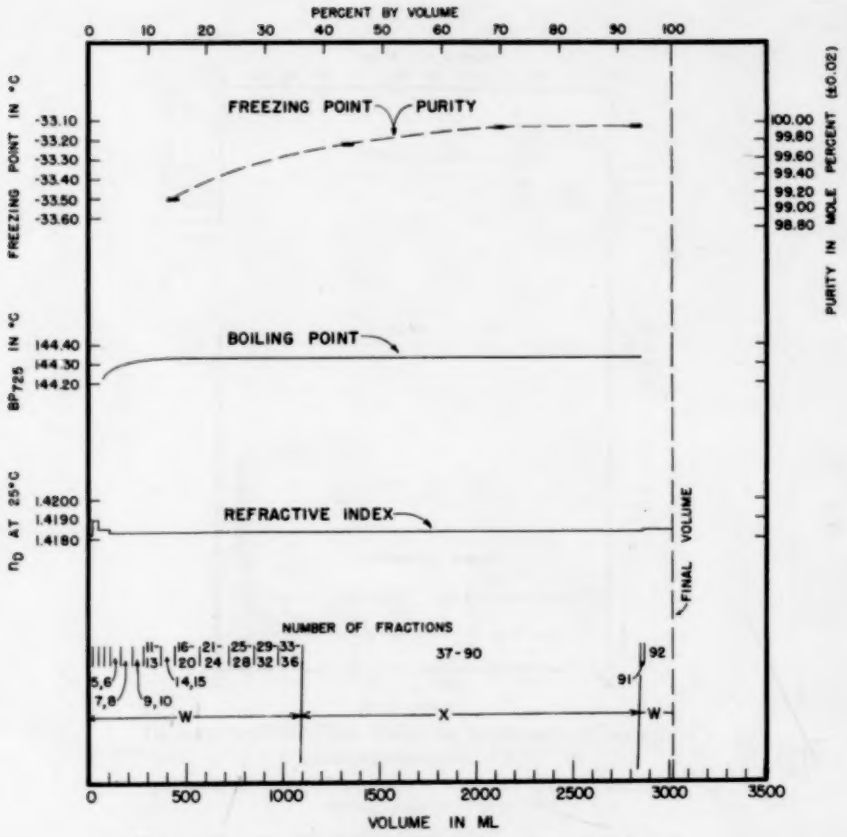

FIGURE 13.—*Results of the first distillation of 3,3-diethylpentane.*

Regular distillation at 725 mm Hg in still 13 (8/13/45 to 9/4/45).

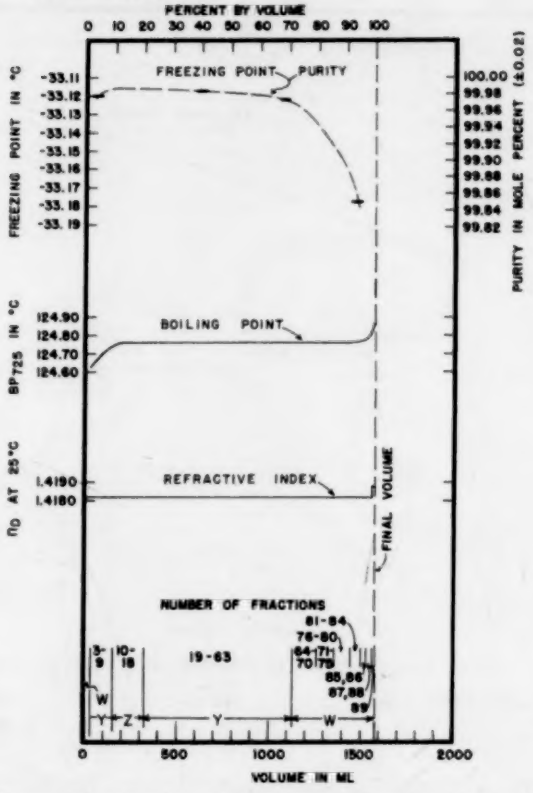

FIGURE 14.—*Results of the second and final distillation of 3,3-diethylpentane.*

Azeotropic distillation with ethylene glycol monoethyl ether at 725 mm Hg in still 13 (11/17/45 to 12/4/45).

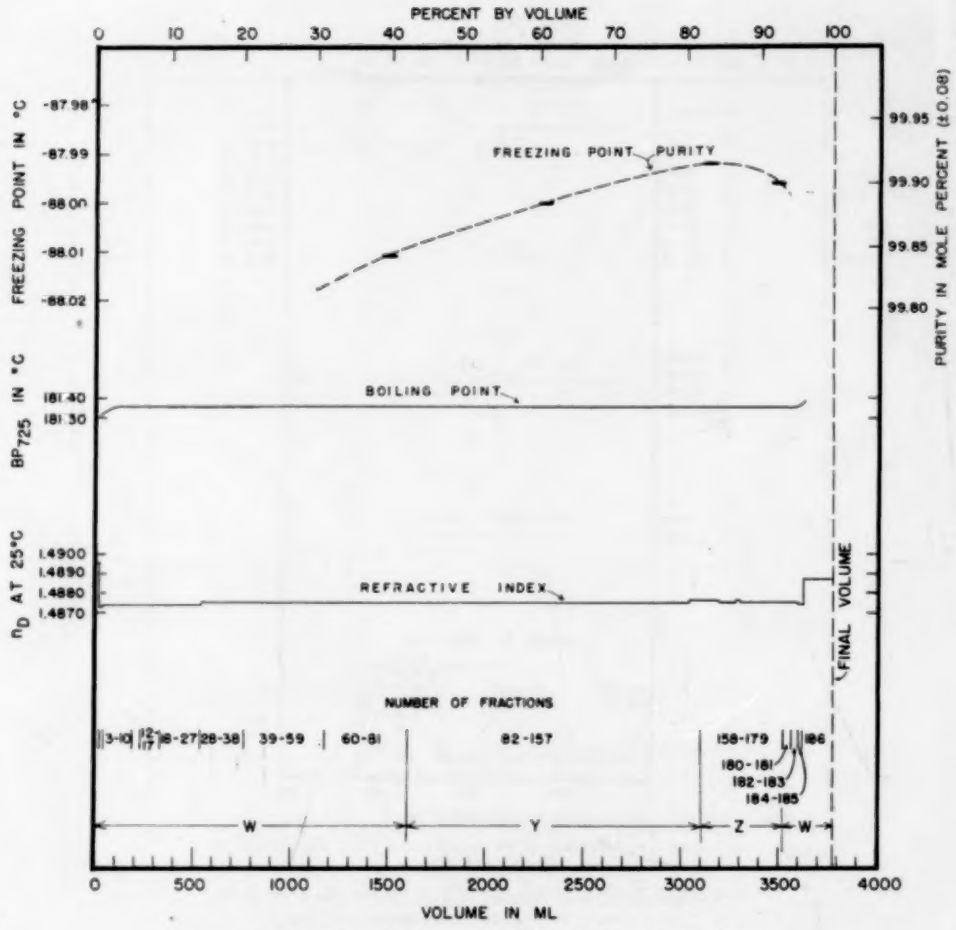

FIGURE 15.—*Results of the first and only distillation of n-butylbenzene.*

Regular distillation at 725 mm Hg in still 9 (7/17/45 to 8/18/45).

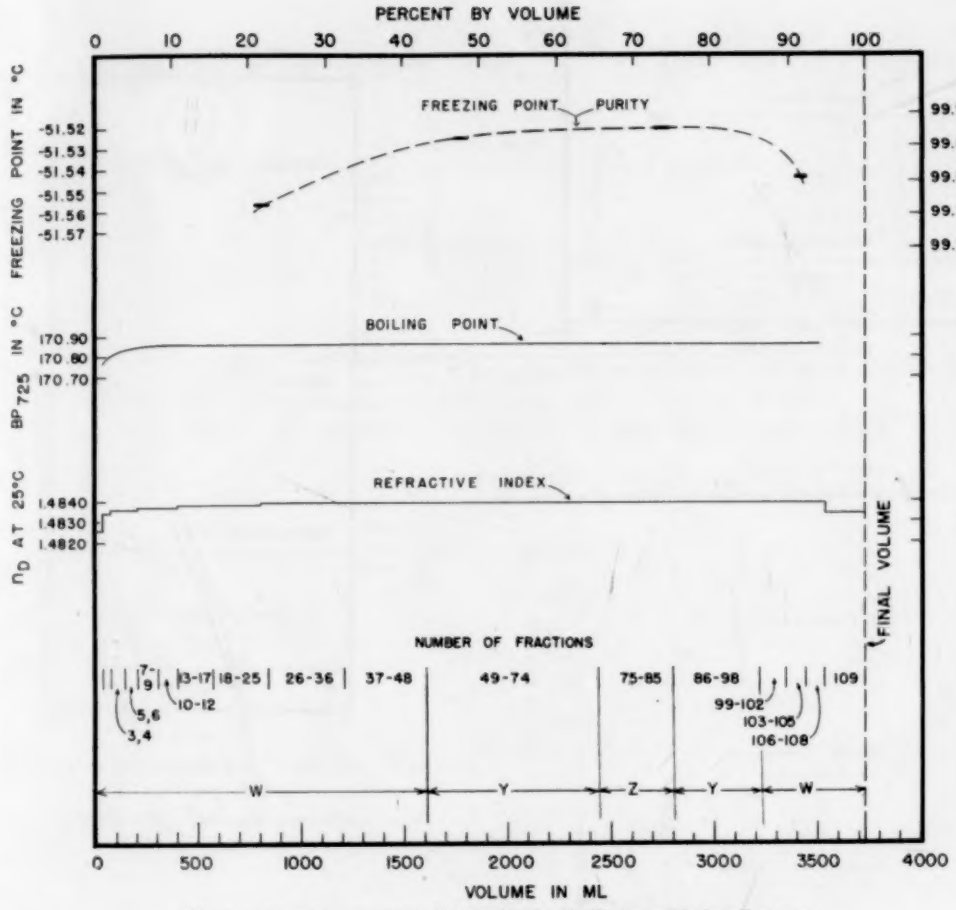

FIGURE 16.—*Results of the first and only distillation of isobutylbenzene.*

Regular distillation at 725 mm Hg in still 8 (8/27/45 to 9/16/45).

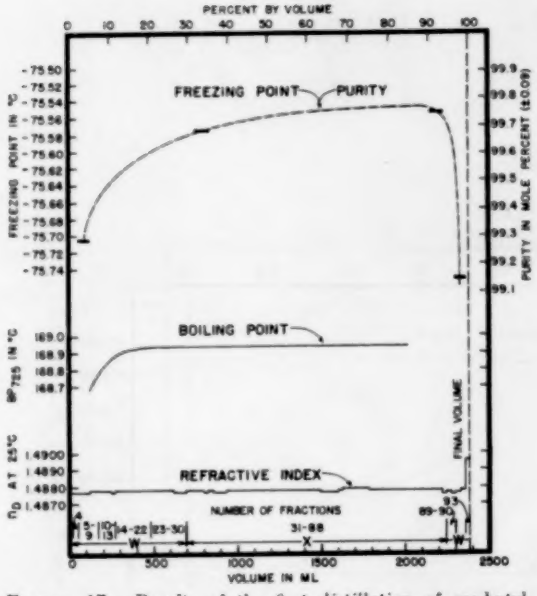

FIGURE 17.—*Results of the first distillation of sec-butylbenzene.*

Azeotropic distillation with diethylene glycol monomethyl ether at 725 mm Hg in still 8 (30/2/44 to 10/19/44).

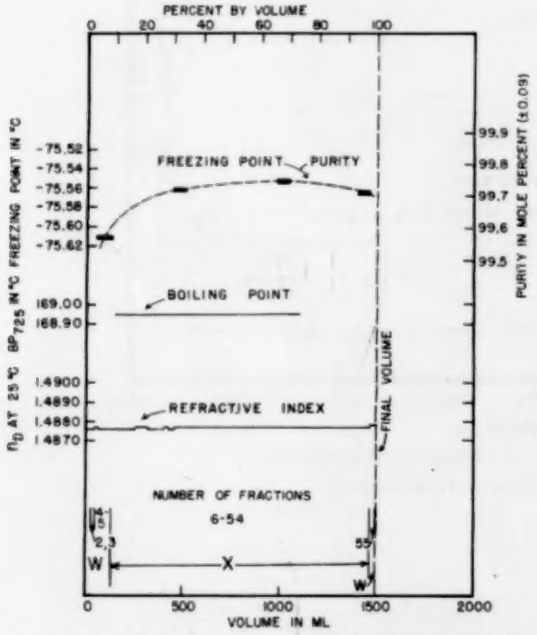

FIGURE 18.—*Results of the second distillation of sec-butylbenzene.*

Azeotropic distillation with diethylene glycol monomethyl ether at 725 mm Hg in still 13 (6/29/45 to 7/12/45).

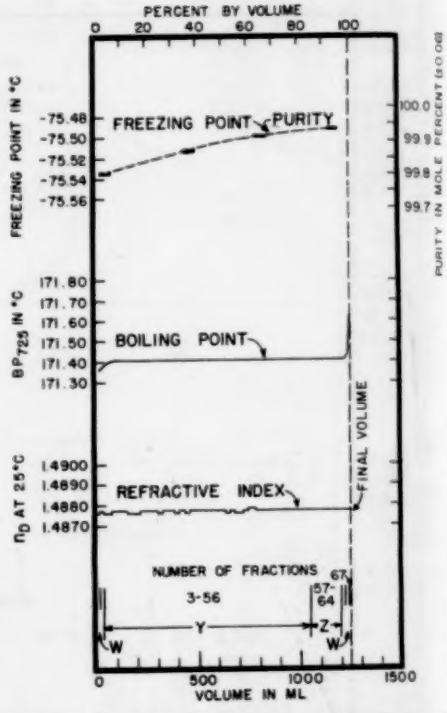

FIGURE 19.—*Results of the third and final distillation of sec-butylbenzene.*

Regular distillation at 725 mm Hg in still 12 (8/17/45 to 9/4/45).

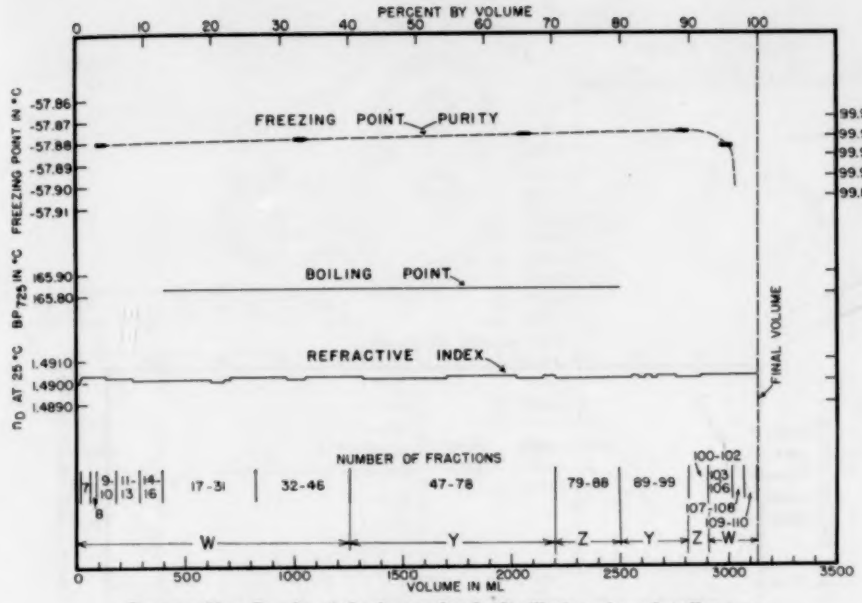

FIGURE 20.—*Results of the first and only distillation of tert-butylbenzene.*

Azeotropic distillation with diethylene glycol monomethyl ether at 725 mm Hg in still 8 (10/19/44 to 11/9/44).

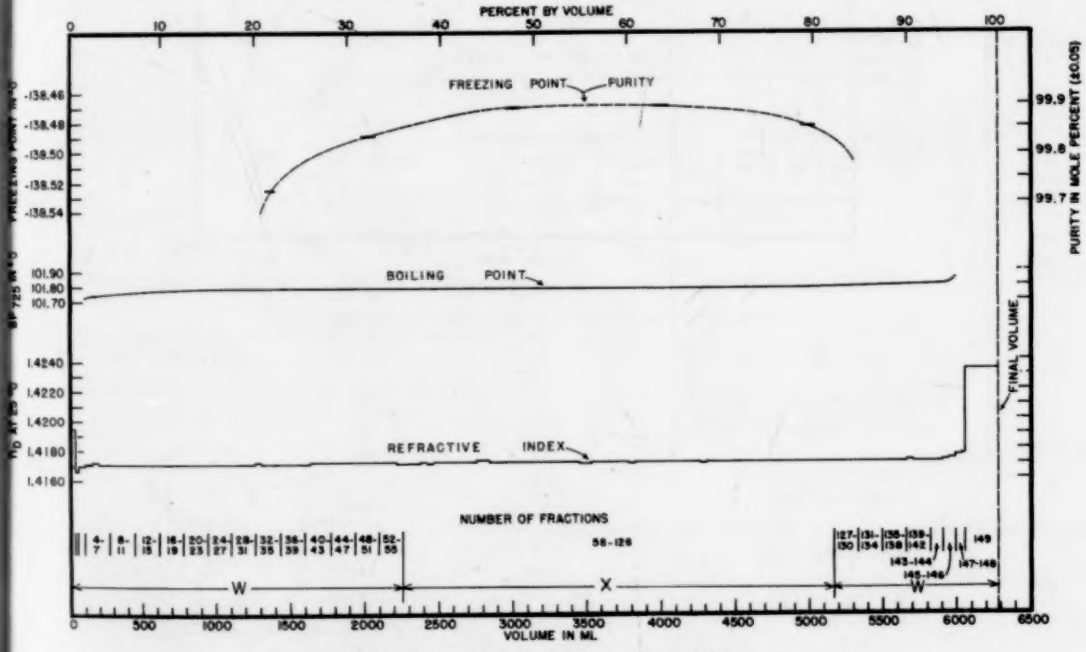

FIGURE 21.—*Results of the first distillation of ethylcyclopentane.*

Regular distillation at 725 mm Hg in still 15 (9/20/44 to 10/10/44).

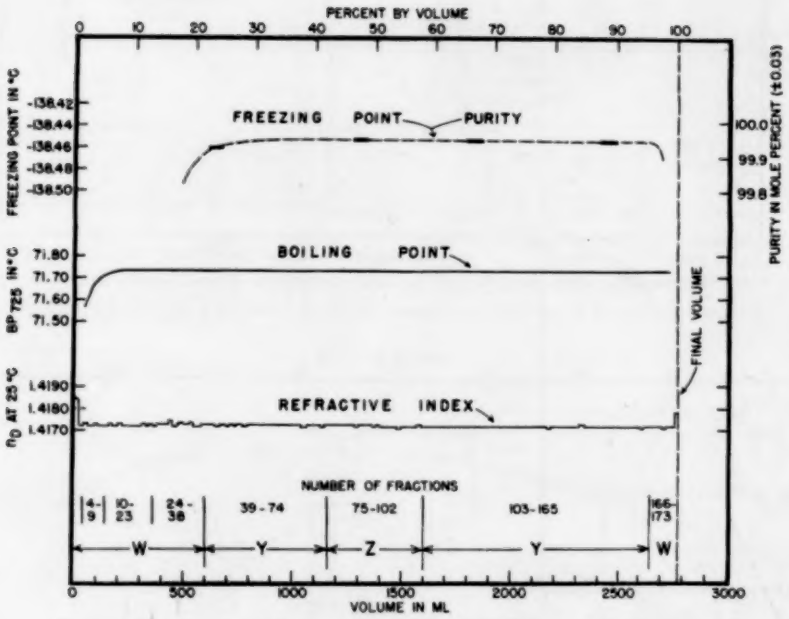

FIGURE 22.—*Results of the second and final distillation of ethylcyclopentane.*

Azeotropic distillation with ethanol at 725 mm Hg in still 13 (3/7/45 to 4/5/45).

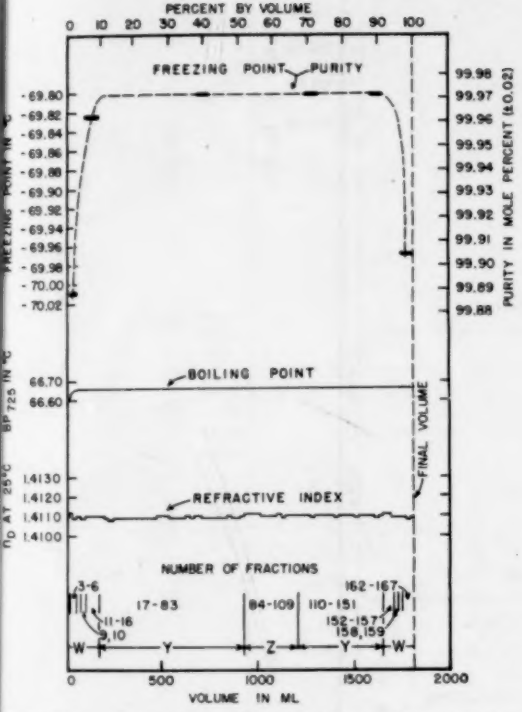

FIGURE 23.—*Results of the first and only distillation of 1,1-dimethylcyclopentane.*

Azeotropic distillation with ethanol at 725 mm Hg in still 9 (8/27/45 to 9/28/45).

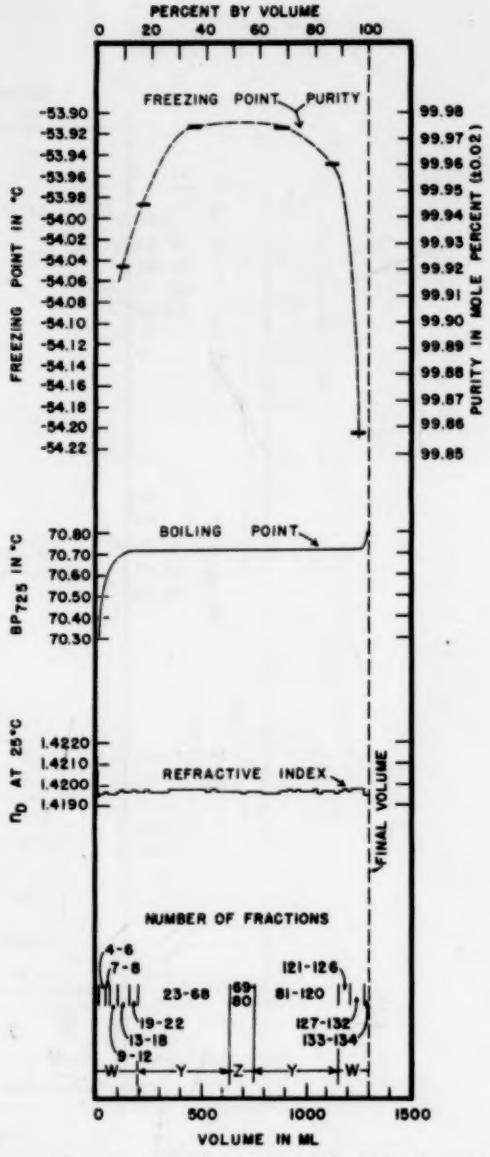

FIGURE 24.—*Results of the first and only distillation of cis-1,2-dimethylcyclopentane.*

Azeotropic distillation with ethanol at 725 mm Hg in still 9 (9/29/45 to 10/24/45).

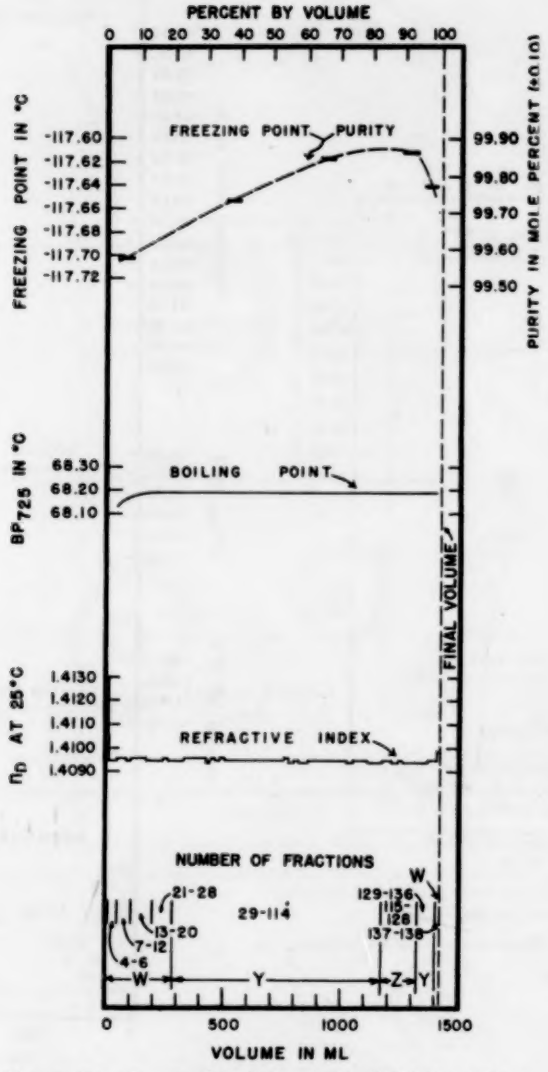

FIGURE 25.—*Results of the first and only distillation of trans-1,2-dimethylcyclopentane.*

Azeotropic distillation with ethanol at 725 mm Hg in still 4 (10/2/45 to 10/28/45).

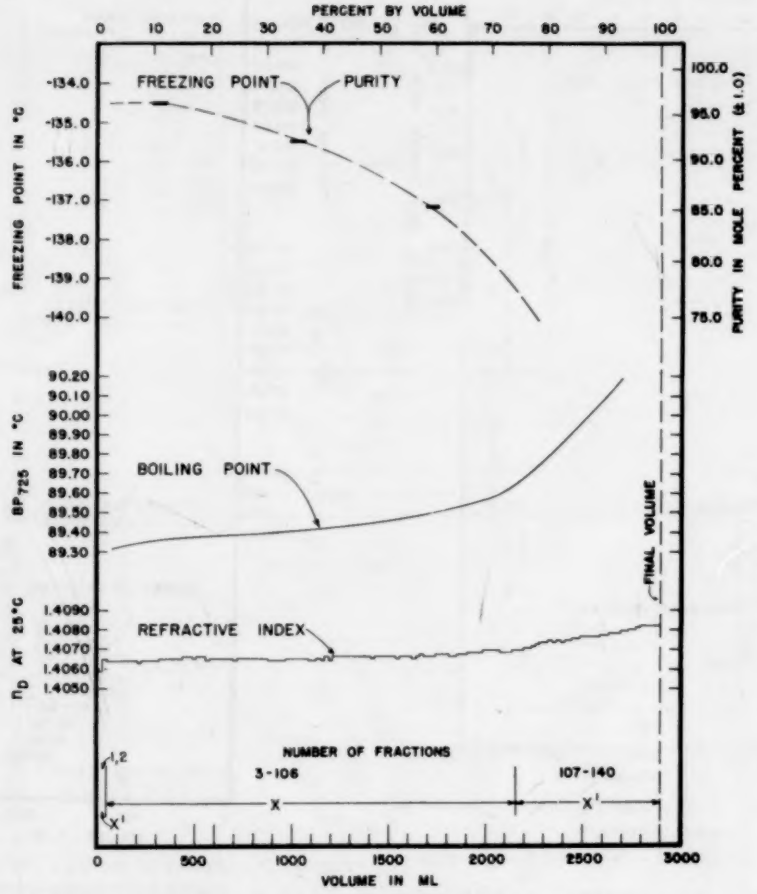

FIGURE 26.—*Results of the first distillation of trans-1,3-dimethylcyclopentane.*

Regular distillation at 725 mm Hg in still 4 (11/6/44 to 12/1/44).
Fractions 1, 2, and 107 to 140 (marked "X'") were retained for further processing by the API Research Project 6.

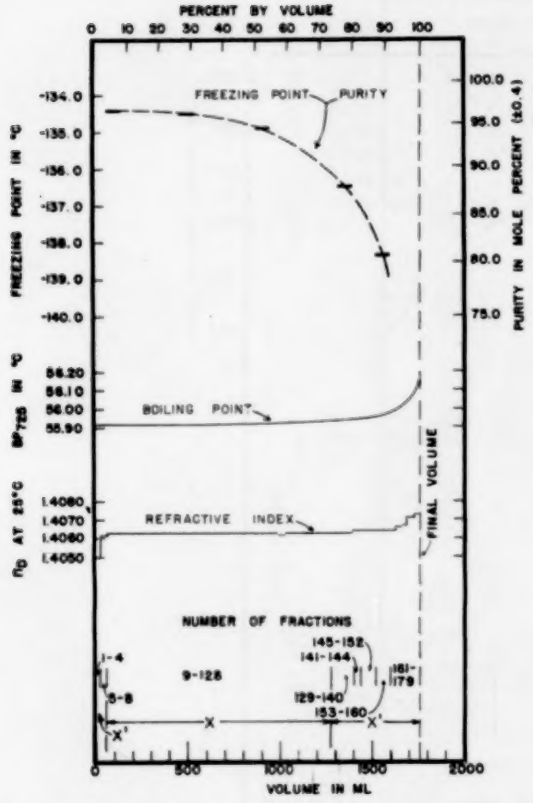

FIGURE 27.—*Results of the second distillation of trans-1,3-dimethylcyclopentane.*

Azeotropic distillation with methanol at 725 mm Hg in still 10 (5/26/45 to 7/4/45).

Fractions 1 to 8 and 153 to 179 (marked "X'") were retained for further processing by the API Research Project 6.

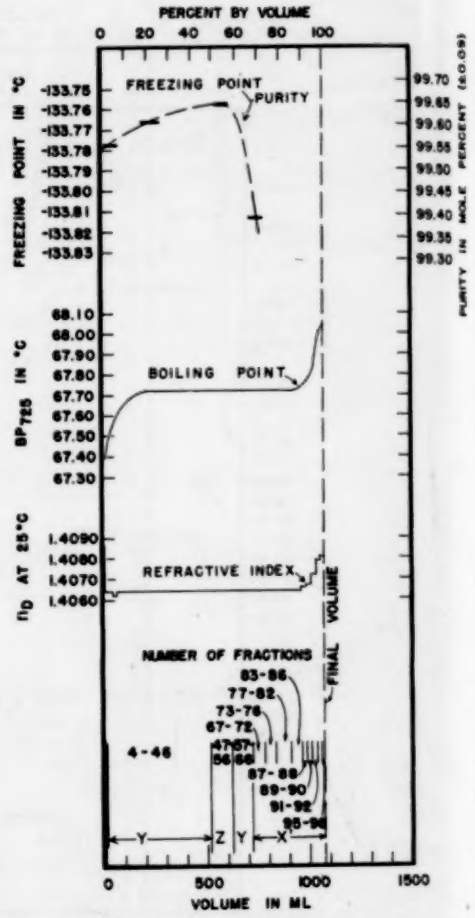

FIGURE 28.—*Results of the third and final distillation of trans-1,3-dimethylcyclopentane.*

Azeotropic distillation with ethanol at 725 mm Hg in still 4 (10/29/45 to 11/20/45).

Fractions 67 to 96 (marked "X'") were retained for further processing by the API Research Project 6.

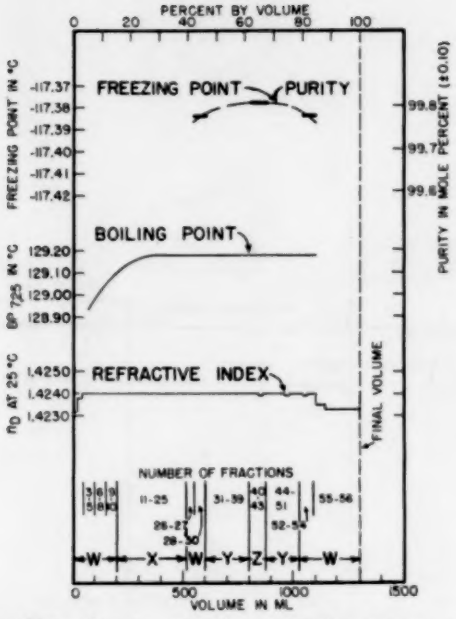

FIGURE 29.—*Results of the first distillation of n-propylcyclopentane.*

Regular distillation at 725 mm Hg in still 4 (6/12/44 to 6/24/44).

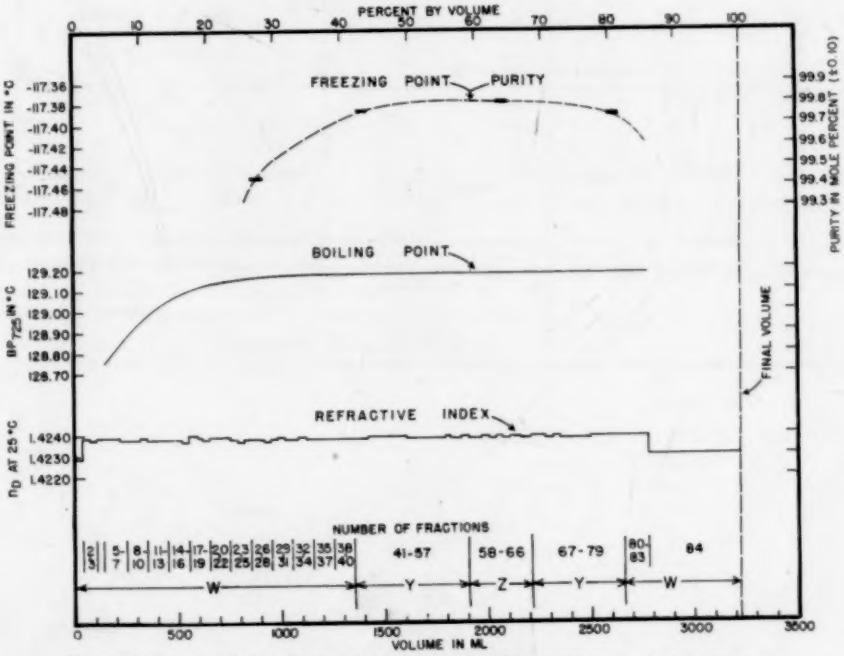

FIGURE 30.—*Results of the second and final distillation of n-propylcyclopentane.*

Regular distillation at 725 mm Hg in still 13 (12/7/44 to 12/22/44).
See table 1 for the composition of the charge for this distillation.

724217—47——6

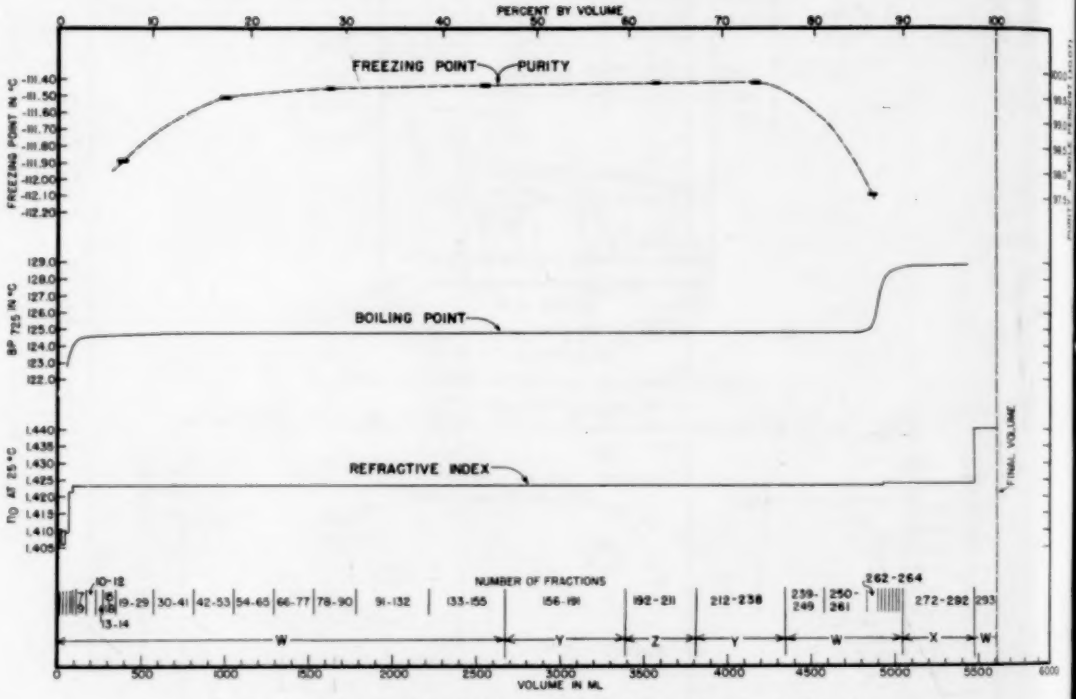

FIGURE 31.—*Results of the first and only distillation of isopropylcyclopentane.*

Regular distillation at 725 mm Hg in still 10 (7/3/44 to 8/20/44.)
The portion marked "X" was used as part of a charge of n-propylcyclopentane (see fig. 30 and footnote n of table 1).

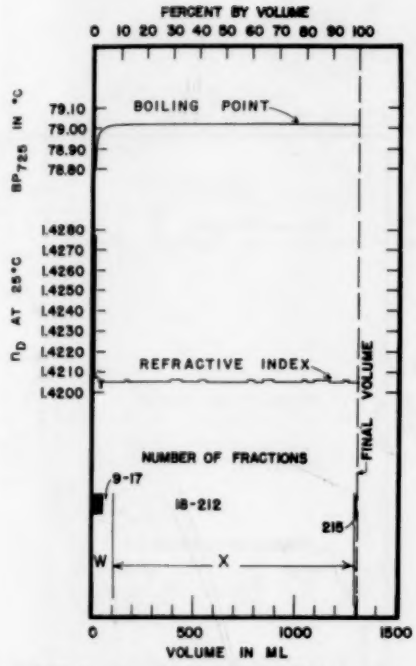

FIGURE 32.—*Results of the first distillation of 1,1,2-trimethylcyclopentane.*

Azeotropic distillation with isopropanol at 725 mm Hg in still 9 (11/23/45 to 1/7/46).

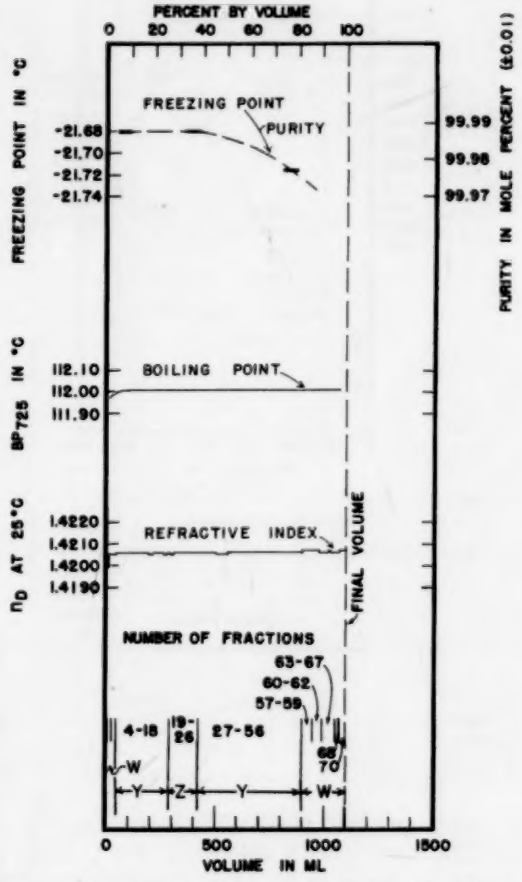

FIGURE 33.—*Results of the second and final distillation of 1,1,2-trimethylcyclopentane.*

Regular distillation at 725 mm Hg in still 3 (1/22/46 to 2/16/46).

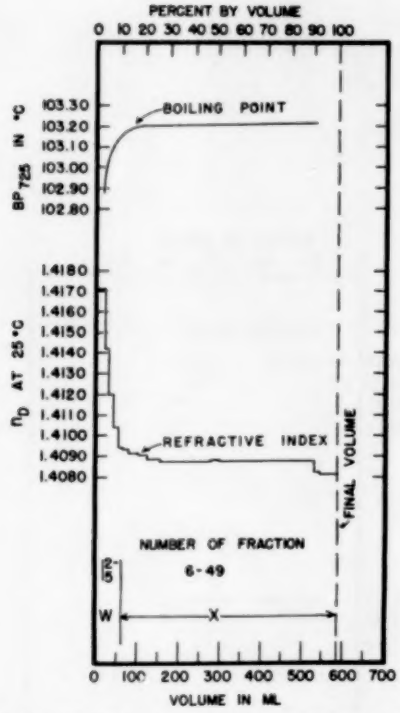

FIGURE 34.—*Results of the first distillation of 1,1,3-trimethylcyclopentane.*

Regular distillation at 725 mm Hg in still 3 (10/6/44 to 10/16/44).

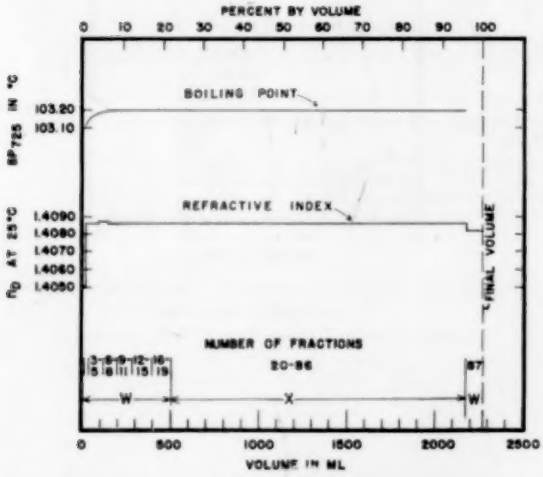

FIGURE 35.—*Results of the second distillation of 1,1,3-trimethylcyclopentane.*

Regular distillation at 725 mm Hg in still 12 (3/13/45 to 4/5/45).
See table 1 for the composition of the charge for this distillation.

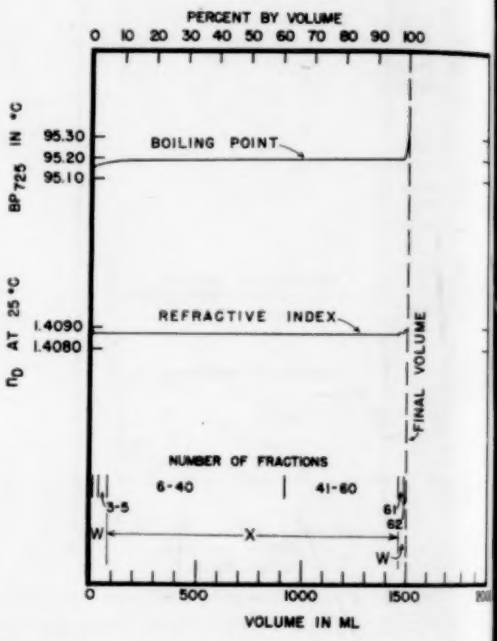

FIGURE 36.—*Results of the third distillation of 1,1,3-trimethylcyclopentane.*

Azeotropic distillation with ethylene glycol monomethyl ether at 725 mm Hg in still 12 (10/1/45 to 10/25/45).

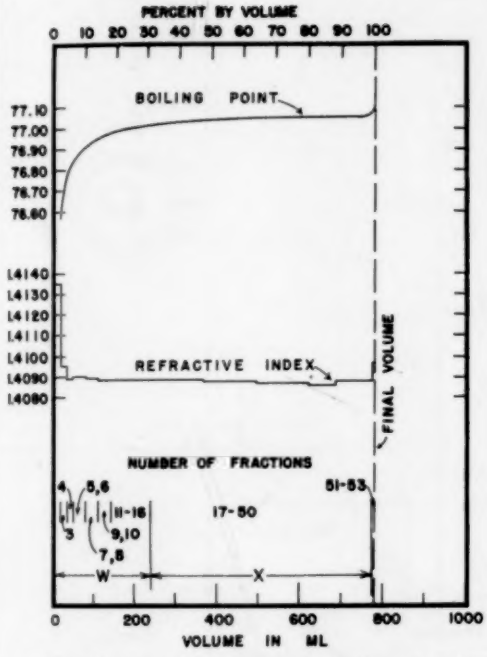

FIGURE 37.—*Results of the fourth distillation of 1,1,3-trimethylcyclopentane.*

Azeotropic distillation with isopropanol at 725 mm Hg in still 7 (11/17/45 to 11/27/45).

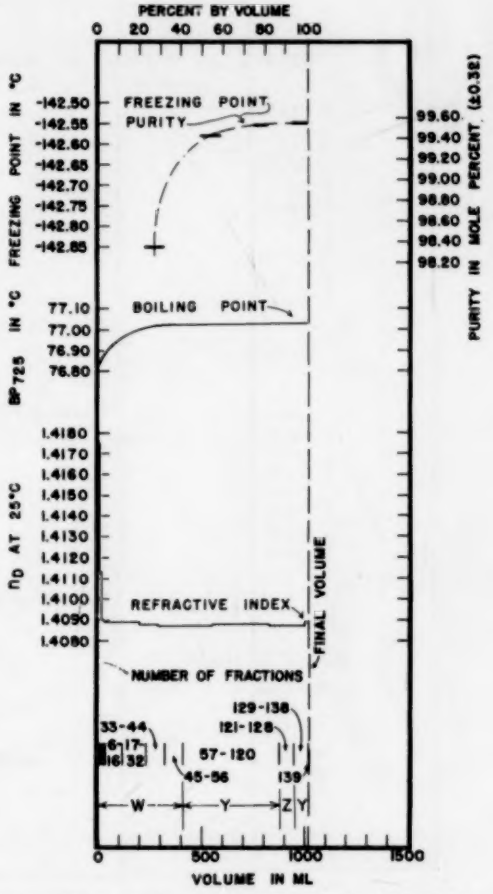

FIGURE 38.—*Results of the fifth and final distillation of 1,1,3-trimethylcyclopentane.*

Azeotropic distillation with isopropanol at 725 mm Hg in still 4 (1/3/46 to 1/29/46).

See table 1 for composition of the charge for this distillation.

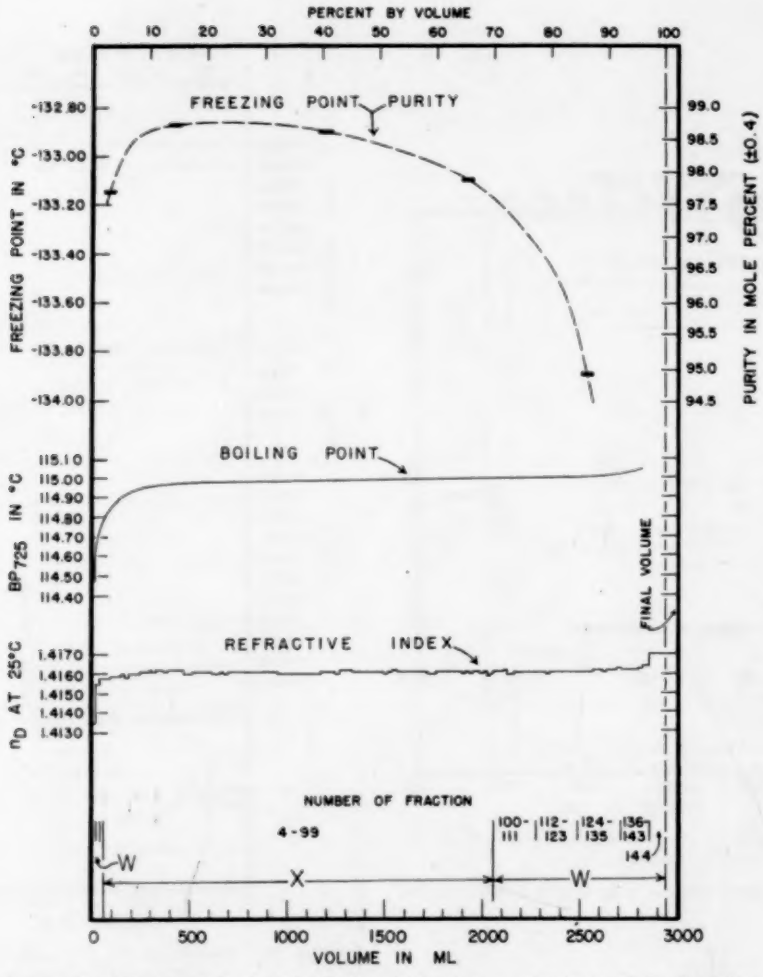

FIGURE 39.—*Results of the first distillation of cis, cis, trans-1,2,4-trimethylcyclopentane.*

Regular distillation at 725 mm Hg in still 4 (12/5/44 to 1/5/45).

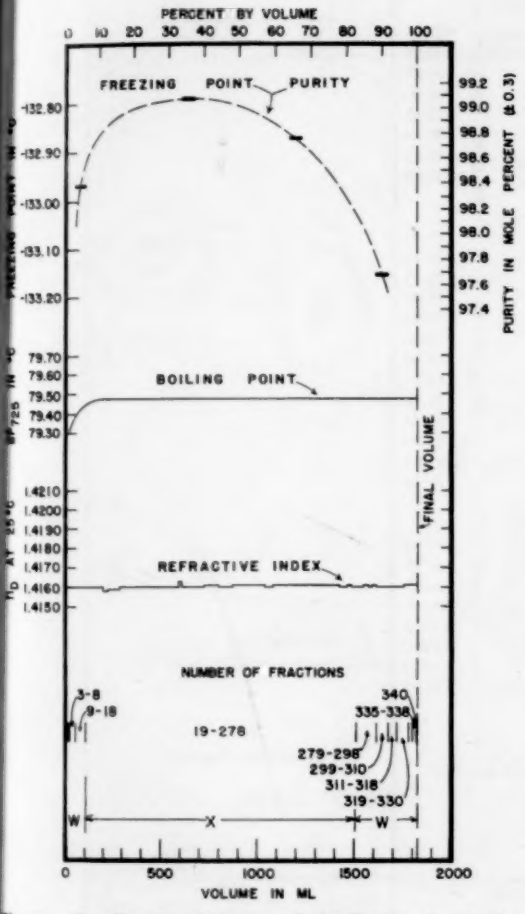

FIGURE 40.—*Results of the second distillation of cis, cis, trans-1,2,4-trimethylcyclopentane.*

Azeotropic distillation with isopropanol at 725 mm Hg in still 11 (6/21/45 to 8/21/45).

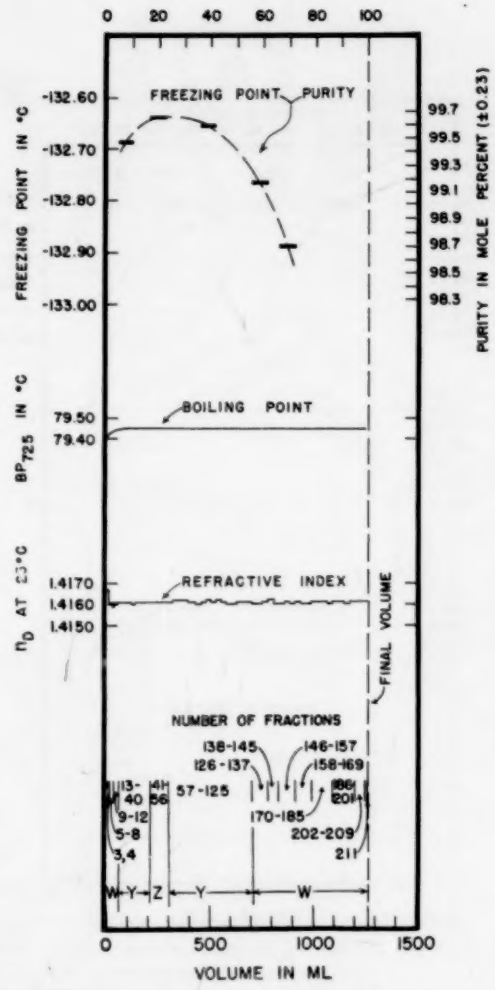

FIGURE 41.—*Results of the third and final distillation of cis, cis, trans-1,2,4-trimethylcyclopentane.*

Azeotropic distillation with isopropanol at 725 mm Hg in still 4 (11/21/45 to 1/3/46).

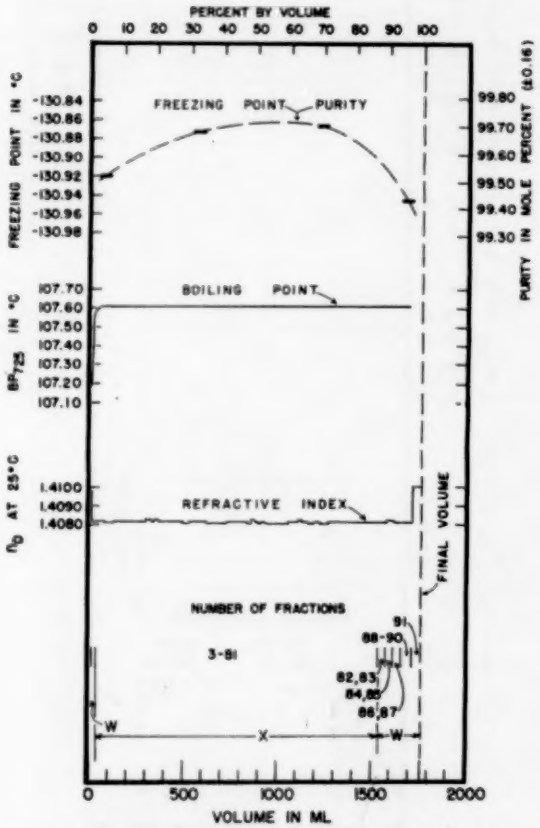

FIGURE 42.—*Results of the first distillation of cis, trans, cis-1,2,4-trimethylcyclopentane.*

Regular distillation at 725 mm Hg in still 2 (7/19/45 to 9/2/45).

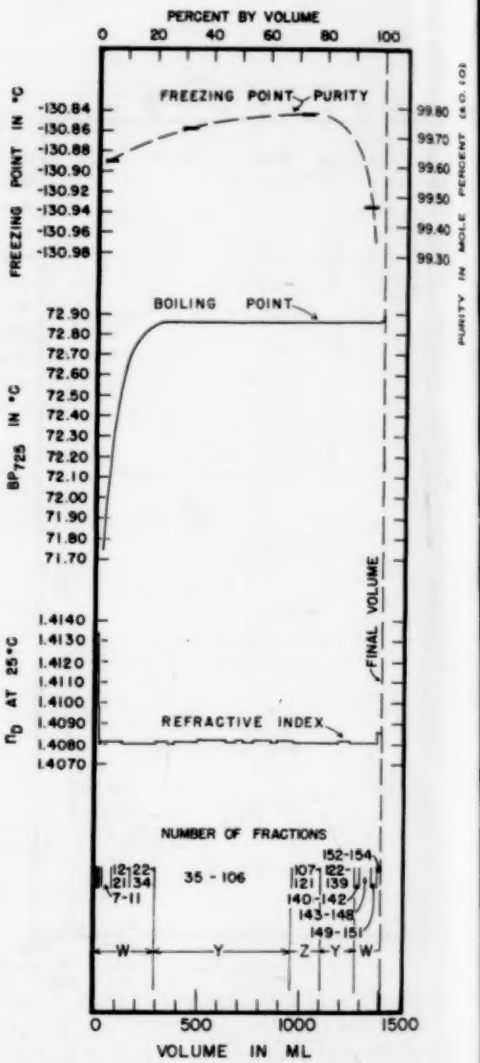

FIGURE 43.—*Results of the second and final distillation of cis, trans, cis-1,2,4-trimethylcyclopentane.*

Azeotropic distillation with ethanol at 725 mm Hg in still 9 (10/26/45 to 11/23/45).

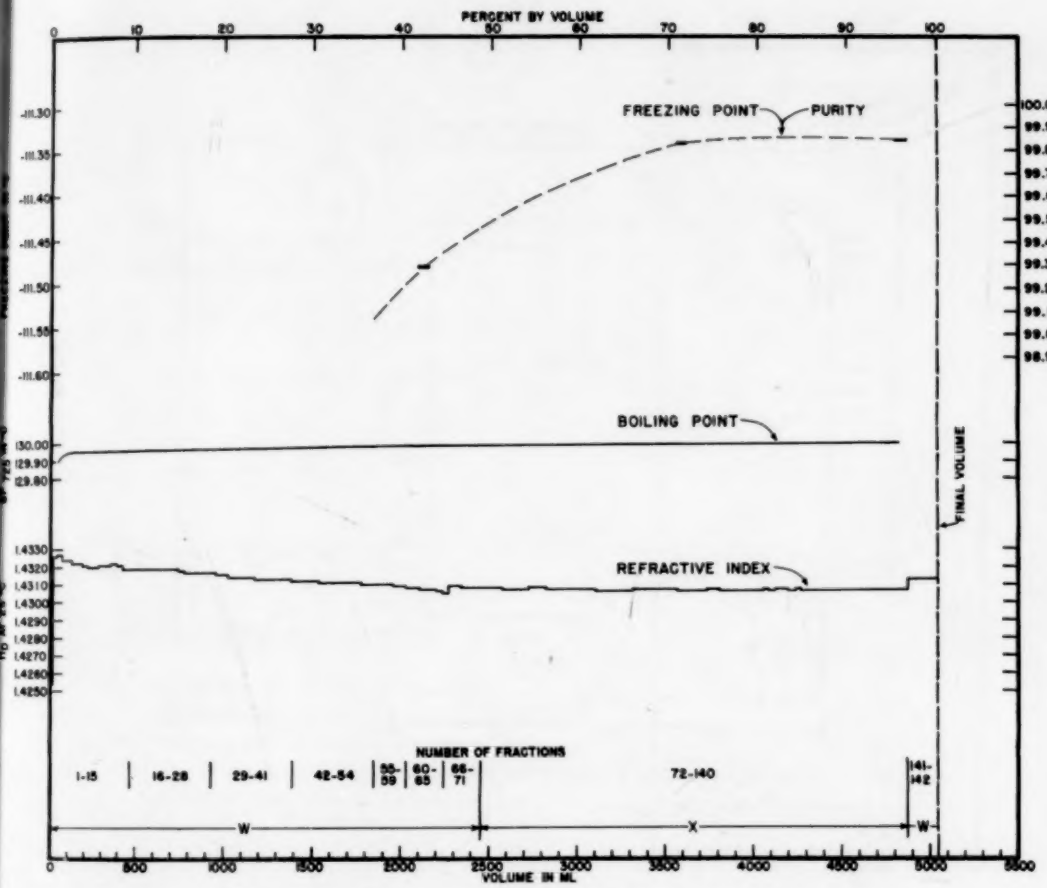

FIGURE 44.—*Results of the first distillation of ethylcyclohexane.*

Regular distillation at 725 mm Hg in still 8 (7/20/44 to 8/15/44).

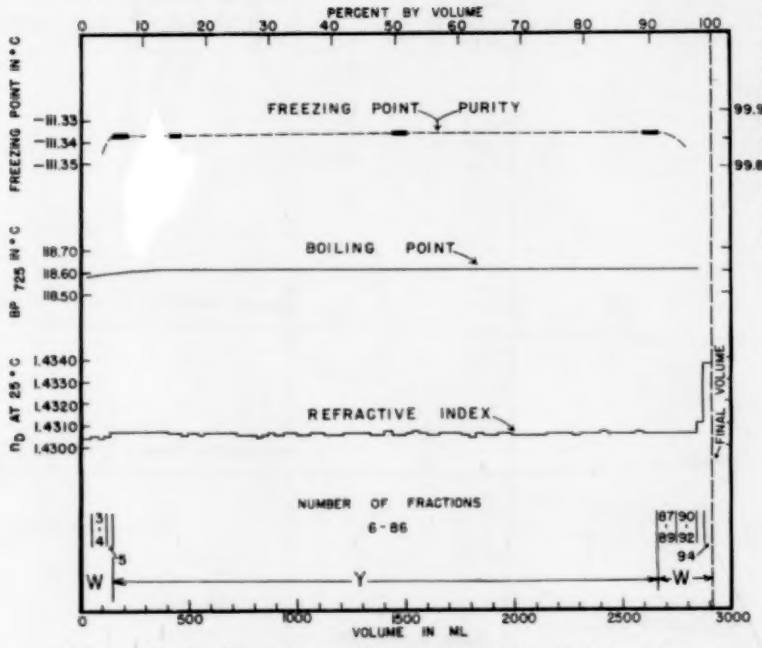

FIGURE 45.—*Results of the second and final distillation of ethylcyclohexane.*

Azeotropic distillation with ethylene glycol monoethyl ether at 725 mm Hg in still 15 (12/16/44 to 1/3/45).
See table 1 for composition of the charge for this distillation.

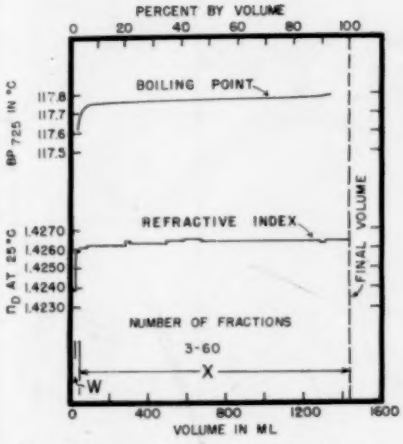

FIGURE 46.—*Results of the first distillation of 1,1-dimethylcyclohexane.*

Regular distillation at 725 mm Hg in still 12 (2/22/45 to 3/11/45).

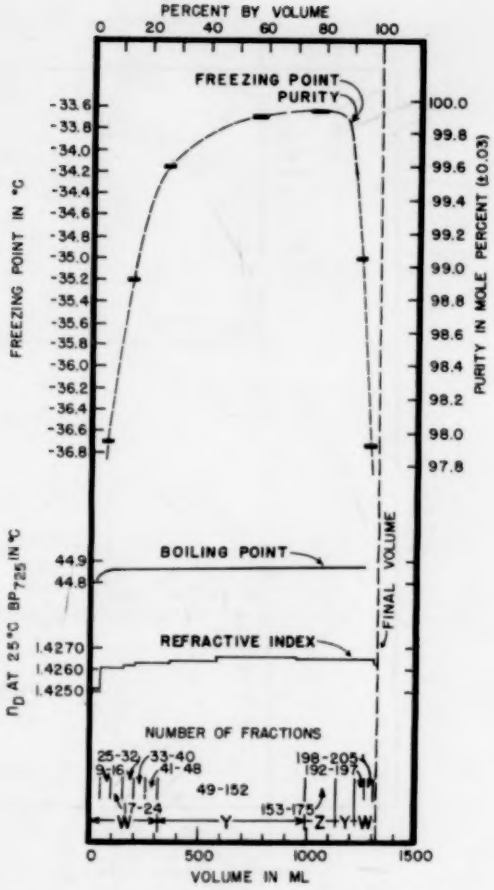

FIGURE 47.—*Results of the second and final distillation of 1,1-dimethylcyclohexane.*

Azeotropic distillation with ethanol at 725 mm Hg in still 9 (3/30/45 to 5/7/45).

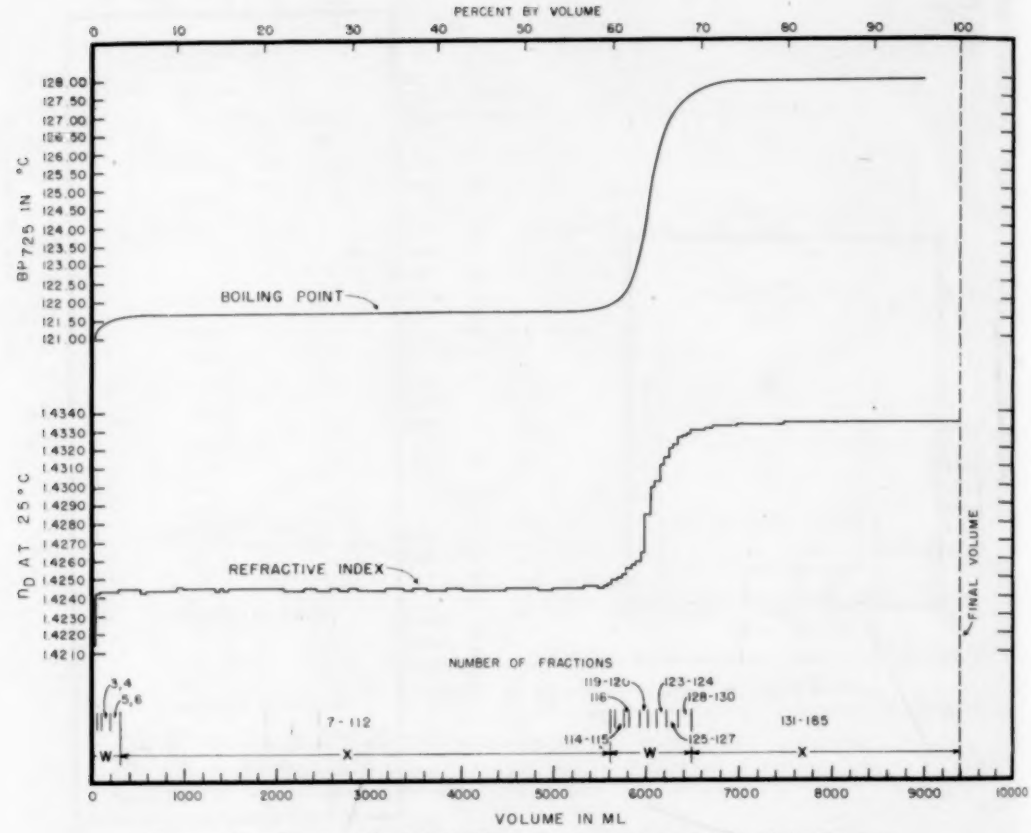

FIGURE 48.—*Results of the first distillation of cis- and trans-1,2-dimethylcyclohexane.*

Regular distillation at 725 mm Hg in still 5 (1/15/45 to 2/16/45).

Fractions 7 to 112 were redistilled to obtain *trans*-1, 2-dimethylcyclohexane (see fig. 50). Fractions 131 to 185 were redistilled to obtain *cis*-1,2-dimethylcyclohexane (see fig. 49).

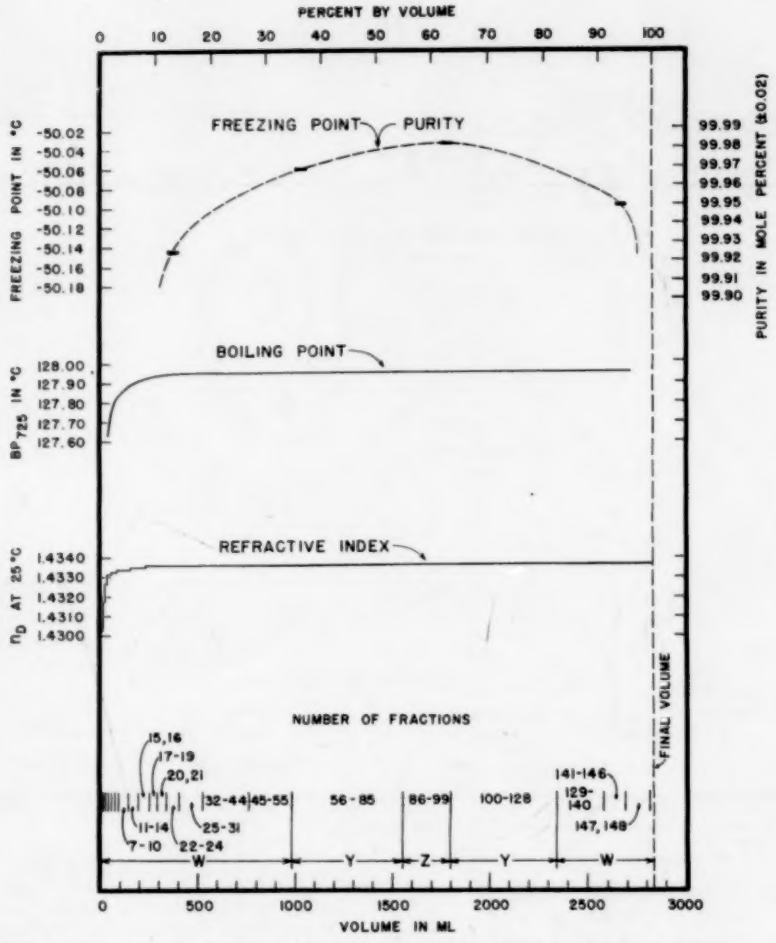

FIGURE 49.—*Results of the second and final distillation of cis-1,2-dimethylcyclohexane.*

Regular distillation at 725 mm Hg in still 9 (5/7/45 to 6/4/45).

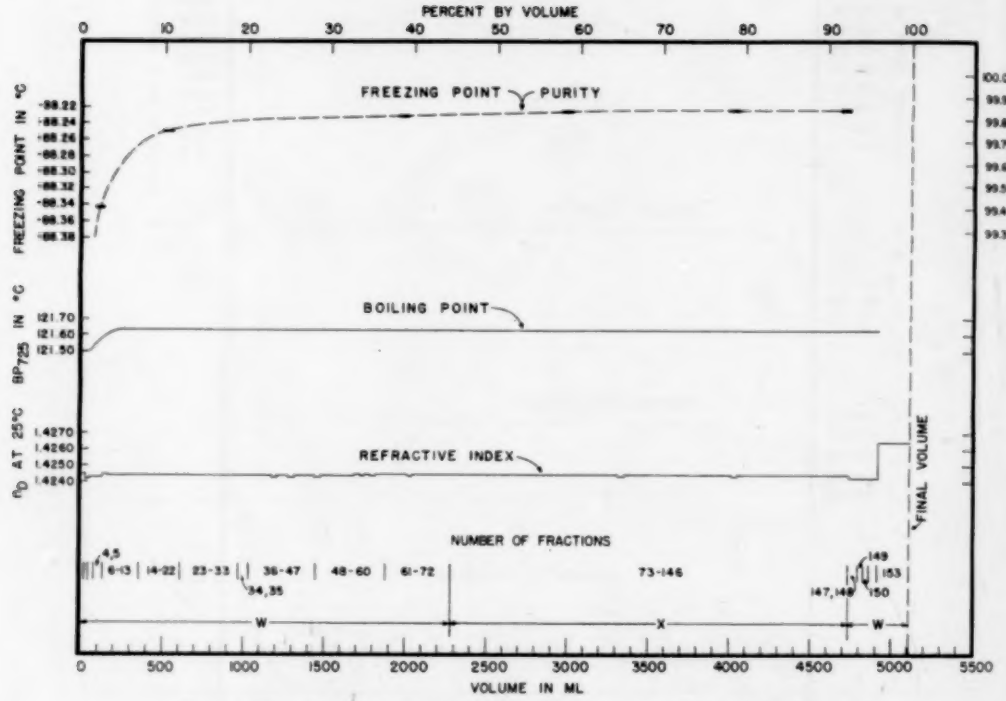

FIGURE 50.—*Results of the second distillation of trans-1,2-dimethylcyclohexane.*

Regular distillation at 725 mm Hg in still 7 (3/21/45 to 4/23/45).

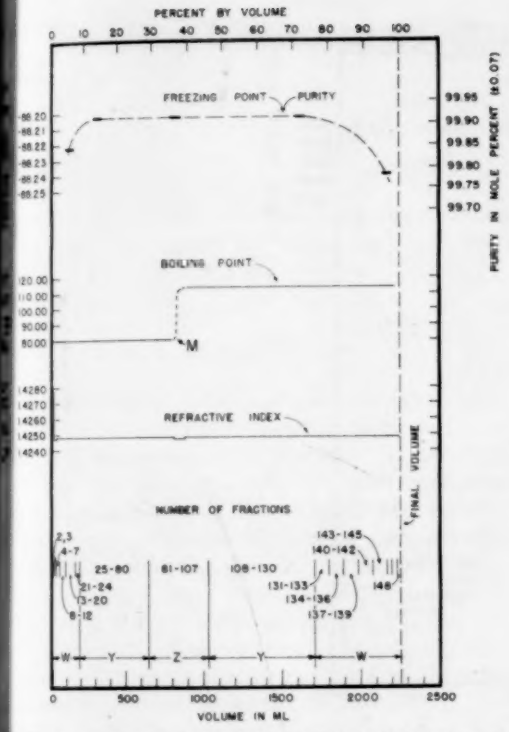

FIGURE 51.—*Results of the third and final distillation of trans-1,2-dimethylcyclohexane.*

Azeotropic distillation with isopropanol and ethylene glycol monoethyl ether at 725 mm Hg in still 13 (9/5/45 to 10/11/45).

The distillate preceding the point marked "M" was distilled with isopropanol as the azeotrope-forming substance, and the remainder of the hydrocarbon was distilled with ethylene glycol monoethyl ether (see footnote *t* of table 1).

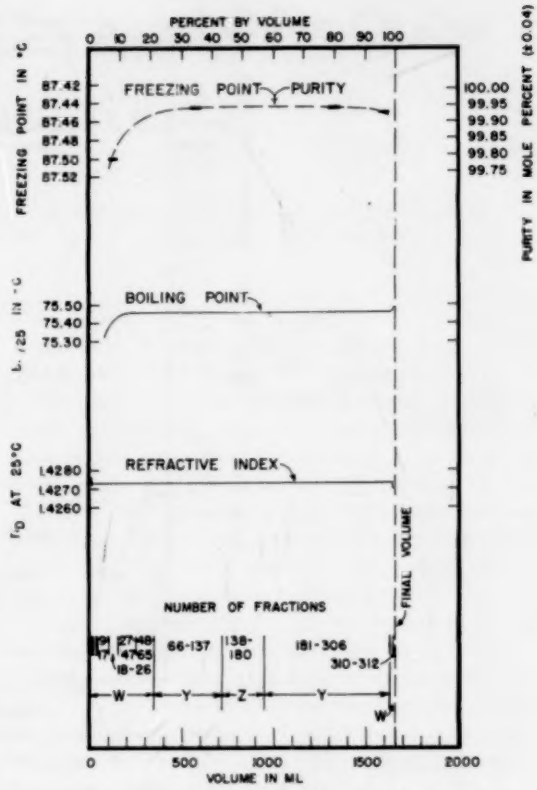

FIGURE 52.—*Results of the first and only distillation of cis-1,4-dimethylcyclohexane.*

Azeotropic distillation with ethanol at 725 mm Hg in still 9 (1/8/46 to 3/7/46).

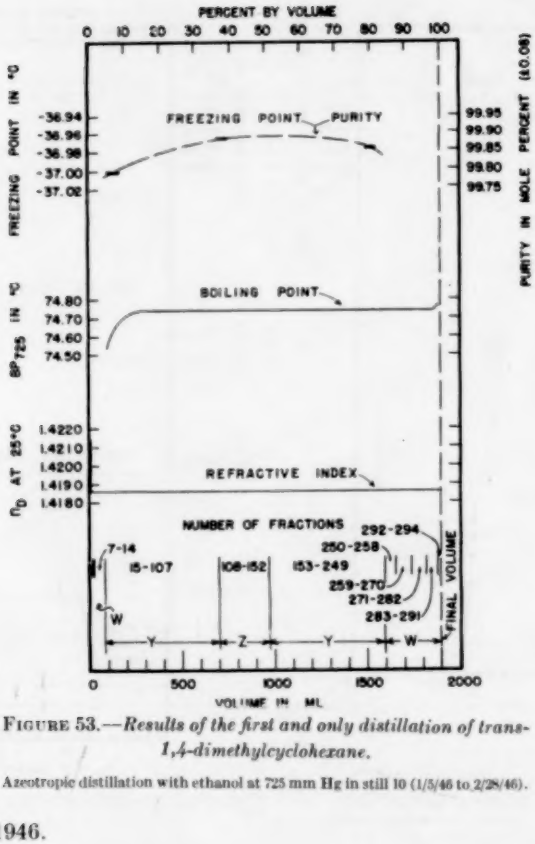

FIGURE 53.—*Results of the first and only distillation of trans-1,4-dimethylcyclohexane.*

Azeotropic distillation with ethanol at 725 mm Hg in still 10 (1/5/46 to 2/28/46).

WASHINGTON, June 15, 1946.

U. S. Department of Commerce
National Bureau of Standards

Research Paper RP1761
Volume 38, January 1947

Part of the Journal of Research of the National Bureau of Standards

Infrared Absorption Spectra of Some Experimental Glasses Containing Rare Earth and Other Oxides

By Ralph Stair and Conrad A. Faick

This paper gives spectral transmission data on soda lime glass containing rare earth (Y, Pr, Nd, Sm, Gd, Er) or other coloring oxides (V, Cr, Mn, Co, Ni, U) in the spectral region of 0.7 to 4.5 microns.

I. Introduction

In connection with experiments upon glass spectral filters and upon the physical properties of certain other glasses as a function of their composition, infrared transmissions were measured upon a number of soda-lime-silica glasses containing some rare earth and other coloring oxides. All glasses were made with the same basic composition, namely: SiO_2, 71.4 percent; Na_2O, 18.4 percent; and CaO, 10.2 percent, as computed from the batch materials. Calcium and anhydrous sodium carbonate of reagent quality and powdered crystalline quartz were employed for the base glass. The other materials were added in the form of oxides.

These glasses were melted in a 25-ml platinum crucible, in a platinum-resistance furnace. The melting procedure followed very closely that used in previous experimental work [1]* and all glasses received the same treatment. Data on the specific refraction and dispersion of some of these glasses have been published elsewhere [12].

The samples obtained often contained a few seeds and a small amount of striation which may have caused small errors in absorption measurements. However, as the complete infrared absorption curve was obtained through the same area of the sample, relative values between the different wavelengths should be adequate.

The rare-earth oxides used in the production of these glasses were from the James collection that had been acquired by the Bureau.[1] According to tests made by the Spectroscopy Section of this Bureau, these rare-earth oxides contained varying amounts of impurities, especially other rare-earth materials, but their purity was judged to be adequate for the purposes of this report.

The praseodymium oxide contained small amounts of lanthanium and yttrium in addition to traces of calcium, copper, iron, magnesium, and silicon. The neodymium oxide was of high purity, containing only traces of calcium, copper, iron, magnesium, and silicon. The samarium oxide was especially good, containing, in addition to small amounts of calcium and silicon, only traces of magnesium and lead, with praseodymium doubtful. The gadolinium oxide contained about 10 percent of europium, about 1 percent each of bismuth and magnesium, in addition to a small amount of calcium, traces of erbium, silicon, and samarium, and possibly traces of potassium and lead. The erbium oxide was not subjected to as thorough spectrochemical study, but it contained

*Figures in brackets indicate the literature references at the end of this paper.

[1] Collection of rare-earth materials prepared by the late Professor James of the University of New Hampshire and subsequently purchased from the University by the National Bureau of Standards.

724217—47——7

about 1 percent of yttrium, smaller amounts of holmium and thulium, and traces of scandium and ytterbium. The purity of the yttrium oxide is not known.

An examination of the different absorption curves shows no significant bands for yttrium (see fig. 2) or for europium (see curve 6 for gadolinium, which contains Eu as an impurity) nor the presence of overlapping of absorption bands that might be expected in mixed materials, where the same impurities are present for a number of the glasses. Hence, in most cases, at least, these impurities were in very small amount or else of a type that is known to produce relatively weak absorption within the region of 0.7 to 4.5 μ. Reagent quality oxides were used for the other coloring materials.

All glasses having a silica base show a high absorption in the region of 2.8 to 4.5 μ, which is caused by some combination of silica with water and other base materials of which the glass is composed. Because this silica absorption may be made to vary between wide limits [9] in the region of 2.9 μ simply by controlling the amount of water within the glass, it is impossible to attempt to make accurate calculations on comparative transmissions within this silica absorption region. Furthermore, analysis of the oxide absorption in the region of 2.8 to 4.5 μ is greatly complicated as the result of the high absorption in the base glass. Either because of this high and variable absorption in the base glass or because the oxides studied have no characteristic bands in this region, no absorption bands between 2.8 and 4.5 μ were discovered that could positively be attributed to the oxides added.

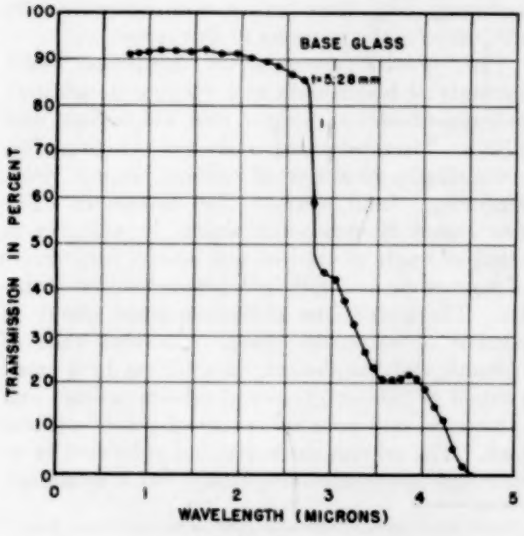

Figure 1.

The transmission of the base glass is given in figure 1. This glass shows no absorption bands at wavelengths shorter than about 2.8 μ. Beyond this wavelength the silica absorption increases rapidly with increase in wavelength.

The glasses vary somewhat in thickness. For several of them two thicknesses were available. This is often useful in infrared studies, because a proper selection of thickness of the specimen permits the structure of the absorption spectrum to be exhibited to best advantage. In this work the more suitable sample was chosen.

II. Instruments and Methods

For a detailed discussion of the experimental procedure, reference is made to previous publications [3, 4, 5, 6, 7, 8]. The spectroradiometer consisted of a mirror spectrometer, with mirrors 50 cm in focal length. A small fluorite prism on a Wadsworth mounting was employed.

The observations were made by the "point by point" method. A portable vacuum thermopile of bismuth-silver, connected with an iron-clad Thomson galvanometer, was used for measuring the radiation. The source of radiation was a Nernst glower, focused upon the entrance slit of the spectrometer by means of a large concave mirror of 1-m focal length. The galvanometer readings were read visually and recorded. The sample was placed in front of the entrance slit of the spectrometer by means of a mechanical carriage which placed it in the same position for each wavelength. The effective spectral slit width varied from about 0.17 at 2 to 0.07 at 4.5 μ.

III. Spectral-Transmission Data

A brief description is given of the glass and its special transmission characteristics. A general summary covering the kinds and amounts of oxides added is given in table 1. The glass numbers correspond to the same samples examined in the visible spectrum and reported on elsewhere [2].

TABLE 1.—*Amount of oxide added to the base glass*

Glass No.	Weight of oxide added	Thickness	Index of refraction wavelength, 5893 A
	Percent	mm	
1	Base glass	5.28	1.5224
2	3.0 V_2O_3	4.73	1.5285
3	1.0 Cr_2O_3	4.21	1.5255
4	1.0 Mn O_2	4.40	1.5237
5	0.04 Co O	4.22	1.5216
6a	.05 Ni O	4.22	----------
6	.50 Ni O	4.47	----------
9	10.0 Y_2O_3	6.81	1.5439
13	10.0 Pr_6O_{11}	7.13	----------
15	10.0 Nd_2O_3	7.27	----------
18	10.0 Sm_2O_3	6.80	----------
19	10.0 Gd_2O_3	6.28	1.5343
20	10.0 Er_2O_3	6.52	----------
23	3.0 U_3O_8	2.52	----------

1. Yttrium Oxide Glass

No appreciable absorption in the near infrared caused by yttrium oxide (Y_2O_3) when added in amount of 10 percent (see fig. 2). Neither was

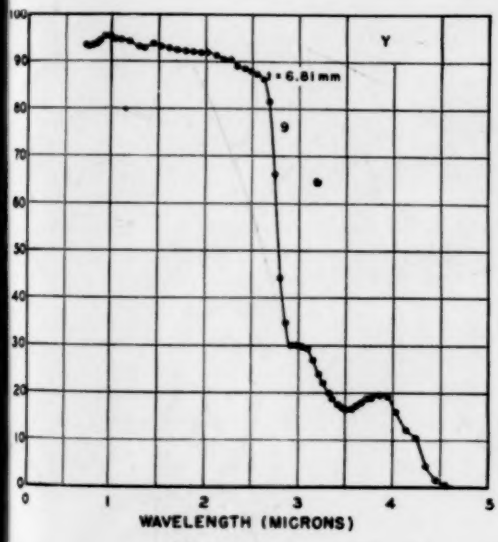

FIGURE 2.

y absorption observed within the visible spec-
um (see reference [2]).

A comparison of the absorption curve for
trium oxide glass with those for the base glass

and the erbium and gadolinium oxide glasses (see figs. 1, 6, and 7) indicates the possibility of some general absorption in the region of 2.7 to 4.2 μ. However, differences in thickness and amounts of water within the glass may account for the greater absorption in this region.

2. Praseodymium Oxide Glass

Two strong absorption maxima occur at about 1.45 and 1.90 μ as the result of the addition of praseodymium (Pr_6O_{11}) in the amount of 10 percent. Weak bands occur at about 0.76 and 1.0 μ (see fig. 3). The general shape of the transmission

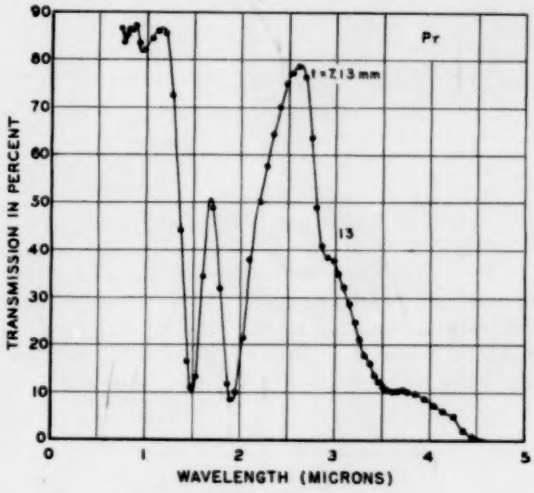

FIGURE 3.

curve indicates the possibility of additional bands in the region of 2.4 and 4.0 μ. Absorption in the visible spectrum gives this glass a light yellowish green color.

3. Neodymium Oxide Glass

The addition of neodymium (Nd_2O_3) in the amount of 10 percent results in three strong absorption bands at about 0.77, 1.63, and 2.43 μ (see fig. 4). It is to be expected that this material would produce a number of absorption bands in the near infrared judging from the number and intensity of the bands in the visible spectrum [2], which give this glass its bright-purple hue.

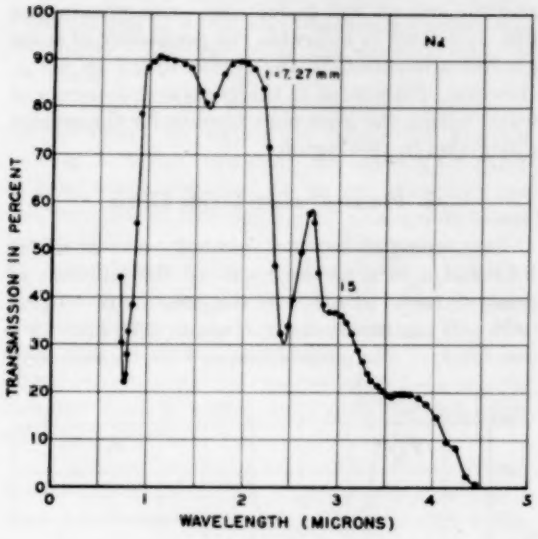

FIGURE 4.

4. Samarium Oxide Glass

The addition of samarium oxide (Sm_2O_3) in an amount of 10 percent gives rise to a very strong absorption band at about 1.47 μ, and weaker bands at about 1.1, 1.92, 2.62, and 4.1 μ (see fig. 5). The strong band at 1.47 μ almost completely masks the one in the neighborhood of 1.1 μ. The presence of so many bands within this part of the infrared spectrum suggests the possibility of other bands at longer wavelengths. Hence it would be interesting to study this material incorporated into a special infrared transmitting glass. Absorption in the visible spectrum gives this glass a light yellowish hue.

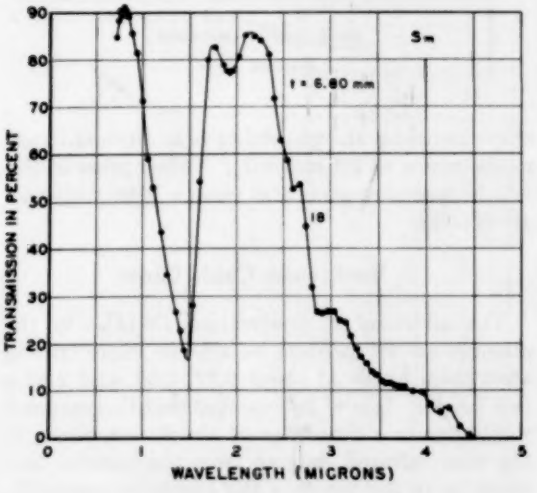

FIGURE 5.

5. Gadolinium Oxide Glass

No appreciable absorption occurs in the near infrared (or in the visible spectrum) because of the addition of gadolinium oxide (Gd_2O_3) (see fig. 6).

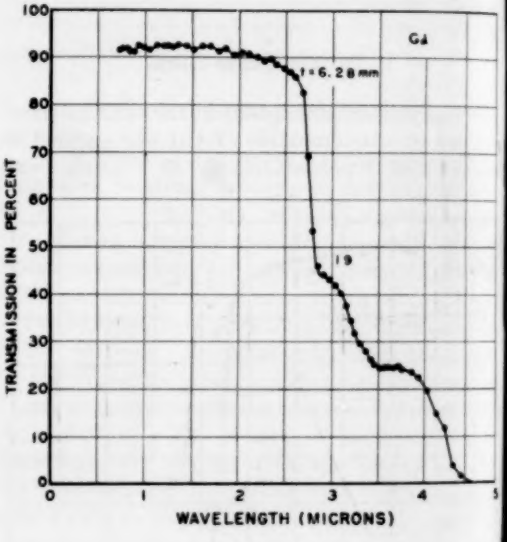

FIGURE 6.

6. Erbium Oxide Glass

The addition of erbium oxide (Er_2O_3) in an amount of 10 percent gives rise to one strong absorption band at about 1.52 μ and two weaker bands at about 0.80 and 0.95 μ, respectively (see fig. 7). A comparison with the transmission curve for gadolinium (fig. 6), which probably produces but little or no absorption in the infrared between 0.6 and 4.5 μ, indicates no other important absorption bands shorter than 4.5 μ. Absorption in the visible spectrum gives this glass a light-pink color.

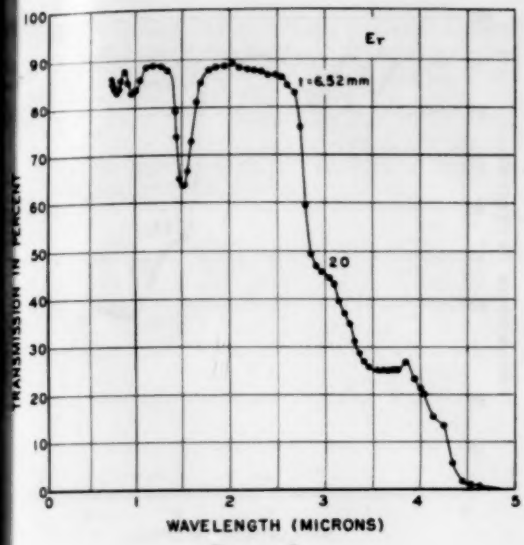

FIGURE 7.

7. Other Oxide Glasses

The addition of vanadium (V_2O_5), cobalt (CoO), nickel (NiO), or uranium (U_3O_8) oxide in small amounts (see table 1) produce strong absorption bands in the spectral region between 1 and 4μ (see figs. 8, 11, 12, and 13). It is to be noted that much smaller concentrations of these metals were required to produce absorption of magnitude similar to that resulting from the addition of 10 percent of some of the rare-earth oxides. In the case of the addition of chromium (Cr_2O_3) and manganese (MnO_2) oxides, little change in absorption occurs within the near infrared region (see figs. 9 and 10).

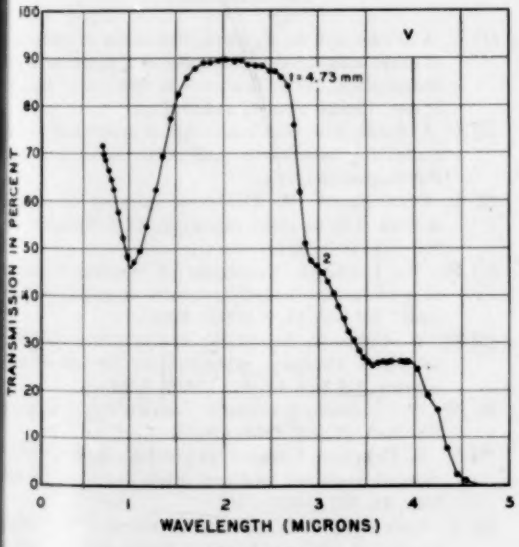

FIGURE 8.

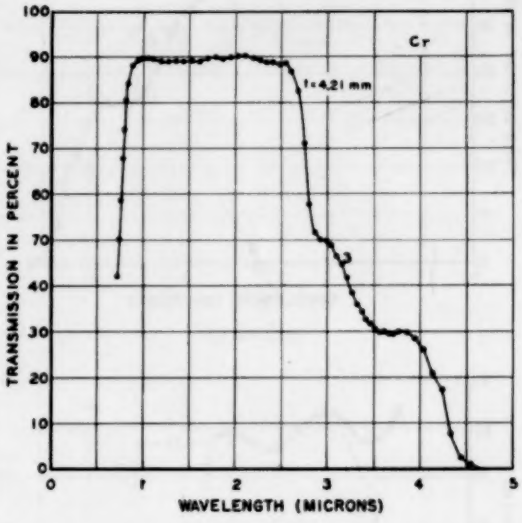

FIGURE 9.

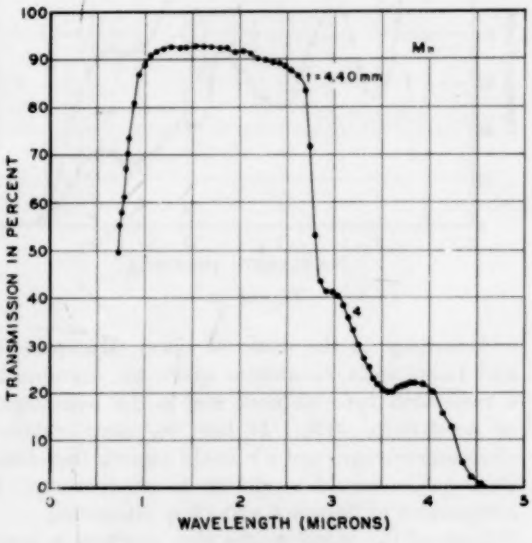

FIGURE 10.

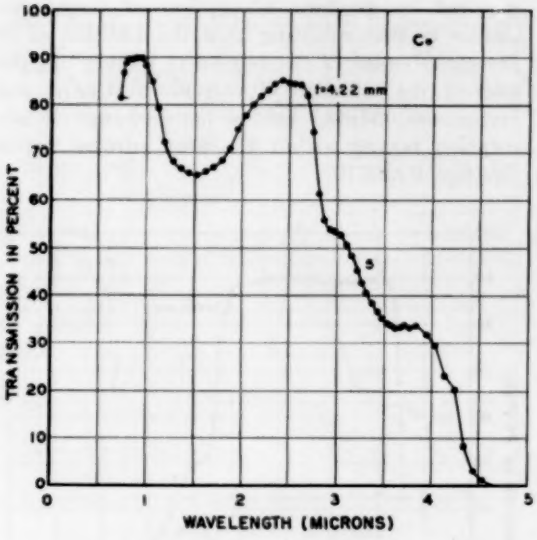

FIGURE 11.

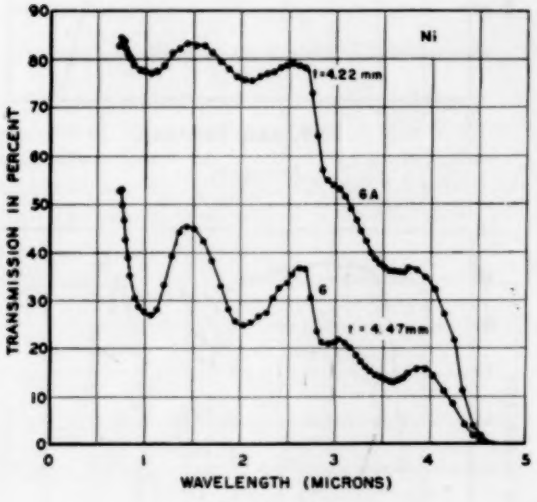

FIGURE 12.

According to the work of Kiess, Humphreys, and Laun upon its atomic spectrum, uranium is a rare-earth type element and is the homologue of neodymium [10]. It has the same valence electron structure and we would expect, therefore, its behavior would be similar to neodymium. A comparison of figures 4 and 13 is interesting.

Each of the metal oxides also produces a large amount of absorption in the visible spectrum resulting in a distinct color for each glass. The

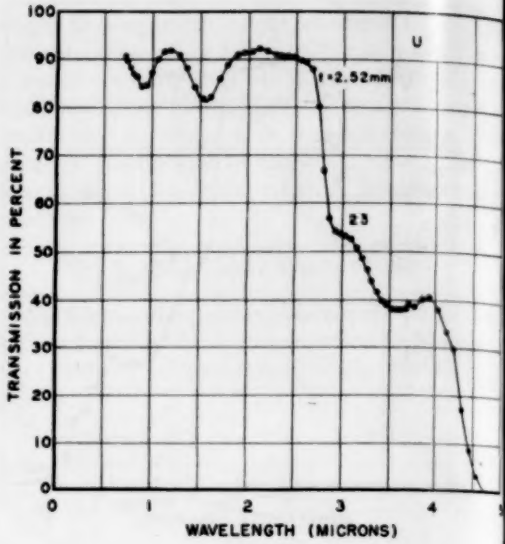

FIGURE 13.

colors resulting in the glasses of this group are as follows for the different oxides: Cobalt, pale blue; nickel, light to dark smoke to dark purple; vanadium, light yellow to yellow green (similar to novial *B*); uranium, light yellow (near novial *C*); chromium, green to yellowish green; and manganese, amethyst.

References

[1] C. A. Faick and A. N. Finn, The index of refraction of some soda-lime-silica glasses as a function of the composition, BS J. Research **6,** 993 (1931) RP320; J. Am. Ceram. Soc. **7,** 518 (1931).

[2] C. A. Faick, The visible absorption spectra of glasses containing rare earth and other coloring oxides. Publication pending.

[3] R. Stair and W. W. Coblentz, Infrared absorption spectra of some plant pigments, BS J. Research **11,** 703 (1933) RP617.

[4] W. W. Coblentz, Constants of spectral radiation of a uniformly heated inclosure, or so-called black body, BS Bul. **10,** 1 (1913) S204.

[5] W. W. Coblentz, Sensitivity and magnetic shielding tests of a Thomson galvanometer for use in radiometry, BS Bul. **13,** 423 (1916) S282.

[6] W. W. Coblentz, A portable vacuum thermopile, BS Sci. Pap. **17,** 187 (1921) S413.

[7] W. W. Coblentz, Infrared transmission and refraction data on standard lens and prism material, BS Sci. Pap. **16,** 701 (1920) S401.

[8] R. Stair and W. W. Coblentz, Infrared absorption spectra of plant and animal tissue and of various other substances, J. Research NBS **15,** 295 (1935) RP830.

[9] Anna J. Harrison, Effect of water content on infrared transmission of simple glasses. Paper given before the Glass Division at the Buffalo meeting of the Amer. Ceram. Soc., May 1, 1946.

[10] C. C. Kiess, C. J. Humphreys, and D. D. Laun, Preliminary report on the description and analysis of the first spectrum of uranium, J. Research NBS **37,** 57 (1946) RP1729.

[11] Woldeman A. Weyl, Colored glasses, J. Soc. Glass Tech. **28,** 158 (1944).

[12] John C. Young and Alfred N. Finn, Effect of composition and other factors on the specific refraction and dispersion of glasses, J. Research NBS **25,** 759 (1940) RP1352.

WASHINGTON, June 5, 1946.

U. S. Department of Commerce
National Bureau of Standards

Research Paper RP1762
Volume 38, January 1947

Part of the Journal of Research of the National Bureau of Standards

Properties of Water-Repellent Fabrics

By John W. Rowen and Domenick Gagliardi

A review and an analysis of the theory of water repellency of textile fabrics have been made. The physicochemical basis underlying the wettability, or water repellency, of treated fabrics is discussed. A survey of the laboratory test methods for evaluating water repellency of textile fabrics is presented. A study was made of the water-repellent properties of 11 commercial raincoat and 4 military fabrics. For this study two of the more recent test methods were examined, the drop-penetration and the contact-angle tests. Two other, and older, test methods were also studied, the spray-rating and the hydrostatic-pressure tests. Several exploratory observations were made in an attempt to determine the mechanism by which water-repellent fabrics lose their repellency when exposed to rain.

I. Introduction

The National Bureau of Standards has been called upon from time to time to supply information dealing with "water-repellent" fabrics. These requests have usually come from Government agencies and the public at large. In recent months there has been an intensified interest in this subject, and the Bureau decided to review the field of "water repellency" and to carry out a laboratory study in order to answer present and future questions regarding this subject.

An examination of the literature [1] [1] revealed the existence of a large number of chemical compounds and commercial treatments about which extraordinary claims were made. Further investigation showed that a large number of laboratory test methods had been devised for evaluating "water repellency." Moreover, considerable confusion was encountered concerning the interpretation of the test results and the meaning of such terms as "waterproof", "water-repellent", "showerproof", and "water-resistant" fabrics. It appeared desirable, therefore, to make a survey of the field of "water repellency" and to carry out some laboratory studies on currently available materials. This report, therefore, will deal mainly with the fundamental nature of "repellency", the laboratory methods used to evaluate it in fabrics, and some laboratory observations by the authors on a variety of raincoat fabrics.

[1] Figures in brackets indicate the literature references at the end of this paper.

II. Theory of "Water Repellency"

We must at the very beginning distinguish between "waterproof" and "water-repellent" textile surfaces. There is still a great tendency to mention both terms simultaneously and interchangeably, in spite of the numerous papers [2, 3, 4] that have been written to call attention to the great difference between them. A waterproof fabric is one in which the pores, the open spaces between the warp and filling yarns and between the fibers, are filled with appropriate substances, resulting in a fabric having a continuous surface and a very low air permeability. A water-repellent fabric is one in which the fibers are usually coated with a "hydrophobic" type of compound, and the pores are not filled in the course of the treatment. The latter types of fabrics are quite

permeable to air and water vapor. The characteristics of the two types of fabric surfaces are summarized below:

	Waterproof	Water repellent
Pores	Filled	Unfilled.
Water-vapor permeability.	Very small	Small or large.
Air permeability	Small	Usually large.
Chief characteristic	Extremely resistant to passage of water even under a hydrostatic head.	Resistant to wetting by rain drops and to the spreading of water over the textile surface, but permits the passage of water under a hydrostatic head.

From the foregoing it is seen that a "water-repellent" textile surface may never be truly waterproof and that a "waterproof" textile surface does not necessarily have to be water repellent. Unless the pores of a raincoat or shower-resistant jacket are large enough to permit transpiration, the wearer will be extremely uncomfortable due to excessive perspiration. The water-repellent fabrics are, therefore, more suited in this respect for making raincoats or shower-resistant jackets. The subject of waterproofing of textiles is very extensive and beyond the scope of this paper, therefore the discussion is restricted to the subject of water-repellent textile surfaces.

As the term implies, a water-repellent textile surface is one that appears to "repel" water. In such cases, the water does not wet or penetrate the surface of the textile fabric. The tendency of a solid to resist wetting is a function of the chemical nature of the solid surface, the roughness of the surface, the porosity of the surface, and the presence of other molecules on the surface. When a drop of water comes to rest on a solid, it may assume one of the forms shown in figure 1, or any intermediate form from complete wetting to complete nonwetting. Which form the drop will take is determined by the above-mentioned variables.

Examination of the angle of contact (fig. 1)—the angle formed by the tangent to the drop at the point of contact with the surface (angle measured through the liquid)—reveals that the size of the angle is related to the repellency of the surface. When the angle of contact is small (under 90 degrees) the surface is said to be wettable [5, 6], and when the angle is large (over 90 degrees) the

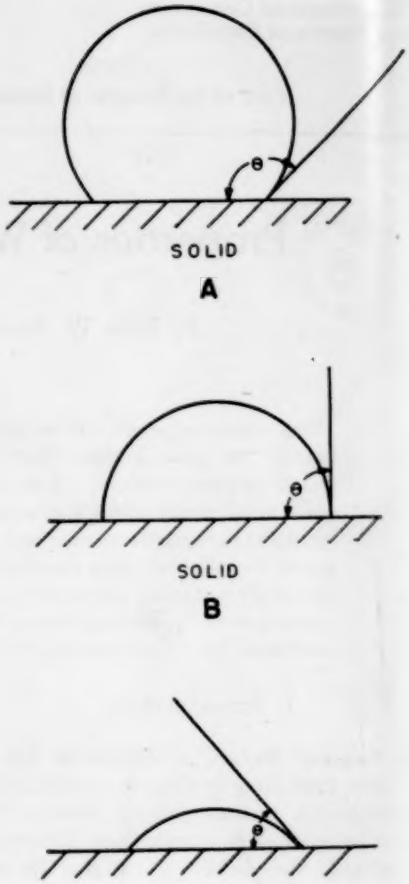

FIGURE 1.—*Shapes of drops on solid surfaces.*

A, Contact angle between 90 and 180 degrees; *B*, contact angle of 90 degrees; *C*, contact angle between 0 and 90 degrees.

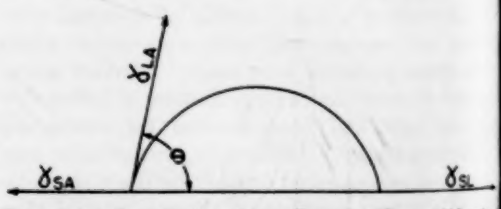

FIGURE 2.—*Forces acting at equilibrium on drop-solid system.*

surface is said to be nonwettable, or repellent. Further consideration of the energy relationship of the drop-surface system as depicted in figure 2 reveals that the equilibrium condition is due to

the following surface energies: γ_{sa}, γ_{la}, γ_{sl}, where γ_{sa} is the free surface energy per square centimeter (numerically and dimensionally equivalent to the surface tension) of the solid in contact with air, γ_{la} is the free surface energy per square centimeter of the liquid when in contact with air, and γ_{sl} is the free surface energy per square centimeter of the solid when in contact with the liquid. At equilibrium, the following relationship holds:

$$\gamma_{sa}=\gamma_{la}\cos\theta+\gamma_{sl}. \tag{1}$$

Dupre [7] first derived the equation relating the free surface energies with the work of adhesion:

$$W=\gamma_{sa}+\gamma_{la}-\gamma_{sl}. \tag{2}$$

From eq 1 and 2 it follows that

$$W=\gamma_{la}\,(1+\cos\theta).^{2} \tag{3}$$

Therefore, by measuring θ and the surface tension of the liquid, one may calculate the work of adhesion between the liquid and the surface of the solid. It is clear that the smaller the work of adhesion, the smaller will be the wettability and the greater will be the repellency. For poorly repellent, easily wettable surfaces, the drop of liquid will assume a shape similar to C in figure 1; and for highly repellent, nonwettable surfaces, the drop will assume shape A.

As textile fabric surfaces are not smooth, continuous surfaces, but rather porous, screen-like surfaces, one must examine the above considerations and see how they apply to textiles. Figure 3 shows the cross section of an idealized fabric.

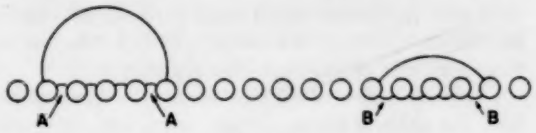

FIGURE 3.—*Drops on surface of idealized yarn.*

In this figure the parallel yarns are shown as circles. If the angle of contact between water and the surface of the fabric is larger than 90 degrees, the equilibrium position of the water level of a drop of water will be, as indicated by the line AA, well outside the fabric. If, however, the angle of contact is much smaller than 90 degrees, the water will penetrate the pores and the level will fall to some position such as BB. Cassie and Baxter [9] have shown that in the case of porous surfaces the apparent angle of contact is related to the continuous surface-water angle of contact in the following way:

$$\cos\theta_a=f_1\cos\theta-f_2, \tag{4}$$

where

θ_a = apparent angle of contact
θ = angle of contact
f_1 = the fraction of the plane geometrical area of unity parallel to the rough surface occupied by the solid-liquid interface.
f_2 = the fraction of the plane geometrical area of unity parallel to the rough surface occupied by the liquid air interface.

They also derived the relationships between the "f" variables, the distance between the fibers in the yarns, the radius of the fibers, and the angle of contact:

$$f_1=\frac{r}{r+d}\left(1-\frac{\theta}{180}\right) \tag{5}$$

$$f_2=\frac{r}{r+d}\sin\theta, \tag{6}$$

[2] The work of adhesion (W) defined above is the amount of energy necessary to destroy 1 cm² of liquid-solid interface and to form 1 cm² of liquid and a 1 cm² of solid surface in contact with air. The energy of a unit area of solid surface in air may be somewhat different from the energy of a unit area of solid surface in vacuum. The difference between these two energies will depend upon the relative humidity, the hydrophobicity of the surface, the presence of transient gaseous or solids in the air, etc. It is physically impossible to separate a solid and a liquid without leaving the solid covered with at least a part of a monolayer [6, p. 62; 8]; however, it is desirable to define a work for such a process, which is shown to be given by

$$W'=\gamma_{so}+\gamma_{lv}-\gamma_{sl}, \tag{1'}$$

where γ_{so} is the free surface energy per square centimeter of solid in vacuum, γ_{lv} is the free surface energy per square centimeter of liquid in equilibrium with its vapor, and γ_{sl} has the same meaning as before. Now, for the clean solid in vacuum, the following relationship (analogous to eq 1) may be postulated:

$$\gamma_{so}=\gamma_{lv}\cos\theta+\gamma_{sl}, \tag{2'}$$

where γ_{sv} is the free surface energy per square centimeter of the solid in equilibrium with saturating vapor of the liquid. It follows from eq 1′ and 2′ that

$$W'=\gamma_{so}-\gamma_{sv}+\gamma_{lv}(1+\cos\theta). \tag{3'}$$

If we assume $\gamma_{lv}=\gamma_{la}$ (which approximation is almost within experimental error), we have

$$W'=\gamma_{so}-\gamma_{sv}+W. \tag{4'}$$

The quantity $\gamma_{so}-\gamma_{sv}$ may be looked upon as the free energy of immersion, at constant temperature, of a unit surface of clean solid immersed in a saturated vapor and is given by [8]

$$\gamma_{so}-\gamma_{sv}=RT\int_0^P\Gamma_2 d\ln P, \tag{5'}$$

where Γ_2 is Gibbs' "surface density" of the vapor on the solid surface and equal to $q/M\Sigma-T/V_2$, where q is the quantity of water vapor adsorbed per gram of absorbent, M is the molecular weight of the vapor, Σ is the area in square centimeters per gram of solid, T is the thickness of the surface region, and V_2 is the molal volume of the vapor.

The right-hand member of 5′ can be integrated if an equation for the adsorption isotherm is known or, if not, a graphical integration of the area under the isothermal curve can be carried out.

where

r = radius of the fibers
d = one-half the distance between the fibers
θ = contact angle between the water and the fiber.

From the above, it appears as though the most water-repellent fabric will be the one on which the drop assumes a form as shown in figure 3, A. This condition may be obtained by adjusting the variables previously mentioned as being responsible for the form of the drop. It is advisable to consider each of the variables separately.

Chemical nature of the solid surface.—When purified, the natural fibers, cotton, wool, silk, etc., are hydrophilic in character and hence the drops assume shapes similar to *C* (fig. 3). It is common practice, therefore, to treat fabrics intended to be water repellent, with various hydrophobic compounds—compositions of waxes, petroleum-like molecules, and soaps of polyvalent metals, which deposit long-chain hydrocarbon molecules on the surface of the fabric. When properly treated with a water-repellent agent, the surface of the fabric will cause a water drop to assume a form very similar to *A* in figure 3.

Roughness of the surface.—Wenzel [10] pointed out that roughness has a peculiar effect on the angle of contact. He employed Freundlich's [11] concept of "adhesion tension," which is defined as follows:

$$AT = \gamma_{la} \cos \theta. \tag{7}$$

It is noted that the adhesion tension is the difference between the work of adhesion per square centimeter (eq 3) and the surface tension. Wenzel recognized that eq 7 was true only in the case where the surface was a mathematical plane. As most surfaces are not of this type, there is associated with each surface a roughness factor R, which is the ratio of the actual surface to the geometric surface. Wenzel showed the validity of the following equation:

$$AT = \gamma_{la} \frac{\cos \theta}{R}. \tag{8}$$

Porosity of the surface.—Cassie and Baxter [9, 12] pursued the idea of the roughness factor and showed that the apparent adhesion tension of a porous surface was given by

$$AT_a = \cos \theta_a \gamma_{la} = \gamma_{la}(f_1 \cos \theta - f_2), \tag{9}$$

where the symbols have the same meaning as in eq 4. Using a hexagonal idealized yarn pattern as a model, the above workers showed that σ, the bulk density of the yarn, was related to the radius of the fibers in the following way:

$$\sigma = \left(\frac{\pi}{2\sqrt{3}}\right) \frac{\rho r^2}{(r+d)^2}, \tag{10}$$

where ρ is the density of the fiber. With the aid of eq 4, 5, 6, and 10, they were able to obtain plots of contact angle versus σ. These plots showed that the angle of contact approaches 180 degrees as σ approaches small values (about 0.1 g/ml). Their theory led them to the position that fabric structure was extremely important in the production of water-repellent fabrics.

Presence of other molecules on the surface.—It is a well-known fact that the surface properties of solids may be greatly altered by covering the surface with impurities, greasy films, dust particles, water vapor and gases, etc. The presence of surface impurities may or may not be related to the fact that numerous workers [12, 13, 14, 15, 16, 17] have reported not one angle of contact with a particular system, but two angles, an advancing and receding angle. One angle is obtained when water has advanced over a surface and the other when water has receded from the surface. This difference in contact angle is often called the hysteresis of the contact angle. The cause of the hysteresis is still not clearly understood. Recently, Harkins [18, 19], working with hydrophobic materials and an improved method of measuring contact angles, found no hysteresis. Langumir [17] suggests that the hysteresis of contact angles, especially with water, is due to the presence of a surface layer of molecules with one end hydrophilic and the other hydrophobic, which are overturned by the receding water.

From the above considerations of the variables involved in water repellency, one would expect that a fabric having a high contact angle would be a water-repellent fabric. In such cases the water level will remain well outside the surface, as shown in figure 3A. At this point it looks as though we may be able to write a prescription for the optimum conditions for water repellency, viz, a textile fabric in which each fiber is completely coated with the material having the highest solid-water angle of contact. It is unfortunate that this prescription has never been tested. The

ason for this is that the present methods of eating fabrics for water repellency do not uarantee the complete coating of each individual ber. These treatments leave many of the inter- vined fibers without any surface coating. The resence of hydrophilic surfaces in the treated bric will of course greatly diminish the over-all sistance of the fabric to wetting.

II. Survey of Methods Used for Measuring Water Repellency in Fabrics

The number of test methods devised for meas- ring water repellency appear to be almost as many as the number of laboratories engaged in this field. Comparative data from and references to the various reports on laboratory test methods have been assembled in table 1. The object in most of these tests has been to offer a sensitive and accurate method of predicting the relative performance of fabrics in the rain. Very few, if any, of the published papers, however, have furnished any data showing the correlation between the particular test method and the performance of fabrics in the rain. Examination of the literature reveals that there is a considerable variation in the methods of testing and the interpretation of the results. It was found convenient for the

TABLE 1.—*Methods and testing conditions used by various laboratories in measuring water-repellent properties of textile fabrics*

Name of test	Reference and year	Test temperature	Sample size	Result units	Extent of use
CLASS *A* TEST					
Hydrostatic pressure	[21] 1941	80°±1° F	3″×3″	cm	Wide, ASTM, and AATCC.
Suter hydrostatic pressure	[22] 1940	80°±1° F	4″×4″	cm	Federal Specification CCC-T-191a and Supplement.
Mullen (high-pressure range)	[22] 1944	? [1]	4″×4″	lb/in.²	Do.
Box test for waterproofness	[24] 1936	?	4½×20″	ml/min	Limited.
British (DSIR)	[25] 1925	?	4.8 cm²	cm	Obsolete.
CLASS *B* TEST					
AATCC spray	[26] 1941	80°±1° F	7″×7″	g, %	Very wide; AATCC; Federal Specification CCC-T-191a and Supplement.
Drop penetration	[27] 1944	80°±1° F	8″ ×9″	min	Federal Specification CCC-T-191a and Supplement.
Water penetration (drip)	[28] 1943	?	4″×4″	sec	ASTM.
Bundesmann	[29] 1935	?	154 cm²	ml	British Specifications; Germany.
Impact penetration	[34] 1943	80°±1° F	6″×8″	g	
Spray test	[31] 1937	?	6″×6″	g, %	Limited.
Kern	[32] 1933	?	4 cm²	No. of drops	Do.
Franz and Henning	[23] 1936	?	12×26 cm	g, %	Germany.
Official German rain	[34] 1910	?	28×38 cm	g, %	Do.
Spray penetration	[35] 1946	12°±2° C	12″×12″	ml	U. S. Navy.
CLASS *C* TEST					
Immersion	[36] 1941	80°±1° F	3″×3″	g, %	Wide; AATCC.
ASTM water-absorption (spray) method	[37] 1943	?	8″×8″	g, %	Federal Specification CCC-T-191a and Supplement.
Dynamic absorption	[38] 1944	80°±1° F	8″×8″	g, %	Do.
Bundesmann	[39] 1935	?	154 cm²	g, %	British Specifications; Germany.
Becker submersion method	[40] 1935	Room temp	5×75 cm	g, %	Germany.
Esslinger submersion method	[41] 1940	?	15× 5 cm	g, %	Do.
CLASS *D* TEST					
Contact angle by tensiometer	[42] 1945	35° C	0.196 in.²	deg	Experimental.
Wetting test	[43] 1945	?	Single yarn	sec	Do.
Wenzel method	[44] 1936	?	1″×3″	deg	Do.

[1] Interrogation mark signifies temperature not indicated.

purpose of this report to arrange the different test methods in four general classes:

Class *A*. Methods by which the hydrostatic pressure required to force water through a fabric is measured.

Class *B*. Methods by which surface wetting and penetration under the influence of falling drops is measured.

Class *C*. Methods by which the absorption of water by the fabric, when immersed or manipulated under water, is measured.

Class *D*. Methods by which the wettability of the surface of the fabric is measured by means of the angle of contact or some function of the angle of contact.

Some timely comments about the more popular test methods in each group are given below.

Class A.—In this class of test methods, the fabric is subjected to the action of water under pressure by a variety of means. Either the amount of water penetrating in a specified time or the pressure required to force water through the fabric is measured. The most widely used test methods in this class are the AATCC [21] and the Suter [22] hydrostatic-pressure tests. Both methods give reproducible test values. It has been reported [45] that a correlation exists between the two methods. The following relationship is supposed to hold at 27°±3° C:

$$A=1.32S-4, \qquad (11)$$

where A is the AATCC test value, S is the Suter test value.

The hydrostatic-pressure test values are dependent mainly on the pore size and the angle of contact. The bulge that occurs when the pressure is applied on the fabric requires a correction [46], but in view of the reproducibility of the test and the smallness of the correction factor, the extra measurements and calculations are usually avoided.

Class B.—The tests in this class are in some cases very different from each other. They are all, moreover, quite different from those in class *A*. All the tests in this class subject the test fabric to the action of water drops. The number, size, frequency, and energy of the drops in the various tests vary considerably. The advantages and disadvantages of these various tests are briefly discussed below:

1. AATCC Spray Test. This test is very widely used in the textile industry for control work. The test will distinguish qualitatively between treated and untreated fabrics. It is not able, however, to distinguish between obviously different water-repellent finishes or to predict the performance of a fabric in the rain.

2. Drop-Penetration Test.—This test was developed for and used by the United States Quartermaster Corps during the war. The energy of the drops used in this apparatus is approximately 10,000 to 15,000 ergs. This value is much larger than that of the drops in a cloudburst (3,000 ergs). It appears that by this test one may be able to arrange fabrics in what seems to be a proper order of protection in the rain. The hardness of the fabric backing has a profound influence on the test value. This is probably also true for the other tests in this group. It should be mentioned that the values obtained in the drop penetration test may differ as much as 20 percent among each other, depending on the particular fabric and its test value.

3. Bundesmann Test.—The Bundesmann test was developed in Germany. It can be used in two ways: (1) to measure the amount of water penetrating the sample, or (2) to measure the amount of water absorbed by the sample in a given time. Again the drops of water in the test have energy of from 15,000 to 30,000 ergs, which is a much larger value than is found in a cloudburst. In this procedure the sample of cloth is in constant motion and is continuously rubbed on the under side during the test. When the amount of water absorbed is measured, the mean deviation [33] of the test value is reported to be about 3 percent. The method seems to offer some advantages over the other tests in class *B* and has been recently adopted by the British Sub-Committee of the General Technical Committee as a standard test method.

4. Impact Penetration Test.—This test involves the spraying of 500 ml of water on the test specimen. At the end of the spray period, a blotter beneath the fabric is weighed. The increase in weight of the blotter represents the amount of water that passed through the cloth. No data are available on correlation with natural rain.

5. Spray Test.—No temperature control is specified in this test. It appears to be similar to the impact penetration test. No data are available for correlating the results of the test with results obtained with fabrics in natural rain.

6. Kern Test.—This novel method has been patented. It employs a single drop of water of definite size. An electric circuit is used to detect the penetration of the water to the under side of the test specimen. The average deviation of the test value from the mean appears to be smaller for smaller size drops. Although there appears to be a tremendous variation in the results, depending upon the fabric, the author states that seven tests are sufficient for obtaining "exact results."

Class C.—All methods in this group measure the resistance that the finish offers to wetting by water. As droplet penetration is not used in these methods, the part played by the structure of the fabric is less important than in other tests in determining the test value. The water absorbed by the fabric is measured by weighing the test specimen after some form of partial drying. In some of the tests (dynamic absorption, Becker, etc.), the sample is in motion during the test period of exposure to the water. In almost all cases the deviation of any particular test value from the mean appears to become smaller as the exposure time gets larger. The dynamic types of tests are definitely to be preferred to the static types in this category. Again, it should be pointed out that little, if any, work has been done to correlate these test results with the performance of fabrics in the rain.

Class D.—Workers who have used the following three technics have done so in an attempt to understand the mechanism of wetting. Various methods for measuring contact angles [47] have been described. The three methods which have been applied to fabrics are discussed below.

1. Wenzel Method.—Wenzel appears to have been the first to attempt to apply methods of measuring contact angles to fabrics [10]. He modified the tilting-plate method [47] to make it applicable to fabrics. Wenzel measured the contact angle of many materials, waxes, cellulose acetate, many metal stearates, rosin, and others. His data indicated that the method was applicable to textile surfaces and was very reproducible. At the Bureau it was found possible to reproduce the values that Wenzel obtained on paraffin wax on glass. It was found, however, that this method lacked control over the following variables: (a) Temperature, (b) rate of flow of the water over the solid surface, (c) rate of rotation of the plate in the water, and (d) cleanliness of the surface of the liquid.

2. Wetting Test.—This test measures the time for the contact angle on a yarn or strip of fabric to decrease to 90 degrees. This time has been called the "wetting time." Cassie and Baxter claim that the wetting test is more sensitive to proofing efficiency than either the Bundesmann or the hydrostatic-pressure tests.

3. Contact Angle by the Tensiometer Method.—Wakeham and Skau [42] found that, by modifying an ordinary interfacial tensiometer and forcing a circular piece of fabric through the surface of the water, they obtained a relationship between the pressure necessary to force the disk of cloth through the surface of the water and the angle of contact of the water to fabric. The method does not appear to be capable of measuring angles greater than 120 degrees. Unfortunately, the upper portion of the measurable range is the most useful from the point of view of water repellency.

The great dependence of all test values on the temperature of the water has been mentioned in several reports [43, 45, 33, 48]. It is quite surprising, therefore, that many of the methods listed in table 1 appeared to be uncontrolled in temperature.

The above review of the methods used to measure water repellency indicates that no one method completely measures the phenomenon. It appears necessary that a combination of tests be used to evaluate the water repellency of a fabric. It appears possible, also, to select one test from each class and report the results in the same units. For example, the hydrostatic pressure is increased at the rate of 1.0 cm a second in the AATCC test. The test value could be expressed in time units. This could also be done with the drop penetration, the dynamic absorption, the wetting and other tests. One could then obtain a summary test value which would be the results of n number of test values, all expressed in time units:

$$T=f\ (a, b, c, \ldots\ n). \qquad (12)$$

It seems reasonable to assume that the value de-

rived from n number of tests would be a more reliable measure of the repellency of a fabric than taking the value of only one test. It would remain to be proved, however, whether such a summary value gives an accurate and reliable indication of the performance of a fabric in the rain.

Considerable information obtained during the war indicates that many of the test methods given in table 1 are not applicable for evaluating the repellency of woolen fabrics [49]. All the test methods mentioned require further investigation to see whether they can be adapted for testing all types of water-repellent fabrics. It is also necessary that some of these methods be studied for the purpose of setting up commercial and Government standard methods of testing.

IV. Evaluation of Water Repellency by Typical Test Methods

In planning the laboratory work, it was necessary to take into account the questions that are asked by Government agencies, industry, and the public at large. The following general questions are frequently asked:

To what degree is a particular fabric water repellent?

To what extent does dry cleaning and/or laundering diminish the water repellency of a fabric?

What causes a fabric to lose its repellency during the course of exposure to the rain?

In order to have available a background of information and data about water-repellent fabrics and common test methods, 11 typical commercial raincoat fabrics and 4 Army fabrics were selected for study. The characteristics of these 15 water-repellent fabrics are given in table 2. The water-repellent properties were examined by the following test methods: AATCC hydrostatic-pressure test, AATCC spray test, drop-penetration test, and angle of contact test (tensiometer type).

Figure 4 shows the results obtained by the four test methods. Each test was done according to the directions prescribed in Government specifications or published papers. It is noted that the most widely used test method, the spray-rating test, did not show any differences among 12 of the 15 fabrics. Great differences among the various fabrics are revealed by the remaining three tests. As each test measures different properties of the fabrics (see section on survey of methods, p. 107), it is not surprising that the 3 tests do not rank the

TABLE 2.— *Properties of 15 water-repellent fabrics*

Sample No.	Type of weave	Number of plies		Thread count		Air permeability at a pressure of 0.5 in. of water across fabric	Weight
		Warp	Filling	Warp	Filling		
WATER-REPELLENT COMMERCIAL FABRICS							
						$(ft^3/min)/ft^2$	Oz/yd^2
1	Twill-tackle	1	3	125	65	20.4	8.6
2	do	1	3	125	67	17.9	8.9
3	Plain-poplin	2	1	107	51	5.0	5.8
4	do	2	1	109	52	6.2	5.9
5	Twill	2	2	135	58	6.4	6.4
6	Plain-poplin	2	1	107	55	8.0	5.7
7	do	2	1	107	54	5.0	6.0
8	Twill-gabardine	2	1	127	54	16.2	6.5
9	Plain-poplin	2	1	106	54	4.6	6.3
10	Twill	1	1	104	60	23.6	7.3
11	Plain-poplin	2	1	107	56	5.3	6.2
ARMY WATER-REPELLENT FABRICS							
12	Sateen	2	2	115	70	3.9	9.1
15	Oxford	1	1	134	53	3.2	6.2
24	Sateen	2	2	115	67	3.8	8.9
26	Poplin	1	1	53	52	4.1	6.2

fabrics in exactly the same order. It is noted, however, that all fabrics can be approximately ted into 3 general groups: good, fair, and poor.

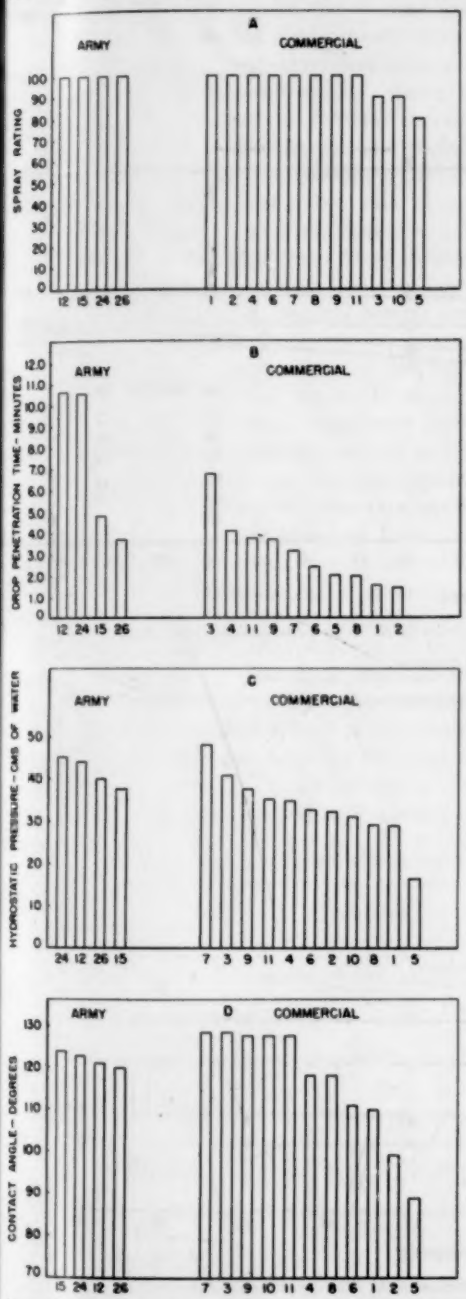

FIGURE 4.—*Comparison of four water-repellency tests.*

Certain samples always appear in a specific group: e. g. No. 5, poor; No. 3, good; No. 6, fair, etc. The fallacy of using only one test method to evaluate water repellency can be clearly seen from the data presented. It would be quite impossible to classify a particular water-repellent fabric on the basis of only one test.

Both the hydrostatic-pressure test and the measurements on contact angles reveal certain differences among the various samples not revealed by the spray test. The drop-penetration test, however, appears to be able to show differences in the fabrics that were not revealed by any of the other tests. The limitations of a particular laboratory test for evaluating water repellence are generally recognized. The most frequent argument against a certain test is that it does not test the fabric under conditions of actual use. Tests that simulate natural rain, therefore, are considered much more useful for practical testing. The drop-penetration test appears to be very useful in predicting the relative performance of fabrics in the rain. It seemed desirable, therefore, to study the present group of fabrics in greater detail on the basis of this test. In view of the arbitrariness of the test value—the time to collect 10 ml of water passing through the test specimen—it was decided to study the rate of penetration of water through water-repellent fabrics for long periods of exposure. It was found that the "rate of penetration (ml/min) versus time curve" was very characteristic of the nature of the particular fabric. Figures 5 and 6 show plots of the rate of penetration of water against time of exposure, for 11 of the fabrics studied. The arrows in figures 5 and 6 indicate the time at which 10 ml of water had passed through the fabric. Each rate curve contains the characteristic portions: an induction period, an S-shaped portion of a curve, and a limiting rate region. It is believed that the penetration of water through a fabric in natural rain follows a similar pattern and that the curves obtained for the drop-penetration apparatus are not a characteristic of the apparatus alone. These curves reveal that during the induction period little or no water comes through the cloth. When the resistance to penetration is finally broken, water passes through the fabric at a very rapid rate (S-shaped region). Finally, the amount of water that penetrates the fabric per unit time reaches a steady state. As

724217—47——8

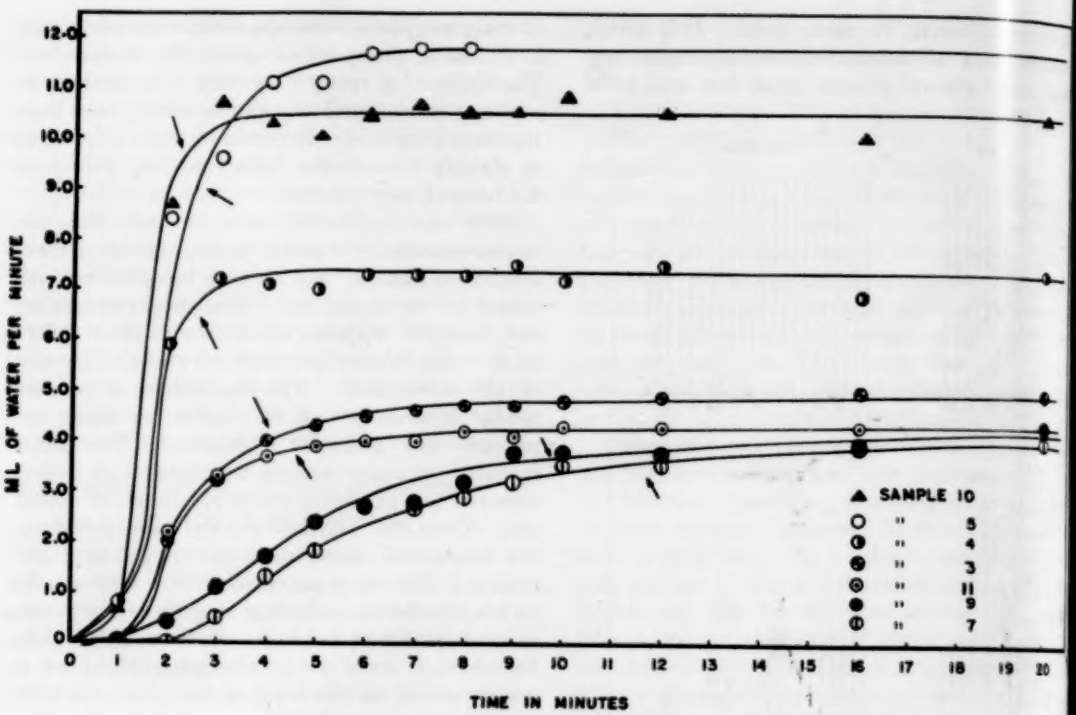

FIGURE 5.— *Rates of penetration of water through fabrics in the drop-penetration apparatus.*

Arrows show the point at which 10 ml of water—test value— have passed through the fabric.

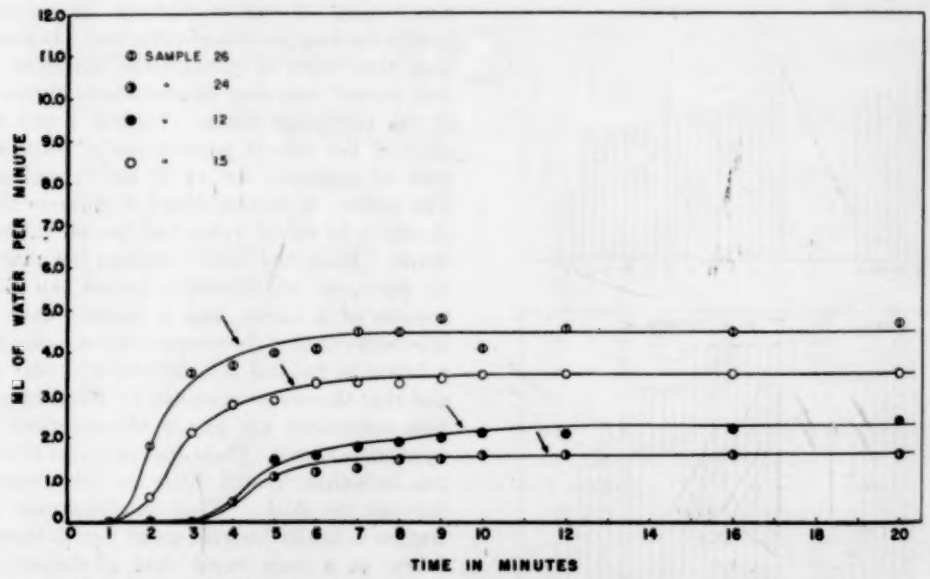

FIGURE 6.— *Rates of penetration of water through fabrics in the drop-penetration apparatus.*

Arrows show the points at which 10 ml of water—test value—have passed through the fabric

ost of the water-repellent fabrics tested are at st only somewhat resistant to penetration, it is ear that, after prolonged exposure of a water-pellent garment to the rain, the wearer would ot keep dry. The curves also indicate that the nger the induction period, the lower will be the quilibrium rate of penetration of water. In signing new water-repellent fabrics, therefore, e object would be to fix the various variables volved so that the resulting product would have long induction period and a low rate of pene-ation. Such a fabric has been designed. The hirley type of cloths that the Army Quarter-aster Corps developed during the war have a ery long induction period (several hours) and a ery low equilibrium rate of penetration (approxi-ately 0.1 ml/min). These types of fabrics are ighly effective for prolonged use in the rain.

The above studies of water repellency lead to e conclusion that obtaining the rate of penetra-on of water with the drop-penetration apparatus ves a more complete picture of the repellency of fabric than the 10-ml test value by itself. This especially significant when one is considering ommercial fabrics (compare fig. 5 with 6). It also concluded that better evaluation of water pellency may be made when a group of tests is mployed. A study of the four test methods ven above reveals that, as the rank correlation mong various tests is very low, it is necessary to rrelate all tests with the behavior of fabrics in tural or artificial rain. The Philadelphia Quar-rmaster Depot has developed and constructed [50] a rain room for fabric and garment testing. By means of specially designed nozzles, it is possible to obtain rainfalls at the rate of 0.1, 1.0, and 3.0 inches an hour, having natural and reproducible drop-size distributions.

V. Durability of Water-Repellent Finishes

The durability of water-repellent finishes is generally taken to be the resistance that the finish shows to the action of dry cleaning or laundering. Durable water-repellent fabrics are those whose water repellency is only slightly diminished by dry cleaning or laundering. Those fabrics whose water repellency is totally or greatly impaired by dry cleaning or laundering are classified as being nondurable. It should be remembered that the two terms are only relative and that the difference between them is a matter of degree of resistance and not necessarily of type of compound.

The effect of dry cleaning and laundering on water repellency was studied, using only the 11 commercial raincoat fabrics given in table 2. Standard methods of dry cleaning and laundering were used [51]. The results of these studies are given in table 3. By the use of three different test methods, it was found possible to distinguish between durable and nondurable repellent finishes. Samples 4, 7, 9, and 11 show a smaller decrease in all test values than do the remaining samples which reveal fairly large changes in all test values. It was found that samples whose water repellency had been totally lost by dry cleaning or laundering,

TABLE 3.—*Effect of dry cleaning and laundering on the water repellency of 11 commercial fabrics*

Sample No.	Spray rating			Hydrostatic pressure (centimeters of water)			Drop-penetration time (time, in minutes, to collect 10 ml of water)		
	Control	Dry cleaned three times	Laundered three times	Control	Dry cleaned three times	Laundered three times	Control	Dry cleaned three times	Laundered three times
1	100	50	50	28.9	36.3	4.0	1.7	1.6	1.4
2	100	50	0	33.0	29.9	3.3	1.5	1.4	(*)
3	90	70	0	40.1	18.4	2.9	6.8	(*)	(*)
4	100	70	70	35.9	33.1	9.0	4.2	2.3	2.7
5	80	0	0	16.5	2.7	0	2.1	(*)	(*)
6	100	50	0	33.1	15.7	2.5	2.4	(*)	(*)
7	100	70	80	48.0	40.1	28.2	3.2	3.1	3.4
8	100	70	0	29.5	23.6	0	2.0	1.1	(*)
9	100	70	50	37.8	32.4	14.9	3.9	2.7	3.2
10	90	0	0	30.5	5.3	2.8	1.6	0.6	(*)
11	100	70	70	36.3	31.6	31.6	3.9	3.0	4.4

* Drop-penetration time could not be measured as the swatches became completely saturated with water at the start of the test.

gave no test value in the drop-penetration test. These samples became completely saturated with water as soon as they were placed in the test apparatus.

The lowering of the water repellency of fabrics by dry cleaning or laundering is commonly attributed to leaching of the repellent compound. The presence of residual soap on the fabric and distortions of the fabric structure are also considered responsible for the loss in repellency. It has been observed, however, that simple wetting by water will also decrease the repellency of a fabric. Tests done at the Philadelphia Quartermaster Depot [52] have shown that water-repellent jackets were more easily wetted if they had been previously exposed to the rain. It was found that drying the jackets after the test exposure, even by heating in an oven, failed to restore to the garments their original water repellency. In view of the interest in the durability of water repellency, it seemed advisable to attempt to establish the rate at which some fabrics lose their repellency when exposed to the rain. For this study, four swatches each of five different water-repellent fabrics were tested five different days in the drop-penetration test. At the end of each test period, the swatches were allowed to dry at room temperature and then were conditioned overnight at 65-percent relative humidity and 70° F. The results of this experiment are shown in figure 7. It was found that the various fabrics lose their repellency at different rates. The drop-penetration test values get progressively lower each time the swatches are tested. This loss in repellency appears to be an irreversible process. Attempts to restore the original repellency by heating in vacuum at elevated temperatures were unsuccessful. An analysis of the factors that could be causing the loss in repellency leads to the following: Loss in the repellent agent by leaching, creation of new uncoated surfaces due to swelling of fibers, and changes in the surface geometry of the fabric due to the pounding of the high energy drops. Any or all of these changes could be taking place, and they all would be irreversible changes.

In order to throw light on the loss in repellency, two simple exploratory experiments were made. The changes in the contact angle of two of the fabrics were measured after various periods of wetting in the drop-penetration apparatus. Also, the change in contact angle and the increase in "standard moisture regain" [3] of one sample were noted after prolonged periods of spraying. The spraying was done with the nozzle of the AATCC spray test and was continuous for the particular period of time. The results of these observations are shown in figures 8 and 9. The contact angle of the dry fabrics was found to be lower after

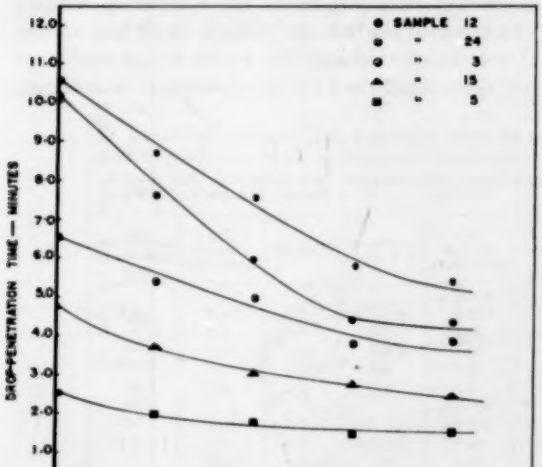

FIGURE 7.— *Lowering of the drop-penetration time owing to repeated testing.*

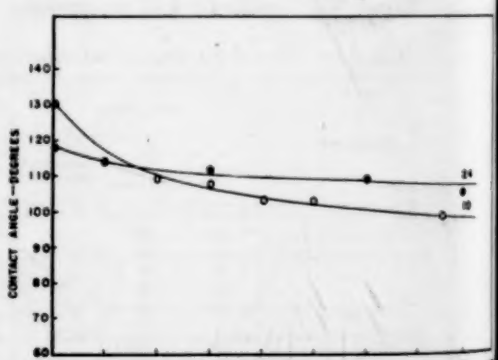

FIGURE 8.— *Change in contact angle of fabrics exposed in the drop-penetration apparatus.*

[3] Regain in weight during a 24-hour exposure period to 65-percent relative humidity and 70° F.

ach period of wetting in the drop-penetration st. The contact angle of one of the fabrics was so lowered after spraying the sample for various mes. Swatches of this fabric, when sprayed nd then tested for standard moisture regain, showed an increase in rate of moisture absorption. It is emphasized that the increase is an increase in rate (per 24-hour period) as the "repellent" fabrics do not always reach equilibrium in this length of time.

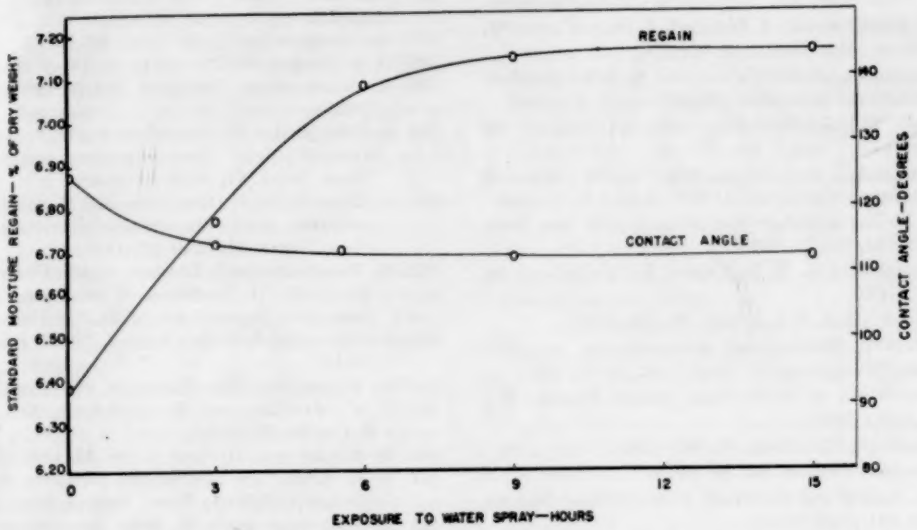

FIGURE 9.— *Changes in the contact angle and the standard moisture regain of a 9-ounce water-repellent fabric after prolonged spraying with water.*

VI. Summary and Conclusions

The theory of water repellency of textile fabrics has been reviewed with special references to the more recent theories of the wetting of fabrics by water. A survey has also been made on the various testing methods that have been devised for measuring water repellency. The results of the present investigation lead to the following conclusions regarding the status of water repellency. There is definite need for a comprehensive study of the role that the structure of a fabric plays in the phenomena of water repellency. In the past, the emphasis has been on developing more efficient compounds. Data available indicate that a better understanding of fabric construction as it applies to repellency, coupled with the now available water-repellent agents, will lead to some more nearly idealized type of water-repellent garment. In regard to testing methods, it is required that correlation be established between the results of laboratory test methods and performance of fabrics in the rain.

As already stated, the contact angle is influenced by the following factors: The chemical nature of the solid surface, the porosity of the surface, and the presence of other molecules on the surface. Again, any one or all of these factors could diminish the contact angle during wetting of the fabric. The change in moisture regain of sample 24 (fig. 9) shows that the rate at which a fabric absorbs moisture increases in proportion to the number of times the sample has been wetted. It is of interest to examine the surface factors that might be responsible for the increase in moisture absorption. The loss in repellent agent, the change in position of the fibers in the yarns, and the creation of new surfaces could all affect the rate of water absorption. The swelling of partially coated or uncoated fibers would also result in making available more hydrophilic surfaces (OH groups) [53].

References

[1] Chemical Abstracts for 1942 and 1943, for example.

[2] H. P. Pearson, Waterproofing textile fabrics (The Chemical Catalog Co., Inc., New York, N. Y., 1924).

[3] D. A. Martin, Am. Dyestuff Reptr. **21,** 126 (1932).

[4] G. A. Slowinske, Am. Dyestuff Reptr. **32,** 85 (1943).

[5] F. E. Bartell and F. J. Osterhof, J. Phys. Chem. **34,** 1399 to 1411 (1930).

[6] J. Alexander, Colloid chemistry **6,** 313 (Reinhold Publishing Corporation, New York, N. Y., 1946).

[7] Dupré, Théorie Méchanique de la Chaleur, 369 (1869).

[8] J. Alexander, Colloid chemistry **6,** 62 (Reinhold Publishing Corporation, New York, N. Y. 1946); G. E. Boyd, Surface chemistry, p. 133 (Am. Assn. Adv. Sci. No. 21, 1943).

[9] S. Baxter and A. B. D. Cassie, J. Textile Inst. **36,** 167 (1945).

[10] R. Wenzel, Ind. Eng. Chem. **28,** 988 (1936).

[11] A. Harvey, Wetting and detergency, p. 18. (The Chemical Catalog Co., New York, N. Y., 1937).

[12] S. Baxter and A. B. D. Cassie, Trans. Faraday Soc. **40,** 546 (1944).

[13] L. Rayleigh, Phil. Mag. [5], **30,** (1890).

[14] A. Pockels, Phys. Z. **15,** 39 (1914).

[15] F. E. Bartell and Cardwell, J. Am. Chem. Soc. **64,** 164, 494, 1530 (1942).

[16] J. Ablett, Phil. Mag. [6] **46,** 244 (1923).

[17] N. K. Adam, The physics and chemistry of surfaces, p. 181, 2d ed. (Clarendon Press, Oxford, England, 1938).

[18] W. D. Harkins, J. Am. Chem. Soc. **62,** 3381 (1940).

[19] J. Alexander, Colloid chemistry **6,** 61 (Reinhold Publishing Corporation, New York, N. Y., 1946).

[20] F. L. Gleysteen and V. R. Dietz, J. Research NBS **35,** 285 (1945) RP1674.

[21] Am. Assn. Textile Chem. Colorists, 1944 Year Book, p. 206.

[22] Am. Assn. Textile Chem. Colorists, 1940 Year Book, p. 223.

[23] U. S. Army Spec. 100–48, p. 20 (May 11, 1945).

[24] Am. Assn. Textile Chem. Colorists, 1937 Year Book, p. 190.

[25] First report of the fabrics coordinating research committee, His Majesty's stationery office, p. 20 (London 1925).

[26] Am. Assn. Textile Chem. Colorists, 1944 Year Book, p. 210.

[27] Federal Spec. CCC–T–191a and its supplement (Oct. 8, 1945).

[28] Standards on textile materials, Am. Soc. Testing Materials, p. 82 (1943).

[29] H. Bundesmann, Melliand Textilber. **16,** 128 (1935)

[30] G. A. Slowinske, Am. Dyestuff Reptr. (Feb. 15, 1943).

[31] A. A. Cook and S. Zaparavik, Am. Dyestuff Reptr. **26,** 323 (1937).

[32] U. S. Patent 2,012,762.

[33] A. Klingelhöfer, H. Mendrzyk, and H. Sommer, Wiss. Abhandl. deut, Materialprüfungsanstalt. 30; Chem. Zentr. **11,** 2249–50 (1940).

[34] A. Klingelhöfer, H. Mendrzyk, and H. Sommer, Wiss. Abhandl. deut. Materialprüfungsanstalt. 23; Chem. Zentr. **11,** 2249–50 (1940).

[35] Harry B. Kime, Am. Dyestuff Reptr. **35,** 261 (1946).

[36] Am. Assn. Textile Chem. Colorists, 1944 Year Book, op. 212.

[37] Standards on textile materials, 83, (1943).

[38] U. S. Army Spec. 100–48, p. 14. (May 11, 1945).

[39] H. Bundesmann, Melliand Textilberichte **16,** 12 (1935).

[40] A. Klingelhöfer, H. Mendrzyk, and H. Sommer, Wiss. Abhandl. deut. Materialprüfungsanstalt. **1,** 1 Chem. Zentr. **11,** 2249–50 (1940).

[41] A. Klingelhöfer, H. Mendrzyk, and H. Sommer, Wiss. Abhandl. deut. Materialprüfungsanstalt. **1,** 1 Chem. Zentr. **11,** 2249–50 (1940).

[42] H. Wakeham and E. L. Skau, J. Am. Chem. Soc. **67** 268 (1945); H. Wakeham, W. Strickland, and E. L. Skau, Am. Dyestuff Reptr. **34,** 178 (1945).

[43] S. Baxter and A. B. D. Cassie, J. Textile Inst. **36,** 167 (1945).

[44] R. Wenzel, Ind. Eng. Chem. **28,** 988 (1936).

[45] G. J. Mandikos and B. A. Ryberg, Am. Dyestuff Reptr. **34,** 37 (1945).

[46] R. Wenzel, Am. Dyestuff Reptr. **25,** 1598 (1936).

[47] N. K. Adam, The physics and chemistry of surfaces (Oxford University Press, London, 1941).

[48] H. W. Stiegler and S. M. Hood, Am. Dyestuff Reptr. **28,** 285 (1939).

[49] Textile research supplement No. 2 (Nov. 1942) and subsequent personal communication from staff of Milton Harris Associates.

[50] J. E. Simpson, Am. Dyestuff Reptr. **35,** 243 (1946).

[51] NBS Commercial Standard CS59–44, par. 24 to 29 and 74 to 76d (1944).

[52] Personal communication from the staff at the Philadelphia Quartermaster Depot.

[53] K. Lauer, Kolloid-Z. **107,** Heft 2, 86 (1944).

ADDITIONAL REFERENCES NOT CITED IN TEXT

S. Mierzinski, The waterproofing of fabrics (D. Van Nostrand Co., New York, N. Y. 1903); also translation of 3d ed. by A. Morris & H. Robson (Scott, Greenwood & Co., 1920).

H. Jaeger, European methods of waterproofing fabrics with formulae for ordinary and continuous processing, Melliand Textilber. **1,** 123 (April 1929); **1,** 253 (May 1929).

Waterproofing and showerproofing, Textile Colorist **51,** 87, and 130 (1932).

A. J. Kelley, Textiles: Flame and waterproofing, cotton **98,** No. 12, 53 (1934).

W. M. Scott, The testing of textiles for waterproofness, Am. Dyestuff Reptr. **27,** 479 (1938).

T. Stenzinger, Review and criticism of the methods of testing waterproof or water repelling impregnations, Am. Dyestuff Reptr. **27,** 407 (1938).

R. Flint, The hydrophobing of artificial fibers and fabrics, Silk And Rayon **13,** 808 (1939).
T. A. Norris, Water-resistant finishes, Textile Colorist **62,** 165 (1940).
T. J. Van Antwerpen, Chemical repellents, Ind. Eng. Chem. **33,** 1514 (1941).
B. Monsaroff, waterproofing textile fabrics, Can. Chem. Process Inds. **26,** 265 (1942).
Eric Croen, Water-repellent and waterproof finishes for Textiles, Cotton **107,** No. 1, 63–66 (1943).
G. A. Slowinske, Evaluating water repellency of fabrics, Textile Mfr. **70,** 268 (1944).
H. P. Holman and T. D. Jarrell, Effects of treating materials and outdoor exposure upon water-resistance and tensile strength of cotton duck, Textile World **73,** 3103 (1928).
Effects of waterproofing materials and outdoor exposure upon the tensile strength of cotton yarn, Ind. Eng. Chem. **15,** 236 (1923).
G. Barr, The determination of waterproofness of "porous" waterproof fabrics, Dept. Sci. & Indl. Research, second Report of the Fabrics Co-ordinating Research Committee, His Majesty's Stationery Office, p. 113–139 (London 1929).
A. J. Hall, Waterproofing with colloidal aluminum hydroxide, Textile Colorist **54,** 616 (1932).
S. Lenher and C. A. Slowinske, Mildewproofing and waterproofing of textile fibers, Am. Dyestuff Reptr. **25,** 326 (1936).
N. K. Adam, Detergent action and its relation to wetting and emulsification, J. Soc. Dyers Colourists **53,** 121 (1937).
Waterproofing cotton duck and canvas, Am. Dyestuff Reptr. **27,** 507 (1938).
H. Zeyferth and O. M. Morgan, The canvas disc wetting test, Am. Dyestuff Reptr. **27,** 525 (1938).
C. E. Mullen, Velan and similar water-repellent finishes, Textile Colorist **60,** 96, 231 (1938).
G. A. Slowinske, A new type water repellent, Am. Dyestuff Reptr. **28,** 647 (1939).
L. Stein, Hygenic and technical aspects of water-repellent clothing, Am. Dyestuff Reptr. **29,** 352 (1940).
C. H. S. Tupholme, Water and Washing resistant finishes on textiles, Am. Dyestuff Reptr. **29,** 466 (1940).
W. C. Hunter-Turner, Fats and waxes in disguise, Am. Dyestuff Reptr. **30,** 371, 399 (1941).
G. A. Slowinske, The Evaluation of water-resisting textile finishes, Am. Dyestuff Reptr. **30,** 6, (1941).
W. Lang, Aluminum acetate proofed khaki, J. Textile Inst. **32,** A563 (1941).
C. E. Salkeld, Some modern war-time finishes, Textile Colorist **64,** 245 (1942).
W. R. Lang, Waterproofing heavy woolens by aluminum acetate, Textile Colorist **64,** 300 (1942).
A. J. Hall, Waterproofing of acetate rayon materials, Textile Colorist **64,** 275 (1942).
Chemical stratagems in waterproofing process, "Critanalyst" Textile Colorist **64,** 95 (1942).
L. G. Lawries, The waterproofness of fabrics permeable to air J. Textile Inst. **33,** 549 to 52 (1942).

WASHINGTON, September 13, 1946.

U. S. Department of Commerce
National Bureau of Standards

Research Paper RP1763
Volume 38, January 1947

Part of the Journal of Research of the National Bureau of Standards

Adsorption of Water Vapor by Untanned Hide and Various Leathers at 100° F

By Joseph R. Kanagy

Adsorption of water vapor by untanned hide and various tannages of leather was determined at relative humidities ranging from 0 to 96 percent at 100° F. The Brunauer, Emmett, and Teller equations for adsorption of gases in multimolecular layers were applied to the data. Adsorption for all of the samples below a relative humidity of 75 percent is a function of the available surface. Above 75-percent relative humidity, other factors exert an influence, the most important of which is probably size of the capillaries. Untanned hide and chrome-tanned leather adsorb the most water vapor except at relative humidities above 75 percent, at which sole leather adsorbs more. The behavior of the sole leather in this region is ascribed to the presence of deliquescent materials used in the finishing process. The other vegetable-tanned leathers adsorb less moisture than either hide or chrome leather. Calculated heats of adsorption indicate that the affinity of groups for water is not appreciably altered by tanning and that the adsorption is physical in nature. Methods by which the data may be applied to practical processes, such as fat-liquoring and tanning, are pointed out.

I. Introduction [1]

The amount of moisture that leather adsorbs or loses is determined by temperature, relative humidity, degree of porosity, and the size of the pores. Moisture has great practical significance because its amount affects the durability of leather, and in articles such as shoes, gloves, and other garments, the comfort of the wearer. High moisture content accelerates deterioration and promotes mildew action. On the other hand, a minimum amount of moisture is required to keep leather properly lubricated and thus prevent cracking. The adsorption of moisture affects comfort by its influence on weight, area, and insulation. Insulation is a function of the amount of water adsorbed, water vapor transmission, rate of condensation, and evaporation.

From data obtained in the study of the moisture adsorption by leather and untanned hide at various relative humidities, theoretical concepts as to the nature and magnitude of the surfaces may be obtained. Such concepts may be of value in determining the nature of tanning and in studying other processes, such as fatliquoring and dyeing.

The effect of relative humidity on strength and stretch of leather has long been known, and it is now customary to make all such tests under controlled conditions of temperature and humidity. Veitch, Frey, and Leinbach [1] [2] studied the strength and stretch of vegetable-tanned calf leather at relative humidities of 35, 55, and 75 percent. Wilson and Kern [2, 3] determined the

[1] This report is made as a part of the project QMC-80, a long-term fundamental program of research sponsored and supported by the Office of the Quartermaster General, War Department. Permission to publish was granted by the Office of the Quartermaster General.

[2] Figures in brackets indicate the literature references at the end of this paper.

variations in strength, stretch and area for both vegetable and chrome-tanned leathers. Evans and Critchfield [4] made an investigation of the amounts of moisture adsorbed by chrome and vegetable-tanned calf leathers at different percentages of relative humidity at a temperature of 21° C. Recently Green [5] determined the moisture content of chrome leather under different percentages of relative humidity at 25° C. These studies have all been somewhat limited in scope and, in general, the results were obtained where static methods for obtaining the relative humidity conditions were used.

Work on the determination of the internal surface area of hide and formaldehyde-tanned hide has recently been done by Zettlemoyer, Schweitzer, and Walker [6]. These determinations were made by studying the adsorption of nitrogen. Bull [7] studied the adsorption of water vapor by a number of different proteins, one of which was collagen.

This paper gives results of an investigation on the moisture relations of collagen and of leather. This is part of a study that is intended to cover a wide range of temperatures and relative humidities. The results given were obtained with collagen (commercial hide powder) and various tannages of leather at 100° F and at relative humidities ranging from 0 to 96 percent.

II. Description of Samples Used

The collagen used was a sample of commercially prepared hide powder. A more highly purified collagen has been prepared since this work was started and will be compared with the commercial hide powder in future work.

Six different samples of leather were used. As there was no precedent to determine the exact nature of the data that would be obtained, the selection of samples was made somewhat arbitrarily, but included leathers which differed from each other in properties and represented some of those most important commercially. Sole leather was used because of its importance and the fact that the addition of salts and glucose in the finishing exerts an influence on the moisture adsorbed. This was compared with a similar tannage of leather from which the grease had been removed, and glucose and salts were removed by washing. Water-soluble material in the leather is mostly vegetable tannin, which it is almost impossible to remove completely by washing. Chrome hydraulic-packing leather was used to represent a mineral tannage. Chrome-retanned leather represents the combination of the mineral and vegetable tannage. Calfskin and belting leather were selected to represent two types of finished vegetable-tanned leathers. The analyses of the leathers are given in table 1.

TABLE 1.—*Chemical analysis of the leathers used in the water-vapor-adsorption measurements, based on moisture-free weight*

Leather	Ash	Grease	Water solubles	Hide substance	Degree of tannage	Acidity	Cr_2O_3
	Percent	*Percent*	*Percent*	*Percent*		pH	*Percent*
Sole	5.6	6.0	36.5	33.0	74	3.3	—
Sole, degreased and washed	0.8	0.4	10.8	52.3	70	3.2	—
Chrome, hydraulic-packing	5.7	7.9	—	76.3	—	3.1	4.6
Chrome-retanned upper, degreased	3.7	2.5	—	52.5	—	3.1	3.6
Calfskin, vegetable-tanned	1.0	16.9	7.8	42.1	78	3.8	—
Belting	0.4	12.8	9.2	45.0	73	3.1	—

III. Methods of Test and Procedure

The conditioning equipment was developed by Carson and Worthington for use in studying water-vapor permeabilities of sheet materials. This equipment is shown in figures 1 and 2, and a detailed description is given in reference [8]. It consists essentially of a sealed temperature-controlled chamber in which a constant relative humidity is maintained by means of the proper saturated salt solution. Air is circulated over the salt solution and throughout the chamber continually. It is equipped with a mechanism for weighing the samples in the chamber. This is done by means of the rotating disk (36), figure 2, from which the samples (1) are suspended. Each sample is weighed by rotating it to the position of the weighing arm (40), and transferring it from the disk to the extended arm of the balance by means of a device on top of the chamber.

The water-adsorption measurements were made with leather samples ground to pass a 4-mm sieve. Weighed portions of the samples were placed in small cylindrical baskets (approximately 2 in. in diameter by 2½ in. high, shown in fig. 3) made

om 40-mesh copper screen. The samples and ontainers were hung from the disk in the chamber. The same sample of each particular material was sed to obtain all the data in the adsorption and esorption procedure. The samples were allowed o come to equilibrium at a constant relative umidity at 100° F. The salt solution was then hanged, and the same samples were brought to quilibrium at a slightly higher relative humidity. This procedure was repeated at 10 different points om 0 to 96 percent. The desorption determinaions were made by reversing this procedure by tarting at 96-percent relative humidity and endng at about 0 percent. The salts used for mainaining the constant relative humidities and their alues as determined by the wet-dry bulb, and by irect vapor-pressure determination [9] are shown n table 2.

To correct for the moisture adsorbed by the ontainer, an empty basket was used as a blank nd weighed each time weighings were made with

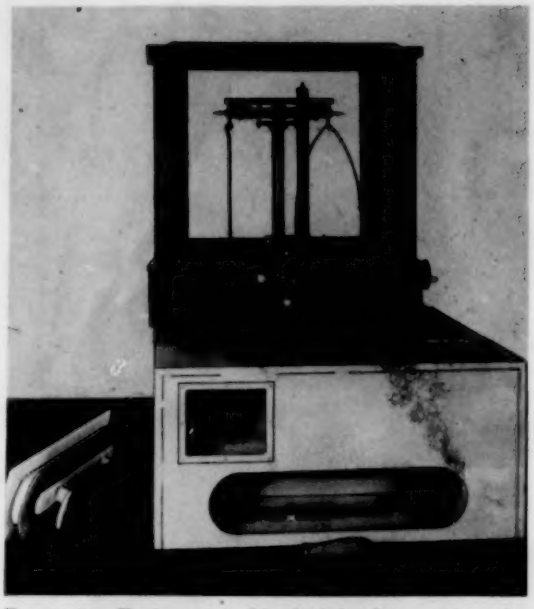

FIGURE 1.—*Equipment used in obtaining data on adsorption of water vapor by untanned hide and various leathers at 100° F.*

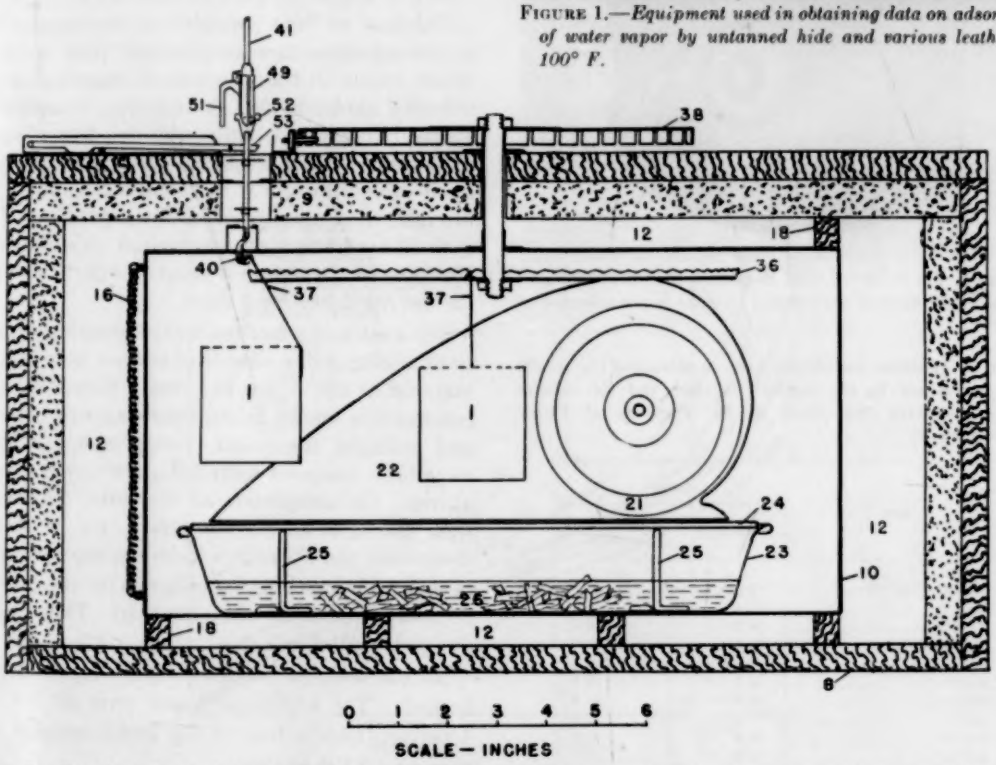

FIGURE 2.—*Details of the conditioning chamber used in obtaining data on the adsorption of water vapor by untanned hide and various leathers at 100° F.*

FIGURE 3.—*Wire basket used to contain the leather samples used in the study of the amount of water vapor adsorbed at 100° F.*

TABLE 2.—*Relative humidities used in obtaining the results as determined by the wet-bulb method and the relative vapor pressure determined at the Institute of Paper Chemistry [9]*

Salt	Method	
	Wet-bulb	Relative vapor-pressure
$MgClO_4$ (Anhydrone)	0 (approx.)	
LiCl	12.4	11.1
$KC_2H_3O_2$	20.2	20.4
$MgCl_2.6H_2O$	31.8	31.9
K_2CO_3	43.0	43.4
NaBr	53.5	53.7
$NaNO_2$	61.3	61.8
NaCl	74.4	75.1
K_2CrO_4	84.3	85.6
K_2SO_4	96.2	

the samples. The increase in the weight of the blank was subtracted from the increase in the weight of the basket and the sample. The amount of moisture adsorbed by the basket was quite low and amounted to a total of only about 0.35 percent for a 5-g sample of leather for all relative humidities up to 96 percent. At 96 percent relative humidity, an additional correction of about 0.45 percent was necessary for the same weight of leather.

No difficulty was experienced in weighing the samples at any condition of relative humidity except at 96 percent. At this humidity, moisture condensed on the rod leading from the balance arm to the sample. It was, however, possible to make a correction for this so that the error in the determinations was minimized.

IV. Results of Measurements

1. "Dry" Weight of the Samples

The base or "dry" weights of the samples used in the experiments were obtained from the equilibrium values in the presence of magenesium perchlorate Anhydrone. A relative humidity of about 10 (dry-wet bulb reading) was obtained with this material by first permitting the attainment of equilibrium with calcium chloride. This brought the humidity to about 2 percent. Then with the addition of magnesium perchlorate, it was possible to obtain a value of approximately 0 for the humidity for 3 days.

The customary method for determining moisture or obtaining a dry sample of leather is to heat the material at 100° C for 18 hours. However, as this treatment is known to alter the structure of leather and collagen somewhat, these materials might have been rendered unfit for use at lower temperatures. On completion of the tests, the samples were placed in an oven at 100° C for 18 hours to determine the difference between the values obtained after reaching equilibrium in the presence of Anhydrone and after heating. These results are given in table 3.

All the samples lost additional weight on being heated. The additional losses were all less than 1 percent and in four of the seven samples, they were under 0.5 percent.

TABLE 3.—*Difference in weights of samples in equilibrium in presence of Anhydrone and after heating 18 hours at 100° C in dry-air stream*

Sample	Weights of samples		Difference	Percent
	After equilibrium in presence of Anhydrone	After heating at 100° C in dry air stream		
	g	g	g	
Untanned hide	6.0326	5.9928	0.0398	0.66
Sole leather	4.3611	4.3199	.0412	.94
Chrome leather	3.3093	3.2756	.0249	.76
Chrome-retanned leather, degreased	4.7728	4.7497	.0231	.49
Sole leather, degreased, washed	5.0098	5.0037	.0061	.12
Vegetable-tanned calfskin	6.2107	6.2011	.0096	.15
Belting leather	5.5106	5.4971	.0135	.25

2. Adsorption Isotherms

The time required to reach equilibrium at a definite relative humidity is shown in figure 4, where the rate at which equilibrium was reached at 11- and 54-percent relative humidity is given. Equilibrium is reached in 1 day at a relative humidity of 11 percent, whereas at 54 percent a 5- to 7-day period was required.

Adsorption isotherms at 100° F for six different leathers and for untanned hide are given in figure 5. The curves are all of the sigmoid type, with a fairly rapid initial rise, then a leveling off, and finally at a relative humidity of 75 percent, again a rapid rise. The very rapid rise shown by sole leather above 75-percent relative humidity is apparently caused by the magnesium sulfate and glucose it contains. The sample of sole leather which was degreased and washed shows no such

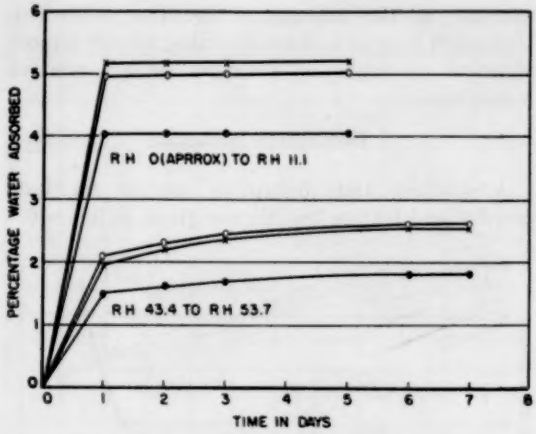

FIGURE 4.—*Rate at which equilibrium is reached at two different relative humidities by hide substance, chrome leather and belting leather when exposed in an atmosphere of water vapor at 100° F.*

○=hide substance; ×=chrome leather; ●=belting leather.

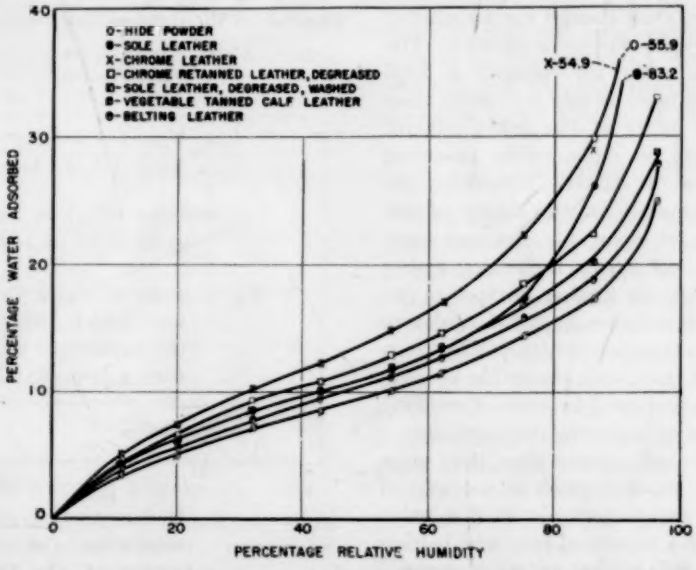

FIGURE 5.—*Increase in the amount of water vapor adsorbed with increase in relative humidity for various leathers and untanned hide at 100° F.*

increase in the amount of moisture adsorbed. Untanned hide and chrome leather adsorb almost identical amounts of moisture at all relative humidities.

3. Desorption Isotherms

Adsorption and desorption curves for hide powder and belting leather are given in figure 6.

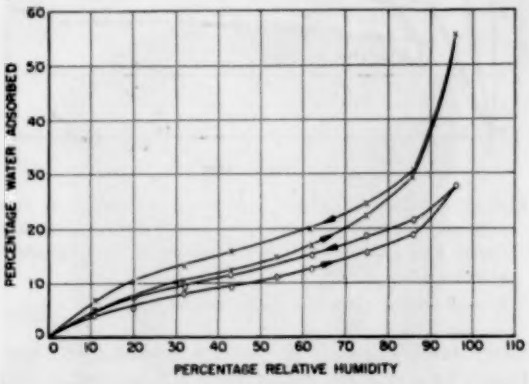

FIGURE 6.—*Adsorption and desorption of water vapor by hide powder and belting leather at various relative humidities at 100° F.*

×=hide powder; ○=belting leather.

The hysteresis for untanned hide is no greater than that for leather, even though the amount of moisture adsorbed by the former is greater. The steep portion of the curve for collagen at high relative humidities is more nearly reversible than the flat part of the curve at the lower relative humidities. This may be explained by assuming that at high values of relative humidity, the adsorption consists mainly in the filling of the larger pores, which is reversible, because condensation of water on water molecules rather than water molecules on leather surface is involved. At the lower relative humidities adsorption consists in condensation where leather surface is involved, and this is not reversible because the surface area has increased because of swelling under the conditions of high relative humidity.

All samples give off practically the same amounts of moisture on desorption as was gained on adsorption; the curves coincide at 0 relative humidity as shown for untanned hide and belting leather in figure 6. Sole leather (table 4) shows a loss of nearly 3 percent more weight on desorption than was gained on adsorption which might be due to loss of salts or glucose. The weight gained on adsorption and lost on desorption for all the samples is given in table 4.

TABLE 4.—*Amounts of moisture adsorbed by samples on adsorption and lost on desorption*

Sample	Adsorption moisture gained	Desorption moisture lost
	Percent	*Percent*
Collagen (hide powder)	55.9	56.2
Sole leather	83.2	86.2
Chrome leather	55.0	55.2
Chrome-retanned leather, degreased	33.1	32.5
Sole leather, degreased, washed	28.7	28.7
Vegetable-tanned calf skin	25.0	24.8
Belting leather	27.9	27.9

V. Calculation of Derived Quantities

1. Application of Brunauer, Emmett, and Teller Equations

Brunauer, Emmett, and Teller [10] have developed a theory to account for the adsorption of gases in multimolecular layers. This theory was developed by a generalization of Langmuir's treatment of the unimolecular layer and has recently been used to calculate surface areas by a number of authors [7, 11].

Two equations are developed [10] that may be applied to the data of this paper.

$$\frac{p}{V(p_0-p)}=\frac{c-1}{V_m c}\frac{p}{p_0} \tag{1}$$

$$V=\frac{V_m cx}{1-x}\frac{1-(n+1)x^n+nx^{n+1}}{1+(c-1)x-cx^{n+1}}, \tag{2}$$

V=volume of water vapor adsorbed per gram at 0° and 760 mm

V_m=volume of water vapor at 0° and 760 mm, which, when adsorbed, covers the surface of 1 g of the adsorbent with a unimolecular layer

p=pressure

x=relative pressure of the water vapor that is equal to p/p_0, where p_0 is the saturation pressure of the water vapor at the temperature of the adsorption

n=maximum number of adsorbed layers

c=a measure of the increase of the heat of adsorption E_1 of the first layer on the adsorbent over the heat of liquefaction (E_L), according to the equation $E_1-E_L=2.303RT \log c$.

From equation 1, which holds only at values of p/p_0 less than 0.5, a straight line may be obtained by plotting experimental values of $p/V(p_0-p)$ as ordinate against p/p_0 as abscissa. The intercept will be $1/V_mc$ and the slope $(c-1)/V_mc$. From the experimental values of intercept and slope thus obtained, c and V_m may be calculated. Typical plots of this type are shown in figure 7, and the values of c and V_m for hide substance and all the leathers are given in table 5.

TABLE 5.—*Values of surface properties for hide powder and various leathers calculated from the Brunauer, Emmett, and Teller equations*

Sample	V_m[1]	c	Surface area	E_1-E_L
	ml/g		*m²/g*	*cal/mole*
Collagen (hide powder)	110.0	8.3	298	1,307
Sole leather	86.7	10.2	235	1,434
Chrome leather	110.1	8.0	298	1,284
Chrome-retanned leather (degreased)	97.2	8.7	263	1,336
Sole leather (degreased and washed)	89.0	9.0	241	1,357
Vegetable-tanned calfskin	76.3	8.2	206	1,299
Vegetable-tanned belting leather	83.3	8.8	225	1,343

[1] V_m is the volume of water vapor at 0°C and 760 mm that is required to form a unimolecular layer on the surface of the sample.

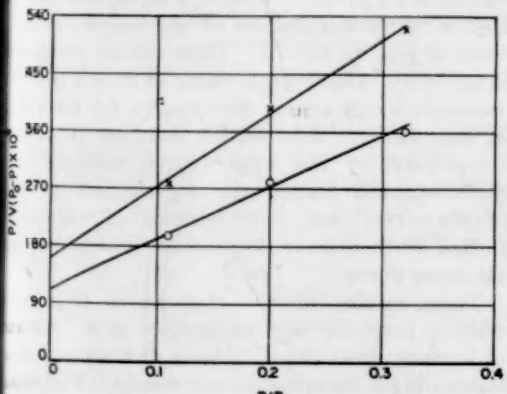

FIGURE 7.—*Linear plot of p/v (p_o-p) against p/p_o for the adsorption of water vapor on vegetable-tanned calfskin and hide powder at 100° F.*

X = vegetable calfskin; O = hide powder.

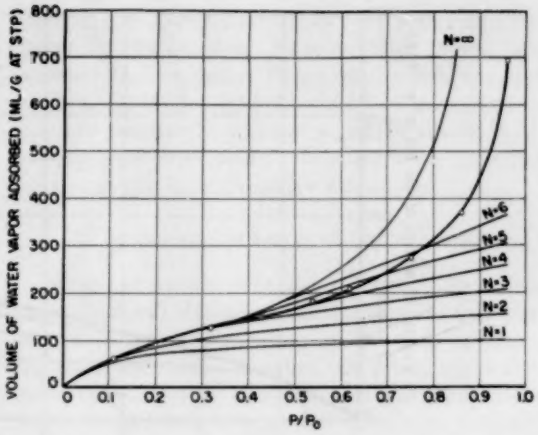

FIGURE 8.—*Observed and calculated isotherms for the adsorption of water vapor on untanned hide at 100° F.*

The values for c and V_m may be substituted into equation 2, and V calculated for different values of n, where n equals the number of adsorbed layers. These values may then be compared with the determined results for the volume of water vapor adsorbed to ascertain the number of adsorbed layers which are equivalent to them. Such results are given in figure 8 for untanned hide, and in figure 9 for leather. The amounts of moisture adsorbed by leather at high relative humidities appear to be equivalent to five or six layers, whereas with untanned hide a large number of layers appears to be formed at these pressures, which probably indicates that the capillaries in the latter are much larger than in the former.

2. Calculation of Surface Areas

With the values for V_m (milliliters of water vapor adsorbed per gram of sample) it is possible to calculate the surface areas of the materials if the volume occupied by each molecule of water is known. Taking the value determined by Smith and Green [12], namely, 10 square angstrom units as the area occupied by the water molecule and 2.705×10^{19}, the number of molecules per milliliter at 0° and 760 mm, the surface area per gram of material is calculated as follows:

$$(V_m\times2.705\times10^{19}\times10\times10^{-20})m^2=2.705V_m.$$

The values for the surface area of all of the samples in square meters per gram are given in table 5.

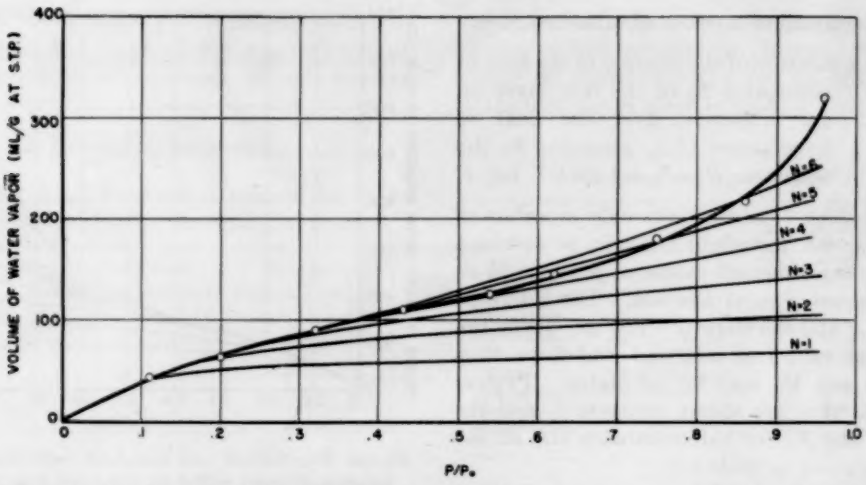

FIGURE 9.—*Observed and calculated isotherms for the adsorption of water vapor on vegetable-tanned calfskin at 100° F.*

Collagen and chrome-tanned leathers have the largest surface areas. The leathers tanned with the vegetable tanning materials have smaller surface areas, as would be expected, since they are composed of less hide substance and the capillaries are reduced to smaller diameters, in some cases probably completely filled by tanning materials. The surface areas of hide and the leathers are lower than that found in general for charcoals. This might be due to the granular nature of ground charcoal. The value of 298 m^2/g of collagen is considered to be in fairly good agreement with the value of 337 m^2/g obtained by Bull [7].

3. Heats of Adsorption

By substituting the values for c given in table 4 in the equation $E_1-E_L=2.303R\ T \log c$, it is possible to calculate the difference between the heat of adsorption and the heat of liquefaction of water on collagen and leather. The values for E_1-E_L are given in table 5. The positive value for E_1-E_L in contrast to the negative value obtained when water is adsorbed on charcoal [13] gives evidence of the effect of polar groups on the attraction of water. The fact that the magnitude of the value obtained for collagen, 1,307 cal/mole, is comparable with that obtained for the leathers, 1,284 to 1,434 cal/mole, may indicate that there is little alteration of groups that attract water when tanning occurs. The small difference between the heats of adsorption and heats of liquefaction, calculated by applying the B. E. T. theory, suggests strong Van der Waals adsorption. Chemisorption is generally accompanied by higher heats of adsorption (20,000 to 50,000 cal/mole) [13]. Further work is planned in which calculations of the differential heats of adsorption will be made.

VI. Discussion

1. Reduction to Unit Surface

If the volumes of water vapor adsorbed at each relative humidity are divided by the calculated values of V_m given in table 5, a factor is obtained that is nearly identical for all the samples at each value of p/p_0 up to 0.75. These results are shown in figure 10. Above a p/p_0 value of 0.75, a definite variation occurs among the samples for the value of this factor. Sole leather assumes the value represented by the upper curve, collagen and chrome-tanned leather are represented by the middle curve, and four samples of vegetable-tanned leathers have the values represented by the lower curve.

These results indicate that up to 75-percent relative humidity the adsorption is a function of surface area alone. Above this value other factors begin to influence the results. The most important of these is probably differences in the sizes of the pores. The rapid increase for sole leather is undoubtedly due to the deliquescent nature of the glucose and magnesium sulfate

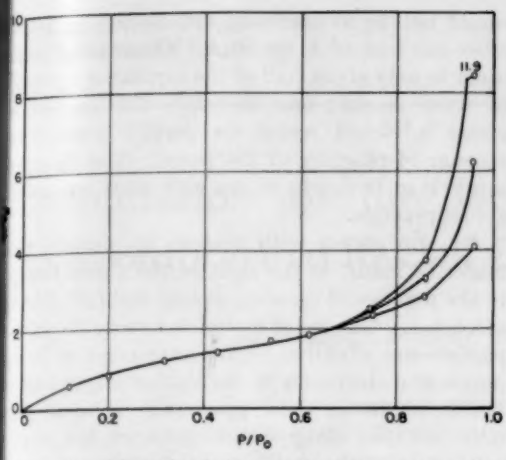

FIGURE 10.—*Adsorption isotherms of water vapor on various leathers and untanned hide at 100° F reduced to unit surface in a plot of V/V_m against p/p_0.*

used in the finishing process. The difference in the behavior of collagen and chrome-tanned leather, on the one hand, and the four vegetable tannages, on the other, can be explained by assuming that the former have larger pores on the average and consequently adsorb more moisture at high relative humidities.

2. Diameter of the Collagen Fiber

As the surface area and the density of collagen are known, it is possible to calculate the diameter of the fiber if it is assumed that it is a uniform cylinder and that the calculated adsorption area is identical with the total surface of collagen fibers. The areas of the ends of cylinder are negligible.

As a cylinder of radius r and length L has a surface $S=2\pi rL$ and a volume $V=\pi r^2L$, the diameter $2r=4V/S$. If the density of collagen is taken as 1.4 g/cm³ (specific volume 0.7 cm³/g), V in the above equation is 0.7 cm³/g and S (table 6) is 298×10^4 cm²/g. Therefore,

$$2r=\frac{4\times0.7}{298\times10^4}=94\times10^{-8}\text{ cm.}$$

Bear [14] found from X-ray data a distance of about 11 A between the polypeptide chains in collagen, which is equivalent to about one-eighth the dimension calculated here. Bear also found a separation of polypeptide chains when he observed the X-ray pattern of wet collagen. Apparently water goes between the chains and spreads them apart. These results indicate that moisture does not go between all of the chains at the low relative humidities at which the B. E. T. calculations were made. It is probable that this occurs at the higher relative humidities.

3. Unimolecular Layer of Oil in Leather

From the surface area of leather it is interesting to make a calculation as to the amount of oil that would be required to cover all the surface with a unimolecular film. Leather oils are composed of a mixture of triolein and tristearin and a number of other constituents that are decomposition products of these two compounds.

From Langmuir's data [15] on the molecular sizes of these compounds, it is possible to make a calculation as to the amount that would be required for a unimolecular layer by using the data for washed and degreased sole leather. If the orientation of the chains is assumed to be perpendicular to surface, with tristearin, 53.7 percent would be required for a single layer; with triolein, 27.7 percent would be required. If it is assumed that the molecules lie flat on the leather surface, with tristearin, 17.7 percent would be necessary; with triolein 24.4 percent would be required. These results are obviously not in harmony with practical experience. The reason is that surface available to water is not available to oils, as the oil molecules are 6 to 10 times larger in diameter.

4. Relation of Adsorption to Capillarity

It has been shown that the adsorption of water vapor by leather and hide shows correlation with the multimolecular adsorption theory of Brunauer, Emmett, and Teller for relative humidities below 50 percent. The adsorption may also be considered especially at the higher relative humidities to be the result of capillary condensation. The surface of leather may be considered as consisting of numerous capillaries of different sizes. This concept arises from its fibrous structure. Between each fibril water may be adsorbed. The openings of various sizes between fibers give, in effect, the same characteristics as capillaries of various sizes. In the first stages of adsorption, the small capillaries will be filled, whereas the last stages will consist in filling the larger pores.

724217—47——9

Calculations may be made in accordance with the Kelvin equation, which applies to the condensation of liquids in cylindrical capillaries.

$$\ln (p/p_0) = -2\gamma v/rRT,$$

in which

γ = surface tension

v = molar volume of the liquid

r = radius of the capillary.

A plot showing the amounts of liquid water adsorbed per gram of sample at values of p/p_0 of 0.3, 0.4, 0.5, 0.6, 0.7, 0.8, and 0.9, in relation to the values for the radius calculated by substituting these values for p/p_0 in the Kelvin equation is shown in figure 11.

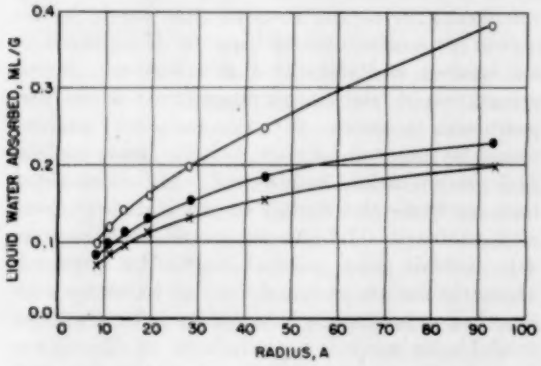

FIGURE 11.—*Adsorption of water vapor at 100° C on untanned hide and two samples of leather in a plot of the volume of liquid water, V_1, per gram of adsorbent against the corresponding radius of a cylindrical capillary as determined from the Kelvin equation.*

(The points for each sample correspond to p/p_0=0.3, 0.4, 0.5, 0.6, 0.7, 0.8, 0.9 consecutively, reading from left to right.) O=hide powder; ●=sole leather degreased and washed; X=vegetable-tanned calfskin.

This figure gives a curve that represents a distribution of capillary sizes in collagen and leather. According to this interpretation, nearly half the water adsorbed by leather below a p/p_0 value of 0.9 could take place in capillaries less than 10 A in radius, whereas about one-third of the water adsorbed by collagen could be taken up in capillaries of this size. It can be seen from these results that much of the surface available to water would not be available to oils having molecular cross sections of 6 to 10 A. Orientation could occur in only about half of the capillaries available to water vapor, and therefore the amount of grease adsorbed would be greatly reduced on account of plugging of the pores. This interpretation is more nearly in line with what is found in actual practice.

An application with respect to particle size might be made, in the light of the above theory, to the practice of tanning, dyeing and fatliquoring of leather. The use of materials having the proper particle-size distribution to correspond with the pore-size distribution in the leather might lead to better results in these processes. If small particles are used along with larger ones, the greater proportion of the smaller particles eventually will be distributed into the small capillaries and the large particles will be in the large pores. Therefore, if an oil having the correct size distribution is used in fat-liquoring, a larger proportion of the surface should become lubricated. Likewise, in tanning, a more uniform distribution of the tanning material would take place.

The author expresses his appreciation to F. T. Carson of the Paper Section for permission to use his equipment, for keeping a daily record of temperature and humidity readings, and for his interest and suggestions.

References

[1] J. Am. Leather Chem. Assn. **17,** 492 (1922).
[2] J. Am. Leather Chem. Assn. **21,** 250 (1926).
[3] J. Am. Leather Chem. Assn. **21,** 351 (1926).
[4] BS Research **11,** 147 (1933) RP583.
[5] J. Am. Leather Chem. Assn. **40,** 378 (1945).
[6] J. Am. Leather Chem. Assn. **41,** 253 (1946).
[7] J. Am. Chem. Soc. **66,** 1499 (1944).
[8] Paper Ind. and Paper World **27,** 1799 (1946).
[9] Inst. Paper Chem., Instrumentation Report No. 40, (February 15, 1945).
[10] J. Am. Chem. Soc. **60,** 309 (1938).
[11] J. Research NBS **29,** 191 (1942) RP1496.
[12] Ind. Eng. Chem., Anal. Ed. **14,** 382 (1942).
[13] Stephen Brunauer, the adsorption of gases and vapors; Physical adsorption (Princeton University Press, Princeton, N. J., 1943).
[14] J. Am. Chem. Soc. **66,** 1297 (1944).
[15] J. Am. Chem. Soc. **39,** 1848 (1917).

WASHINGTON, October 15, 1946.

U. S. Department of Commerce
National Bureau of Standards

Research Paper RP1764
Volume 38, January 1947

Concentration of the Isotopes of Mercury by Free Evaporation in a 10-Cell Counter-Current Reflux Still[1]

By A. Keith Brewer[2] and Samuel L. Madorsky

Concentration of the isotopes of mercury was carried out in a counter-current molecular still consisting of 10 stages. Distillation temperatures varied from 55° to 100° C. A single-stage molecular still was operated, also with mercury, at temperatures varying from 108.1° to 128° C. The results agree with those obtained previously by other investigators operating with single-stage stills.

I. Introduction

Molecular distillation has been used by a number of investigators for concentrating the isotopes of mercury. The technic employed in each instance was essentially the same. Brönsted and Hevesy [1][3] used a Dewar flask type still in which the mercury evaporating in the heated outer flask was frozen out on the chilled inner flask. Mulliken and Harkins [2] condensed the vapor on a cooled sloping glass roof, from which it ran into a side reservoir. Harkins and Madorsky [3] used a large steel annular trough with a Λ-shaped condensing roof.

Each investigator used a single still with one evaporating and one condensing surface. In order to obtain an appreciable concentration it was necessary to repeat the process many times. This required an elaborate system for collecting, recombining, and redistilling fractions.

Wollner, Matchett, and Levine [4] describe a multiple distillation apparatus which they used in purifying acetylated marihuana "red oil". No details are given as to temperature, rate of distillation, pressure inside the still, or as to whether a volatile fraction collected in the dry-ice-cooled trap. In view of the fact that organic liquids are subject to decomposition during high vacuum, high temperature, distillation, and that no provision was made to cool the condensing part of the still, except contact with air, it is doubtful whether they operated under conditions of nonequilibrium distillation.

The present paper describes an apparatus and technic in which a series of molecular stills have been arranged to operate under counter-current reflux. The new still is so designed that recombination of fractions is accomplished automatically by means of gravity feeds. The system acts as a reflux column in which each cell is a separate plate.

The mechanism of operation, under total reflux, is shown graphically in figure 2, *A*. The vapor rising from the surface a_3 of the liquid in cell A_3 condenses on the sloping surface b_3 and runs down to drop into the adjacent cell A_4 higher up in the series. At the same time, the liquid level in cell A_4 is kept constant by means of a spillover, S, which allows the liquid to flow back into cell A_3. The flowback, in consequence, is exactly equal to the forward throughput. The over-all operation is such that the light fraction increases in concentration toward the upper end while the heavy fraction increases in concentration toward the lower end of the still.

[1] This paper covers experimental work carried out during the period June 7, 1940, to April 3, 1941. Two statements describing the method and most of the experimental work and dated June 24, 1940, and Nov. 25, 1940, respectively, were submitted to the Director of the National Bureau of Standards. Until recently it has been withheld from publication because of wartime security restrictions. It will be included in vol. 6, Div. III, of the Manhattan Project Technical Series.

[2] Now at the U. S. Navy Department.

[3] Numbers in brackets indicate the literature references at the end of this paper.

II. Apparatus

The evaporation apparatus is shown diagrammatically in figure 1. The evaporating reservoirs were machined from an iron plate, *B*. Each reservoir was 2 cm wide, 7.5 cm long, and 0.8 cm deep at the shallow side. Spillovers *S*, figure 2, *B*, were cut at alternate ends for adjacent cells to provide thorough mixing of the liquid. The capacity of each cell was 9 ml, and that of the entire system was 90 ml. The reservoirs were heated by a Nichrome coil imbedded in an alundum plate that was bolted directly to the reservoir block.

The condensing roofs, *C*, figure 1, were made of iron wedges screwed to a supporting plate, *D*. The angle of slope could be varied by changing the wedges. The roofs were cooled by circulating alcohol at $-18°$ C through an iron coil immersed in a pool of mercury, *E*, in contact with plate *D*. The temperature of the mercury was kept near 0° C by a thermoregulator that operated the alcohol-circulating pump.

Loss of mercury from the evaporators was prevented by glass plates provided with notches to allow proper evacuation of each cell.

A high vacuum was obtained by enclosing the entire still in a glass cylinder with machined metal plates bolted across the ends; rubber gaskets coated with stopcock grease made the system vacuum-tight. The operating pressure, as read by a McLeod gage, was below 10^{-5} mm Hg.

Considerable difficulty was experienced in obtaining roofs that did not allow most of the condensed mercury to drop back into the same cell. In the first apparatus the machined surface of the iron wedges was used directly as the condensing surface; the angle was 25 degrees. A large fraction of the mercury dropped back into the same cell instead of running down into the next pool. Changing the slope of the wedges to 40 degrees made only a slight improvement. The condensing surfaces were then polished and blued at 300° C. The results were fairly satisfactory. A special study of condensing surfaces carried out with a single-cell apparatus showed that glass was by far the most effective material. Glass plates 1 mm thick were then cemented to the iron roofs. This change was effective in giving a complete forward transport of the condensing mercury. An angle of 33 degrees was satisfactory.

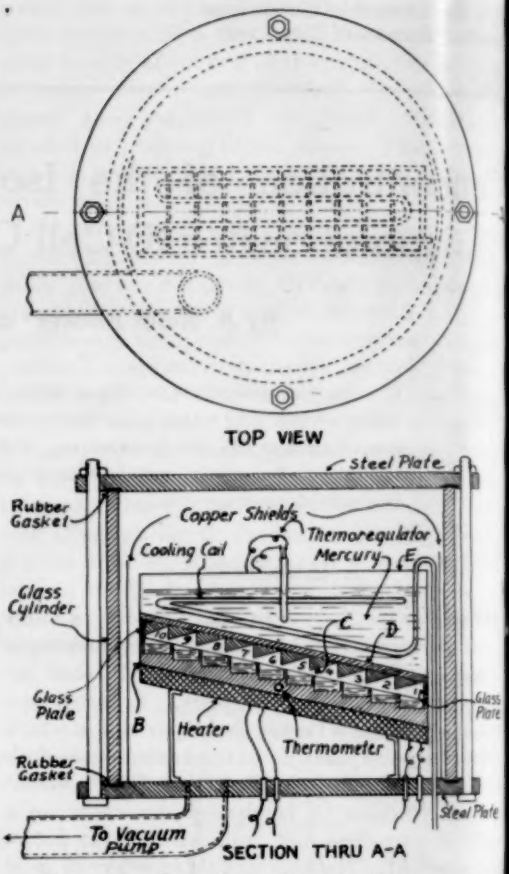

FIGURE 1.—*Ten-cell cascade evaporation apparatus.*

Purification and density determination of the mercury

The mercury was first purified by aeration for 24 hours in 10-percent nitric acid. It was then distilled three times, rejecting 10-percent fractions at the beginning and end of each distillation.

The change in the isotope ratio was determined by the density method described by Mulliken and Harkins [2] and Harkins and Madorsky [3]. Several modifications were introduced to increase the accuracy of the measurements. The picnometer had a capacity of about 3 ml and held about 40 g of Hg. It was filled with the Hg sample at about 10° C, then placed in a thermostat at 31.7° ±0.003° C. The overflow of Hg was brushed off with the sharp edge of a piece of paper exactly at the time when the reading on a thermometer was

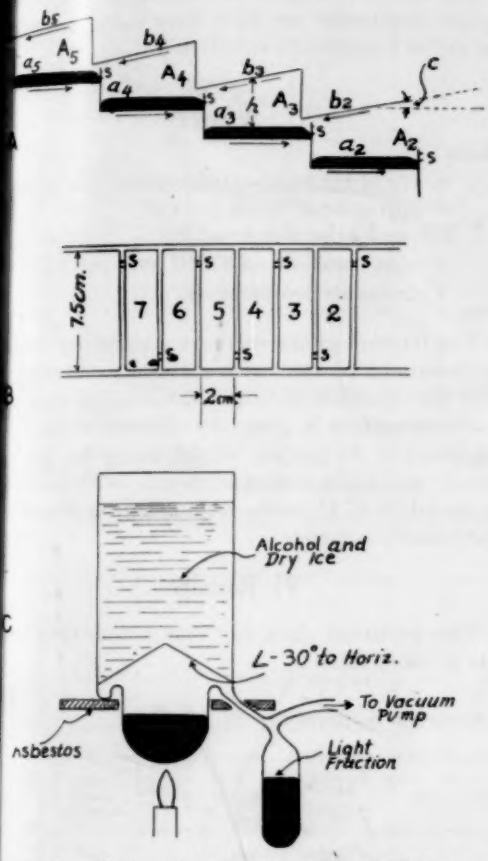

FIGURE 2.—*Diagramatic view of cascade distillation and apparatus for single-stage operation.*

A, diagram showing mechanism of cascade distillation; *B*, section through cells showing spillovers; *C*, Mulliken-type single-stage molecular still.

at a given point on the downward temperature variation of the bath. At first a razor blade was used to wipe off the mercury overflow, but it was found that the picnometer lost weight owing to scraping of the glass.

Weighings were made on a new chainomatic balance, using a counterpois picnometer having the dimensions as close to the original as possible. Magnifying glasses were used to read the zero on the pointer scale and the divisions on the chain dial. An accuracy of about 2 parts per million was obtained. As the total weight of the Hg was 40 g, 2 ppm involved an accuracy of 0.08 mg.

In order to check the density measurements against isotope abundance ratios, samples of mercury of known density labeled No. 1 ordinary, No. 2 ordinary, and *A*, *B*, *C*, and *D* were sent to A. O. C. Nier, at the University of Minnesota, for mass spectrometric analysis. The ratios for ^{198}Hg to ^{204}Hg were measured. These ratios with comparative density measurements are given in table 1.

TABLE 1.—*Comparison between mass spectrograph analysis and density determinations of mercury*

Sample	Change of density of mercury	Ratio $^{198}Hg/^{204}Hg$
	ppm	
University of Minnesota, ordinary	.....	1.456
No. 1, ordinary	.....	1.459
No. 2, ordinary	.....	1.457
A	+10.9	1.450
B	−11.2	1.466
C	+30.6	1.438
D	−15.2	1.470
E	+14.2	1.452

III. Temperature Measurements

The temperature of the mercury in the cells was first determined by a thermometer and thermocouple inserted in plate *B* (fig. 1). It was evident, however, that the power input was much too small to account for the evaporation of Hg at a rate corresponding to the plate temperature. A Pt-Pt-Rh thermocouple inserted in the mercury gave incorrect readings because of stray contact potentials. In consequence, it was found necessary to estimate the temperature of the evaporating Hg surface from the power input into the heater, after correcting for radiation and conduction losses.

IV. Operational Procedure

After the cell had been filled with mercury, the system was closed and evacuated to a sticking vacuum. In all the runs the operation was continuous. The mercury cooling bath was maintained at about 0° C.

Runs II, III, and IV were made with the 40-degree polished and blued roofs; the average distance from the evaporating surface was 19 mm. The duration was 2, 5, and 3 days, respectively. Run V+VI was carried out for the first 6 days with blued iron roofs; the experiment was then stopped, and the glass-covered roofs were installed. The run was then continued for another 6 days. The slope angle was 33 degrees from the horizontal,

and the average distance from the evaporating surface was 15 mm. Runs VII, VIII, and IX were made with the same glass-covered roofs and lasted 3, 5, and 2 days, respectively. In run VII the mercury in the two lowest cells became mixed in sample taking. The conditions in run X were the same as in run IX, except that the temperature was higher. Soon after this run was started the glass plate fell off the roof in cell 5, and most of the condensate in this cell dropped back without reaching cell 6. In consequence, the lower four cells and the upper six cells in run X operated as separate systems.

V. Throughput

The throughput in the present still is determined by the quantity of mercury carried forward from cell to cell. As the stills were operated under total reflux, this is necessarily the same as the quantity of mercury spilling back. The forward movement of mercury is determined by three factors: (1) the rate of escape from the liquid surface, (2) the fraction condensed on the roofs, and (3) the fraction of condensate dropping back into the same cell.

The rates of evaporation of Hg in grams per square centimeter per hour were calculated with the aid of Langmuir's equation [5]

$$m = P\sqrt{\frac{M}{2\pi RT}},$$

where

m = (g of Hg evaporated per cm^2) per second
P = pressure in dynes per cm^2
M = molecular weight of Hg
R = gas constant = 8.3×10^7 ergs per 1 deg C
T = absolute temperature.

The fraction of the mercury condensing on the roofs cannot be told with certainity. Assuming that the direction of escape of molecules from the mercury surface is given by the cosine law, approximately 75 percent of the molecules leaving should strike the sloping surface. As this surface is cooled to 0° C condensation thereon should be very nearly complete.

VI. Results

The pertinent data for nine consecutive runs are given in table 2.

TABLE 2.—*Concentration of isotopes of mercury in the 10-cell apparatus*

Experiment No.	Time	Temperature	Vapor pressure	Rate of evaporation	Kind of roof	Angle to horizon	Average, Δ	Number of plates	Total change in density
	Days	*°C*	mm Hg	*(g/cm²)/hr*		*Degrees*	*mm*		*ppm*
II	2	55	0.017	2.95	Iron	40	19	9	21.8
III	5	70	.048	7.75	do	40	19	9	45.9
IV	3	70	.048	7.75	do	40	19	9	29.6
V+VI	12	75	.067	10.26	Iron and glass	40, 33	19, 15	9	129.4
VII	3	75	.067	10.26	Glass	33	15	8	78.2
VIII	5	75	.067	10.26	do	33	15	9	161.6
IX	2	75	.067	10.26	do	33	15	9	85.7
X	2	100	.273	42.03	do	33	15	5	79.8

The change in density of the mercury in the individual cells for each run is given in figures 3 and 4.

Runs II and IV are of the type to be expected in a reflux column in the initial stages of operation. The concentration predominates at the ends with very little effect in the central portion. Run III is characterized by a nonuniformity of transport between cells. All three runs were made with iron roofs in which a large fraction of the condensed mercury fell back into the cells from which it evaporated. As some of the roofs behaved more efficiently than others, the erratic shape of line III is to be expected.

Run V+VI shows a uniform rate of change in density from cells 5 to 10. This is indicative of equilibrium having been established in that portion of the column. In the lower cells from 4 down, the difference in density decreases slightly toward the bottom. This dropping off in the efficiency in the lower cells was expected as droplets of mercury were regularly observed to form in the upper part of the column and run along the walls to fall principally into cell 1. The constant

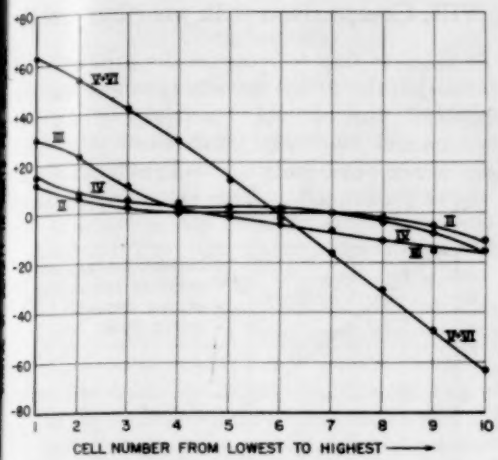

FIGURE 3.—*Results obtained in runs II, III, IV, and V plus VI where polished steel roofs were used.*

II, 2 days at 55°; III, 5 days at 70°, IV, 3 days at 70°; V plus VI, 12 days at 75°.

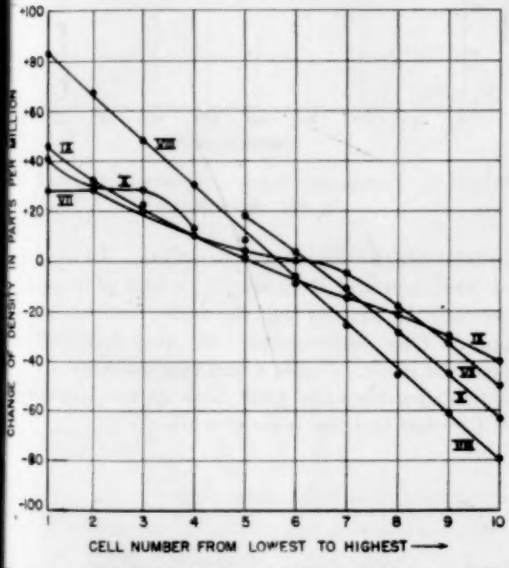

FIGURE 4.—*Results obtained in runs VII, VIII, IX, and X, where glass-covered roofs were used.*

VII, 3 days at 75°; VIII, 5 days at 75°; IX, 2 days at 75°; X, 2 days at 100°.

addition of light mercury from the top cells to the bottom cell gives rise to the observed decrease in rate.

It should be pointed out that a small difference in density between the two lowest cells might indicate impurity in the mercury. As any impurity that might be present would of necessity be lighter than mercury and at the same time have a lower vapor pressure, it would soon concentrate in the lowest cell and lower the density of the Hq in that cell. The possibility of impurities in the mercury, however, has been carefully considered and shown to be absent. The straight line obtained in run VIII is also definite proof for the absence of impurities.

Runs VII, VIII, IX, and X were made with glass plates on the condensing roofs. Visual observation showed most of the mercury droplets falling into the next cell higher up. The quantity of mercury running down the walls and dropping into the lower cells was small.

Runs VII and IX are of the character to be expected when equilibrium has not been attained between the various cells. The contour of the curve for run VII indicates that the throughput is not uniform between the various cells as equilibrium is much nearer attained in the top three cells than in the remainder.

Run VIII is characteristic of a counter-current system operating under total reflux when equilibrium has been established between all cells.

The results obtained at 100° C are illustrated in run X. As the glass plate on cell 5 fell off during operation, the data are not complete for the entire system. They do show, however, that cells from 6 to 10 were in equilibrium. The separation per plate, as shown by figure 4, is 17.3 ppm.

Figure 5 shows that the separation values are in general agreement with those to be expected from single-stage stills. As the exact temperature of the evaporating surface was not known in any instance, a more precise agreement cannot be expected.

VII. Free Evaporation of Mercury at High Temperatures

The 10-cell cascade system was not designed for a study of free evaporation at temperatures above about 100° C. As such knowledge is essential in working out more efficient still designs, tests at temperatures above 100° C were made in a single-stage glass molecular still similar to the one used by Mulliken and Harkins [2]. The still is illustrated in figure 2, C.

The capacity of the evaporator was 200 g of Hg (fig. 2, C), the evaporating surface was 10 cm^2, and the condensing surface had an angle of

30 degrees. The roof was cooled by an alcohol–dry-ice mixture, and the evaporator was heated with an oxy-gas blast-lamp. The temperature of the mercury evaporating surface was calculated from the quantity of mercury evaporated per unit time, using Langmuir's equation.

Four runs at different temperatures were made. In the final run the full force of the oxy-gas flame was used. The cut, C, in each run was approximately 2. The pertinent data for these experiments are given in table 3.

TABLE 3.—*Concentration of isotopes of mercury in a single-stage apparatus*

Experiment No.	Time	Temperature	Vapor pressure	Rate of evaporation	Change in density of light fraction per cut	Change in density per plate
	min	*°C*	*mm Hg*	*(g/cm²)/hr*	*ppm*	*ppm*
XI	11	108.1	0.417	62.8	10.50	15.15
XII	8	114.8	.570	87.3	10.40	15.01
XIII	6	120.7	.770	113.7	8.05	11.62
XIV	4	128.0	1.075	161.0	4.80	6.93

The change in density, ΔD, of the light fractions was obtained by dividing the total difference in density between the light and heavy fractions by 2. The change of density per plate, $\Delta D'$, was computed from the equation given by Mulliken and Harkins [2]:

$$\Delta D = \Delta D' \frac{\ln C}{C-1}, \qquad (1)$$

where ΔD and $\Delta D'$ are expressed in parts per million. Then

$$\Delta D' = \Delta D / 0.69315. \qquad (2)$$

VIII. Comparison with previous work

It is interesting to compare the present results obtained in the 10-cell cascade apparatus with the single-cell work at the University of Chicago. Harkins and Madorsky [3] obtained about 16.50 ppm decrease in density for the light fraction when a cut of 2 was made. This value corresponds to

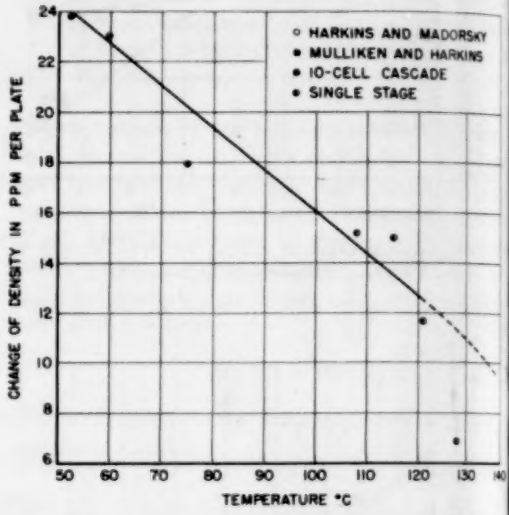

FIGURE 5.—*Comparison between the present work and that by other investigators*

16.50/0.69315=23.80 ppm per plate. In the work of Mulliken and Harkins [2], a cut of 2 gave a decrease in density for the light fractions of 16 ppm. This corresponds to 16/0.69315=23.08 ppm per plate. Table 4 and figure 5 show a comparison between the work done at the University of Chicago and the present work.

TABLE 4.—*Concentration of isotopes of mercury: comparison with previous work*

Reference	Number of cells in still	Rate of evaporation	Calculated	Vapor pressure	Cut	Change in density of light fraction per cut	Change in density per plate
		(g/cm²)/hr	*T°C*	*mm Hg*		*ppm*	*ppm*
Harkins and Madorsky	1	2.37	52.0	0.015	2	16.50	23.08
Mulliken and Harkins	1	4.60	59.5	.025	2	16.00	23.80
Present work, experiment VIII	10	10.27	75.0	.067	.....	.....	17.95
Present work, experiment XI	1	62.8	108.1	.417	2	10.50	15.15
Present work, experiment XII	1	87.3	114.8	.570	2	10.40	15.01
Present work, experiment XIII	1	113.7	120.7	.770	2	8.05	11.62
Present work, experiment XIV	1	161.0	128.0	1.075	2	4.08	6.93

IX. Conclusions

The results presented in this paper demonstrate that a series of individual molecular stills can be arranged in counter-current reflux in such a manner that the throughput between cells is entirely controlled by gravity feed. The advantages of the present reflux still over the single-stage still are many: (1) The quantity of material required to give a desired separation is materially smaller, (2) the holdup is vastly lower, (3) the time required for a given separation is very much shorter, (4) the labor involved is less; this is illustrated by the fact that to realize the separation obtained in one operation in the present 10-compartment still, 55 individual recombinations and distillations would have to be made with single-stage stills, (5) the operation can be made continuous; the material to be concentrated can be fed into the system at one end or at the midpoint, if both light and heavy fractions are of interest, and the concentrate can be withdrawn continuously at the ends, and (6) The entire separation can be run without exposing the material to the atmosphere. This is particularly desirable for liquids that are susceptible to decomposition upon exposure to air.

The authors express their appreciation to J. W. Westhaver for his many basic contributions to this research.

References

[1] Brönsted and Hevesy, Phil. Mag. [6] **43,** 31 (1922).
[2] Robert S. Mulliken and W. D. Harkins, J. Am. Chem. Soc. **44,** 37 to 65 (1922).
[3] W. D. Harkins and S. L. Madorsky, J. Am. Chem. Soc. **45,** 591 (1923).
[4] H. J. Wollner, John R. Matchett, and Joseph Levine, Ind. Eng. Chem., Anal. Ed. **16,** 529 (1944).
[5] I. Langmuir, Phys. Rev. **2,** 329 (1913).

WASHINGTON, November 19, 1946.